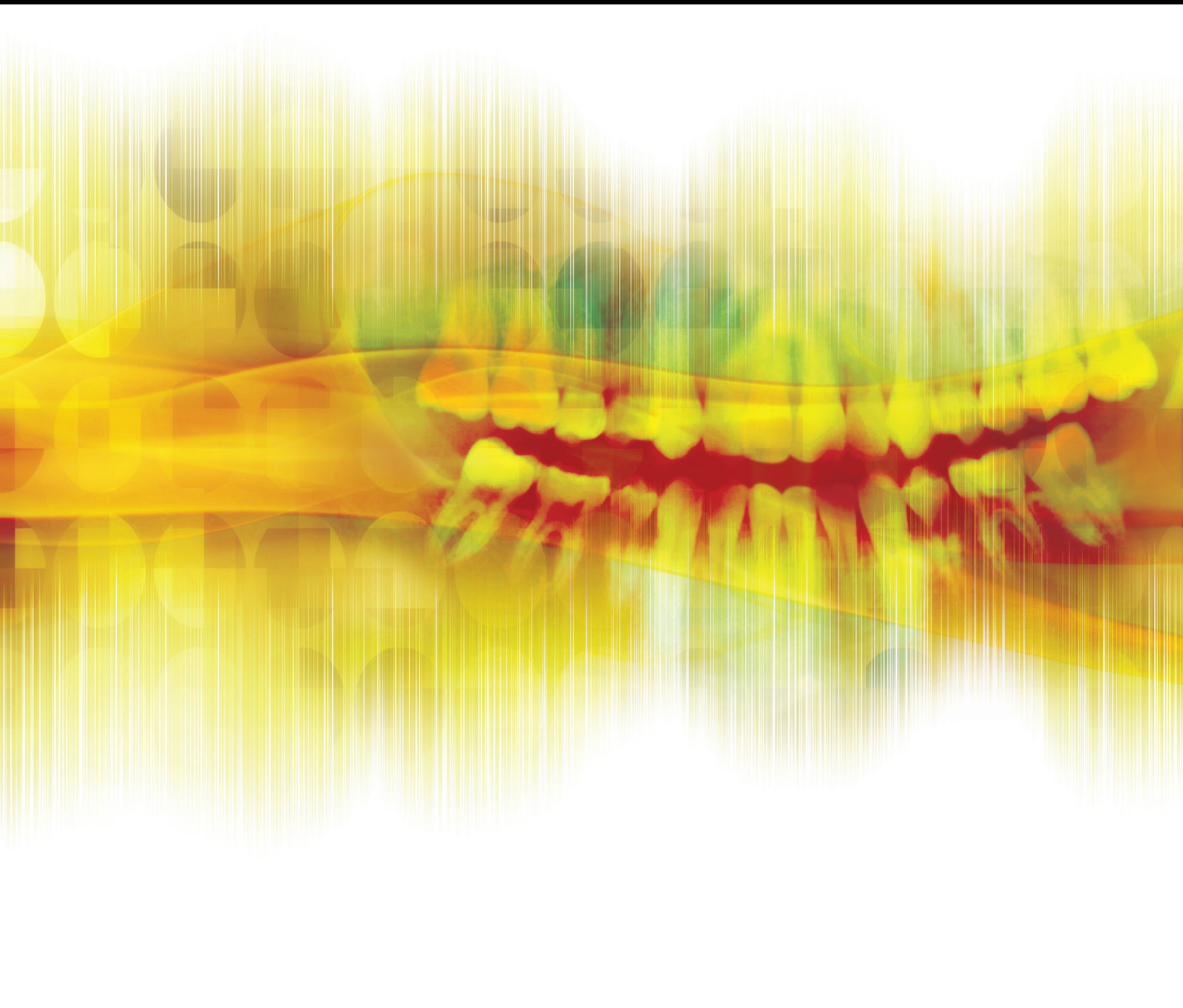


International Journal of Dentistry

Dental Implants in the Third Millennium

Lead Guest Editor: Luigi Canullo

Guest Editors: Eitan Mijiritsky and Silvio M. Meloni



Dental Implants in the Third Millennium

International Journal of Dentistry

Dental Implants in the Third Millennium

Lead Guest Editor: Luigi Canullo

Guest Editors: Eitan Mijiritsky and Silvio M. Meloni



Copyright © 2018 Hindawi. All rights reserved.

This is a special issue published in “International Journal of Dentistry.” All articles are open access articles distributed under the Creative Commons Attribution License, which permits unrestricted use, distribution, and reproduction in any medium, provided the original work is properly cited.

Editorial Board

Ali I. Abdalla, Egypt
Manal Awad, UAE
Ashraf F. Ayoub, UK
Silvana Barros, USA
Sema Belli, Turkey
Giuseppina Campisi, Italy
Dong Mei Deng, Netherlands
Shinn-Jyh Ding, Taiwan
J. D. Eick, USA
Annika Ekestubbe, Sweden
Carla Evans, USA
Yoshitaka Hara, Japan
Saso Ivanovski, Australia
Chia-Tze Kao, Taiwan
Kee Y. Kum, Republic of Korea

Manuel Lagraverre, Canada
Claudio Rodrigues Leles, Brazil
Louis M. Lin, USA
A. D. Loguercio, Brazil
Tommaso Lombardi, Switzerland
Martin Lorenzoni, Austria
Jukka H. Meurman, Finland
Masashi Miyazaki, Japan
Yasuhiro Morimoto, Japan
Carlos A. Munoz-Viveros, USA
Hiroshi Murata, Japan
Joseph Nissan, Israel
Patricia Pereira, USA
Roberta Pileggi, USA
André Reis, Brazil

Georgios E. Romanos, USA
Gilberto Sammartino, Italy
Andrea Scribante, Italy
Robin Seymour, UK
Timo Sorsa, Finland
Gianrico Spagnuolo, Italy
Andreas Stavropoulos, Sweden
Dimitris N. Tatakis, USA
Ahmad Waseem, UK
Izzet Yavuz, Turkey
Cynthia Yiu, Hong Kong
Li Wu Zheng, Hong Kong
Qiang Zhu, USA
Spiros Zinelis, Greece

Contents

Dental Implants in the Third Millennium

Luigi Canullo , Eitan Mijiritsky , and Silvio Mario Meloni 
Editorial (2 pages), Article ID 9752141, Volume 2018 (2018)

Survival and Success Rates of Different Shoulder Designs: A Systematic Review of the Literature

Marco Tallarico, Marco Caneva, Silvio Mario Meloni , Erta Khanari, Yuki Omori, and Luigi Canullo 
Review Article (10 pages), Article ID 6812875, Volume 2018 (2018)

Self-Assembled Monolayers for Dental Implants

Sidónio C. Freitas , Alejandra Correa-Urbe, M. Cristina L. Martins , and Alejandro Pelaez-Vargas 
Review Article (21 pages), Article ID 4395460, Volume 2018 (2018)

Double Guided Surgery in All-on-4® Concept: When Ostectomy Is Needed

Gabriele Tonellini , Raquel Saez Vigo , and Giorgio Novelli
Clinical Study (7 pages), Article ID 2672549, Volume 2018 (2018)

Soft Lithography and Minimally Human Invasive Technique for Rapid Screening of Oral Biofilm Formation on New Microfabricated Dental Material Surfaces

Marta Alvarez-Escobar, Sidónio C. Freitas , Derek Hansford, Fernando J. Monteiro, and Alejandro Pelaez-Vargas 
Research Article (5 pages), Article ID 4219625, Volume 2018 (2018)

Osseointegration of a 3D Printed Stemmed Titanium Dental Implant: A Pilot Study

James Tedesco, Bryan E. J. Lee, Alex Y. W. Lin, Dakota M. Binkley, Kathleen H. Delaney, Jacek M. Kwiecien, and Kathryn Grandfield
Research Article (11 pages), Article ID 5920714, Volume 2017 (2018)

Morse Taper Connection Implants Placed in Grafted Sinuses in 65 Patients: A Retrospective Clinical Study with 10 Years of Follow-Up

Francesco Mangano, Renata Bakaj, Irene Frezzato, Alberto Frezzato, Sergio Montini, and Carlo Mangano
Clinical Study (9 pages), Article ID 4573037, Volume 2017 (2018)

The Ball Welding Bar: A New Solution for the Immediate Loading of Screw-Retained, Mandibular Fixed Full Arch Prostheses

Danilo Bacchiocchi and Andrea Guida
Clinical Study (9 pages), Article ID 2679085, Volume 2017 (2018)

Cumulative Success Rate of Short and Ultrashort Implants Supporting Single Crowns in the Posterior Maxilla: A 3-Year Retrospective Study

Giorgio Lombardo, Jacopo Pighi, Mauro Marincola, Giovanni Corrocher, Miguel Simancas-Pallares, and Pier Francesco Nocini
Clinical Study (10 pages), Article ID 8434281, Volume 2017 (2018)

Immediate Loading of Single Implants in the Anterior Maxilla: A 1-Year Prospective Clinical Study on 34 Patients

Miguel Stanley, Filipa Calheiros Braga, and Beatriz Mota Jordao
Clinical Study (11 pages), Article ID 8346496, Volume 2017 (2018)

Editorial

Dental Implants in the Third Millennium

Luigi Canullo , **Eitan Mijiritsky** , **and Silvio Mario Meloni** 

¹University of Valencia, Valencia, Spain

²Maxillofacial Surgery, Department of Otolaryngology, Tel-Aviv Sourasky Medical Center, Sackler Faculty of Medicine, Tel-Aviv University, Tel Aviv, Israel

³School of Dentistry, University of Sassari, Sassari, Italy

Correspondence should be addressed to Luigi Canullo; luigicanullo@yahoo.com

Received 27 March 2018; Accepted 28 March 2018; Published 2 May 2018

Copyright © 2018 Luigi Canullo et al. This is an open access article distributed under the Creative Commons Attribution License, which permits unrestricted use, distribution, and reproduction in any medium, provided the original work is properly cited.

From Galileo to Bacon, the science has always tried to bring the scientific discipline on the road of “evidence” in face of many possible and arbitrary “opinions.” For instance, the Cochrane Library exists so that healthcare decisions could get better. This organization tried to certify this “evidence” using a methodologic approach. Nevertheless, in oral and maxillofacial surgery, most of systematic reviews founded weak or no evidence that any particular type of intervention is better than any other.

Evidence medicine (EBM) has been defined as “the judicious use of the best current evidence in making decisions about the care of the individual patient” [1]. It was assumed that only randomized trials can generate level I evidence. Particularly, due to its rigor in design and control for different types of bias, randomized double-blind placebo controlled trials have had the largest impact in leading clinicians toward the concept of EBM. However, other methods, such as prospective cohort studies, can also be used for evidence-based decision making.

The rationale behind the EBM is to analyze only the effect of the drug, removing the patients’ and operators’ variables. To cancel patient variability, sample size should be in the order of thousands. At the same time, the only skill required to the operator is to display a pill. EBM has been applied to surgery over the past decades with increasing numbers of randomized controlled trials (RCTs). Nevertheless, interpretation of its clinical meaning might be problematic in the dental surgical field. In fact, despite a test technique can be compared to a control one in a randomized modality, to ensure that the techniques can be precisely defined and then performed in a standardized

manner for each operator remains challenging. The skill of the operator, which remains the most important variable, must not be underestimated. Finally, due to the ethical conflicts intrinsic to the surgical field, sample size is very often small, and despite statistical tricky analyses and strict inclusion/exclusion medical criteria, patient variability cannot be excluded. Very often, in fact, to statistically increase numbers and apparently generalize the meaning of the message, the biology behind the cases is underestimated and the outcomes are so generalized to lose a specific clinical effectiveness.

Although the start of this methodologic approach was really promising, its, so far, extensive and maybe misinterpreted use in the surgical field might represent only a tricky way to publish.

Controversially, in the modern implant dentistry, biologic (a composite neologism to express the need to combine knowledge of biology and the use of the logic) could be the key factor to interpret and choose the correct surgical (and not only) techniques to treat a clinical case. At the light of the third millennium clinical demands, interpretation of the evidence in surgical dentistry through Cochrane’s guidelines might appear problematic due to the nature of surgery itself. Outcomes of systematic reviews (at least with the actual standards) should be used as approximate indications.

Randomized controlled trial and systematic review will continue to be a safety margin not to go beyond, but the message to spread to the scientific community should be to encourage the production of long-term prospective and also retrospective study conducted in clinical practice. These might provide less high levels but without forgetting the

importance of the experience and the operator skill, just focusing on the potential limits and complications of the technique itself.

Luigi Canullo
Eitan Mijiritsky
Silvio Mario Meloni

References

- [1] D. L. Sackett, W. M. C. Rosenberg, J. A. M. Gray, R. B. Haynes, and W. S. Richardson, "Evidence based medicine: what it is and what it isn't," *BMJ*, vol. 312, no. 7023, pp. 71-72, 1996.

Review Article

Survival and Success Rates of Different Shoulder Designs: A Systematic Review of the Literature

Marco Tallarico,^{1,2} Marco Caneva,³ Silvio Mario Meloni ,⁴ Erta Xhanari,⁵ Yuki Omori,^{3,6} and Luigi Canullo ²

¹Implantology and Prosthetic Aspects, Master of Science in Dentistry Program, Aldent University, Tirana, Albania

²Private Practice, Rome, Italy

³ARDEC Academy, Ariminum Odontologica Srl, Rimini, Italy

⁴Dentistry Unit, University Hospital of Sassari, Sassari, Italy

⁵Private Practice, Tirana, Albania

⁶Department of Oral Implantology, Osaka Dental University, Hirakata, Osaka, Japan

Correspondence should be addressed to Luigi Canullo; luigicanullo@yahoo.com

Received 16 January 2018; Accepted 1 March 2018; Published 26 April 2018

Academic Editor: Shinn-Jyh Ding

Copyright © 2018 Marco Tallarico et al. This is an open access article distributed under the Creative Commons Attribution License, which permits unrestricted use, distribution, and reproduction in any medium, provided the original work is properly cited.

Objectives. To identify whether there is a relationship between different implant shoulder positions/orientations/designs and prosthetic and/or implant failures, biological or mechanical complications, radiographic marginal bone loss (MBL), peri-implant buccal recession (RC), aesthetic scores (Papilla Index, PES, and WES), and patient satisfaction after a minimum of 1 year function in the aesthetic zone, compared to the two-piece, conventional implant neck architecture. **Materials and Methods.** The systematic review was written according to the PRISMA guidelines. The search strategy encompassed the English literature from 1967 to September 2016 and was performed online (in the PubMed database of the U.S. National Library of Medicine, Embase, and the Cochrane Library) to identify relevant studies that met the inclusion criteria. The assessment of quality and risk of bias of the selected manuscripts was performed according to the guidelines provided by CONSORT and STROBE statements. **Results.** A total of 16 articles (7 randomized controlled trials, 4 observational comparative studies, and 5 systematic reviews) were selected to fulfill the inclusion criteria. A trend of higher implant failure and prosthetic complications were experienced in the one-piece group compared to the two-piece group, although no statistically significant differences were found. Higher marginal bone loss was found in the test group (one-piece, scalloped implants) compared to the control group (two-piece, flat implants). No comparative studies reporting data on sloped implants were found that fulfilled the inclusion and exclusion criteria of this systematic review. No differences were experienced between groups regarding aesthetic outcomes and patient satisfaction. **Conclusions.** There was sufficient evidence that different implant shoulder positions/orientations/designs (scalloped, sloped, and one piece) offer no benefit when compared to two-piece, conventional flat implants. Current evidence is limited due to the quality of available studies.

1. Introduction

Stability of the peri-implant soft and hard tissues is a prerequisite for a long-term aesthetic and function of implant-supported restoration [1]. In two-piece implants, early bone loss is observed after the connection of the abutment and delivery of final prosthesis, mostly due to the biologic width establishment [2–6]. This concept is being hypothesized as one of the most likely causes of early implant bone loss [2, 3].

The effect of surgical trauma, implant surface characteristics, macrodesign of the implant, and type of implant-abutment connection, as well as implant placement depth, soft tissue thickness, distance between adjacent implants, and abutment height, may all contribute to this process [4–6].

Traditionally, implants are two pieces, and they were placed in a two-step surgical procedure [7]. Two-piece designs can offer increased flexibility, with connections possible at the bone level, and wound closure can be easier.

In the 1980s [8], Schroeder and colleagues introduced an implant where the bone anchorage unit and contiguous transmucosal component were manufactured in a single unit. With one-piece implant designs, the transmucosal part is incorporated into the implants. This was an attempt to minimize crestal bone loss that reduces contamination of the implant-abutment junction. Furthermore, by using a one-piece implant, the second surgery procedure is avoided, as well as abutment connection/disconnection. The advantage of this procedure is to avoid the presence of a gap or micromovement at the implant-abutment junction for a beneficial effect on the peri-implant soft and hard tissues [9]. Nevertheless, compared with two-piece implants, they are much more difficult to place in the prosthetically driven position (height and angulation), which makes one-piece implants even more difficult to finalize. On the other hand, new implant and abutment designs have been proposed to minimize the crestal bone loss. Platform switching is done whenever an abutment is used that is smaller in diameter than the implant platform. This concept has been proposed as an effective prosthetic concept to reduce the amount of peri-implant bone loss around dental implants [10]. The concept of horizontal offset (platform switching) has made it possible to place implant shoulders at the crestal bone level with predictable minimal marginal bone resorption [10]. Scalloped and sloped implants represent other design changes that advocate for maintaining marginal bone levels [11–13]. The scalloped implant was designed with a modified platform that mirrors the natural cement-enamel junction of the anterior teeth and follows the anatomic contour of the anterior alveolar bone crest. The scalloped implants were developed with the intent of preserving interdental bony peaks, supporting the soft tissue, thereby maintaining or creating interimplant papillae [11, 12]. Recently, a dental implant with a sloped marginal contour and a height difference of the implant shoulder of approximately 1.5 mm has been developed with the aim of improving the congruence between the implant and the bone in extraction sites and sloped ridges [13].

The main objective of this systematic review was to compare the prosthetic and/or implant failures, biological or mechanical complications, radiographic marginal bone loss, peri-implant buccal recession, aesthetic scores, and patient satisfaction after at least 1 year of function, around single- or multiple-tooth implant-supported restorations in the aesthetic zone, on the two-piece, conventional implant neck architecture (flat implants with the same level on 360°) and one-piece, scalloped, or sloped implants.

2. Materials and Methods

This systematic review was written according to the Preferred Reporting Items for Systematic Reviews and Meta-Analyses (PRISMA) guidelines [14]. The focused question was to identify whether there is a relationship between different implant shoulder positions/orientations/designs (one piece, scalloped, and sloped) and prosthetic and/or implant failures, biological or mechanical complications, radiographic marginal bone loss, peri-implant buccal

recession, aesthetic scores, and patient satisfaction after at least 1 year of function, compared to two-piece, flat implants with the same level on 360°. Initially, PICOS question (population (P), intervention (I), comparison (C), outcomes and study design (O), and study type (S)) defined the search strategy, where P = single and partial edentulous patients required an implant-supported restoration in the aesthetic zone; I = different implant shoulder positions/orientations/designs (scalloped, sloped, and one piece), after at least 1 year of function; C = two piece and same level on 360° (flat implants); O = prosthetic and/or implant failures, biological or mechanical complications, radiographic marginal bone loss (MBL), peri-implant buccal recession (BR), aesthetic scores (Papilla Index, PES, and WES), and patient satisfaction (patient questionnaire and VAS); and S = randomized controlled clinical trials (RCTs), case-control studies, and cohort studies.

2.1. Search Strategy. An initial search strategy that includes the English literature from 1967 to September 2016 was performed to identify relevant studies that met the inclusion criteria of this systematic review. The following databases were consulted: Embase (Excerpta Medica dataBASE), PubMed database of the U.S. National Library of Medicine, Grey Literature Database (New York Academy of Medicine Grey Literature Report), and the Cochrane Library. Screening was performed independently and simultaneously by two calibrated examiners (MT and SMM). The electronic databases were searched using the following terms: (((“dental implants”[Mesh] AND “dental implant abutment design”[Mesh]) OR “dental implant abutment interface”[All Fields]) OR (one[All Fields] AND piece[All Fields] AND implant[All Fields])) OR (“scalloped”[All Fields] AND implant[All Fields]) OR (sloped[All Fields] AND implant [All Fields]) AND English[lang].

2.2. Eligibility Criteria. The following inclusion criteria were defined for the selection of articles:

- (i) Written in English
- (ii) Evaluate in their protocol the prosthetic and/or implant failures, biological or mechanical complications, radiographic marginal bone loss, peri-implant buccal recession, aesthetic scores, patient satisfaction, and/or the influence of the implant shoulder position/orientation/design on soft and hard tissue levels around single or multiple implants in the aesthetic zone with scalloped, sloped, and one-piece implants and a two-piece, conventional implant neck architecture (flat implants featured with the same level on 360°)
- (iii) Randomized controlled clinical trials of implants of ≥ 1 year in function
- (iv) Observational (prospective and retrospective) case-control studies of implants of ≥ 1 year in function
- (v) Cross-sectional comparative studies of ≥ 1 year in function

- (vi) Systematic reviews, narrative reviews, consensus statements, commentaries, or editorials

Articles were excluded if they were

- (i) observational (prospective or retrospective) cohort studies without the control group;
- (ii) in vitro studies;
- (iii) finite element analyses;
- (iv) animal studies;
- (v) reports with <5 cases;
- (vi) reports involving mini-implants, zirconia implants, or blade implants;
- (vii) reports on implants of <1 year in function.

2.3. Data Extraction. The two calibrated reviewers screened all the data from the selected papers. Cohen's kappa values between examiners were calculated at both the stages of the research. Discrepancies were resolved by consensus, and a third examiner was consulted (LC). Articles without abstracts but with titles related to the objectives of this study were included, and their full texts were screened for possible eligibility. Reference lists of the selected articles, including published systematic reviews, were screened for possible additional papers.

The following outcome measures were analyzed when available: [1] prosthetic and/or implant failures leading to loss or removal of the prosthesis and/or implant [2], biological or mechanical complications [3], radiographic marginal bone loss (MBL) [4], peri-implant buccal recession (BR) [5], Papilla Index, pink aesthetic score (PES), and white aesthetic score (WES) [6], and patient satisfaction (patient questionnaire and VAS).

2.4. Assessment of Quality, Heterogeneity, and Risk of Bias of Individual Studies. The same reviewers assessed the quality of the included manuscripts, heterogeneity, and the risk of bias according to the guidelines provided by the CONSORT statement for the evaluation of randomized controlled trials (<http://www.consort-statement.org>) [15] and the STROBE statement for observational studies (<http://www.strobe-statement.org>), as well as the modified items from the Cochrane Collaboration's tool for assessing risk of bias [16]. The overall risk of bias was expressed as the percentage of negatively graded items [16]. Quality assessment was performed on the published full-text articles, independently by both reviewers. Disagreements between them were resolved upon discussion. An estimation of plausible risk of bias (low, moderate, or high) was completed for each selected study according to the Cochrane Handbook for Systematic Reviews of Interventions (version 5.1.0. <http://www.cochrane.org/resources/handbook>).

3. Results

3.1. Study Selection. A total of 945 potentially relevant titles and abstracts were found after the initial electronic and

manual search. At this stage, 810 articles were excluded (% of agreement: 89.2%; Cohen's k : 0.35). Complete full-text manuscripts of the remaining 135 articles were evaluated, and 119 articles were excluded since they did not fulfill the inclusion criteria (% of agreement: 97.0; Cohen's k : 0.85), scoring an almost perfect agreement. Finally, a total of 16 articles that fulfilled the inclusion criteria of this systematic review were included in the qualitative analysis. Overall, data from 221 one-piece implants placed in 107 patients, 139 scalloped implants placed in 96 patients, and 366 flat implants (same level on 360°) placed in 207 patients were evaluated. No comparative studies reporting data on sloped implants that fulfilled the inclusion criteria were founded. Of the 16 selected studies, 7 were randomized controlled trials [9, 17–22], 4 were observational comparative studies (2 retrospective and 2 prospective) [23–26], and 5 were systematic reviews [27–31]. A diagram of the search strategy is shown in Figure 1.

Three pairs of manuscripts reported data from the same cohort of patients. Sanz Martin et al. [17] and Thoma et al. [18] published two manuscripts based on the same cohort of 60 patients, reporting volumetric soft tissue change and demographic and radiographic results, respectively. Van Nimwegen et al. [19] published a 5-year follow-up report on the 1-year report of Tymstra et al. [22]. Finally, den Hartog et al. published two manuscripts reporting data from single implants in the aesthetic zone with different neck designs. The first manuscript was published in 2011 and was aimed at reporting radiological and clinical outcome measures [20], while the second manuscript, published 2 years later, focused on the aesthetic outcomes from both professional's and patient's perception [21].

3.2. Risk of Bias. The 16 selected studies were published between 1993 and September 2016. None of the publications were associated with a low risk of bias, while five with a high risk of bias and six with a moderate risk of bias (Table 1). The included articles received minimum grading when written in agreement with the CONSORT/STROBE statement guidelines (0/11), evaluating submission to ethical committees (5/11), none or unclear randomization procedures (7/11), none or unclear allocation concealment (9/11), and blinding of participants/outcome assessors (0/11) (Table 1).

3.3. Prosthetic and/or Implant Failures and Biological or Mechanical Complications. Nine of the eleven clinical studies reported data on implant failure/success. Two studies regarding one-piece implants compared with two-piece implants scored a cumulative survival rate of 100% in both test and control groups [23, 26]. Thoma et al. [18] reported one implant failure in the one-piece group and none in the two-piece group. Duda et al. [24] reported 9 implant failures in the one-piece group (7 immediately loaded and 2 delayed loaded), while no implant failure was reported in the two-piece group. Most of these failures were experienced due to biological complications (peri-implantitis and lack of osseointegration). Conversely, Heijdenrijk et al. [9] reported 2 implant failures in the

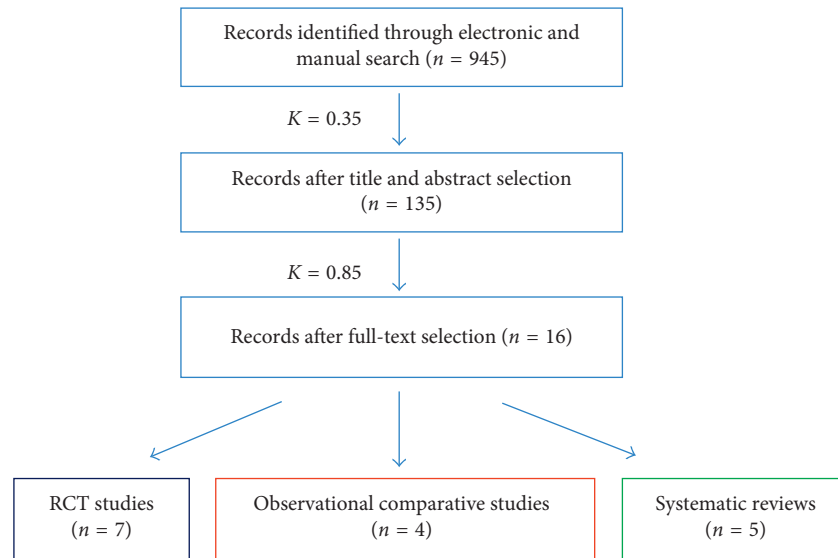


FIGURE 1: Flow chart.

two-piece implants compared to no failure in the one-piece group. All the implant failures were reported within the first year after function.

Three studies reported data from scalloped implants. den Hartog et al. [20, 21] reported only 1 implant failure in the control group (same level on 360°) compared with scalloped implants. Tymstra et al. [22] reported a cumulative survival rate of 100% in both groups at 1 year of follow-up, while Van Nimwegen et al. [19], over the same cohort of patients, reported 2 implant failures in the scalloped group, 4 years after their placement, due to extensive peri-implant bone loss.

Only one study included clinical complications as an outcome measure [23]. In this study, Ormianer et al. reported 8 porcelain fractures in the two-piece group and 4 in the one-piece group. Nevertheless, no statistically significant difference was found. All data are reported in Table 2. Finally, two systematic reviews of Barrachina-Díez et al. [27, 28] reported a high long-term survival rate but also high frequency of technical and biological complications in one-piece implants, both in one-part and two-part designs.

3.4. One-Piece versus Two-Piece Implants (MBL and BR).

Sanz Martin et al. [17] and Thoma et al. [18] published two randomized controlled clinical trials on the same cohort of 60 patients (151 implants), aimed at assess the volumetric changes of the buccal soft tissues between baseline and 1 year after loading follow-up, [17] and to compare the clinical and radiographic outcomes using one-piece ($n = 65$; Straumann) and two-piece ($n = 86$; Nobel Biocare External Hex) dental implant systems [18]. These researches failed to find significant differences between the one- and two-piece implant types with regard to tissue thickness, crown height (CHC), and facial tissue volume (VC). Conversely, the two-piece group exhibited slightly less bone loss during the evaluated period. Differences between the two groups reached a statistical significance with less bone loss for the two-piece group.

Ormianer et al. [23] analyzed retrospectively one-piece ($n = 34$; Zimmer One-Piece, Zimmer Biomet) and two-piece ($n = 38$; Tapered Screw-Vent, Zimmer Biomet) implants placed in the mandible of the same patients ($n = 24$) according to a split-mouth design. After 5 years of function, marginal bone loss did not significantly differ between one- and two-piece dental implant systems (the mean MBL is not reported).

Duda et al. [24] in a retrospective comparative study evaluated clinical outcomes of immediate insertion and loading of one-piece implants (49 implants in 13 patients; Q-Implant; Triron Titanium GmbH, Karlsruhe, Germany), compared to delayed loading of immediately placed one-piece implants (24 implants in 11 patients; Q-Implant; Triron Titanium GmbH), and delayed placed two-piece nonsubmerged implants (39 implants in 10 patients; Q-Implant; Triron Titanium GmbH). Mean MBL was 1.45 mm and 1.71 mm at the 5-year follow-up for one-piece implants with immediate loading and delayed loading, respectively. In case of two-piece implants, the mean MBL was 0.9 mm at the 3-year follow-up. The authors concluded that two-piece implants showed less MBL compared with one-piece implants in both the maxilla and mandible [24]. On the other hand, there was no statistical difference in MBL between immediate and delayed loaded one-piece implants, but immediate loaded implants showed more MBL in the maxilla [24].

Finally, Heijdenrijk et al. [9] in a randomized controlled trial with 5-year follow-up reported that the microgap at the implant-abutment interface in two-piece implants does not appear to have an adverse effect on the amount of peri-implant bone loss compared with one-piece implants [9]. All of the data are reported in Table 2.

3.5. Scalloped Implants (MBL and BR).

Van Nimwegen et al. [19] randomly compared 20 patients with two adjacent implant-supported restorations delivered on scalloped implants ($n = 20$; NobelPerfect Groovy, Nobel Biocare) and implants with a flat

TABLE 1: Reporting quality of all selected full-text articles.

Author and year	Implant shoulder design	Study characteristics			Selection bias			Performance bias	Detection bias	Attrition bias	Reporting bias		Overall risk of bias
		Study design	Follow-up	CONSORT/STROBE	Ethical board approval	Random sequence generation	Allocation concealment				Blinding of participants and personnel	Blinding of outcome assessors	
Heijdenrijk et al. 2006 [9]	Scalloped	RCT	5 years	No	No	Unclear	Unclear	No	No	Medium risk	Low risk	Low risk	Medium risk
Sanz Martin et al. 2015 [17]*	One piece	RCT	1 year	No	Yes	Computer-generated list	No	No	Unclear	Low risk	Low risk	Low risk	Medium risk
Thoma et al. 2014 [18]*	One piece	RCT	1 year	No	Yes	Computer-generated list	No	No	No	Low risk	Low risk	Low risk	Medium risk
Nimwegen et al. 2015 [19]*	Scalloped	RCT	5 years	Unclear	No	Unclear	No	No	No	Low risk	Low risk	Low risk	High risk
den Hartog et al. 2011 [20]*	Scalloped	RCT	1 year	No	Yes	Randomization by minimization	Yes	No	No	Low risk	Low risk	Low risk	Medium risk
den Hartog et al. 2013 [21]*	Scalloped	RCT	1 year	No	Yes	Randomization by minimization	Yes	No	No	Low risk	Low risk	Low risk	Medium risk
Tymstra et al. 2011 [22]*	Scalloped	RCT	1 year	Unclear	No	Unclear	No	No	No	Low risk	Low risk	Low risk	High risk
Ormianer et al. 2016 [23]	One piece	Retrospective	5 years	No	No	Arbitrary	No	No	No	Low risk	Medium risk	Medium risk	High risk
Duda et al. 2016 [24]	One piece	Retrospective	3 years	No	No	No	No	No	No	Low risk	Medium risk	Medium risk	High risk
Khraisat et al. 2013 [25]	Scalloped	Prospective	3 years	No	Yes	No	No	No	No	Low risk	Low risk	Low risk	Medium risk
McAllister 2007 [26]	Scalloped/one piece	Prospective	4 to 28 months	No	No	No	No	No	No	Medium risk	Medium risk	Medium risk	High risk

*Manuscripts that included the same cohort of patients.

TABLE 2: Results of the included studies.

Author and year	Patients/implants	Follow-up	Failed implants	Complications	MBL (mm)	BR	Papilla Index	PES/WES	Patient questionnaire/VAS
<i>One-piece (test, T) versus two-piece (control, C) implants</i>									
Heijdenrijk et al. 2006 [9]	T	20/40	5 years	0	NR	1.8	NR	NR	NR
	C	20/40	5 years	1	NR	1.6	NR	NR	NR
	C	20/40	5 years	1	NR	1.4	NR	NR	NR
Sanz Martin et al. 2015 [17]*	T	30/65	1 year	NR	NR	NR	CHC: -0.17; VC: -0.03	NR	NR
	C	30/86	1 year	NR	NR	NR	CHC: 0.02; VC: -0.12	NR	NR
Thoma et al. 2014 [18]*	T	30/65	1 year	1	NR	0.27	NR	NR	NR
	C	30/86	1 year	0	NR	0.05	NR	NR	NR
Ormianer et al. 2016 [23]	T	24/34	5 years	0	4 ^c	NR	NR	NR	NR
	C	24/38	5 years	0	8 ^c	NR	NR	NR	NR
Duda et al. 2016 [24]	T	13/49 [§]	5 years	7	NR	1.45	NR	NR	NR
	T	11/24 [°]	5 years	2	NR	1.71	NR	NR	NR
	C	10/39	3 years	0	NR	0.9	NR	NR	NR
<i>One-piece (test, T) versus two-piece (control, C) scalloped implants</i>									
McAllister 2007 [26]	T	9/9	18 months	0	NR	NR	NR	16:3; 2:2	NR
	T	13/16	28 months	0	NR	NR	NR	25:3; 7:2	NR
	C	NR/12	12 months	0	NR	NR	NR	NR	NR
<i>Scalloped (test, T) versus flat (control, C) implants</i>									
Van Nimwegen et al. 2015 [19]*	T	20/40	5 years	2	2	3.4/2.4	NR	16, 32	NR
	C	20/40	5 years	0	0	1.5/1.3	NR	19, 38	NR
den Hartog et al. 2011 [20]*	T	31/31	18 months	0	NR	2.01	0.25	36:3; 41:2; 23:1	NR
	C	31/31	18 months	1	NR	1.19	0.18	31:3; 53:2; 16:1	NR
	C	31/31	18 months	0	NR	0.9	0.28	34:3; 45:2; 19:1	NR
den Hartog et al. 2013 [21]*	T	31/31	18 months	0	NR	2.01	NR	NR	6.6/7.2
	C	31/31	18 months	1	NR	1.19	NR	NR	6.0/7.2
	C	31/31	18 months	0	NR	0.9	NR	NR	6.3/7.4
Tymstra et al. 2011 [22]*	T	20/40	1 year	0	NR	2.7/2.6	0.3	19, 38	NR
	C	20/40	1 year	0	NR	0.9	0.1	19, 38	NR
Khraisat et al. 2013 [25]	T	12/12	3 years	NR	NR	3.48/3.52	NR	NR	NR
	C	12/12	3 years	NR	NR	1.35/1.27	NR	NR	NR

* Manuscripts that included the same cohort of patients; ^c porcelain fractures; [§] immediately loaded one-piece; [°] delayed loaded one-piece; NR: not reported; CHC: crown height changes in mm; VC: volume changes in mm.

platform ($n = 20$; NobelPerfect Groovy). This study is a 5-year follow-up on the 1-year preliminary report of Tymstra et al. [22]. More bone loss and more BoP with compromised interimplant papilla regeneration were found around scalloped implants. Nevertheless, the implant crown aesthetic index, as well as patient satisfaction, was not significantly different between the groups [19, 22].

den Hartog et al., in two similar randomized controlled trials with 18 months of follow-up [20, 21], evaluated the aesthetic outcome and the marginal bone level changes of anterior single-tooth implants with three different implant shoulder (neck) designs: a 1.5 mm machined implant neck (Replace Select Tapered, Nobel Biocare AB, Göteborg, Sweden), a rough implant neck with grooves (NobelReplace

Tapered Groovy, Nobel Biocare AB), and a scalloped rough implant neck with grooves (NobelPerfect Groovy, Nobel Biocare AB). Although there was a statistically significant difference in MBL between different implant shoulder designs (smooth neck 1.19 ± 0.82 mm, rough neck 0.90 ± 0.57 mm, and scalloped neck 2.01 ± 0.77 mm), there were no differences between groups regarding the PES/WES outcomes, as well as patient satisfaction. In a prospective comparative study, Khraisat et al. [25] evaluated MBL and soft tissues around single implants with the scalloped shoulder design (Nobel Perfect, Nobel Biocare) and a smooth collar of 1.5 mm, within 3 years of function. The mean MBLs around scalloped implants were compared to MBLs around conventional flat platform 3.75 mm diameter TiUnite surface implants with external hex (MK III RP, Nobel Biocare), after both 1 and 3 years of function. The results of the present prospective study demonstrated that scalloped implants did not maintain marginal bone levels. All of the data are reported in Table 2.

Data from other reviews provide insufficient evidence about the efficacy of scalloped implant designs in the stability of peri-implant tissues [30, 31]. On the other hand, favorable results regarding scalloped implants were reported by Prasad et al. [29].

3.6. One-Piece versus Two-Piece Scalloped Implants. Consecutively, restored one-piece (NobelPerfect One-Piece) and two-piece (NobelPerfect, Nobel Biocare) scalloped dental implants were radiographically and clinically compared in a study of McAllister [26]. Radiographic evaluation of 16 two-piece scalloped implants and 9 one-piece scalloped implants revealed enhanced interproximal bone levels compared to a nonscalloped conventional flat-top implant design. Based on the Jemt system for interproximal soft tissue level evaluation, 78% of the two-piece implants scored 3 and 22% scored 2 and 89% of the one-piece implants scored 3 and 11% scored 2. The authors concluded that enhanced interproximal tissue preservation from scalloped implant designs may lead to more predictable aesthetic dental implant restorations in the anterior maxilla. All of the data are reported in Table 2.

3.7. Sloped Implants (MBL and BR). No comparative studies reporting data on sloped implants were found that fulfilled the inclusion and exclusion criteria of this systematic review.

3.8. Aesthetic Outcomes (Papilla Index, PES, and WES) and Patient Satisfaction. Four studies reported no differences in aesthetic outcomes between scalloped and flat implants [19–22]. Tymstra et al. [22] and Van Nimwegen et al. [19] evaluated the soft tissues around the adjacent implants and the neighbouring teeth using the Papilla Index according to Jemt [32]. den Hartog et al. [20, 21] analyzed the volume of the interproximal papilla using the Papilla Index in the first study [20] and two objective aesthetic indexes, pink aesthetic score/white aesthetic score (PES/WES) and implant crown aesthetic index (ICAI), in the second study [21]. Three of them reported outcomes on patient satisfaction, using the

patient questionnaire or VAS, scoring no differences between groups [19, 21, 22]. All the data are reported in Table 2.

4. Discussion

The aim of this systematic review was to identify whether there is a relationship between different implant shoulder positions/orientations/designs in the anterior dentition and prosthetic and/or implant failures, biological or mechanical complications, radiographic marginal bone loss, peri-implant buccal recession, aesthetic scores, and patient satisfaction after a minimum of 1-year function. The types of the implant analyzed were one-piece implants, compared with two-piece implants, and scalloped and sloped implants, compared with the conventional implant neck architecture (flat implants with the same level on 360°).

The results of the present systematic review indicate that different implant shoulder positions (scalloped, sloped, and one piece) seem to offer no benefit when compared to conventional, two-piece, flat implants.

A trend of higher implant failure and prosthetic complications were experienced in the one-piece group compared to the two-piece group, even if no statistically significant differences were found. This is in agreement with two systematic reviews by the same author [27, 28] which concluded that, despite high long-term prosthetic survival rates, technical and biological complications are frequent in one-piece implants independently by the loading protocols, implant surfaces, or type of edentulism.

One-piece implants are generally placed in a non-submerged approach. This means that implant placement is performed in a single surgical procedure, with no need for surgical reopening. Compared to a two-stage procedure, this approach is more comfortable for the patient, due to the fewer number of surgeries, and reduces the healing period. Implant shoulder placed at the level of the soft tissue offers many advantages since it is easily accessible for procedures such as impression taking and represents an excellent basis for cemented implant restorations [17, 18]. Moreover, due to its design, one-piece implants have their transmucosal surface unaltered during all of the prosthetic procedures since abutment reconnection is avoided (one-piece, one-part implants) or it is performed at the supramucosa or marginal mucosa level (one-piece, two-part implants). This avoids trauma to the soft tissue, which could result in a more apical position of the connective tissue and be responsible for additional marginal bone resorption.

A clinical study by Heijdenrijk et al. [9] evaluated the feasibility of using a two-piece implant system in a nonsubmerged procedure compared to the two-piece implant system placed in the traditional submerged procedure and one-piece implants placed in a nonsubmerged procedure. After 5 years of functioning, no association was found between the level of the microgap and the amount of bone loss, suggesting that two-piece implants used in a nonsubmerged procedure may be as predictable as when used in a submerged procedure or as one-piece implants [9].

Three studies included in this review reported differences in MBL between one- and two-piece implants. Thoma et al.

[18] and Duda et al. [24] reported higher MBL in the one-piece implants, whilst Ormianer et al. [23] reported no differences between groups. Sanz Martin et al. [17] assessed the volumetric changes of the buccal soft tissue between baseline and 1 year of loading between one- and two-piece dental implants. This research failed to find significant differences between the one- and two-piece implant types with regard to tissue thickness, crown height, and facial tissue volume.

The concept of scalloped implants was introduced to maintain the alveolar ridge and the peri-implant soft tissue contour by mimicking the scalloped shape of natural topography of the healthy marginal bone contour [12]. The long-term results showed stable soft tissues around the scalloped implants in spite of some loss of marginal bone support in relation to the originally intended marginal bone level [33].

The primary aesthetic goal of the scalloped implant design is to avoid the dark, triangular space known as the “black triangle.” This space appears when bone remodeling results in loss of osseous support for the papillae [34]. The aesthetic concern is increased when a patient presents an alveolar morphotype, with a pronounced scalloped profile of the hard and soft tissues. This can be further complicated by the gingival display of a high smile line [34]. A five-year randomized controlled trial [19] was realized as follow-up of a 1-year report [22] to evaluate peri-implant soft and hard tissue of two adjacent implant-support restorations in the aesthetic region using a scalloped or flat platform. More bone loss and compromised interimplant papilla regeneration were obtained around scalloped implants, indicating that scalloped implants do not offer benefits in the aesthetic region [19, 22]. The other articles included in this review [20, 21, 25] comparing scalloped implants with the conventional implant neck architecture reported higher marginal bone loss in the test group (scalloped implants) compared to implants with the same level on 360°. Other than MBL, Khraisat [25] also analyzed the soft tissue level around scalloped single implants compared to conventional rough surface implants with external hex in the aesthetic zone over a 3-year period. The Jemt system was used to clinically assess sizes of the mesial and distal interproximal papillae, showing that soft tissue height was not consistently maintained around the scalloped area of the implants. Different results were obtained in a study of McAllister [26] where consecutively restored one- and two-piece scalloped implants were radiographically and clinically compared to a flat-top implant with similar implant geometry regarding taper and thread design. Enhanced interproximal hard and soft tissue preservation was obtained for scalloped implants leading to predictable aesthetic restorations in the anterior maxilla. The authors concluded that interproximal soft tissue levels may be enhanced by maintaining the crestal bone level and avoiding interproximal soft tissue attachment manipulation during abutment connection.

No comparative studies were found that fulfilled the inclusion and exclusion criteria of the sloped implants’ systematic review. Nevertheless, the available data provide encouraging results for sloped implants in preserving the bone crest and the interplant papilla [13]. Placing an implant

in a healed alveolar ridge with differences in height between the buccal and lingual bone crest will not allow the buccal part of the marginal portion of the implant to be completely invested in the bone, resulting in a risk of aesthetic complications [13]. In a prospective multicenter study, non-submerged implants (OsseoSpeed Profile implants; Astra Tech AB, Molndal, Sweden) were placed in a recipient site with a buccal-lingual bone height discrepancy of 2.0–5.0 mm, and the sloped part of the device was located at the buccal and most apical position of the preparation. Sixteen weeks later, bone level alterations were 0.02 mm lingually and 0.30 mm buccally, and at the 1-year reexamination, the average change in interproximal bone levels was 0.54 mm. The authors concluded that sloped implant placement in an alveolar ridge with a sloped marginal configuration resulted in minor remodeling, preserving discrepancies between buccal and lingual bone levels [13].

5. Conclusions

- (i) Although no statistically significant differences were found, a trend of higher implant failure and prosthetic complications were experienced in the one-piece group compared to the two-piece group.
- (ii) A trend of higher marginal bone loss was found in the test group compared to the control group. This trend is moderate when comparing one-piece versus two-piece implants and high when comparing scalloped versus flat implants.
- (iii) Although no studies were found comparing sloped versus flat implants, preliminary results may encourage future studies.
- (iv) No differences were experienced between groups regarding aesthetic outcomes and patient satisfaction.

There was sufficient evidence that different implant shoulder positions/orientations/designs (scalloped, sloped, and one piece) offer no benefit when compared to two-piece, conventional flat implants. Current evidence is limited due to the quality of available studies. Marginal bone loss seems to be affected by the implant neck design, while aesthetics and patient satisfaction appear to be independent. Further studies, designed as randomized controlled clinical trials reported according to the CONSORT statement, are needed.

Conflicts of Interest

The authors declare that they have no conflicts of interest.

References

- [1] T. Albrektsson, G. Zarb, P. Worthington, and A. R. Eriksson, “The long-term efficacy of currently used dental implants: a review and proposed criteria of success,” *International Journal of Oral and Maxillofacial Implants*, vol. 1, no. 1, pp. 11–25, 1986.
- [2] T. J. Oh, J. Yoon, C. E. Misch, and H. L. Wang, “The causes of early implant bone loss: myth or science?,” *Journal of Periodontology*, vol. 73, no. 3, pp. 322–333, 2002.

- [3] D. L. Cochran, J. S. Hermann, R. K. Schenk, F. L. Higginbottom, and D. Buser, "Biologic width around titanium implants: a histometric analysis of the implant-gingival junction around unloaded and loaded nonsubmerged implants in the canine mandible," *Journal of Periodontology*, vol. 68, no. 2, pp. 186–198, 1997.
- [4] N. Elian, M. Bloom, M. Dard, S. C. Cho, R. D. Trushkowsky, and D. Tarnow, "Effect of interimplant distance (2 and 3 mm) on the height of interimplant bone crest: a histomorphometric evaluation," *Journal of Periodontology*, vol. 82, no. 12, pp. 1749–1756, 2011.
- [5] D. P. Tarnow, S. C. Cho, and S. S. Wallace, "The effect of inter-implant distance on the height of inter-implant bone crest," *Journal of Periodontology*, vol. 71, no. 4, pp. 546–549, 2000.
- [6] A. Pozzi, E. L. Agliardi, M. Tallarico, and A. Barlattani, "Clinical and radiological outcomes of two implants with different prosthetic interfaces and neck configurations: randomized, controlled, split-mouth clinical trial," *Clinical Implant Dentistry and Related Research*, vol. 16, no. 1, pp. 96–106, 2014.
- [7] M. Tallarico, A. Vaccarella, and G. C. Marzi, "Clinical and radiological outcomes of 1- versus 2-stage implant placement: 1-year results of a randomised clinical trial," *European Journal of Oral Implantology*, vol. 4, no. 1, pp. 13–20, 2011.
- [8] A. Schroeder, B. Maeglin, and F. Sutter, "ITI (Internationales Team für orale Implantologie) type-F hollow cylinder implant for denture retention in the edentulous jaw," *Schweizerische Monatsschrift für Zahnheilkunde*, vol. 93, no. 9, pp. 720–733, 1983.
- [9] K. Heijdenrijk, G. M. Raghoobar, H. J. Meijer, B. Stegenga, and W. A. van der Reijden, "Feasibility and influence of the microgap of two implants placed in a non-submerged procedure: a five-year follow-up clinical trial," *Journal of Periodontology*, vol. 77, no. 6, pp. 1051–1060, 2006.
- [10] L. Canullo, M. Caneva, and M. Tallarico, "Ten-year hard and soft tissue results of a pilot double-blinded randomized controlled trial on immediately loaded post-extractive implants using platform-switching concept," *Clinical Oral Implants Research*, vol. 28, no. 10, pp. 1195–1203, 2016.
- [11] J. Y. Kan, K. Rungcharassaeng, G. Liddelov, P. Henry, and C. J. Goodacre, "Periimplant tissue response following immediate provisional restoration of scalloped implants in the esthetic zone: a one-year pilot prospective multicenter study," *Journal of Prosthetic Dentistry*, vol. 97, no. 6, pp. S109–S118, 2007.
- [12] P. S. Wohrle, "Nobel perfect esthetic scalloped implant: rationale for a new design," *Clinical Implant Dentistry and Related Research*, vol. 5, no. 1, pp. 64–73, 2003.
- [13] R. Noelken, M. Donati, J. Fiorellini et al., "Soft and hard tissue alterations around implants placed in an alveolar ridge with a sloped configuration," *Clinical Oral Implants Research*, vol. 25, no. 1, pp. 3–9, 2014.
- [14] D. Moher, A. Liberati, J. Tetzlaff, D. G. Altman, and The PRISMA Group, "Preferred reporting items for systematic reviews and meta-analyses: the PRISMA statement," *PLoS Medicine*, vol. 6, no. 7, p. e1000097, 2009.
- [15] K. F. Schulz, D. G. Altman, D. Moher, and CONSORT Group, "CONSORT 2010 statement: updated guidelines for reporting parallel group randomised trials," *European Journal of Oral Implantology*, vol. 8, pp. 129–140, 2015.
- [16] J. P. T. Higgins, D. G. Altman, P. C. Gotzsche et al., "The Cochrane Collaboration's tool for assessing risk of bias in randomised trials," *BMJ*, vol. 343, no. 2, p. d5928, 2011.
- [17] I. Sanz Martin, G. I. Benic, C. H. Hämmerle, and D. S. Thoma, "Prospective randomized controlled clinical study comparing two dental implant types: volumetric soft tissue changes at 1 year of loading," *Clinical Oral Implants Research*, vol. 27, no. 4, pp. 406–411, 2015.
- [18] D. S. Thoma, I. Sanz Martin, G. I. Benic, M. Roos, and C. H. Hämmerle, "Prospective randomized controlled clinical study comparing two dental implant systems: demographic and radiographic results at one year of loading," *Clinical Oral Implants Research*, vol. 25, no. 2, pp. 142–149, 2014.
- [19] W. G. Van Nimwegen, G. M. Raghoobar, K. Stellingsma, N. Tymstra, A. Vissink, and H. J. Meijer, "Treatment outcome of two adjacent implant-supported restorations with different implant platform designs in the esthetic region: a five-year randomized clinical trial," *International Journal of Prosthodontics*, vol. 28, no. 5, pp. 490–498, 2015.
- [20] L. den Hartog, H. J. Meijer, B. Stegenga, N. Tymstra, A. Vissink, and G. M. Raghoobar, "Single implants with different neck designs in the aesthetic zone: a randomized clinical trial," *Clinical Oral Implants Research*, vol. 22, no. 11, pp. 1289–1297, 2011.
- [21] L. den Hartog, G. M. Raghoobar, J. J. Slater, K. Stellingsma, A. Vissink, and H. J. Meijer, "Single-tooth implants with different neck designs: a randomized clinical trial evaluating the aesthetic outcome," *Clinical Implant Dentistry and Related Research*, vol. 15, no. 3, pp. 311–321, 2013.
- [22] N. Tymstra, G. M. Raghoobar, A. Vissink, L. den Hartog, K. Stellingsma, and H. J. Meijer, "Treatment outcome of two adjacent implant crowns with different implant platform designs in the aesthetic zone: a 1-year randomized clinical trial," *Journal of Clinical Periodontology*, vol. 38, no. 1, pp. 74–85, 2011.
- [23] Z. Ormianer, M. Duda, J. Block, and S. Matalon, "One- and two-piece implants placed in the same patients: clinical outcomes after 5 years of function," *International Journal of Prosthodontics*, vol. 29, no. 6, pp. 608–610, 2016.
- [24] M. Duda, S. Matalon, I. Lewinstein, N. Harel, J. Block, and Z. Ormianer, "One piece immediately loaded implants versus 1 piece or 2 pieces delayed: 3 years outcome," *Implant Dentistry*, vol. 25, no. 1, pp. 109–113, 2016.
- [25] A. Khraisat, A. Zembic, R. E. Jung, and C. H. Hammerle, "Marginal bone levels and soft tissue conditions around single-tooth implants with a scalloped neck design: results of a prospective 3-year study," *International Journal of Oral & Maxillofacial Implants*, vol. 28, no. 2, pp. 550–555, 2013.
- [26] B. S. McAllister, "Scalloped implant designs enhance interproximal bone levels," *International Journal of Periodontics & Restorative Dentistry*, vol. 27, no. 1, pp. 9–15, 2007.
- [27] J. M. Barrachina-Díez, E. Tashkandi, S. Stampf, and W. Att, "Long-term outcome of one-piece implants. Part I: implant characteristics and loading protocols. A systematic literature review with meta analysis," *International Journal of Oral & Maxillofacial Implants*, vol. 28, no. 2, pp. 503–518, 2013.
- [28] J. M. Barrachina-Díez, E. Tashkandi, S. Stampf, and W. Att, "Long-term outcome of one-piece implants. Part II: prosthetic outcomes. A systematic literature review with meta-analysis," *International Journal of Oral & Maxillofacial Implants*, vol. 28, no. 6, pp. 1470–1482, 2013.
- [29] D. K. Prasad, M. Shetty, N. Bansal, and C. Hegde, "Crestal bone preservation: a review of different approaches for successful implant therapy," *Indian Journal of Dental Research*, vol. 22, pp. 317–323, 2011.
- [30] M. Bateli, W. Att, and J. R. Strub, "Implant neck configurations for preservation of marginal bone level: a systematic review," *International Journal of Oral and Maxillofacial Implants*, vol. 26, no. 2, pp. 290–303, 2011.

- [31] S. Bishti, J. R. Strub, and W. Att, "Effect of the implant-abutment interface on peri-implant tissues: a systematic review," *Acta Odontologica Scandinavica*, vol. 72, no. 1, pp. 13–25, 2014.
- [32] T. Jemt, "Regeneration of gingival papillae after single-implant treatment," *International Journal of Periodontics and Restorative Dentistry*, vol. 17, no. 4, pp. 326–333, 1997.
- [33] S. Paul and U. Held, "Immediate supracrestal implant placement with immediate temporization in the anterior dentition: a retrospective study of 31 implants in 26 patients with up to 5.5-years follow-up," *Clinical Oral Implants Research*, vol. 24, no. 6, pp. 710–717, 2013.
- [34] R. Noelken, F. Oberhansl, M. Kunkel, and W. Wagner, "Immediately provisionalized OsseoSpeed™ Profile implants inserted into extraction sockets: 3-year results," *Clinical Oral Implants Research*, vol. 27, no. 6, pp. 744–749, 2016.

Review Article

Self-Assembled Monolayers for Dental Implants

Sidónio C. Freitas ¹, Alejandra Correa-Uribe,² M. Cristina L. Martins ³ and Alejandro Pelaez-Vargas ¹

¹Faculty of Dentistry, Universidad Cooperativa de Colombia, Medellín, Colombia

²Private Practice in Periodontology, Medellín, Colombia

³Instituto de Investigação e Inovação em Saúde (I3S), Instituto de Engenharia Biomédica (INEB) and Instituto de Ciências Biomédicas Abel Salazar (ICBAS), Universidade do Porto, Porto, Portugal

Correspondence should be addressed to Sidónio C. Freitas; sidonio.freitas@campusucc.edu.co

Received 22 April 2017; Accepted 26 October 2017; Published 6 February 2018

Academic Editor: Silvio M. Meloni

Copyright © 2018 Sidónio C. Freitas et al. This is an open access article distributed under the Creative Commons Attribution License, which permits unrestricted use, distribution, and reproduction in any medium, provided the original work is properly cited.

Implant-based therapy is a mature approach to recover the health conditions of patients affected by edentulism. Thousands of dental implants are placed each year since their introduction in the 80s. However, implantology faces challenges that require more research strategies such as new support therapies for a world population with a continuous increase of life expectancy, to control periodontal status and new bioactive surfaces for implants. The present review is focused on self-assembled monolayers (SAMs) for dental implant materials as a nanoscale-processing approach to modify titanium surfaces. SAMs represent an easy, accurate, and precise approach to modify surface properties. These are stable, well-defined, and well-organized organic structures that allow to control the chemical properties of the interface at the molecular scale. The ability to control the composition and properties of SAMs precisely through synthesis (i.e., the synthetic chemistry of organic compounds with a wide range of functional groups is well established and in general very simple, being commercially available), combined with the simple methods to pattern their functional groups on complex geometry appliances, makes them a good system for fundamental studies regarding the interaction between surfaces, proteins, and cells, as well as to engineering surfaces in order to develop new biomaterials.

1. Introduction

The World Health Organization points out two entities of bacterial origin, caries and periodontitis, which are the most disseminated diseases in human, and both are associated with frequent surgical procedures [1]. These infectious diseases and other noninfectious diseases such as dentoalveolar trauma and congenital absences are the main causes of edentulism. Several preventives and educational programs are used to avoid or reduce the role of these infectious diseases in the early loss of teeth. However, dentoalveolar trauma has been increased due to human activities such as extreme and contact sports [2–4].

Partial edentulism produces deleterious effects on the balance of the cranio-cervico-facial system because it may affect soft and hard tissues. Intra-arch changes include missing of interproximal contacts, misalignment, diastema, rotation, inclination, periodontal defects, impaction, and

mesial drift displacement. Inter-arch changes have been described as occlusal collapse, premature occlusal contact, infraocclusion, and altered vertical dimension. These changes are synergic, increasing the bruxism, muscle parafunction, teeth wear, ATM symptom, otologic pain, and craniocervical position [5].

Recovering aesthetics and function is possible using orthodontics when space closing is an alternative feasible while in other cases are required surgical and oral rehabilitation procedures such as implant-supported or removable prostheses. Titanium implant-based therapy appears as the “gold standard,” with a record of ~95% survival rates reported after 5 years [6]. However, other concepts have been introduced such as “the success” (Figure 1), which is different from long-term survival because it is focused on integral evaluation in terms of aesthetic, function, and biological response, with less than 0.2 mm of apical migration [7].

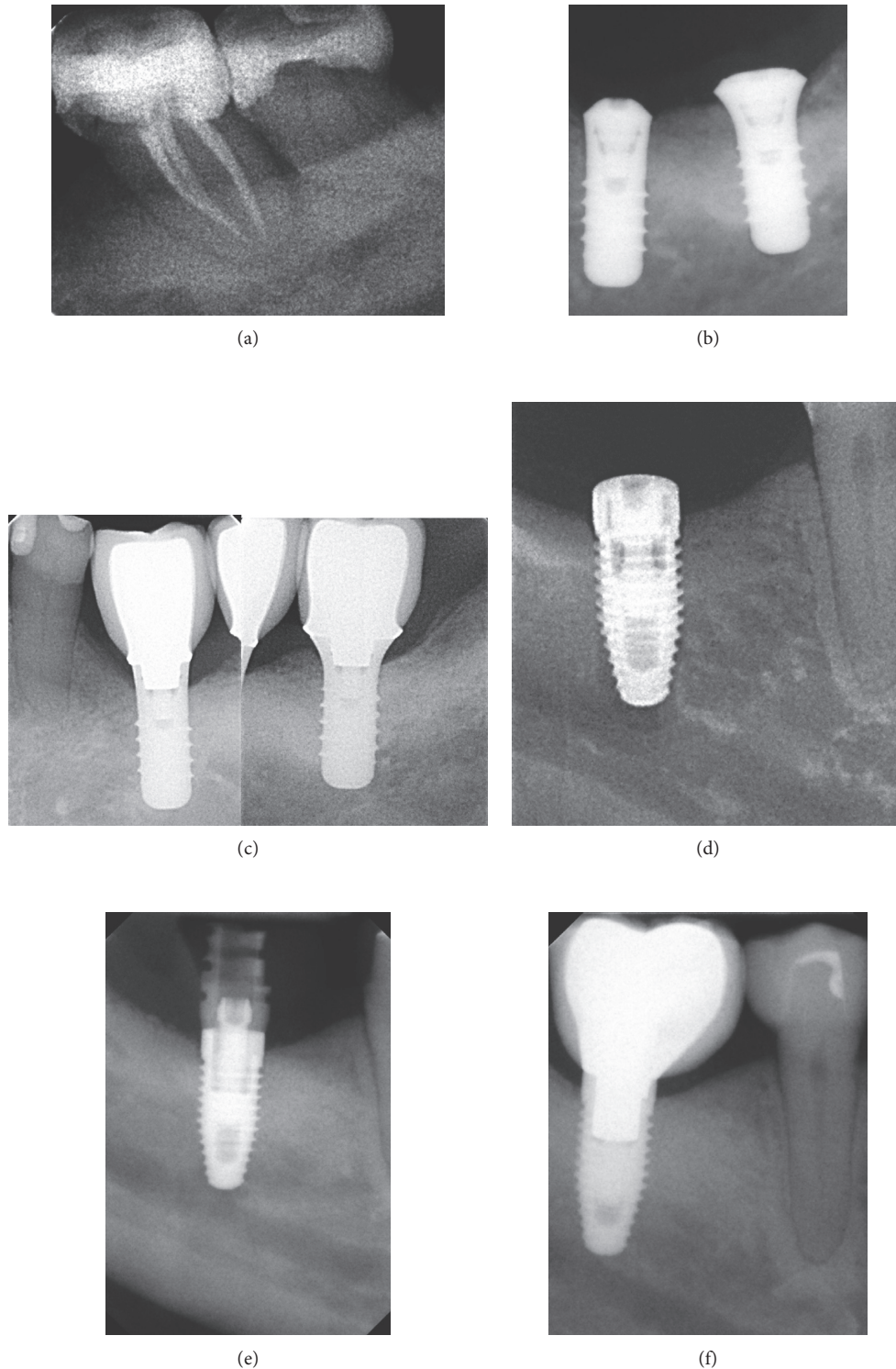


FIGURE 1: Successful cases. Patient 1: initially, an important reduction of support tissues was observed (a), and periapical X-ray obtained during the surgical procedure (b) and 5 years of follow-up (c). Patient 2: periapical X-ray obtained during implant surgery (d), restorative processing (e), and 5 years of follow-up (f).

The implantology history shows two different phases defined as pre-osseointegration and post-osseointegration eras. During the pre-osseointegration era, blade- and plate-form implants were developed using cobalt-chromium-molybdenum and different stainless steel types. However,

a limited long-term success was achieved. Post-osseointegration era started with Branemark's research a decade before that his research were presented to scientific community, followed by Albrektsson et al. studies to verify clinically the osseointegration of implants [8]. The osseointegration concept was

defined as a biological phenomenon involving direct contact between bone and Ti surfaces, opening a new paradigm of therapy. A wide revision about this topic is available [8, 9].

Implant therapy has high levels of predictability in a short term presenting few contraindications to restore partial and full edentulism. Many factors have been evaluated to predict the short-term effect including surgical stability, individual inflammatory response, periodontal covering, and blood clot formation. However, long-term predictability has been associated with several aspects such as implant-related designs, surgical procedures, anatomic and osseous conditions, systemic diseases, habits like bruxism, prosthetic design, susceptibility, periodontal status, oral microenvironment, native or augmented bone, two-stage or immediate loading, and adherence to support therapy. A poor prognosis is observed in patients with an insufficient quality and/or quantity of bone; patients exhibiting poor quality of bone (type IV) in the posterior area of the maxilla had a 35% implant failure while patients with types I, II, and III showed only 3% failure [10].

The long-term success of an implant (Figure 1) largely depends on the balance between occlusal equilibrium, osseointegration, and epithelial/connective tissue attachment. A complete sealing of the soft tissue protects the newly formed bone from bacterial metabolic products originated in the biofilm formed around implant [11].

Several animal and *in vitro* studies have shown similar epithelial and connective structures between the gingiva and the peri-implant mucosa. The outer surface of the peri-implant mucosa is aligned by a continuous stratified keratinized oral epithelium with a junctional epithelium attached to the Ti surface by a basal lamina and hemidesmosomes. The nonkeratinized junctional epithelium has only a few cell layers in the apical portion and is separated from the alveolar bone by a collagen-rich connective tissue. This 3–4 mm biological barrier, which is formed regardless of the original mucosal thickness, protects the osseointegration zone from factors released by the plaque and the oral cavity [12]. The main differences between the soft tissues around natural teeth and those around implants are the collagen fibre orientation, which run parallel from the implant surface to the crest bone, the low number of fibroblasts, the reduced vascularization revealed as scar tissue, and the loss of the irrigation system of the periodontal ligament [13].

An osseointegrated implant is not exempt from failure and complications. They are classified as biological, mechanical, material surface, iatrogenic, and patient-related failures. Mobility is a sign of implant failure and can be presented as rotational, lateral or horizontal, and axial or vertical [14]. There are different terms in the literature associated with biological implant failures like peri-implant diseases, mucositis, and peri-implantitis (Figure 2), where the first two are reversible inflammatory reactions around a functioning implant while peri-implantitis is a chronic inflammation with a loss of the supporting tissues around the implant induced by bacterial colonization and facilitated by the implant/abutment gap and by the chemistry and surface roughness of screw and restorative components [15].

Bacteria colonize and develop biofilms on the transmucosal abutment of osseointegrated dental implants. Like

the gingival crevice around the natural tooth, the peri-implant mucosa covering the alveolar bone is closely adapted to the implant. In partially edentulous subjects, the developing microbiota around implants closely resembles the microflora of the natural teeth [12]. In addition to the dark-pigmented, Gram-negative anaerobic rods, other bacteria are associated with peri-implant infections (*Tannerella forsythia*, *Fusobacterium nucleatum*, *Campylobacter rectus*, *Parvimonas micra*, and *Prevotella intermedia*) [16], and eventually with *Staphylococcus* spp. and *Candida* spp. [17].

The surface texture of dental implants affects the rate of osseointegration [18] and biomechanical fixation. Surface roughness may be classified as “macro,” “micro,” and “nano” sized topologies. The “macro” ranges from millimetres to 10 μm and is directly related to implant geometry with threaded screws and macroporous coatings helping the primary stability of the implants during the early phases of implantation. However, high surface roughness may increase peri-implantitis risk compared with moderate roughness (1–2 μm) within “micro” range (1–10 μm), maximizing bone/implant interlocking. Surface profiles in the “nano” range play an important role in protein adsorption and osteoblast adhesion and, thus, in osseointegration [19], but no reproducible surface roughness is currently clinically available.

This review firstly presents a brief overview of different coating strategies to increase the osseointegration of titanium and is followed by a detailed description of self-assembled monolayers as a nanoscale approach to modify dental implant surfaces.

2. Biofunctionalization Strategies Available for Dental Implants

All surface modification strategies described below aimed to improve the long-term clinical survival and success of those dental biomaterials without altering their bulk properties (e.g., mechanical and nontoxicity). These coating strategies are mainly focused to increase the osseointegration than to reduce the bacterial colonization.

Bioactive surfaces have been developed to improve the osseointegration of bone with dental materials like titanium through coating strategies with immobilized biomolecules such as cell adhesive peptides having the Arg-Gly-Asp (RGD) sequence or bone morphogenetic proteins (BMPs) that play important roles in bone formation *in vivo* [20], to promote the adhesion of bone cells (i.e., osteoblasts) and subsequent proliferation and mineralization activities [21, 22], to induce alkaline phosphatase activity in fibroblast [23] or the attachment of osteoblast [24].

Antiadhesive surfaces have been used to avoid/resist protein adsorption and microbial adhesion by immobilization or coating of synthetic polymers like poly(ethylene glycol) (PEG)/poly(ethylene oxide) (PEO) [25] and poly(methacrylic acid) [26] or natural polymers as chitosan [27].

Finally, antibacterial coatings have been applied using biocidal substances (e.g., antibiotics and antimicrobial peptides) through two systems: (a) a continuous release system, creating a local effect around the implant and (b)

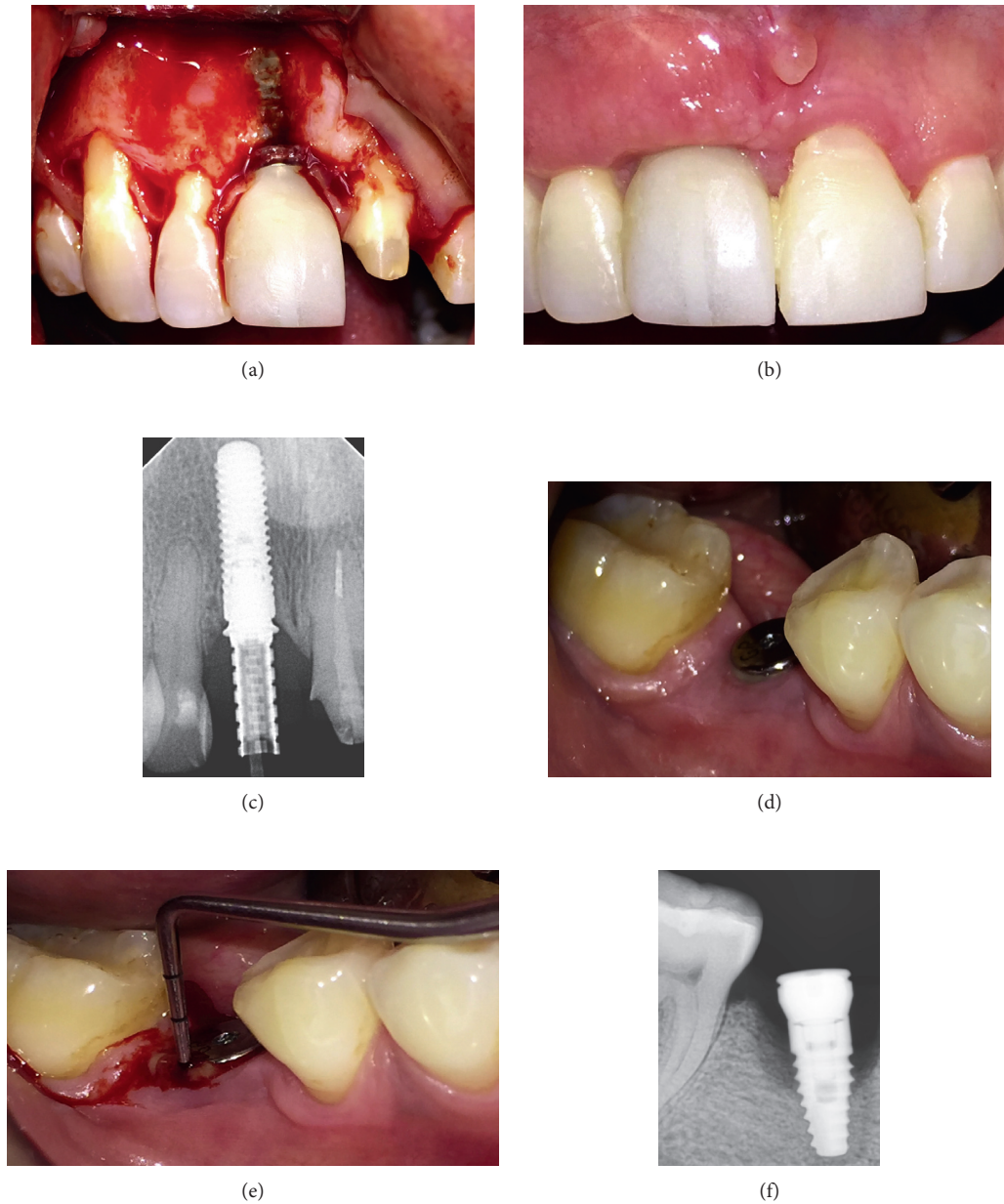


FIGURE 2: Failure cases. Patient 3: exploratory surgical procedure for peri-implantitis (a), soft tissues after a bone graft healing (b), and periapical X-ray after 4 months (c). Patient 4: intraoral photograph of implant (d), periodontal probing (e), and periapical X-ray showing vertical bone loss around implant (f).

a permanent immobilization scheme, acting on local microorganisms that contact the surface.

Furthermore, one promising strategy to enhance tissue integration is to develop a selective biointeractive surface that simultaneously enhances bone cell function while decreasing bacterial adhesion [20, 22, 28].

A resume of surface modification methods and effects is presented in Table 1.

3. Basic Aspects of Self-Assembled Monolayers (SAMs)

SAMs are spontaneously formed by solution deposition through the immersion of an appropriate substrate into

a solution of an active surfactant in an appropriate solvent (e.g., organic or aqueous) or by aerosol spraying or vapor deposition of the active organic compound onto the solid surface, being immersion the most popular and widely studied method for monolayer formation since it is the easiest and most inexpensive way to be applied to appliances with complex geometries [62–64]. In a typical procedure, freshly prepared or clean substrate is immersed in a dilute 1–10 mm solution of surfactant compound(s) in high purity solvent for 12–48 h at room temperature. After this period, the slides are withdrawn, rinsed with solvent, and dried under a stream of nitrogen [62].

The driving force for self-assembly is usually the specific interaction between the head group of the surfactant and

TABLE 1: Bioactive osseointegration, antiadhesive, and antibacterial coatings on titanium.

Surface	Coating type	Molecule	Study type	Effect	Ref.	
Bioactive osseointegration	Covalent immobilization of osseointegration molecules	RGD peptide	<i>In vitro</i>	Supports osteoblast attachment and spreading, and significant mineralization after 14 and 21 days	[21]	
			<i>In vitro</i>	Significantly improves the osteoblast adhesion, proliferation, and alkaline phosphatase (ALP) activity while retaining high antibacterial efficacy after aging for 21 days in PBS	[22]	
		BMP4	<i>In vivo</i>	Significant increase in bone formation after 4 weeks <i>in vivo</i> in rat femurs and in a rabbit model	[29, 30]	
			<i>In vitro</i>	Induces significant alkaline phosphatase activity in pluripotent C3H10T1/2 cells	[24]	
			<i>In vitro</i>	Only 8% of the immobilized BMP2 seems to be available for interaction with the cells and able to induce the signaling cascade with cytochrome compatible for C3H10T1/2 cells	[31]	
Antiadhesive	—	BMP2	<i>In vitro</i>	Reduces the bacterial adhesion (<i>S. aureus</i> and <i>S. epidermidis</i>) and significantly promotes attachment, alkaline phosphatase activity, and calcium mineral deposition of both osteoblast and human bone marrow-derived mesenchymal stem cells	[20]	
			<i>In vivo</i>	Titanium screw implants with nano-anchored oligonucleotides strands hybridized with conjugated rhBMP2 exhibited enhanced bone ingrowth into the perforations and increased bone implant contact after 1 and 4 weeks compared to controls. No difference was seen after 13 weeks. Bone density around the outer implant surface did not differ significantly at any of the intervals. Therefore, rhBMP2 immobilized on the surface of titanium implants through nanoanchored oligonucleotide strands can enhance bone implant contact	[32]	
			<i>In vitro</i>	Inhibits salivary protein adsorption and the attachment of <i>S. gordonii</i> and <i>S. mutans</i> biofilm was easier to be detached	[25]	
		Polymer coating	PLL-g-PEG	<i>In vitro</i>	Human serum adsorbed was below the detection limit of the optical sensor technique (OWLS) (<1-2 ng/cm ²). Reduces fibrinogen adsorption by 96%. Decreases <i>S. aureus</i> adhesion by 89-93%	[33, 34]
			PLL-g-PEG conjugated to catechols groups ¹	<i>In vitro</i>	Suppresses fibrinogen adsorption. Resists attachment of the cyanobacterium <i>Lyngbya</i> spp. for at least 100 days	[35]
Antibacterial	Metal ion incorporation	Multivalent PEGylated peptides	<i>In vitro</i>	Resistant to serum proteins (<1 ng/cm ² to detection limit of OWLS). Almost free of blood protein adsorption. No cytotoxicity against bone-marrow stem cells. Reduces 95% of serum protein adsorption	[36-38]	
			<i>In vitro</i>	90% PEGylated peptides remain in surface. 90% reduction in <i>S. aureus</i> biofilm	[39]	
		Silver	<i>In vitro</i>	Activity effects against periodontal and peri-implant pathogens, including <i>P. gingivalis</i> , <i>P. intermedia</i> , <i>A. actinomycetemcomitans</i> , <i>F. nucleatum</i> , <i>Tannerella forsythia</i> , and <i>S. aureus</i>	[40, 41]	
			<i>In vitro</i>	Limits antibacterial activity against <i>P. gingivalis</i> and <i>A. actinomycetemcomitans</i> , probably due to the formation of silver compounds such as AgCl, Ag ₂ O, and Ag ₂ S	[42, 43]	
			<i>In vitro</i>	Improves the antibacterial effect against <i>S. aureus</i> and preserves human gingival fibroblasts viability	[44]	
Zinc	<i>In vitro</i>	Very strong (greater than 4-log or 99.99% reduction) antibacterial effect against <i>P. aeruginosa</i> for 24 h. Osteoblast adhesion, spread, and proliferation higher than bare-Ti and so does not cause cytotoxicity	[45]			
	<i>In vitro</i>	No antibacterial activity against the periodontal bacteria <i>P. gingivalis</i> and <i>A. actinomycetemcomitans</i> , possibly due to the formation of zinc halogens, oxides, or sulphides	[43]			
	<i>In vitro</i>	Antimicrobial effect on <i>E. coli</i> and especially on <i>S. aureus</i> , with the lethal concentration for <i>S. aureus</i> of 5 µg/ml	[46]			
Copper	<i>In vitro</i>	Antibacterial activity (90%) against <i>S. aureus</i>	[47]			

TABLE 1: Continued.

Surface	Coating type	Molecule	Study type	Effect	Ref.
		Gentamicin into a degradable PDLLA	<i>In vivo</i>	Animals receiving systemic therapy alone had a recovery rate of about 15%, whereas animals receiving the gentamicin-coated implants had an 85% recovery rate. Human patient with infection-free after 1 year and no gentamycin levels in blood	[48]
		Mixtures of antibiotics or antiseptics into PLLA	<i>In vitro</i> and <i>in vivo</i>	Effective in eliminating <i>S. aureus</i> infection without cytotoxic effects	[49]
		Chlorhexidine into PLLA and politerefate	<i>In vitro</i>	Concentration of chlorhexidine remained at therapeutic levels for 200 h (8 days) before disappearing completely. Cytocompatible to hTERT fibroblast cells	[50]
	Biocidal release	Gendine (chlorhexidine + gentian violet)	<i>In vitro</i>	Active against methicillin-resistant <i>S. aureus</i> (MRSA), preventing the formation of biofilm (90% reduction)	[51]
		Vancomycin into silica sol-gel thin film	<i>In vitro</i>	Releases drug above the MIC and degrades after about 2 weeks <i>in vitro</i>	[52]
		Minocycline and rifampicin	<i>In vivo</i>	In a rabbit model that induced infection by inoculating <i>S. aureus</i> in the femoral medullary canal, the coated implants had an infection rate of 38% compared with 100% for the noncoated	[53]
		Vancomycin	<i>In vitro</i> and <i>in vivo</i>	Strong bactericidal activity against <i>S. epidermidis</i> and <i>S. aureus</i> over long periods of time (up to 6 weeks) <i>in vitro</i> . Stable bactericidal activity and reduced infection rates when implanted in an infected rat model	[54]
		Vancomycin conjugated to PEG-anachelin	<i>In vitro</i>	Only dead cells (<i>B. subtilis</i>) were detected on surface	[55]
		Gentamicin and penicillin	<i>In vitro</i>	The covalently immobilized antibiotics retain the antibacterial properties as indicated by a significant reduction in the viability of contacting <i>S. aureus</i>	[56]
	Covalent immobilization of biocidal	AMP Tet213	<i>In vitro</i>	Activity against both Gram-positive (<i>S. aureus</i>) and Gram-negative (<i>P. aeruginosa</i>) bacteria with 10 ⁶ -fold reductions of both bacterial strains within 30 min	[57]
		AMP GL13K	<i>In vitro</i>	Significantly fewer live cells of <i>P. gingivalis</i> than disks coated with a control peptide and uncoated Ti under static culture conditions. This GL13K coating showed to be cytocompatible by an adequate proliferation of osteoblasts and human gingival fibroblasts. Kills bacteria and prevents formation and growth of <i>S. gordonii</i> biofilms in a drip-flow bioreactor and under regular mild-agitation conditions, with rupture of the cell wall	[58, 59]
		Tet-20	<i>In vitro</i> and <i>in vivo</i>	Excellent activity against Gram-negative <i>P. aeruginosa</i> and Gram-positive <i>S. aureus</i> , as well as biofilm resistance <i>in vitro</i> . The coating had no toxicity to osteoblast-like cells and showed insignificant platelet activation and adhesion, and complement activation in human blood. Protects bacterial infection <i>in vivo</i> (rat model) against infected <i>S. aureus</i>	[60]
		hLf1-11	<i>In vitro</i>	Reduction in bacterial adhesion, early-stage biofilm formation, and growth of planktonic of <i>S. sanguinis</i> and <i>L. salivarius</i>	[61]

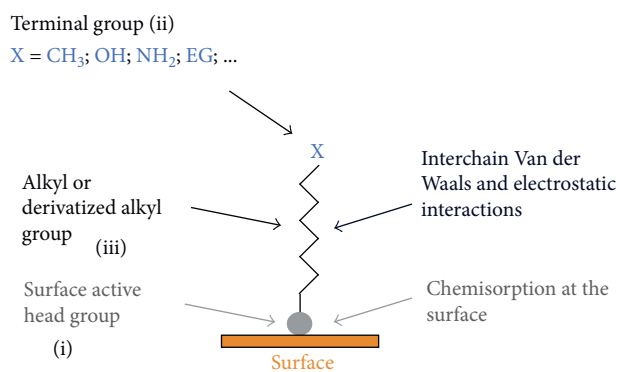


FIGURE 3: Schematic representation of a surfactant that can form a SAM.

the surface of the substrate. Most surfactants used for monolayer studies consist of three distinctive parts: (i) the surface active head group which binds strongly to the surface, (ii) the terminal group that is located at the monolayer surface and normally determines the interfacial properties of the assembly, and (iii) the alkane chain serves as a linker between the head and the terminal groups and facilitates the packing of the molecules in the monolayer with the Van der Waals interactions between adjacent methylene groups that orient and stabilize the monolayer (Figure 3) [62–66].

Considering that SAMs surface modifications are at nanoscale, physical and chemical characterizations appear as an important challenge to develop new market products based on this technology. Currently, several specialized surface analytical techniques are available to characterize SAMs for scientific approaches. The most commonly used techniques in routine SAMs characterization are as follows: ellipsometry, infrared reflection absorption spectroscopy (IRRAS), X-ray photoelectron spectroscopy (XPS), contact angle measurements, near edge X-ray absorption fine structure (NEXAFS), static time-of-flight secondary ion mass spectrometry (ToF-SIMS), surface imaging techniques such as scanning tunneling (STM) and atomic force microscopy (AFM), and electrochemical methods such as capacitance measurements (with cyclic voltammetry or impedance spectroscopy) and heterogeneous electron transfer (cyclic voltammetry). The general analytical capabilities of some of these techniques are presented in Table 2.

SAMs can be of different nature according to the surface described in Table 3.

The most widely studied and characterized class of SAMs is alkanethiols on gold, which have been used in model systems for various purposes, including corrosion resistance, protein adsorption, cell adhesion, and biosensors. Therefore, taking into account the focus of this chapter, a brief description of alkanethiols-SAMs on gold with bioactive osseointegration, antiadhesive, and antibacterial properties is presented below. (For more details on the structure and assembly, preparation, and characterization of gold-alkanethiol monolayers, see references [62, 66, 72]).

4. SAMs on Gold as Model Surface for Biomaterials

SAMs of alkanethiols on gold have been used as model surfaces for modulate cells adhesion, including osteoblasts and fibroblasts, by the immobilization of specific ligands or proteins such as RGD peptides and fibronectin [80–82].

Concerning antiadhesive surfaces, SAMs presenting oligomers of ethylene glycol, commonly prepared using the alkanethiols $\text{HS}(\text{CH}_2)_{11}(\text{OCH}_2\text{CH}_2)_n\text{OH}$ (EG_n , $n = 3-7$ or OEG), resist the adsorption of several proteins and the adhesion of cells [83–91]. OEG-SAMs on gold present low adsorption of several blood proteins and blood cell adhesion as well as adhesion of the gastrointestinal bacterial species *H. pylori* as reported by us [86, 92–94]. This antiadhesive effect has been explained through theoretical and experimental research [95–99], indicating that water penetrates into the $(\text{EG})_n\text{OH}$ layers of the SAMs forming a stable interfacial water layer, which prevents the direct contact between the underlying surface and the proteins and/cells. In addition, SAMs that comprise an OEG-terminated thiol with an alkanethiol terminated with either a biological ligand or a reactive site for linking to a biological ligand can present the ligands of interest in a structurally well-defined manner against a background that resists the nonspecific adsorption of other biomolecules or adhesion of cells. Moreover, the OEG terminal group also does not compromise receptor function either to promote the attachment and proliferation of eukaryotic cells as osteoblast and fibroblast for improving osseointegration or to avoid the adhesion and colonization of prokaryotic cells following an antibacterial strategy as described below [62].

Antibacterial SAMs strategies have been performed through the immobilization of biomolecules such as antibodies, antibiotics, and antimicrobial peptides by covalent or affinity binding. One of the strongest noncovalent receptor-ligand binding interactions known in nature is the biotin-avidin/streptavidin system, where both streptavidin and avidin have a very high degree of specificity and affinity to biotin ($K_d = 10^{-13}$ M) with four equivalent sites for biotin [100]. This high binding affinity and selectivity, the symmetry of the biotin-binding pockets that are positioned in pairs at opposite faces of the protein, and the ease of functionalization of diverse biomolecules (e.g., antibodies, peptides, and nucleotides) with biotin make the streptavidin-biotin system extremely useful in a wide range of biotechnological applications such as in affinity separations, in diagnostic assays, and for “tagging” of molecules for imaging or delivery of therapeutics [101]. This affinity system is also applied to immobilize biomolecules/ligands onto SAMs surfaces by using alkanethiol terminally functionalized with a biotin moiety (Figure 4) [102–104]. These SAMs can bind streptavidin or avidin with high coverage, specificity, and activity in such a way to expose two of its binding sites away from the surface. Secondary molecules modified with biotin can then be rapidly and conveniently immobilized on these streptavidin/avidin-activated surfaces with minimal impact on their biological activity (e.g., specificity) [105].

TABLE 2: Analytical capabilities of commonly used techniques for SAM characterization. Adapted from Liedberg and Cooper [67].

Experimental technique	Analytical capability							
	Thickness	Interfacial tension	Coverage	Chemical composition	Orientation of molecule or group	Alkyl chain density	Defects and their distribution	Roughness chemical homogeneity
Ellipsometry	++	--	0	--	--	0	--	0
Contact angle goniometry	--	++	-	0	+	0	-	+
Cycle voltammetry	-	--	++	--	--	++	++	--
Infrared spectroscopy	+	-	+	+	++	++	-	--
XPS	0	--	++	++	+	0	--	--
QCM	+	--	++	--	--	0	--	--
AFM	--	0	+	-	-	-	++	++

Analytical capability: ++, excellent; +, good, 0, fair; -, poor; --, not applied.

TABLE 3: Types of SAMs according to the surface.

Surface	Surface active head group			Ref.
Noble metals	Gold, silver, copper, platinum, and palladium	Organosulfur compounds	Alkanethiols (R-SH), dialkyl sulfide (R-S-R), dialkyl disulfide (R-S-R)	[62, 64, 68–73]
Hydroxylated surfaces	Silicon oxide/silica (SiO ₂), aluminum oxide (Al ₂ O ₃), quartz, glass, and mica	Organosilanes or organosilicon derivatives	Alkylchlorosilanes (R-Si-Cl ₃), alkylalkoxysilanes (R-Si-(OCH ₃) ₃), and alkylaminosilanes (R-Si-(NHCH ₃) ₃)	[64, 65, 74]
Metal oxide	Silver oxide, aluminum oxide (Al ₂ O ₃), zirconium dioxide (ZnO ₂ , zirconia), titanium/titanium oxide (TiO ₂), and native oxide stainless steel	Carboxylic acids Organophosphorus compounds	<i>n</i> -Alkanoic (carboxylic) acids (C _n H _{2n+1} COOH) Phosphates (RPO ₃ ²⁻), phosphonates/phosphonic acids (RP(O)(OH) ₂)	[64, 74, 75] [65, 74, 76–79]

Biotin-containing SAMs (BTMs) have been used in both antiadhesive and antibacterial surface strategies as discussed in Table 4. However, although this system is successful and widely used, it shares the disadvantages of most immobilization schemes requiring chemical modification of a protein: (i) chemical modification may lead to denaturation or loss of activity and (ii) the presence of multiple sites on the protein available for modification results in loss of control over its orientation after immobilization [106].

On the contrary, immobilization by covalent binding provides an irreversible attachment that is required for some application such as coating of implants or microarrays because the ligand should not dissociate or exchange with other compounds [62, 85]. Covalent immobilization of some antibacterial ligands on thiol/gold SAMs is presented in Table 4.

5. Nanostructured SAMs: Trend for Dental Implants

As described previously, SAMs of alkanethiol on gold are the most used, but the formation of well-ordered and strong alkanethiol monolayers has been extremely limited on metal oxides such as the titanium since alkanethiols generally do

not adhere to metal oxides or are easily removed by rinsing. Among the self-assembled organic molecules, organophosphorus compounds are somewhat less often characterized compared to thiols but are becoming of great practical interest because of their ability to produce SAMs on a range of metal oxide surfaces including titanium [127, 128]. They also have attracted interest as an alternative to organosilane compounds in the functionalization of metal oxide surfaces due to the large number of available organophosphorus functional molecules and because the reaction mechanisms are not water sensitive [127, 129]. As indicated in Table 3, organophosphorus compounds for SAMs can be of organophosphonates (or phosphonic acids) and organophosphates (or phosphate ester), being structurally identical. An organophosphate has 4 oxygens with an alkyl group connected via a phosphoester bond, while organophosphonates have 3 oxygens with a carbon attached directly to phosphorus (Figure 5(a)). The lack of a hydrolysable P-O-C linkage makes phosphonate compounds more stable in aqueous solution and easier to make SAMs than organophosphate compounds. Phosphonates and phosphonic acids form SAMs on TiO₂ surfaces by the formation of Ti-O-P bonds [127].

The reaction of long-chain alkylphosphonic acids with metal oxide leads to dense, well-ordered SAMs [76, 131] that

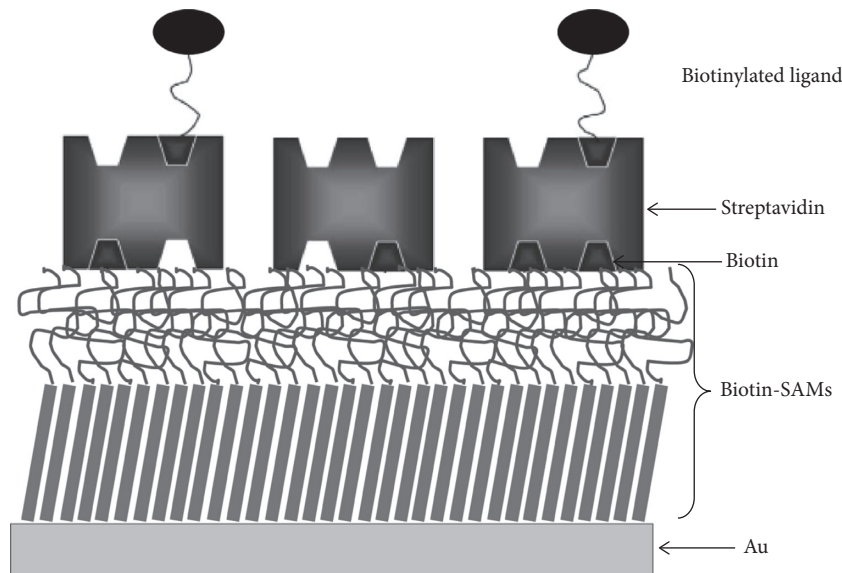


FIGURE 4: Schematic representation of mixed SAMs prepared with biotinylated alkanethiol (BAT) and triethylene glycol alkanethiol (EG3) followed by streptavidin adsorption and ligand immobilization (not scale). Adapted from Freitas et al. [107].

can find applications in a wide range of fields such as catalysis, corrosion resistance, microelectronics, chemical sensors [127], and in biomedical field, particularly in dental biomaterials for implants and orthodontic appliances. Like alkanethiol on gold and phosph(on)ate metal oxide, SAMs form monolayers with a “tail-up” orientation and a tilt angle of the hydrocarbon chains of about 30° with respect to the surface normal [128]. The binding mode of organophosphorus molecules has been proposed to be mono-, bi-, and tridentate (Figure 5(b)), which is dependent on both the surface (i.e., titanium) and the nature of the organophosphorus compounds (i.e., phosphonate or phosphate), and being bidentate for titanium [132].

Gawalt et al. [133] have reported that self-assembly of alkanephosphonates on the native oxide surface of Ti can be affected by a simple procedure of aerosol deposition of octadecylphosphonic acid followed by solvent evaporation with subsequent heating at 120°C for 18 h giving strongly surface-bound, ordered films of the alkanephosphonate species, which resist removal by solvent washing or mechanical peel testing. Hähner et al. [134] studied the adsorption of octadecyl phosphate (ODP) onto several oxide surfaces including titanium, showing densely packed SAMs with the packing density analogous to that of alkanethiols on gold. Clair et al. [135] studied and compared the assembly of dodecylphosphoric acid (DDPA) on polished and on nanotextured titanium disks. After immersion on DDPA, smooth Ti surfaces presented a water contact angle of 88° , demonstrating successful deposition of a hydrophobic molecular film, and an average thickness of 20 Å, suggesting that a monolayer of material was deposited (the theoretical length of straight molecules is 18 Å). However, nanotextured Ti surfaces presented a greater hydrophobicity because of its nanoroughness, with contact angle as high as 120° , which is higher than that in an ideally flat surface. Due to the difference between the molecular height (2 nm) and the

substrate average pit size (20 nm), the binding behavior of DDPA molecules is expected to be similar on smooth and nanotextured surfaces; considering the fact that previous studies showed that alkanephosphoric acid forms only monolayers on titanium, the authors assumed a similarity in the formation of a monolayer on this (nanorough) surface. Infrared spectroscopy for a flat surface provides characteristic methylene group peaks ($\text{CH}_{2_{\text{v asymm}}}$ 2933 cm^{-1} and $\text{CH}_{2_{\text{v symm}}}$ 2858 cm^{-1}) while the nanotextured surface presented peaks shifted ($\text{CH}_{2_{\text{v asymm}}}$ 2924 cm^{-1} and $\text{CH}_{2_{\text{v symm}}}$ 2854 cm^{-1}), with these differences in frequencies reflecting physical states of the phosphate monolayer on the surface, from a relatively densely packed phase on nanotextured Ti to a low-density disordered film on flat-polished Ti. In addition, some deterioration of the hydrophobic properties of the films was observed after 20 days in air and 10 days in buffer solution without further degradation after an additional storage for 1 month in ambient air. However, prolonged exposure of the samples (3 weeks) to the buffer solution resulted in a significant desorption of the organic film. The authors emphasize that alkanephosphoric acid films are relatively resistant to aging in a physiological-like environment when compared to thiol-based SAMs, in which spontaneous desorption occurs within a few days of immersion in various solvents, and that a further increase of their durability should be possible by optimizing film properties (e.g., by using longer alkyl chain molecules which should produce better molecular packing in the film). Spori et al. [136] reported the influence of chain length on phosphate SAMs showing a higher degree of order and packing density within the monolayers with alkyl chain lengths exceeding 15 carbon atoms forming crystalline structures and with an average alkyl chain tilt angle of 30° to the surface normal, similar to thiol/gold system. Lecollinet et al. [137] studied the adsorption of a monolayer of five bisphosphonates on oxidized surfaces of titanium and

TABLE 4: Bioactive osseointegration, antiadhesive, and antibacterial gold SAMs.

Surface	Strategy	SAMs terminal group	+Ligand	Effect	Ref.		
Bioactive osseointegration		Maleimide	CGGRGDS-NH2 Ac-CGGGRGDSP-NH ₂	Efficient and specific attachment of 3T3 fibroblasts	[108]		
		Chloroacetylated		Fibroblast adhesion and spreading	[109]		
	Covalent binding of osseointegration molecules	Azide (click chemistry reaction)	RGDSP	Minimal nonspecific protein adsorption (lysozyme and proteins in fetal bovine serum) and selective adhesion and spreading of human mesenchymal stem cells (hMSC). Moreover, RGDSP intermolecular spacing of 36 nm or less (≥ 0.01 mol% on the surface) is sufficient for hMSC adhesion and a spacing of 11 nm or less (≥ 0.05 mol% on the surface) is sufficient for cell spreading and focal adhesion complex formation	[110]		
		Phosphonates	Engineered fusion protein comprising cutinase and sections of fibronectin (FnIII10)	Leaves the cutinase bound to the surface, but the attached protein extends into the ambient solution with a defined orientation. Substrates presenting cutinase-FnIII ₁₀ -mediated rapid attachment and spreading of Swiss 3T3 fibroblasts, while substrates presenting cutinase or the phosphonate ligand alone did not support cell attachment	[111]		
Antiadhesive		Hydroquinone ⁵	RGD cyclopentadiene	Promotes Swiss 3T3 fibroblasts attachment, spreading, and migration from surface with adsorbed fibronectin to immobilized RGD	[112]		
		Ethylene glycol, HS(CH ₂) ₁₁ (OCH ₂ CH ₂) _n OH (EG, n = 3-7 or OEG)			Low adsorption of several blood proteins such as albumin, heparin, and thrombin as well as blood cell adhesion of leukocytes and platelets	[92, 93, 113-116]	
					Prevents <i>H. pylori</i> adhesion and significantly reduces the viability of adhered bacteria	[86]	
						SAMs prepared with latent aldehyde and OEG terminal showed high protein resistance (IgG) and ability to efficiently bound small bioligands or small heterobifunctional crosslinkers with hydrazide functions to the aldehyde functions on the SAM	[117]
						SAMs prepared with anhydride having H ₂ N(EG) _n =3-6-H resist nonspecific protein adsorption (fibrinogen, lysozyme, and ribonuclease A) similar to a single-component SAMs involving chemisorption of OEG-terminated alkanethiols on gold	
						Mixed SAMs (HS-EG6-COOH + HS-EG3-OH) resist to adsorption of cytochrome c and lysozyme	[118]
						Mixed SAMs (HS-EG6-COOH + HS-EG3-OH) resist to adsorption of cytochrome c and lysozyme	[119]
						Biotin-containing SAMs having an ethylene glycol background improve the selectivity to streptavidin, by avoiding nonspecific protein adsorption, and to subsequent biotin-labelled molecules with a right surface orientation	[105, 120-122]
						A natural direct thrombin inhibitor (<i>boophilin</i>) was successfully expressed, purified, biotinylated, and immobilized on biotin SAMs, able to adsorb thrombin in a selective way to delay surface-induced plasma coagulation, and so be used for the development of novel hemocompatible materials for blood-contacting devices	[107]

TABLE 4: Continued.

Surface	Strategy	SAMs terminal group	+Ligand	Effect	Ref.
		Anhydride ³	N- α -Ac-L-Lys-D-Ala-D-Ala (N-R-Ac-KDADA)	Biospecific interaction of vancomycin with this fragment from the bacterial cell wall	[123]
		Free carboxylic acid ⁴ (HS-EG6-COOH + HS-EG3-OH) + EDC/NHS chemistry	Anti- <i>E. coli</i> O157:H7	SPR biosensor with alkane monothiol surface was demonstrated to be very rapid, sensitive, and specific for potential application in detection of <i>E. coli</i> O157:H7	[124]
Antibacterial	Covalent binding of antibacterial molecules		Magainin I	Reduces by more than 50% the adhesion of bacteria (<i>L. ivanovii</i> , <i>E. faecalis</i> , and <i>S. aureus</i>) at the surface, together with the killing of the bacteria that nonetheless adhered to the surface	[125]
		Biotin	Biotin- <i>H. pylori</i> glycan structures	Several biotinylated adhesins specific to different strains of <i>H. pylori</i> were bound onto biotin SAMs showing that these immobilized ligands maintain an ability to specifically bind <i>H. pylori</i> and thus offering new insights into innovative strategies against <i>H. pylori</i> infection based on the scavenging of bacteria from the stomach using specific <i>H. pylori</i> -chelating biomaterials	[126]

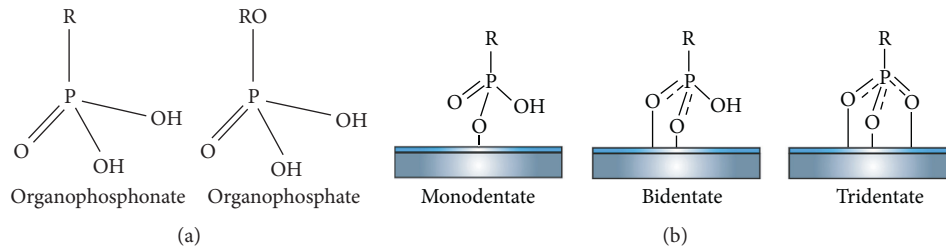


FIGURE 5: (a) Structure of organophosphate and phosphonate compounds. Adapted from Durmaz [127]. (b) Different bonding modes of a phosphonate unit to a metal oxide surface [130].

stainless steel. The authors highlighted that the molecule having a perfluoropolyether linked to a bisphosphonate moiety can resist harsh conditions, such as lasting water immersion at 50°C for 6 months, at different pHs, autoclaving at 121°C, and biocorrosion required for dental application.

However, in those studies and others described below for immobilized bioactive molecules [138–147], the amphiphile adlayers were produced from solutions of alkylphosphonates in organic solvents, which can reduce the biocompatibility of the surface [127, 130]. Tosatti et al. [148] applied aqueous phosphates to titanium oxide and titanium metal films to serve as smooth, flat model surfaces, and a special titanium dental implant surface with a rough, highly corrugated surface. XPS showed to form densely packed SAMs onto titanium not only as flat surface but also for high surface area materials, such as the SLA dental implant surface, with the phosphate headgroups attaching to the titanium (oxide) surface and the terminal end group (either methyl or hydroxy) pointing toward the ambient environment (air, vacuum, or water). The authors point out that “The technique of spontaneous organization of organophosphate molecules on titanium (oxide) surfaces from aqueous solution is believed to have potential for the modification of titanium-based medical implants and devices with the aim of tailoring the surface chemistry (chemical or biological functionalities), including groups such as poly(ethylene glycol), cell-adhesive peptides or growth factors.” Complementarily, Zwahlen et al. [149] showed that dodecyl phosphate adsorbed from aqueous solution formed SAMs of comparable quality to those of the longer octadecyl phosphate prepared from organic solvent and those of similar thiol/gold systems. Therefore, such mixed SAMs on metal oxide surfaces are of particular interest to the biosensor and biomaterial field, because they allow tailoring surface properties in a precise manner and may prove to be highly relevant for controlling the interaction between the SAM-modified surface and biological systems, such as proteins, antibodies, and cells.

5.1. SAMs for Bioactive Osseointegration on Titanium. Viornery et al. [150] firstly showed the formation of a chemical link between Ti disks and three phosphonic acids in water. The bioactivity of the modified Ti disks was evaluated by incubating these disks in a physiological solution (Hank’s balanced salt solution (HBSS)) for 1, 7, and 14 days. Modified

surfaces showed only slightly higher calcium levels in the XPS analysis compared to the reference Ti surface, with the surface modified with ethane-1,1,2-triphosphonic acid (ETP) inducing the highest calcium phosphate deposition after 14 days incubation [150]. Afterwards, these same types of phosphonic acid-modified titanium disks were evaluated *in vitro* related to the proliferation, differentiation, and protein production of rat osteoblastic cells (CRP10/30) [151]. No statistical differences were found in osteoblast proliferation among the phosphonic acid-modified titanium, unmodified titanium, and tissue culture plastic (used as a positive control), indicating that the phosphonic acids used were not cytotoxic to the osteoblasts. For all surfaces evaluated, the alkaline phosphatase activity was comparable as negative control (tissue culture plastic). However, the total amount of protein, and especially the collagen type I synthesis, was sensitive to surface modification. On titanium modified with ETP, the total amount of synthesized protein was significantly higher than the titanium control surfaces [151]. Then, the authors stated that “The covalently attached phosphonic acid molecules on the Ti-metal surface thus may form a scaffold for new bone formation, ultimately leading to bonding of the implant to the host tissue.”

A different strategy to enhance titanium osseointegration was explored by Liu et al. [145] firstly through the introduction of different end groups including hydroxyl, carboxylic acid, phosphate, and vinyl via the formation of alkyl-based SAM on a Ti foil. Accordingly, a hydroxyapatite coating was successfully obtained with phosphate and carboxylic acid after soaking the Ti foil in a solution that contained ions at a concentration 1.5 times higher than SBF. Then, these authors [146] investigated hydroxyapatite formation on Ti surfaces with various end groups, demonstrating that carboxylic acid as an end group provided the optimal SAM surface for nucleation and growth of biomimetic crystalline HA. It seems that the affinity of carboxylic acid for nuclei of CaP plays a pivotal role in the promotion of HA crystallization at surface. In addition to the functional groups, alkyl chain length of phosphonic acids should also be considered as a factor that influences hydroxyapatite crystallization at surface. Next, Wu et al. [147] evaluated the deposition from simulated body fluid of CaP onto carboxylic acid-terminated phosphonic acid SAMs with three different lengths of an alkyl chain (3, 6, and 16 methylene units) to compare the ability of promoting CaP crystallization. SEM, XPS, and X-ray diffraction revealed

that the formation of PA SAMs accelerates the deposition of poorly crystallized HA in an alkyl chain length-dependent manner, primarily due to the higher surface density of Ca^{2+} -attracting carboxylic acids. Among PAs studied here, PA containing a 16-carbon alkyl chain gave rise to the titanium surface most effective for the deposition of hydroxyapatite.

Gawalt et al. [138, 139] reported that alkylphosphonic acids (11-hydroxyundecylphosphonic acid) self-assemble on the native oxide surfaces of Ti and Ti6Al4V, followed by a heating step that binds the acids strongly to these surfaces as ordered phosphonate films. These SAMs with OH-terminated groups were activated to a maleimide group and then immersed in an aqueous solution of cell-adhesive peptide RGD-cysteine. The adhesion and spreading of the osteoblasts on RGD-modified Ti surface were quite substantial after 24 h and even more so after 3 days. Indeed, cell proliferation continued unabated throughout the test period on this surface. The morphology and actin cytoskeleton of cells were observed by staining with rhodamine phalloidin, with cells remaining small and rounded with no organized actin cytoskeleton on control substrates. However, more than 90% of cells adherent to RGD-modified substrates became well spread and organized their actin filaments into robust stress fibres. Danahy et al. [140] constructed more complex SAMs from α,ω -diphosphonic acids self-assembled on the native oxide surfaces of Ti and Ti6Al4V and thermally treated to get strongly bonded phosphonate monolayers. Data from infrared and X-ray spectroscopies and water contact angle showed that the films bind to the surface by one phosphonate unit while the other remains free as a phosphonic acid. Then, the SAMs were treated with zirconium tetra(tert-butoxide) to give surface Zr complex species. Finally, these surface-bound alkoxides can be further derivatized with the insertion of maleimide group followed by binding the RGD-cysteine peptide. Surfaces modified with RGD were stable to hydrolysis under physiological conditions and mechanically strong and shown to be effective to promote osteoblast adhesion and proliferation with organized actin filaments and vinculin-positive focal adhesions.

Adden et al. [141] used two different phosphonic acid monolayer films for immobilization of bioactive molecule BMP2 on titanium surfaces. Monolayers of (11-hydroxyundecyl) phosphonic acid and (12-carboxydodecyl) phosphonic acid molecules were produced by a simple dipping process and the terminal functional groups on these monolayers were activated (carbonyldiimidazole for hydroxyl groups and *N*-hydroxysuccinimide for carboxyl groups) to bind amine-containing molecules as the BMP2. The hydroxyl-terminated SAM is better ordered and orientated than the carboxyl-terminated SAM, and the CDI-activated surfaces (OH-terminated SAMs) gave higher amounts of BMP2 bound than the NHS-activated surfaces (COOH-terminated SAMs).

A different bioactive SAMs coating strategy was done by Mani et al. [152, 153] with the use of OH-terminated phosphonic acid SAM on Ti prepared from aqueous solution followed by the chemical attachment of a model drug flufenamic acid through three different methods of esterification (acid chloride esterification, dry heat esterification,

and direct esterification). The drug release profiles of TSAMs prepared via acid-chloride esterification exhibited large data scatter, probably because the drug molecules were not uniformly attached to SAM-coated metal surfaces while TSAMs prepared by dry heat and direct esterification methods showed an initial burst release of the drug followed by a sustained slow release for up to 2 weeks. Thus, this study suggests “the potential for using SAMs as an alternate system for delivering drugs from coronary stents and other metal implants” [152]. Then, Mani et al. [153] used SAMs with flufenamic acid only attached by direct esterification to study their interaction with human aortic endothelial cells (HAECs), showing that the adhesion of HAECs on TSAMs was equivalent to that of control metal surfaces and superior to that of plain glass surfaces with the cells continued to proliferate on TSAMs even though the rate of proliferation was slower than plain glass or control-Ti. Moreover, the spreading of HAECs on TSAMs with typical polygonal shape indicated that these surfaces are conducive to endothelialization. The expression of surface adhesion protein (platelet endothelial cell adhesion molecule-1) on TSAMs indicated that the endothelial cells preserved their phenotype on these surfaces. Thus, this study demonstrated that TSAMs do not elicit an adverse response from endothelial cells in *in vitro* conditions.

Recently, Rudzka et al. [154] modified cpTi surfaces by producing mixed and patterned SAMs in order to induce hydroxyapatite nucleation and growth for bone tissue engineering. Mixed-SAMs were prepared from aqueous solutions having different fractions of 11-hydroxyundecylphosphonic acid (UDPA, -OH terminal group) and 12-phosphonododecylphosphonic acid (PDDPA, -PO(OH)₂ terminal group) and patterned-SAMs from single THF solutions of 16-phosphonohexadecanoic acid (PHDA, -COOH terminal group) and octadecylphosphonic acid (ODPA, -CH₃ terminal group) followed by laser ablation. These authors have shown that the PHDA-SAMs without laser treatment promote significantly the hydroxyapatite formation with smaller clusters, demonstrating that the presence of carboxyl groups on the cpTi surface is more favorable for the hydroxyapatite nucleation and growth in SBF than on the laser-ablated surface.

Rojo et al. [155] used a simple, effective, and clean methodology through the self-assembly chemisorption onto Ti6Al4V alloy surfaces of alendronate, which is a well-known bisphosphonate commonly used in osteoporosis therapy and treatment of other bone diseases. XPS spectroscopy revealed that an effective mode of bonding is created between the metal oxide surface and the phosphate residue of alendronate, leading to the formation of homogeneous drug distribution along the surface. In addition, *in vitro* studies showed that alendronate SAMs induce differentiation of hMSC to a bone cell phenotype and promote bone formation on modified surfaces, as evidenced by upregulation in the expression of early markers of osteogenic differentiation (Runx2, osteopontin (OPN), alkaline phosphatase (ALP), and BMP2).

5.2. SAMs with Antiadhesive and Antibacterial Properties on Titanium. Byun et al. [156] synthesized a PEG-phosphonic acid terminated with an amino group (PA-C11-EG3-NH2)

that is used to make SAMs onto titanium surface by aqueous immersion. This denominated pSAM was sequentially modified by EMPISA conjugation through EDC/NHS chemistry to insert a terminal thioester functional group followed by PEGylation through NH₂-Cys-PEG. Ellipsometry, goniometry, and XPS unambiguously confirmed the presence of PEGs, which provided nonfouling effects of surfaces, preventing the biological adhesion of cells as the NIH-3T3 adhered cells were reduced by 92.3% after PEGylation.

Amalric et al. [142, 143] developed antibacterial nanocoatings on titanium and stainless steel through the functionalization of phosphonate monolayers of mercaptododecylphosphonic acid (MDPA) with silver nitrate (AgNO₃) by a two-step scheme: (i) deposition of a thiol-functionalized monolayer by reaction with MDPA solution and (ii) reaction of the terminating thiol groups with silver nitrate to form silver thiolate species. Thiol-terminated groups are expected to react readily with silver cations to form silver thiolates with high formation constants and, accordingly, the silver thiolate groups should be stable toward hydrolysis, but silver ions can be selectively released by exchange between the silver thiolate groups at the surface of the monolayers and the free thiol groups exposed at the surface of the bacterial membrane proteins, with the reaction of Ag⁺ ions with thiol groups in the bacterial membrane proteins playing an essential role in bacterial inactivation. FTIR confirmed the binding of MDPA to the surface on both the titanium and the stainless steel, suggesting the formation of moderately ordered monolayers compared to alkylphosphonic acid monolayers deposited on similar substrates. XPS analysis confirmed the effectiveness of these surface modifications. Postmodification with AgNO₃ resulted in the conversion of most of the terminal thiol groups into silver thiolate species, which represented about 60% of all sulfur species in the final samples, with the density of silver at the surface estimated to $3.5 \pm 1 \text{ Ag-nm}^{-2}$, corresponding to about $0.6 \text{ nmol-Ag-cm}^{-2}$. Thus, the amount of silver was very low compared to other antibacterial silver-coated materials reported in the literature, such as the silver content in stainless steel or titanium samples modified by ion implantation or by physical vapor deposition ranging from 80 to 1700 nmol-Ag-cm⁻². Despite their very low silver content, MDPA + AgNO₃ monolayers strongly decreased the bacterial adhesion of the surface compared to the bare titanium or stainless steel substrates: a 3- to 5-log reduction in the number of viable adherent bacteria was found for the four bacterial strains tested (*E. coli*, *S. aureus*, *S. epidermidis*, and *P. aeruginosa*). Furthermore, the antibacterial efficiency of MDPA + AgNO₃ monolayers remained excellent even after incubation for 3 days at 37°C in fresh human blood plasma, with a 4-log reduction of the number of viable adherent bacteria on the coated substrate compared to unmodified substrate. The MDPA + AgNO₃ coating deposited on titanium or stainless steel also strongly decreased the density of bacterial biofilm formed after incubation for 3 days in a culture of *E. coli*, *S. epidermidis*, or *P. aeruginosa*. In addition, the growth of *E. coli* biofilm on titanium modified by MDPA + AgNO₃ was significantly inhibited for about 1 week. Even more, since the release of silver ions by hydrolysis of the silver thiolate groups was negligible, the antibacterial effect observed in this study could result from the exchange of

silver between the thiolate groups at the surface of the MDPA + AgNO₃ monolayers and the free thiol groups exposed at the surface of the bacterial membrane proteins. Antibacterial transitory effect was obtained for an extremely low Ag content compared to conventional coatings, which is important to avoid any toxicity issue and to minimize the release of silver in the environment, which could facilitate the selection of resistant strains. Rather, the aim of these coatings is to prevent contamination during handling of the implant and surgery, then for the first few days after the implantation, which are considered critical. Then, Tilmaciu et al. [144] showed that these SAMs on titanium significantly inhibited *E. coli* and *S. epidermidis* adhesion and biofilm formation *in vitro*, while allowing attachment and proliferation of MC3T3-E1 preosteoblasts. Moreover, osteogenic differentiation of MC3T3 cells and murine mesenchymal stem cells was not affected by the nanocoatings. Sterilization by ethylene oxide did not alter the antibacterial activity and biocompatibility of the nanocoatings. After subcutaneous implantation of the materials in mice, MDPA + AgNO₃ nanocoatings exhibit significant antibacterial activity and excellent biocompatibility, both *in vitro* and *in vivo*, after postoperative seeding with *S. epidermidis*.

Vaithilingam et al. [157] immobilized Ciprofloxacin® (an antibacterial drug) to a carboxylic acid-terminated phosphonic acid based self-assembled monolayers (SAMs) adsorbed on a selectively laser melting (SLM) Ti6Al4V structure by immersion deposition method in THF. Ciprofloxacin-coated Ti6Al4V surfaces are highly stable under the oxidative ambient laboratory conditions for 1, 2, 4, and 6 weeks. When immersed in 10 mm of Tris-HCl buffer (pH 7.4), the drug was observed to release in a sustained manner with 50% of the drug released after 4 weeks and approximately 40% of the drug remaining after 6 weeks. Antibacterial susceptibility tests revealed that the immobilized drug was therapeutically active upon its release against *S. aureus* and *E. coli*. Then, these authors also used the same strategy to immobilize paracetamol, which was stable for over four weeks and then began to desorb from the surface, showing a potential to improve biocompatibility and reduce surgical complications after implant placement [158].

5.3. SAMs with Dual Biofunctions. Kang et al. [28] coated titanium with a nonbiofouling poly(poly(ethylene glycol) methacrylate) (pPEGMA) by surface-initiated polymerization to Br-terminated SAMs of phosphonic acid, and BMP2 was chemically conjugated to the activated pPEGMA films by DSC/DMAP chemistry. The BMP2-conjugated pPEGMA films induced adhesion and differentiation of mesenchymal stem cells.

Moreover, Gnauck et al. [159] synthesized a carboxy-terminated oligo (ethylene glycol) alkanephosphate with the OEG for resistance against nonspecific protein adsorption and cells/bacteria adhesion and the COOH-terminal functional group as a linker for the attachment of specific bioligands, such as peptides and proteins to be present at the

surface. XPS data showed that the monomolecular layer is attached with the phosphate group to the substrate but not fully ordered or taking an all-trans conformation. However, this study did not present any result concerning protein adsorption or cell adhesion with only chemical and structure characterization. Bozzini et al. [160, 161] synthesized PEG-terminated alkanephosphate that was codeposited with OH-terminated alkane phosphates from aqueous solution onto TiO₂ films. XPS and ellipsometry of the resulting mixed SAMs indicate that the PEG density can be controlled by varying the mole fraction of PEG-terminated phosphates in the solutions used during the deposition process, leading to surfaces with different degrees of protein resistance [160] and reduction of bacterial adhesion (*S. mutans*): As the PEG surface density increased, the protein adsorption and bacterial adhesion considerably decreased when compared to uncoated titanium surfaces, while maintaining osteoblast proliferation up to 7 days of culture *in vitro* with the greatest levels of metabolic activity at the highest PEG surface concentrations [161]. These results are extremely promising in view of a potential clinical application in dental implants, where reduction of bacteria adhesion and stimulation of bone formation are both highly desirable.

Other approaches using nonphosphate SAMs have been reported, showing results oriented to improve the osseointegration and reduce the bacterial adhesion [162–165].

6. Conclusions

The present review shows that dental-based implant therapy after 30 years is a predictable short-term treatment to patient with full or partial edentulism. However, long-term success and survival of implant need more research looking for a more stable interface tissue/implant. Nanoscale modifications of surface implants have been an active scientific area, where new approaches such as SAMs are providing strategies to modulate tissue response and microbiota microenvironment in terms of bioactivity, antiadhesion, antibacterial, or combined effects.

- (i) Titanium with SAMs for bioactive osseointegration effect has been highly studied with several strategies such as exposure of carboxylic terminal to promote calcium phosphate or hydroxyapatite deposition, with immobilized cell adhesive RGD peptides to induce osteoblast attachment, spreading, and proliferation and with immobilized bone morphogenetic proteins (BMPs) to promote bone formation.
- (ii) Antiadhesive and antibacterial SAMs on titanium have been sparsely worked with few studies, based on monolayers with protruding group of ethylene glycol and in the immobilization of metals ions and molecules with activity against bacteria, respectively.
- (iii) SAMs on titanium with combined bioactivity and antiadhesion or antibacterial effect have been little described with a monolayer of ethylene glycol to which pro-osseointegration molecules might be immobilized.

Conflicts of Interest

The authors declare that there are no conflicts of interest.

Acknowledgments

This study was supported by the CONADI funds, Universidad Cooperativa de Colombia (Code ID1527). The authors are also grateful to Professor S. Arango-Santander for the help in discussing several aspects in this review.

References

- [1] P. E. Petersen, “The World Oral Health Report 2003: continuous improvement of oral health in the 21st century. The approach of the WHO Global Oral Health Programme,” *Community Dentistry and Oral Epidemiology*, vol. 31, no. 1, pp. 3–24, 2003.
- [2] A. K. Mascarenhas, “Mouthguards reduce orofacial injury during sport activities, but may not reduce concussion,” *Journal of Evidence Based Dental Practice*, vol. 12, no. 2, pp. 90–91, 2012.
- [3] K. Bücher, C. Neumann, R. Hickel, and J. Kühnisch, “Traumatic dental injuries at a German University Clinic 2004–2008,” *Dental Traumatology*, vol. 29, no. 2, pp. 127–133, 2013.
- [4] V. Tiwari, V. Saxena, U. Tiwari, A. Singh, M. Jain, and S. Goud, “Dental trauma and mouthguard awareness and use among contact and noncontact athletes in central India,” *Journal of Oral Science*, vol. 56, no. 4, pp. 239–243, 2014.
- [5] H. E. Gonzalez and A. Manns, “Forward head posture: its structural and functional influence on the stomatognathic system, a conceptual study,” *Cranio*, vol. 14, no. 1, pp. 71–80, 1996.
- [6] B. E. Pjetursson, U. Brägger, N. P. Lang, and M. Zwahlen, “Comparison of survival and complication rates of tooth-supported fixed dental prostheses (FDPs) and implant-supported FDPs and single crowns (SCs),” *Clinical Oral Implants Research*, vol. 18, pp. 97–113, 2007.
- [7] I. K. Karoussis, G. E. Salvi, L. J. A. Heitz-Mayfield, U. Brägger, C. H. F. Hämmerle, and N. P. Lang, “Long-term implant prognosis in patients with and without a history of chronic periodontitis: a 10-year prospective cohort study of the ITI Dental Implant System,” *Clinical Oral Implants Research*, vol. 14, no. 3, pp. 329–339, 2003.
- [8] T. Albrektsson, L. Sennerby, and A. Wennerberg, “State of the art of oral implants,” *Periodontology 2000*, vol. 47, no. 1, pp. 15–26, 2008.
- [9] L. Sennerby, “Dental implants: matters of course and controversies,” *Periodontology 2000*, vol. 47, no. 1, pp. 9–14, 2008.
- [10] R. A. Jaffin and C. L. Berman, “The excessive loss of Branemark fixtures in type IV bone: a 5-year analysis,” *Journal of Periodontology*, vol. 62, no. 1, pp. 2–4, 1991.
- [11] A. Pelaez-Vargas, D. Gallego-Perez, N. Higueta-Castro et al., “Micropatterned coatings for guided tissue regeneration in dental implantology,” in *Cell Interaction*, S. Gowder, Ed., pp. 273–302, InTech, London, UK, 2012.
- [12] B. Klinge, M. Hultin, and T. Berglundh, “Peri-implantitis,” *Dental Clinics of North America*, vol. 49, no. 3, pp. 661–676, 2005.
- [13] E. Silva, S. Félix, A. Rodriguez-Archilla, P. Oliveira, and J. Martins dos Santos, “Revisiting peri-implant soft tissue - histopathological study of the peri-implant soft tissue,”

- International Journal of Clinical and Experimental Pathology*, vol. 7, no. 2, pp. 611–618, 2014.
- [14] M. Esposito, J.-M. Hirsch, U. Lekholm, and P. Thomsen, “Biological factors contributing to failures of osseointegrated oral implants. (I). Success criteria and epidemiology,” *European Journal of Oral Sciences*, vol. 106, no. 1, pp. 527–551, 1998.
- [15] L. Rimondini, L. Cerroni, A. Carrassi, and P. Torricelli, “Bacterial colonization of zirconia ceramic surfaces: an in vitro and in vivo study,” *International Journal of Oral & Maxillofacial Implants*, vol. 17, no. 6, pp. 793–798, 2002.
- [16] A. Tanner, M. F. J. Maiden, K. Lee, L. B. Shulman, and H. P. Weber, “Dental implant infections,” *Clinical Infectious Diseases*, vol. 25, no. 2, pp. S213–S217, 1997.
- [17] A. Leonhardt, S. Renvert, and G. Dahlen, “Microbial findings at failing implants,” *Clinical Oral Implants Research*, vol. 10, no. 5, pp. 339–345, 1999.
- [18] B. D. Boyan, C. H. Lohmann, D. D. Dean, V. L. Sylvia, D. L. Cochran, and Z. Schwartz, “Mechanisms involved in osteoblast response to implant surface morphology,” *Annual Review of Materials Research*, vol. 31, no. 1, pp. 357–371, 2001.
- [19] P. M. Brett, J. Harle, V. Salih et al., “Roughness response genes in osteoblasts,” *Bone*, vol. 35, no. 1, pp. 124–133, 2004.
- [20] Z. Shi, K. G. Neoh, E. T. Kang, K. P. Chye, and W. Wang, “Surface functionalization of titanium with carboxymethyl chitosan and immobilized bone morphogenetic protein-2 for enhanced osseointegration,” *Biomacromolecules*, vol. 10, no. 6, pp. 1603–1611, 2009.
- [21] T. A. Barber, L. J. Gamble, D. G. Castner, and K. E. Healy, “In vitro characterization of peptide-modified p(AAm-co-EG/AAc) IPN-coated titanium implants,” *Journal of Orthopaedic Research*, vol. 24, no. 7, pp. 1366–1376, 2006.
- [22] P. H. Chua, K. G. Neoh, E. T. Kang, and W. Wang, “Surface functionalization of titanium with hyaluronic acid/chitosan polyelectrolyte multilayers and RGD for promoting osteoblast functions and inhibiting bacterial adhesion,” *Biomaterials*, vol. 29, no. 10, pp. 1412–1421, 2008.
- [23] X. Zhou, S. Park, H. Mao, T. Isoshima, Y. Wang, and Y. Ito, “Nanolayer formation on titanium by phosphonated gelatin for cell adhesion and growth enhancement,” *International Journal of Nanomedicine*, vol. 10, pp. 5597–5607, 2015.
- [24] D. A. Puleo, R. A. Kissling, and M. S. Sheu, “A technique to immobilize bioactive proteins, including bone morphogenetic protein-4 (BMP-4), on titanium alloy,” *Biomaterials*, vol. 23, no. 9, pp. 2079–2087, 2002.
- [25] Y. Tanaka, K. Matin, M. Gyo et al., “Effects of electro-deposited poly(ethylene glycol) on biofilm adherence to titanium,” *Journal of Biomedical Materials Research Part A*, vol. 95, no. 4, pp. 1105–1113, 2010.
- [26] F. Zhang, Z. Zhang, X. Zhu, E. T. Kang, and K. G. Neoh, “Silk-functionalized titanium surfaces for enhancing osteoblast functions and reducing bacterial adhesion,” *Biomaterials*, vol. 29, no. 36, pp. 4751–4759, 2008.
- [27] P. Renoud, B. Toury, S. Benayoun, G. Attik, and B. Grosgeat, “Functionalization of titanium with chitosan via silanation: evaluation of biological and mechanical performances,” *PLoS One*, vol. 7, no. 7, Article ID e39367, 2012.
- [28] S. M. Kang, B. Kong, E. Oh, J. S. Choi, and I. S. Choi, “Osteoconductive conjugation of bone morphogenetic protein-2 onto titanium/titanium oxide surfaces coated with non-biofouling poly(poly(ethylene glycol) methacrylate),” *Colloids Surfaces B: Biointerfaces*, vol. 75, no. 1, pp. 385–389, 2010.
- [29] D. Ferris, “RGD-coated titanium implants stimulate increased bone formation in vivo,” *Biomaterials*, vol. 20, no. 23–24, pp. 2323–2331, 1999.
- [30] H. C. Kroese-Deutman, J. van den Dolder, P. H. M. Spauwen, and J. A. Jansen, “Influence of RGD-loaded titanium implants on bone formation in vivo,” *Tissue Engineering*, vol. 11, no. 11–12, pp. 1867–1875, 2005.
- [31] C. Lorenz, A. Hoffmann, G. Gross et al., “Coating of titanium implant materials with thin polymeric films for binding the signaling protein BMP2,” *Macromolecular Bioscience*, vol. 11, no. 2, pp. 234–244, 2011.
- [32] H. Schliephake, J. Rublack, N. Aeckerle et al., “In vivo effect of immobilisation of bone morphogenetic protein 2 on titanium implants through nano-anchored oligonucleotides,” *European Cells and Materials*, vol. 30, pp. 28–40, 2015.
- [33] N. P. Huang, R. Michel, J. Voros et al., “Poly(l-lysine)-g-poly(ethylene glycol) layers on metal oxide surfaces: surface-analytical characterization and resistance to serum and fibrinogen adsorption,” *Langmuir*, vol. 17, no. 2, pp. 489–498, 2001.
- [34] L. G. Harris, S. Tosatti, M. Wieland, M. Textor, and R. G. Richards, “*Staphylococcus aureus* adhesion to titanium oxide surfaces coated with non-functionalized and peptide-functionalized poly(l-lysine)-grafted- poly(ethylene glycol) copolymers,” *Biomaterials*, vol. 25, no. 18, pp. 4135–4148, 2004.
- [35] S. Saxer, C. Portmann, S. Tosatti, K. Gademann, S. Zürcher, and M. Textor, “Surface assembly of catechol-functionalized poly(l-lysine)-graftpoly(ethylene glycol) copolymer on titanium exploiting combined electrostatically driven self-organization and biomimetic strong adhesion,” *Macromolecules*, vol. 43, no. 2, pp. 1050–1060, 2010.
- [36] J. L. Dalsin, L. Lin, S. Tosatti, J. Vörös, M. Textor, and P. B. Messersmith, “Protein resistance of titanium oxide surfaces modified by biologically inspired mPEG-DOPA,” *Langmuir*, vol. 21, no. 2, pp. 640–646, 2005.
- [37] F. Khalil, E. Franzmann, J. Ramcke et al., “Biomimetic PEG-catecholates for stable antifouling coatings on metal surfaces: applications on TiO₂ and stainless steel,” *Colloids Surfaces B: Biointerfaces*, vol. 117, pp. 185–192, 2014.
- [38] J.-Y. Wach, B. Malisova, S. Bonazzi et al., “Protein-resistant surfaces through mild dopamine surface functionalization,” *Chemistry*, vol. 14, no. 34, pp. 10579–10584, 2008.
- [39] X. Khoo, G. A. O’Toole, S. A. Nair, B. D. Snyder, D. J. Kenan, and M. W. Grinstaff, “*Staphylococcus aureus* resistance on titanium coated with multivalent PEGylated-peptides,” *Biomaterials*, vol. 31, no. 35, pp. 9285–9292, 2010.
- [40] D. Jedrzejczyk, T. Zdziech, and M. Hajduga, “Influence of modifying treatment of titanic implants on periimplantitis,” in *Met 2012: Conference Proceedings, 21st International Conference on Metallurgy and Materials*, pp. 1037–1043, Tanager Ltd., Brno, Czech Republic, 2012.
- [41] Y. Z. Wan, S. Raman, F. He, and Y. Huang, “Surface modification of medical metals by ion implantation of silver and copper,” *Vacuum*, vol. 81, no. 9, pp. 1114–1118, 2007.
- [42] M. Yoshinari, Y. Oda, T. Kato, and K. Okuda, “Influence of surface modifications to titanium on antibacterial activity in vitro,” *Biomaterials*, vol. 22, no. 14, pp. 2043–2048, 2001.
- [43] M. Yoshinari, Y. Oda, T. Kato, K. Okuda, and A. Hirayama, “Influence of surface modifications to titanium on oral bacterial adhesion in vitro,” *Journal of Biomedical Materials Research*, vol. 52, no. 2, pp. 388–394, 2000.
- [44] H. L. Huang, Y. Y. Chang, M. C. Lai, C. R. Lin, C. H. Lai, and T. M. Shieh, “Antibacterial TaN-Ag coatings on titanium

- dental implants,” *Surface and Coatings Technology*, vol. 205, no. 5, pp. 1636–1641, 2010.
- [45] K. Das, S. Bose, A. Bandyopadhyay, B. Karandikar, and B. L. Gibbins, “Surface coatings for improvement of bone cell materials and antimicrobial activities of Ti implants,” *Journal of Biomedical Materials Research Part B: Applied Biomaterials*, vol. 87, no. 2, pp. 455–460, 2008.
- [46] N. Ryter, J. Köser, W. Hoffmann et al., “Antimicrobial effects on titanium surfaces with incorporated copper,” in *Proceedings of Annual Meeting of the Swiss Society for Biomedical Engineering (SSBE)*, vol. 39, p. 12, Bern, Switzerland, 2011.
- [47] Y. Z. Wan, G. Y. Xiong, H. Liang, S. Raman, F. He, and Y. Huang, “Modification of medical metals by ion implantation of copper,” *Applied Surface Scienc*, vol. 253, no. 24, pp. 9426–9429, 2007.
- [48] G. Schmidmaier, M. Lucke, B. Wildemann, N. P. Haas, and M. Raschke, “Prophylaxis and treatment of implant-related infections by antibiotic-coated implants: a review,” *Injury*, vol. 37, no. 2, pp. S105–S112, 2006.
- [49] T. Kalicke, J. Schierholz, U. Schlegel et al., “Effect on infection resistance of a local antiseptic and antibiotic coating on osteosynthesis implants: an in vitro and in vivo study,” *Journal of Orthopaedic Research*, vol. 24, no. 8, pp. 1622–1640, 2006.
- [50] L. G. Harris, L. Mead, E. Muller-Oberlander, and R. G. Richards, “Bacteria and cell cytocompatibility studies on coated medical grade titanium surfaces,” *Journal of Biomedical Materials Research Part A*, vol. 78, no. 1, pp. 50–58, 2006.
- [51] P. Bahna, T. Dvorak, H. Hanna, A. W. Yasko, R. Hachem, and I. Raad, “Orthopaedic metal devices coated with a novel antiseptic dye for the prevention of bacterial infections,” *International Journal of Antimicrobial Agents*, vol. 29, no. 5, pp. 593–596, 2007.
- [52] S. Radin and P. Ducheyne, “Controlled release of vancomycin from thin sol-gel films on titanium alloy fracture plate material,” *Biomaterials*, vol. 28, no. 9, pp. 1721–1729, 2007.
- [53] R. O. Darouiche, M. D. Mansouri, D. Zakarevicz, A. Alsharif, and G. C. Landon, “In vivo efficacy of antimicrobial-coated devices,” *Journal of Bone and Joint Surgery*, vol. 89, no. 4, pp. 792–797, 2007.
- [54] S. Zürcher, D. Wäckerlin, Y. Bethuel et al., “Biomimetic surface modifications based on the cyanobacterial iron chelator anachelin,” *Journal of the American Chemical Society*, vol. 128, no. 4, pp. 1064–1065, 2006.
- [55] J. Y. Wach, S. Bonazzi, and K. Gademann, “Antimicrobial surfaces through natural product hybrids,” *Angewandte Chemie International Edition*, vol. 47, no. 37, pp. 7123–7126, 2008.
- [56] F. Zhang, Z. L. Shi, P. H. Chua, E. T. Kang, and K. G. Neoh, “Functionalization of titanium surfaces via controlled living radical polymerization: from antibacterial surface to surface for osteoblast adhesion,” *Industrial & Engineering Chemistry Research*, vol. 46, no. 26, pp. 9077–9086, 2007.
- [57] M. Kazemzadeh-Narbat, J. Kindrachuk, K. Duan, H. Jenssen, R. E. W. Hancock, and R. Wang, “Antimicrobial peptides on calcium phosphate-coated titanium for the prevention of implant-associated infections,” *Biomaterials*, vol. 31, no. 36, pp. 9519–9526, 2010.
- [58] K. V. Holmberg, M. Abdolhosseini, Y. Li, X. Chen, S. U. Gorr, and C. Aparicio, “Bio-inspired stable antimicrobial peptide coatings for dental applications,” *Acta Biomaterialia*, vol. 9, no. 9, pp. 8224–8231, 2013.
- [59] X. Chen, H. Hirt, Y. Li, S. U. Gorr, and C. Aparicio, “Antimicrobial GL13K peptide coatings killed and ruptured the wall of streptococcus gordonii and prevented formation and growth of biofilms,” *PLoS One*, vol. 9, no. 11, Article ID e111579, 2014.
- [60] G. Gao, D. Lange, K. Hilpert et al., “The biocompatibility and biofilm resistance of implant coatings based on hydrophilic polymer brushes conjugated with antimicrobial peptides,” *Biomaterials*, vol. 32, no. 16, pp. 3899–3909, 2011.
- [61] M. Godoy-Gallardo, C. Mas-Moruno, M. C. Fernández-Calderón et al., “Covalent immobilization of hLf1-11 peptide on a titanium surface reduces bacterial adhesion and biofilm formation,” *Acta Biomaterialia*, vol. 10, no. 8, pp. 3522–3534, 2014.
- [62] J. C. Love, L. A. Estroff, J. K. Kriebel, R. G. Nuzzo, and G. M. Whitesides, “Self-assembled monolayers of thiolates on methals as a form of nanotechnology,” *Chemical Reviews*, vol. 105, no. 4, pp. 1103–1169, 2005.
- [63] M. Kind and C. Woll, “Organic surfaces exposed by self-assembled organothiols monolayers: preparation, characterization, and application,” *Progress in Surface Science*, vol. 84, no. 7-8, pp. 230–278, 2009.
- [64] A. Ulman, “Formation and structure of self-assembled monolayers,” *Chemical Reviews*, vol. 96, no. 4, pp. 1533–1554, 1996.
- [65] F. Mastrangelo, G. Fioravanti, R. Quaresima, R. Vinci, and E. Gherlone, “Self-assembled monolayers (SAMs): which perspectives in implant dentistry?,” *Journal of Biomaterials and Nanobiotechnology*, vol. 2, no. 5, pp. 533–543, 2011.
- [66] V. Chechik and C. J. M. Stirling, “Gold-thiol self-assembled monolayers,” in *The Chemistry of Organic Derivatives of Gold and Silver*, S. Patai and Z. Rappoport, Eds., pp. 551–640, John Wiley & Sons, Ltd., New York, NY, USA, 1999.
- [67] B. Liedberg and J. M. Cooper, “Bioanalytical applications of self-assembled monolayers,” in *Immobilized Biomolecules in Analysis: A Practical Approach*, T. Cass and F. S. Ligler, Eds., pp. 55–78, Oxford University Press, Oxford, UK, 1998.
- [68] P. Laibinis and G. Whitesides, “Comparison of the structures and wetting properties of self-assembled monolayers of n-alkanethiols on the coinage metal surfaces, copper, silver, and gold,” *Journal of the American Chemical Society*, vol. 113, no. 19, pp. 7152–7167, 1991.
- [69] C. D. Bain, E. B. Troughton, Y. T. Tao, J. Evall, G. M. Whitesides, and R. G. Nuzzo, “Formation of monolayer films by the spontaneous assembly of organic thiols from solution onto gold,” *Journal of the American Chemical Society*, vol. 111, no. 1, pp. 321–335, 1989.
- [70] C. D. Bain, J. Evall, and G. M. Whitesides, “Formation of monolayers by the coadsorption of thiols on gold: variation in the head group, tail group, and solvent,” *Journal of the American Chemical Society*, vol. 111, no. 18, pp. 7155–7164, 1989.
- [71] C. D. Bain and G. M. Whitesides, “Molecular-level control over surface order in self-assembled monolayer films of thiols on gold,” *Science*, vol. 240, no. 4848, pp. 62–63, 1988.
- [72] C. Vericat, M. E. Vela, G. Benitez, P. Carro, and R. C. Salvarezza, “Self-assembled monolayers of thiols and dithiols on gold: new challenges for a well-known system,” *Chemical Society Reviews*, vol. 39, no. 5, pp. 1805–1834, 2010.
- [73] C. D. Bain and G. M. Whitesides, “Formation of monolayers by the coadsorption of thiols on gold: variation in the length of the alkyl chain,” *Journal of the American Chemical Society*, vol. 111, no. 18, pp. 7164–7175, 1989.

- [74] S. P. Pujari, L. Scheres, A. T. M. Marcelis, and H. Zuilhof, "Covalent surface modification of oxide surfaces," *Angewandte Chemie International Edition*, vol. 53, no. 25, pp. 6322–6356, 2014.
- [75] Y.-T. Tao, "Structural comparison of self-assembled monolayers of n-alkanoic acids on the surfaces of silver, copper, and aluminum," *Journal of the American Chemical Society*, vol. 115, no. 23, pp. 4350–4358, 1993.
- [76] W. Gao, L. Dickinson, C. Grozinger, F. G. Morin, and L. Reven, "Self-assembled monolayers of alkylphosphonic acids on metal oxides," *Langmuir*, vol. 12, no. 26, pp. 6429–6435, 1996.
- [77] C. Queffelec, M. Petit, P. Janvier, D. A. Knight, and B. Bujoli, "Surface modification using phosphonic acids and esters," *Chemical Reviews*, vol. 112, no. 7, pp. 3777–3807, 2012.
- [78] Y. Paz, "Self-assembled monolayers and titanium dioxide: from surface patterning to potential applications," *Beilstein Journal of Nanotechnology*, vol. 2, no. 1, pp. 845–861, 2011.
- [79] A. Raman, M. Dubey, I. Gouzman, and E. S. Gawalt, "Formation of self-assembled monolayers of alkylphosphonic acid on the native oxide surface of SS316L," *Langmuir*, vol. 22, no. 15, pp. 6469–6472, 2006.
- [80] C. A. Scotchford, E. Cooper, G. J. Leggett, and S. Downes, "Growth of human osteoblast-like cells on alkanethiol on gold self-assembled monolayers: the effect of surface chemistry," *Journal of Biomedical Materials Research*, vol. 41, no. 3, pp. 431–442, 1998.
- [81] C. A. Scotchford, C. P. Gilmore, E. Cooper, G. J. Leggett, and S. Downes, "Protein adsorption and human osteoblast-like cell attachment and growth on alkylthiol on gold self-assembled monolayers," *Journal of Biomedical Materials Research*, vol. 59, no. 1, pp. 84–99, 2002.
- [82] K. B. McClary, T. Ugarova, and D. W. Grainger, "Modulating fibroblast adhesion, spreading, and proliferation using self-assembled monolayer films of alkylthiolates on gold," *Journal of Biomedical Materials Research*, vol. 50, no. 3, pp. 428–439, 2000.
- [83] C. Pale-Grosdemange, E. S. Simon, K. L. Prime, and G. M. Whitesides, "Formation of self-assembled monolayers by chemisorption of derivatives of oligo(ethylene glycol) of structure $\text{HS}(\text{CH}_2)_{11}(\text{OCH}_2\text{CH}_2)_m\text{OH}$ on gold," *Journal of the American Chemical Society*, vol. 113, no. 1, pp. 12–20, 1991.
- [84] K. L. Prime and G. M. Whitesides, "Adsorption of proteins onto surfaces containing end-attached oligo(ethylene oxide): a model system using self-assembled monolayers," *Journal of the American Chemical Society*, vol. 115, no. 23, pp. 10714–10721, 1993.
- [85] E. Ostuni, L. Yan, and G. M. Whitesides, "The interaction of proteins and cells with self-assembled monolayers of alkanethiolates on gold and silver," *Colloids and Surfaces B: Biointerfaces*, vol. 15, no. 1, pp. 3–30, 1999.
- [86] P. Parreira, A. Magalhaes, I. C. Gonaçalves et al., "Effect of surface chemistry on bacterial adhesion, viability, and morphology," *Journal of Biomedical Materials Research Part A*, vol. 99, no. 3, pp. 344–353, 2011.
- [87] G. Cheng, Z. Zhang, S. Chen, J. D. Bryers, and S. Jiang, "Inhibition of bacterial adhesion and biofilm formation on zwitterionic surfaces," *Biomaterials*, vol. 28, no. 29, pp. 4192–4199, 2007.
- [88] S. Hou, E. A. Burton, K. A. Simon, D. Blodgett, Y. Y. Luk, and D. Ren, "Inhibition of *Escherichia coli* biofilm formation by self-assembled monolayers of functional alkanethiols on gold," *Applied and Environmental Microbiology*, vol. 73, no. 13, pp. 4300–4307, 2007.
- [89] E. Ostuni, R. G. Chapman, M. N. Liang et al., "Self-assembled monolayers that resist the adsorption of cells," *Langmuir*, vol. 17, no. 20, pp. 6336–6343, 2001.
- [90] B. Zhu, T. Eurell, R. Gunawan, and D. Leckband, "Chain-length dependence of the protein and cell resistance of oligo(ethylene glycol)-terminated self-assembled monolayers on gold," *Journal of Biomedical Materials Research*, vol. 56, no. 3, pp. 406–416, 2001.
- [91] L. K. Ista, H. Fan, O. Baca, and G. P. López, "Attachment of bacteria to model solid surfaces' oligo(ethylene glycol) surfaces inhibit bacterial attachment," *FEMS Microbiology Letters*, vol. 142, no. 1, pp. 59–63, 1996.
- [92] S. C. Freitas, M. A. Barbosa, and M. C. L. Martins, "The effect of immobilization of thrombin inhibitors onto self-assembled monolayers on the adsorption and activity of thrombin," *Biomaterials*, vol. 31, no. 14, pp. 3772–3780, 2010.
- [93] M. C. L. Martins, V. Ochoa-Mendes, G. Ferreira et al., "Interactions of leukocytes and platelets with poly(lysine/leucine) immobilized on tetraethylene glycol-terminated self-assembled monolayers," *Acta Biomaterialia*, vol. 7, no. 5, pp. 1949–1955, 2011.
- [94] S. C. Freitas, S. Maia, A. C. Figueiredo et al., "Selective albumin-binding surfaces modified with a thrombin-inhibiting peptide," *Acta Biomaterialia*, vol. 10, no. 3, pp. 1227–1237, 2014.
- [95] R. L. C. Wang, H. J. Kreuzer, and M. Grunze, "Molecular conformation and solvation of oligo(ethylene glycol)-terminated self-assembled monolayers and their resistance to protein adsorption," *Journal of Physical Chemistry B*, vol. 101, no. 47, pp. 9767–9773, 1997.
- [96] R. Y. Wang, M. Himmelhaus, J. Fick, S. Herrwerth, W. Eck, and M. Grunze, "Interaction of self-assembled monolayers of oligo(ethylene glycol)-terminated alkanethiols with water studied by vibrational sum-frequency generation," *Journal of Chemical Physics*, vol. 122, no. 16, p. 164702, 2005.
- [97] P. Harder, M. Grunze, R. Dahint, G. M. Whitesides, and P. E. Laibinis, "Molecular conformation in oligo(ethylene glycol)-terminated self-assembled monolayers on gold and silver surfaces determines their ability to resist protein adsorption," *Journal of Physical Chemistry B*, vol. 102, no. 2, pp. 426–436, 1998.
- [98] M. Zolk, F. Eisert, J. Pipper et al., "Solvation of oligo(ethylene glycol)-terminated self-assembled monolayers studied by vibrational sum frequency spectroscopy," *Langmuir*, vol. 16, no. 14, pp. 5849–5852, 2000.
- [99] M. Zwahlen, S. Herrwerth, W. Eck, M. Grunze, and G. Hähner, "Conformational order in oligo(ethylene glycol)-terminated self-assembled monolayers on gold determined by soft X-ray absorption," *Langmuir*, vol. 19, no. 22, pp. 9305–9310, 2003.
- [100] N. M. Green, "Avidin and streptavidin," *Methods in Enzymology*, Elsevier, vol. 184pp. 51–67, Elsevier, Amsterdam, Netherlands, 1990.
- [101] V. H. Pérez-Luna, M. J. O'Brien, K. A. Opperman et al., "Molecular recognition between genetically engineered streptavidin and surface-bound biotin," *Journal of the American Chemical Society*, vol. 121, no. 12, pp. 6469–6478, 1999.
- [102] L. Häußling, H. Ringsdorf, F. J. Schmitt, and W. Knoll, "Biotin-functionalized self-assembled monolayers on gold: surface plasmon optical studies of specific recognition reactions," *Langmuir*, vol. 7, no. 9, pp. 1837–1840, 1991.
- [103] J. Spinke, M. Liley, H. J. Guder, L. Angermaier, and W. Knoll, "Molecular recognition at self-assembled monolayers: the

- construction of multicomponent multilayers," *Langmuir*, vol. 9, no. 7, pp. 1821–1825, 1993.
- [104] J. Spinke, M. Liley, F. J. Schmitt, H. J. Guder, L. Angermaier, and W. Knoll, "Molecular recognition at a self-assembled monolayers: optimization of surface functionalization," *Journal of Chemical Physics*, vol. 99, no. 9, pp. 7012–7019, 1993.
- [105] L. S. Jung, K. E. Nelson, C. T. Campbell et al., "Surface plasmon resonance measurement of binding and dissociation of wild-type and mutant streptavidin on mixed biotin-containing alkylthiolate monolayers," *Sensors and Actuators B: Chemical*, vol. 54, no. 1, pp. 137–144, 1999.
- [106] G. B. Sigal, C. Bamdad, A. Barberis, J. Strominger, and G. M. Whitesides, "A self-assembled monolayer for the binding and study of histidine-tagged proteins by surface plasmon resonance," *Analytical Chemistry*, vol. 68, no. 3, pp. 490–497, 1996.
- [107] S. C. Freitas, T. B. Cereija, A. C. Figueiredo et al., "Bio-engineered surfaces to improve the blood compatibility of biomaterials through direct thrombin inactivation," *Acta Biomaterialia*, vol. 8, no. 11, pp. 4101–4110, 2012.
- [108] B. T. Houseman, E. S. Gawalt, and M. Mrksich, "Maleimide-functionalized self-assembled monolayers for the preparation of peptide and carbohydrate biochips," *Langmuir*, vol. 19, no. 5, pp. 1522–1531, 2003.
- [109] K. V. Gujrati, R. Ashton, S. R. Bethi et al., "Thiol-mediated anchoring of ligands to self-assembled monolayers for studies of biospecific interactions," *Langmuir*, vol. 22, no. 24, pp. 10157–10162, 2006.
- [110] G. A. Hudalla and W. L. Murphy, "Using "click" chemistry to prepare SAM substrates to study stem cell adhesion," *Langmuir*, vol. 25, no. 10, pp. 5737–5746, 2009.
- [111] W. L. Murphy, K. O. Mercurius, S. Koide, and M. Mrksich, "Substrates for cell adhesion prepared via active site-directed immobilization of a protein domain," *Langmuir*, vol. 20, no. 4, pp. 1026–1030, 2004.
- [112] M. N. Yousaf, B. T. Houseman, and M. Mrksich, "Turning on cell migration with electroactive substrates," *Angewandte Chemie International Edition*, vol. 40, no. 6, pp. 1093–1096, 2001.
- [113] M. C. Martins, E. Naemi, B. D. Ratner, and M. A. Barbosa, "Albumin adsorption on cibacron blue F3G-A immobilized onto oligo(ethylene glycol)-terminated self-assembled monolayers," *Journal of Materials Science: Materials in Medicine*, vol. 14, no. 11, pp. 945–954, 2003.
- [114] I. C. Gonçalves, M. C. L. Martins, J. N. Barbosa, P. Oliveira, M. A. Barbosa, and B. D. Ratner, "Platelet and leukocyte adhesion to albumin binding self-assembled monolayers," *Journal of Materials Science: Materials in Medicine*, vol. 22, no. 9, pp. 2053–2063, 2011.
- [115] M. C. L. Martins, S. A. Curtin, S. C. Freitas, P. Salgueiro, B. D. Ratner, and M. A. Barbosa, "Molecularly designed surfaces for blood deheparinization using an immobilized heparin-binding peptide," *Journal of Biomedical Materials Research Part A*, vol. 88, no. 1, pp. 162–173, 2009.
- [116] J. N. Barbosa, M. C. L. Martins, S. C. Freitas, I. C. Gonçalves, A. Aguas, and M. A. Barbosa, "Adhesion of human leukocytes on mixtures of hydroxyl- and methyl-terminated self-assembled monolayers: effect of blood protein adsorption," *Journal of Biomedical Materials Research Part A*, vol. 93, no. 1, pp. 12–19, 2010.
- [117] M. Hölzl, A. Tinazli, C. Leitner et al., "Protein-resistant self-assembled monolayers on gold with latent aldehyde functions," *Langmuir*, vol. 23, no. 10, pp. 5571–5577, 2007.
- [118] R. G. Chapman, E. Ostuni, L. Yan, and G. M. Whitesides, "Preparation of mixed self-assembled monolayers (SAMs) that resist adsorption of proteins using the reaction of amines with a SAM that presents interchain carboxylic anhydride groups," *Langmuir*, vol. 16, no. 17, pp. 6927–6936, 2000.
- [119] J. Lahiri, L. Isaacs, J. Tien, and G. M. Whitesides, "A strategy for the generation of surfaces presenting ligands for studies of binding based on an active ester as a common reactive intermediate: a surface plasmon resonance study," *Analytical Chemistry*, vol. 71, no. 4, pp. 777–790, 1999.
- [120] O. Azzaroni, M. Mir, and W. Knoll, "Supramolecular architectures of streptavidin on biotinylated self-assembled monolayers. Tracking biomolecular reorganization after bioconjugation," *Journal of Physical Chemistry B*, vol. 111, no. 48, pp. 13499–13503, 2007.
- [121] L. S. Jung, K. E. Nelson, P. S. Stayton, and C. T. Campbell, "Binding and dissociation kinetics of wild-type and mutant streptavidins on mixed biotin-containing alkylthiolate monolayers," *Langmuir*, vol. 16, no. 24, pp. 9421–9432, 2000.
- [122] K. E. Nelson, L. Gamble, L. S. Jung et al., "Surface characterization of mixed self-assembled monolayers designed for streptavidin immobilization," *Langmuir*, vol. 17, no. 9, pp. 2807–2816, 2001.
- [123] J. H. Rao, L. Yan, B. Xu, and G. M. Whitesides, "Using surface plasmon resonance to study the binding of vancomycin and its dimer to self-assembled monolayers presenting d-Ala-d-Ala," *Journal of the American Chemical Society*, vol. 121, no. 16, pp. 2629–2630, 1999.
- [124] A. Subramanian, J. Irudayaraj, and T. Ryan, "A mixed self-assembled monolayer-based surface plasmon immunosensor for detection of *E. coli* O157:H7," *Biosensors and Bioelectronics*, vol. 21, no. 7, pp. 998–1006, 2006.
- [125] V. Humblot, J. F. Yala, P. Thebault et al., "The antibacterial activity of magainin I immobilized onto mixed thiols self-assembled monolayers," *Biomaterials*, vol. 30, no. 21, pp. 3503–3512, 2009.
- [126] P. Parreira, A. Magalhães, C. A. Reis, T. Borén, D. Leckband, and M. C. L. Martins, "Bioengineered surfaces promote specific protein-glycan mediated binding of the gastric pathogen *Helicobacter pylori*," *Acta Biomaterialia*, vol. 9, no. 11, pp. 8885–8893, 2013.
- [127] F. A. Durmaz, "Modular approach to functional self-assembled monolayers," ETH Zurich, Zürich, Switzerland-ETH Zurich, 2006 Doctoral thesis, Thesis.
- [128] R. Hofer, "Surface modification for optical biosensor applications," ETH Zurich, Zürich, Switzerland-ETH Zurich, 2000 Ph.D. thesis, Thesis.
- [129] P. H. Mutin, G. Guerrero, and A. Vioux, "Hybrid materials from organophosphorus coupling molecules," *Journal of Materials Chemistry*, vol. 15, no. 35–36, pp. 3761–3768, 2005.
- [130] R. Hofer, M. Textor, and N. D. Spencer, "Alkyl phosphate monolayers, self-assembled from aqueous solution onto metal oxide surfaces," *Langmuir*, vol. 17, no. 13, pp. 4014–4020, 2001.
- [131] R. Helmy and A. Y. Fadeev, "Self-assembled monolayers supported on TiO₂: comparison of C₁₈H₃₇SiX₃ (X = H, Cl, OCH₃), C₁₈H₃₇Si(CH₃)₂Cl, and C₁₈H₃₇PO(OH)₂," *Langmuir*, vol. 18, no. 23, pp. 8924–8928, 2002.
- [132] A. Raman, R. Quiñones, L. Barriger, R. Eastman, A. Parsi, and E. S. Gawalt, "Understanding organic film behavior on alloy and metal oxides," *Langmuir*, vol. 26, no. 3, pp. 1747–1754, 2010.
- [133] E. S. Gawalt, M. J. Avaltroni, N. Koch, and J. Schwartz, "Self-assembly and bonding of alkanephosphonic acids on the

- native oxide surface of titanium,” *Langmuir*, vol. 17, no. 19, pp. 5736–5738, 2001.
- [134] G. Hähner, R. Hofer, and I. Klingenfuss, “Order and orientation in self-assembled long chain alkanephosphate monolayers adsorbed on metal oxide surfaces,” *Langmuir*, vol. 17, no. 22, pp. 7047–7052, 2001.
- [135] S. Clair, F. Variola, M. Kondratenko et al., “Self-assembled monolayer of alkanephosphoric acid on nanotextured Ti,” *Journal of Chemical Physics*, vol. 128, no. 14, pp. 1–7, 2008.
- [136] D. M. Spori, N. V. Venkataraman, S. G. P. Tosatti, F. Durmaz, N. D. Spencer, and S. Zürcher, “Influence of alkyl chain length on phosphate,” *Langmuir*, vol. 23, no. 15, pp. 8053–8060, 2007.
- [137] G. Lecollinet, N. Delorme, M. Edely et al., “Self-assembled monolayers of bisphosphonates: influence of side chain steric hindrance,” *Langmuir*, vol. 25, no. 14, pp. 7828–7835, 2009.
- [138] E. S. Gawalt, M. J. Avaltroni, M. P. Danahy et al., “Bonding organics to Ti alloys: facilitating human osteoblast attachment and spreading on surgical implant materials,” *Langmuir*, vol. 19, no. 1, pp. 200–204, 2003.
- [139] J. Schwartz, M. J. Avaltroni, M. P. Danahy et al., “Cell attachment and spreading on metal implant materials,” *Materials Science and Engineering: C*, vol. 23, no. 3, pp. 395–400, 2003.
- [140] M. P. Danahy, M. J. Avaltroni, K. S. Midwood, J. E. Schwarzbauer, and J. Schwartz, “Self-assembled monolayers of α,ω -diphosphonic acids on Ti enable complete or spatially controlled surface derivatization,” *Langmuir*, vol. 20, no. 13, pp. 5333–5337, 2004.
- [141] N. Adden, L. J. Gamble, D. G. Castner, A. Hoffmann, G. Gross, and H. Menzel, “Phosphonic acid monolayers for binding of bioactive molecules to titanium surfaces,” *Langmuir*, vol. 22, no. 19, pp. 8197–8204, 2006.
- [142] H. Mutin, G. Guerrero, and J. Amalric, “Preparation of an inorganic substrate having antimicrobial properties,” US 8586758 B2, 2007.
- [143] J. Amalric, P. H. Mutin, G. Guerrero, A. Ponche, A. Sotto, and J.-P. Lavigne, “Phosphonate monolayers functionalized by silver thiolate species as antibacterial nanocoatings on titanium and stainless steel,” *Journal of Materials Chemistry*, vol. 19, no. 1, pp. 141–149, 2009.
- [144] C. M. Tilmaciu, M. Mathieu, J. P. Lavigne et al., “In vitro and in vivo characterization of antibacterial activity and biocompatibility: a study on silver-containing phosphonate monolayers on titanium,” *Acta Biomaterialia*, vol. 15, pp. 266–277, 2015.
- [145] Q. Liu, J. Ding, F. K. Mante, S. L. Wunder, and G. R. Baran, “The role of surface functional groups in calcium phosphate nucleation on titanium foil: a self-assembled monolayer technique,” *Biomaterials*, vol. 23, no. 15, pp. 3103–3111, 2002.
- [146] D. P. Liu, P. Majewski, B. K. O’Neill, Y. Ngothai, and C. B. Colby, “The optimal SAM surface functional group for producing a biomimetic HA coating on Ti,” *Journal of Biomedical Materials Research Part A*, vol. 77, no. 4, pp. 763–772, 2006.
- [147] J. Wu, I. Hirata, X. Zhao, B. Gao, M. Okazaki, and K. Kato, “Influence of alkyl chain length on calcium phosphate deposition onto titanium surfaces modified with alkylphosphonic acid monolayers,” *Journal of Biomedical Materials Research Part A*, vol. 101, no. 8, pp. 2267–2272, 2013.
- [148] S. Tosatti, R. Michel, M. Textor, and N. D. Spencer, “Self-assembled monolayers of dodecyl and hydroxy-dodecyl phosphates on both smooth and rough titanium and titanium oxide surfaces,” *Langmuir*, vol. 18, no. 9, pp. 3537–3548, 2002.
- [149] M. Zwahlen, S. Tosatti, M. Textor, G. Hähner, and G. Hähner, “Orientation in methyl- and hydroxyl-terminated self-assembled alkanephosphate monolayers on titanium oxide surfaces investigated with soft X-ray absorption,” *Langmuir*, vol. 18, no. 10, pp. 3957–3962, 2002.
- [150] C. Viorner, Y. Chevolut, D. Léonard et al., “Surface modification of titanium with phosphonic acid to improve bone bonding: characterization by XPS and ToF-SIMS,” *Langmuir*, vol. 18, no. 7, pp. 2582–2589, 2002.
- [151] C. Viorner, H. L. Guenther, B. O. Aronsson, P. Péchy, P. Descouts, and M. Grätzel, “Osteoblast culture on polished titanium disks modified with phosphonic acids,” *Journal of Biomedical Materials Research*, vol. 62, no. 1, pp. 149–155, 2002.
- [152] G. Mani, D. M. Johnson, D. Marton et al., “Drug delivery from gold and titanium surfaces using self-assembled monolayers,” *Biomaterials*, vol. 29, no. 34, pp. 4561–4573, 2008.
- [153] G. Mani, B. Chandrasekar, M. D. Feldman, D. Patel, and C. M. Agrawal, “Interaction of endothelial cells with self-assembled monolayers for potential use in drug-eluting coronary stents,” *Journal of Biomedical Materials Research Part B: Applied Biomaterials*, vol. 90, no. 2, pp. 789–801, 2009.
- [154] K. Rudzka, A. Y. Sanchez Treviño, M. A. Rodríguez-Valverde, and M. A. Cabrerizo-Vílchez, “Formation of mixed and patterned self-assembled films of alkylphosphonates on commercially pure titanium surfaces,” *Applied Surface Science*, vol. 389, pp. 270–277, 2016.
- [155] L. Rojo, B. Gharibi, R. McLister, B. J. Meenan, and S. Deb, “Self-assembled monolayers of alendronate on Ti6Al4V alloy surfaces enhance osteogenesis in mesenchymal stem cells,” *Scientific Reports*, vol. 6, no. 1, p. 30548, 2016.
- [156] E. Byun, J. Kim, S. M. Kang, H. Lee, D. Bang, and H. Lee, “Surface PEGylation via native chemical ligation,” *Bioconjugate Chemistry*, vol. 22, no. 1, pp. 4–8, 2011.
- [157] J. Vaithilingam, S. Kilsby, R. D. Goodridge, S. D. R. Christie, S. Edmondson, and R. J. M. Hague, “Immobilisation of an antibacterial drug to Ti6Al4V components fabricated using selective laser melting,” *Applied Surface Science*, vol. 314, pp. 642–654, 2014.
- [158] J. Vaithilingam, S. Kilsby, R. D. Goodridge, S. D. R. Christie, S. Edmondson, and R. J. M. Hague, “Functionalisation of Ti6Al4V components fabricated using selective laser melting with a bioactive compound,” *Materials Science and Engineering: C*, vol. 46, pp. 52–61, 2015.
- [159] M. Gnauck, E. Jaehne, T. Blaettler, S. Tosatti, M. Textor, and H. J. P. Adler, “Carboxy-terminated oligo(ethylene glycol)-alkane phosphate: synthesis and self-assembly on titanium oxide surfaces,” *Langmuir*, vol. 23, no. 2, pp. 377–381, 2007.
- [160] S. Bozzini, P. Petrini, M. C. Tanzi, S. Zürcher, and S. Tosatti, “Poly(ethylene glycol) and hydroxy functionalized alkane phosphate mixed self-assembled monolayers to control nonspecific adsorption of proteins on titanium oxide surfaces,” *Langmuir*, vol. 26, no. 9, pp. 6529–6534, 2010.
- [161] S. Bozzini, P. Petrini, M. C. Tanzi, C. R. Arciola, S. Tosatti, and L. Visai, “Poly(ethylene glycol) and hydroxy functionalized alkane phosphate self-assembled monolayers reduce bacterial adhesion and support osteoblast proliferation,” *International Journal of Artificial Organs*, vol. 34, no. 9, pp. 898–907, 2011.
- [162] L. Tack, K. Schickle, F. Böke, and H. Fischer, “Immobilization of specific proteins to titanium surface using self-assembled monolayer technique,” *Dental Materials*, vol. 31, no. 10, pp. 1169–1179, 2015.
- [163] G. Tan, K. Ouyang, H. Wang et al., “Effect of amino-, methyl- and epoxy-silane coupling as a molecular bridge for

formatting a biomimetic hydroxyapatite coating on titanium by electrochemical deposition,” *Journal of Materials Science & Technology*, vol. 32, no. 9, pp. 956–965, 2016.

- [164] J. Shen, Y. Qi, B. Jin, X. Wang, Y. Hu, and Q. Jiang, “Control of hydroxyapatite coating by self-assembled monolayers on titanium and improvement of osteoblast adhesion,” *Journal of Biomedical Materials Research Part B: Applied Biomaterials*, vol. 105, no. 1, pp. 124–135, 2015.
- [165] M. Nishida, T. Nakaji-Hirabayashi, H. Kitano, Y. Saruwatari, and K. Matsuoka, “Titanium alloy modified with anti-biofouling zwitterionic polymer to facilitate formation of bio-mineral layer,” *Colloids and Surfaces B: Biointerfaces*, vol. 152, pp. 302–310, 2017.

Clinical Study

Double Guided Surgery in All-on-4[®] Concept: When Osteotomy Is Needed

Gabriele Tonellini , **Raquel Saez Vigo** , and **Giorgio Novelli**

San Gerardo Hospital, Department of Maxillofacial Surgery, University of Milano-Bicocca, Milan, Italy

Correspondence should be addressed to Raquel Saez Vigo; raquelsaezvigo@gmail.com

Received 27 June 2017; Revised 28 November 2017; Accepted 11 December 2017; Published 4 February 2018

Academic Editor: Silvio M. Meloni

Copyright © 2018 Gabriele Tonellini et al. This is an open access article distributed under the Creative Commons Attribution License, which permits unrestricted use, distribution, and reproduction in any medium, provided the original work is properly cited.

Background. The rehabilitation of edentulous jaws with guided and flapless surgery applied to the All-on-4 concepts is a predictable treatment with a high implant and prosthetic survival rates, but there are several contraindications for this technique like when bone reduction is needed due to a high smile line in the maxilla or when there is an irregular or thin bone crest. *Purpose.* To report a technique with double guided surgery for bone reduction and implant placement with the All-on-4 concept. *Materials and Methods.* 7 patients were included in the study. Guided implant planning was performed using CBCT, and the virtual templates were created with three dedicated software. Custom surgical templates were made for the osteotomy and for implants positioning. *Results.* 28 implants were placed using a double bone-supported surgical guide. The mean angular errors between the preoperative-planned implant and the postoperative-placed implant were $2.155^\circ \pm 2.03^\circ$; the mean distance errors between the planned and the placed implants were $0.763 \text{ mm} \pm 0.55 \text{ mm}$ on the shoulder implant and $0.570 \text{ mm} \pm 0.40 \text{ mm}$ on the apex implant. *Conclusions.* The results of our study indicate that this treatment is predictable with an excellent survival rate allowing excellent results even when bone reduction is mandatory.

1. Introduction

One of most important things for edentulous rehabilitation is to optimize the patient's treatment and comfort in the fastest and safest way. In the last years, the use of one-stage surgical protocols with immediate function has demonstrated to be an effective treatment in full or partial-arch edentulous rehabilitation, giving patients the chance of having a fixed dentition as soon as possible [1].

Sometimes, the lost of posterior teeth of the mandible can make complex the treatment plan because of the impediment in using the alveolar bone posterior to the inferior alveolar nerve without the addition of complicate surgical steps like bone grafting procedures or nerve transposition [2].

The same can happen in the maxilla when the atrophic bone makes difficult the rehabilitation without a sinus lift.

The All-on-4 treatment concept introduced by Maló allows the rehabilitation of edentulous jaws without bone

graft in one surgical step through the placement of 4 implants, optimizing the available bone. The implants are placed two posteriorly tilted between 30° and 45° and two anteriorly axial, well anchored achieving a primary stability of at least 30 Ncm. The survival rate implant related was 98% for the maxilla and 98.1% for the mandible after 5 to 10 years of follow-up [3–5]. The use of tilted and longer implants increases primary stability, allows cantilever decrease with excellent prosthetic support, and maximizes the use of available bone [6].

The clinical outcome of optimal implant placement is based on precise preoperative planning. Computer-aided surgery techniques are suggested for reaching a precise implant position avoiding lesions for important anatomical structures such as the maxillary sinus or the mandibular nerve [7].

Several authors introduce a variance from the protocol presented by Maló using the guided surgery for the All-on-4 procedure [8, 9]. According to the guided surgery protocol,

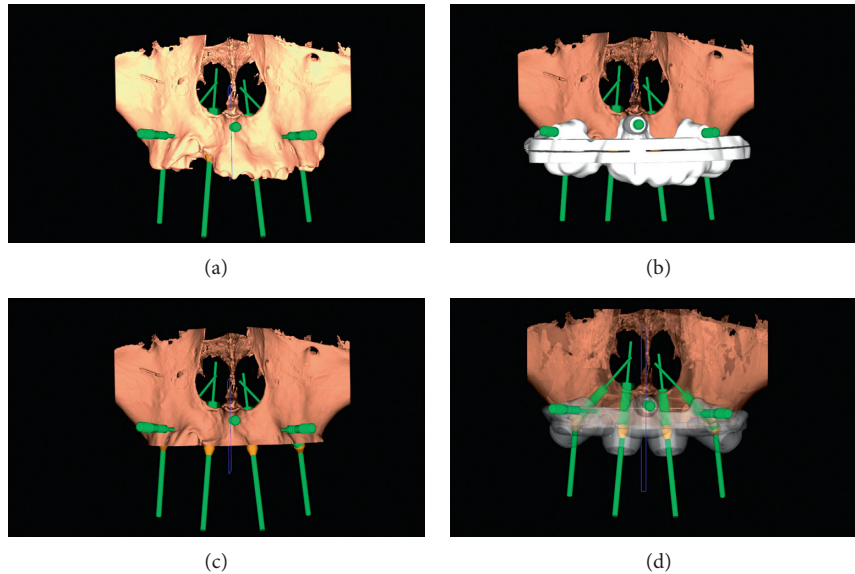


FIGURE 1: (a) 3D implant planning. (b) Resection guide. (c) 3D implant planning with osteotomy performed. (d) Implant guide.

a surgical guide is made based on data obtained through CBCT [10].

Naziri et al. have proven the precision and predictability of implant placement when using CAD-CAM surgical guides based on CBCT. The analysis of Naziri shows a median deviation between preoperative plan and post-operative implant positions of 1 mm at the implant shoulder and 1.4 mm at the implant apex, with a median angular deviation of 3.6° [11].

There are three kinds of tissue that can sustain stereolithographic surgical guides: bone, mucosa, and tooth. The first templates used for the treatment of edentulous full-arch were the bone-supported guides. In 2006, Fortin et al. introduced the flapless surgical technique with mucosa- and tooth-supported template. This is a minimally invasive technique that allows us to decrease surgical time, patient discomfort, postoperative bleeding, and the healing period, but it is important to remember that bone template provides the best visualization of the surgical field, allowing for better control of the whole procedure [7, 12, 13].

The results of Maló studies suggest that the rehabilitation of edentulous jaws using surgical planning and surgical-customized templates with prosthetic rehabilitation through CBCT, CAD-CAM technology, and flapless surgery is a predictable treatment with a high implant and prosthetic survival rates when is applied to the All-on-4 concept. However, there are several contraindications for this technique; one of the most important is when bone reduction is necessary due to a gummy smile in the maxilla or when an irregular or thin bone crest in the jaws prevents a correct treatment [6].

The smile line must be considered when planning an implant-supported fixed prosthesis. We must ensure that the prosthesis tissue junction (PTJ) is not visible during the patient's maximum smile. This is primarily because of

the difficulty to match with precision of the colour of the prosthetic gingiva with the natural gingival tissues [14–17].

The second cause for bone reduction is to allow adequate implant and prosthetic space. In all these cases, it is necessary to perform a bone reduction or osteotomy of the jaws, but it is no easy to know how many bone it must be reduced; underreduction of bone can lead to prosthetic failure, and overreduction of bone can produce a divestment of available bone and risks encroachment of vital anatomic structures [14–16].

This article describes a technique with double-guided surgery for bone reduction and implant placement in the All-on-4 concept, avoiding risks of vital anatomic structures and guarantying a good aesthetic result. This protocol can be used with edentulous patients and also patients with failure dentition.

2. Materials and Methods

Seven patients with edentulous or partial edentulous arches were included and treated in 3 private center practices. The patients were 45 to 72 years old.

A total of 28 implants were placed between February 2015 and October 2016.

The treatment's plannings were performed always by the same surgeon.

Four implants were placed in the maxilla and 24 implants in the mandible. One osteotomy guide was used in the maxilla, and 6 were used in the mandible.

The procedure and the evaluation of the aesthetic parameters were based on a planning data and 2D photographs. A prosthesis was manufactured prior to the implant surgery and was immediately inserted after surgery.

Panoramic radiographs and CT scan were examined.

Patients with minimum bone volume available with thin crest bone or with gingival display to perform an All-on-4

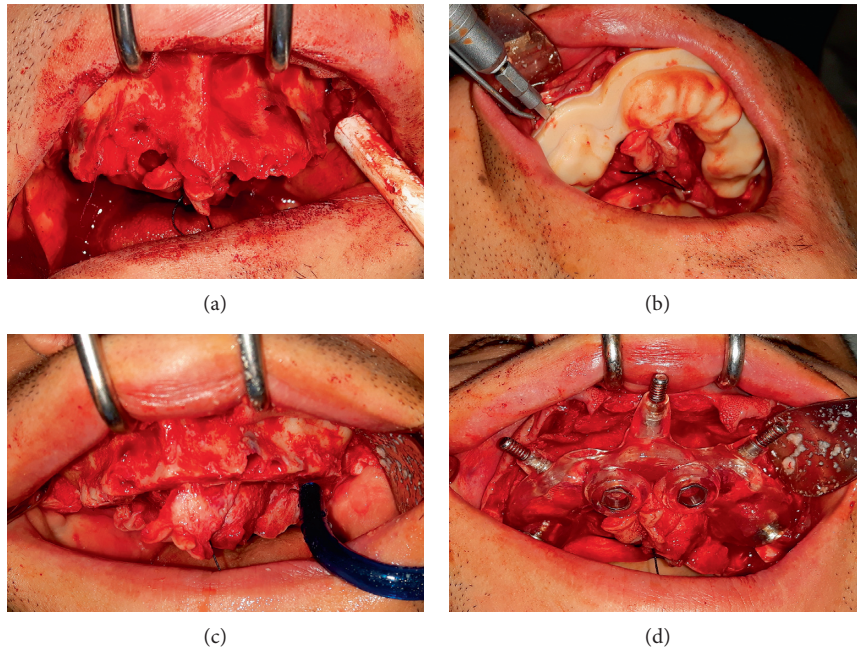


FIGURE 2: (a) Maxillary postextraction. (b) Osteotomy performed by saw through the guide. (c) Removal of the osteotomized bone. (d) Implant guide placed on the same holes used to fix the resection guide.



FIGURE 3: Super imposition of the postop CT scan and the preop 3D panning.

rehabilitation were selected, so patients with bone reduction were needed.

2.1. Planning Protocol. Guided implant planning was performed using CBCT, and computer-assisted implant treatment planning software 3Diagnosis (3Diemme, Cantù, Italy), Mimics 10.01 (Materialise, Leuven, Belgium), and PlastyCAD 1.5 (3Diemme) were used to create the virtual templates.

Custom surgical templates were made for the osteotomy and for implants position (3Diemme, Cantù, Italy) (Figure 1).

The planning protocol includes alveolar osteotomy of the maxilla up to 2 mm from line smile when there was a gingival display and as much as necessary bone reduction when there was an irregular or thin crest in the maxilla or in the mandible. The measurements were

made directly on the patient and then reported to the software.

The implants were planned according to the All-on-4 protocol, two tilted and two axial, to take advantage of the available bone. The implants were not prosthetically driven.

The STL file of templates was then sent to fabricate. These templates were made in all-acrylic resin with 3D DWS Digitalwax 020D printer that could print with a minimum of 0.01 mm thickness.

2.2. Surgical Protocol. The surgical procedures for both jaws were performed under local anaesthesia with sedation. Antibiotics (clavulanic acid + amoxicillin) were given 1 hour before surgery and daily for six days thereafter. Prednisone was administrated daily in a regression mode (from 15 mg to



FIGURE 4: (a) Preop clinical presentation. Partially edentulous with high mobility of the teeth and gummy smile. (b) Immediate postop with provisional prosthesis. With ostectomy of the maxilla we correct the defect of the patient's smile.

TABLE 1: Accuracy: angular and distance errors.

Patient	Position of implant	Angular error (°)	Shoulder error (mm)	Apical error (mm)
1	#45	0.65	0.1	0
	#42	0	0.1	0.5
	#32	3.37	1.37	1.09
	#35	4.19	0.91	0.72
2	#15	0.67	0.59	0.75
	#12	3.40	0.45	0.66
	#22	4.11	1.33	0.82
3	#25	0.83	1.77	0.20
	#45	0	0.75	0.1
	#42	2.21	0.47	0.42
	#32	9.49	0.36	1.82
4	#35	2.99	0.40	0.89
	#45	5.56	1.22	0.27
	#42	1.09	0.39	0.58
	#32	0	0	0
5	#35	0.79	0.80	0.42
	#45	2.03	1.01	0.32
	#42	1.01	0.30	0.65
	#32	3	0.81	0.87
6	#35	1.05	0.93	0.41
	#45	0.80	0.23	0.29
	#42	2.03	1.76	1.05
	#32	1.10	1.14	0.58
7	#35	3.01	0.89	0.27
	#45	3.21	1.79	1.20
	#42	0.65	0.40	0.46
	#32	2.20	0.95	0.62
	#35	0.9	0.32	0.31
Mean ± standard deviation	—	2.155 ± 2.03	0.763 ± 0.55	0.570 ± 0.40

5 mg) from the day of surgery until 4 days postoperatively. Analgesics were given for 4 days and then just if needed.

A mucosal incision was made to raise a mucoperiosteal flap; the bone-supported surgical template for ostectomy was positioned and fixed with three anchor pins. Then the ostectomy was performed with a saw (W&H).

After the ostectomy, the second template was fixed in the same holes of the first anchor pins. The precise fit of surgical templates was visually and manually checked before surgery.

Implants were placed through the sleeves of the surgical template in the planning anatomic sites (Figure 2). Four different types of implants were used, *Nobel speedy*,

Nobel parallel CC, *Prodent twinner collar*, and *Leader Implus*, depending on the preference of implant connection required by the dentist. The implant site was under preparation according to the bone density achieving an insertion torque of 35 to 50 Nmc in the maxilla, and 30 to 70 Nmc in the mandible was applied to obtain a primary stability for loading immediately the fixed denture prosthesis.

2.3. Immediate Provisional Prosthetic Protocol. Implant-supported fixed prosthesis of high-density acrylic resin with titanium cylinders were manufactured at the dental laboratory and inserted at the same day. The provisional

TABLE 2: Implant survival rate.

	Patient 1	Patient 2	Patient 3	Patient 4	Patient 5	Patient 6	Patient 7
Number of implants stable	4	4	4	4	4	4	4
Number of implants functional	4	4	4	4	4	4	4
Number of implants with infection	0	0	0	0	0	0	0
Number of implants with radiolucent areas	0	0	0	0	0	0	0

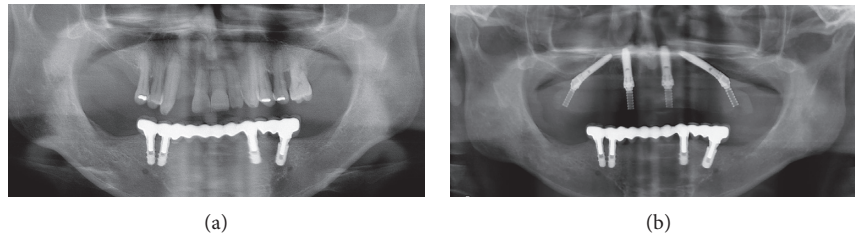


FIGURE 5: Pre- and post-OPG. In the postop OPG, we can see the guided osteotomy of the maxilla and the implants positioning.

TABLE 3: Aesthetic parameter results.

	Patient 1	Patient 2	Patient 3	Patient 4	Patient 5	Patient 6	Patient 7
PTJ visible	No						
Black space posterior	No						

prosthesis was positioned in the mouth using the patient's occlusion. Just anterior occlusal contacts were preferred in the provisional prosthesis, and no cantilevers were used. Emergence positions at the posterior implants were normally at the second premolar or first molar allowing the prosthesis to hold 10 to 12 teeth [18].

2.4. Outcome Measures. The first parameter evaluated was the accuracy of implants position according to the surgical planning. It was confronted that the 3D CT scan reconstruction of the planning is obtained with 3Diagnosis software with a postsurgery CT scan. In order to analyse differences between preoperative planned implants and postoperative placed implants, angular errors and distance errors were evaluated [19] (Figure 3).

The second outcome evaluated was the implant survival rates. To analyse this parameter, Maló Clinic survival criteria were used: clinical stability, function without any discomfort, absence of suppuration, infection, or radiolucent areas around the implants during the follow-up [6].

The third and last outcome evaluated was the aesthetic of smile with the fixed complete denture prosthesis. "Dental aesthetics" has been defined as "the application of the principles of esthetics to the natural or artificial teeth and restorations." It is difficult to find studies in the literature that can be considered as evidence based. The parameters considered in this study were the concealment of prosthesis tissue junction and an adequate posterior tooth extension to avoid "black space" behind the prosthesis [15, 16] (Figure 4).

3. Results

Twenty-eight implants were placed in 7 patients, and all implants were inserted using bone-supported surgical guide, created with 3 dedicated software. To place the implants, the All-on-4 protocol was performed. All implants were loaded immediately.

The angular and distance errors are summarized in Table 1. The mean angular error between the preoperative planned implant and the postoperative placed implant was 2.155 ± 2.03 ; the mean distance errors between the planned and the placed implants were 0.763 ± 0.55 on the shoulder implant and 0.570 ± 0.40 on the apex implant.

Life table analysis is reported in Table 2. At one year of follow-up, 0 implants failed, resulting in a cumulative implant survival rate of 100%; all implants are functional with 0% of infection or radiolucent areas. It was not reported any complication during the entire follow-up.

In all patients, the prosthesis tissue junction was not visible during the maximum smile, and there was no black space posterior on prosthesis. The aesthetic result evaluated from patients was excellent (Figure 5). The aesthetic parameters results are summarized in Table 3.

4. Discussion

The present study was planned to estimate the accuracy of implants position, the survival rate of implants placed, and the aesthetic of smile using a new protocol that expects a double surgical guide. The first guide is to perform an osteotomy in all cases when bone reduction is mandatory,

and the second guide is to place the implants in a perfect position to avoid anatomical damages and avoiding bone grafts. The protocol was planned first virtually with computer-assisted planning software, and the virtual templates with bone support were created. Computer-guided implant surgery consents accurate implant positioning with safety application and has the advantage of surgical time reduction and the optimization of available bone [20]. The templates used were bone supported as we must raise the flap to perform the bone reduction; this kind of templates provides better accuracy than conventional flapless guides because the limiting factor of soft tissue is removed after flap elevation [7]. The fit of template was based on bone anatomy, and the soft tissue does not interfere with it. Our technique offers the option to fabricate a guide with increased thickness that improves the mechanical proprieties avoiding the fracture of the guide during the surgery.

With this method it is not necessary to use the classic protocol of double CT scanning, like flapless guided surgery, to obtain the gingival surface because we use only bone surface to create the template. So the time and the final cost of the treatment were reduced. Another advantage over the free-hand approach is the precision of implant positioning using all distal available bone and the accuracy of the millimeters of ostectomy.

The results of this study are in agreement with previously published works [20–25].

The transfer of the virtual planning to the surgical template for the operation time results in a very accurate technique.

Nowadays, it is mandatory to expect the best aesthetic results so as to correct the excessive gingival display which becomes also a priority, such as to prevent black spaces posterior in the final prosthesis and a good outcome to the PTJ. It does not exist as a simple technique to perform bone reduction with a guided surgery in a safest and quick way [26–28].

5. Conclusions

The results of this preliminary study suggest that this treatment modality for total or partial edentulous patients is predictable with an excellent implant survival rate. By combining 3D planning for a double surgical guide, the All-on-4 protocol, and immediate loading implants, it is possible to increase the advantages of each one, resulting in a more accurate and safer technique with high predictable results. Patients can rehabilitate full-arches even when bone reduction is mandatory because of a gummy smile or because of an irregular or thin bone crest. Our technique demonstrated excellent aesthetic outcomes with a reduction surgery time without any complication.

Conflicts of Interest

The authors declare that they have no conflicts of interest.

Authors' Contributions

All the authors contributed to concept and design of the study, were involved in acquisition, analysis, and interpretation of

the data and in writing and revision of the article, and approved the final version to be published.

References

- [1] A. Lopes, P. Maló, M. De Araujo Nobre, and E. Sanchez-Fernández, “The NobelGuide All-on-4 treatment concept for rehabilitation of edentulous jaws: a prospective Report on Medium and long term outcomes,” *Clinical Implant Dentistry and Related Research*, vol. 17, pp. e406–e416, 2015.
- [2] P. Maló, M. De Araujo Nobre, A. Lopes, A. Ferro, and I. Gravito, “All-on-4 treatment concept for the rehabilitation of the completely edentulous mandible: a 7 year clinical and 5 year radiographic retrospective case series with risk assessment for implant failure and marginal bone level,” *Clinical Implant Dentistry and Related Research*, vol. 17, pp. e531–e541, 2015.
- [3] P. Maló, M. De Araujo Nobre, A. Lopes, C. Francischone, and M. Rigolizzo, ““All-on-4” immediate-function concept for completely Edentulous Maxilla: a clinical report on the medium (3 years) and long-term (5 years) outcomes,” *Clinical Implant Dentistry and Related Research*, vol. 14, pp. 139–150, 2012.
- [4] P. Maló, B. Rangert, and M. Nobre, “All-on-Four immediate function concept with Branemark System implants for completely edentulous mandibles: a retrospective clinical study,” *Clinical Implant Dentistry and Related Research*, vol. 5, pp. 2–9, 2003.
- [5] P. Maló, M. De Araujo Nobre, A. Lopes, S. Moss, and G. Molina, “A longitudinal study of the survival of All-on-4 implants in the mandible with up to 10 years of follow-up,” *Journal of the American Dental Association*, vol. 142, no. 3, pp. 310–320, 2011.
- [6] P. Maló, M. De Araujo Nobre, and A. Lopes, “The use of computer-guided flapless implant surgery and four implants placed in immediate function to support a fixed denture: preliminary results after a mean follow-up period of thirteen months,” *Journal of Prosthetic Dentistry*, vol. 97, no. 6, pp. S26–S34, 2007.
- [7] Y. N. R. Gallardo, I. R. Teixeira da Silva-Olivio, E. Mukai, S. Morimoto, N. Sesma, and L. Cordaro, “Accuracy comparison of guided surgery for dental implants according to the tissue of support: a systematic review and meta-analysis,” *Clinical Oral Implants Research*, vol. 28, no. 5, pp. 1–11, 2016.
- [8] P. Maló, M. Rigolizzo, M. D. Nobre, A. Lopes, and E. Agliardi, “Clinical outcomes in the presence and absence of keratinized mucosa in mandibular guided implant surgeries: a pilot study with proposal for the modification of the technique,” *Quintessence International*, vol. 44, no. 2, pp. 149–157, 2013.
- [9] A. Lopes, P. Maló, M. De Araujo Nobre, E. Sanchez-Fernandez, and I. Gravito, “The NobelGuide® All-on-4® treatment concept for rehabilitation of edentulous jaws: a retrospective report on the 7-years clinical and 5-years radiographic outcomes,” *Clinical Implant Dentistry and Related Research*, vol. 19, no. 2, pp. 233–244, 2017.
- [10] S. M. Meloni, M. Tallarico, M. Pisano, E. Khanari, and L. Canullo, “Immediate loading of fixed complete denture prosthesis supported by 4-8 Implants placed using guided surgery: a 5 year prospective study on 66 patients with 356 implants,” *Clinical Implant Dentistry and Related Research*, vol. 19, no. 1, 2016.
- [11] E. Naziri, A. Schramm, and F. Wilde, “Accuracy of computer-assisted implant placement with insertion templates,” *Interdisciplinary Plastic and Reconstructive Surgery*, vol. 5, 2016.

- [12] T. Fortin, J. L. Bosson, M. Isidori, and E. Blanchet, "Effect of flapless surgery on pain experienced in implant placement using an image-guided system," *International Journal of Oral and Maxillofacial Implants*, vol. 21, no. 2, pp. 298–304, 2006.
- [13] A. Azari and S. Nikzad, "Flapless implant surgery: review of the literature and report of 2 cases with computer-guided surgical approach," *Journal of Oral and Maxillofacial Surgery*, vol. 66, no. 5, pp. 1015–1021, 2008.
- [14] A. S. Bidra, "Technique for systematic bone reduction for fixed implant-supported prosthesis in the edentulous maxilla," *Journal of Prosthetic Dentistry*, vol. 113, no. 6, pp. 520–523, 2015.
- [15] A. S. Bidra, J. R. Agar, and S. M. Parel, "Management of patient with excessive gingival display for maxillary complete arch fixed implant-supported prostheses," *Journal of Prosthetic Dentistry*, vol. 108, no. 5, pp. 324–331, 2012.
- [16] A. S. Bidra, "Three-dimensional esthetic analysis in treatment planning for implant-supported fixed prosthesis in the edentulous Maxilla: review of the esthetics literature," *Journal of Esthetic and Restorative Dentistry*, vol. 23, no. 4, pp. 219–236, 2011.
- [17] F. Nejad, P. Proussaefs, and J. Lozada, "Combining guided ridge reduction and guided implant placement for all-on-4 surgery: a clinical report," *Journal of Prosthetic Dentistry*, vol. 115, no. 6, pp. 662–667, 2016.
- [18] G. A. Dolcini, M. Colombo, and C. Mangano, "From guided surgery to final prosthesis with a fully digital procedure: a prospective clinical study on 15 partially edentulous patients," *International Journal of Dentistry*, vol. 2016, Article ID 7358423, 7 pages, 2016.
- [19] S.-Y. Moon, K.-R. Lee, S.-G. Kim, and M.-K. Son, "Clinical problems of computer-guided implant surgery," *Maxillofacial Plastic and Reconstructive Surgery*, vol. 38, no. 1, p. 15, 2016.
- [20] D. Schneiderm, P. Marquardt, M. Zwahlen, and R. E. Jung, "A systematic review on the accuracy and the clinical outcome of computer-guided template-based implant dentistry," *Clinical Oral Implants Research*, vol. 20, pp. 73–86, 2009.
- [21] A. Komiyama, B. Klinge, and M. Hultin, "Treatment outcome of immediately loaded implants installed in edentulous jaws following computer-assisted virtual treatment planning and flapless surgery," *Clinical Oral Implants Research*, vol. 19, no. 7, pp. 677–685, 2008.
- [22] R. A. Landázuri-Del Barrio, J. Cosyn, W. N. De Paula, H. De Bruyn, and E. Marcantonio Jr., "A prospective study on implants installed with flapless-guided surgery using the all on-four concept in the mandible," *Clinical Oral Implants Research*, vol. 24, no. 4, pp. 428–433, 2013.
- [23] L. Gillot, R. Noharet, and B. Cannas, "Guided surgery and presurgical prosthesis: preliminary results of 33 fully edentulous maxillae treated in accordance with the NobelGuide protocol," *Clinical Implant Dentistry and Related Research*, vol. 12, pp. e104–e113, 2010.
- [24] S. M. Meloni, G. De Riu, M. Pisano, O. Massarelli, and A. Tullio, "Computer assisted dental rehabilitation in free flaps reconstructed jaws: one year follow-up of a prospective clinical study," *British Journal of Oral and Maxillofacial Surgery*, vol. 50, no. 8, pp. 726–731, 2012.
- [25] P. Maló, M. De Araujo Nobre, and A. Lopes, "The use of computer guided flapless implant surgery and four implants placed in immediate function to support a fixed denture: preliminary results after a mean follow-up period of thirteen months," *Journal of Prosthetic Dentistry*, vol. 97, no. 6, pp. S26–S34, 2007.
- [26] N. Silberberg, M. Goldstein, and A. Smidt, "Excessive gingival display—etiology, diagnosis, and treatment modalities," *Quintessence International*, vol. 40, no. 10, pp. 809–818, 2009.
- [27] A. Rosenblatt and Z. Simon, "Lip repositioning for reduction of excessive gingival display: a clinical report," *International Journal of Periodontics and Restorative Dentistry*, vol. 26, no. 5, pp. 433–437, 2006.
- [28] S. A. Miskinyar, "A new method for correcting a gummy smile," *Plastic and Reconstructive Surgery*, vol. 72, no. 3, pp. 397–400, 1983.

Research Article

Soft Lithography and Minimally Human Invasive Technique for Rapid Screening of Oral Biofilm Formation on New Microfabricated Dental Material Surfaces

Marta Alvarez-Escobar,¹ Sidónio C. Freitas ¹, Derek Hansford,² Fernando J. Monteiro,³ and Alejandro Pelaez-Vargas ¹

¹Faculty of Dentistry, Universidad Cooperativa de Colombia, Medellín, Colombia

²Department of Biomedical Engineering, The Ohio State University, Columbus, OH 43210, USA

³Instituto de Investigação e Inovação em Saúde (i3S), Instituto de Engenharia Biomédica (INEB) and DMME, Faculdade de Engenharia, Universidade do Porto (FEUP), Porto, Portugal

Correspondence should be addressed to Alejandro Pelaez-Vargas; alejandro.pelaezv@campusucc.edu.co

Received 29 April 2017; Accepted 19 November 2017; Published 14 January 2018

Academic Editor: Silvio M. Meloni

Copyright © 2018 Marta Alvarez-Escobar et al. This is an open access article distributed under the Creative Commons Attribution License, which permits unrestricted use, distribution, and reproduction in any medium, provided the original work is properly cited.

Introduction. Microfabrication offers opportunities to study surface concepts focused to reduce bacterial adhesion on implants using human minimally invasive rapid screening (hMIRS). Wide information is available about cell/biomaterial interactions using eukaryotic and prokaryotic cells on surfaces of dental materials with different topographies, but studies using human being are still limited. **Objective.** To evaluate a synergy of microfabrication and hMIRS to study the bacterial adhesion on micropatterned surfaces for dental materials. **Materials and Methods.** Micropatterned and flat surfaces on biomedical PDMS disks were produced by soft lithography. The hMIRS approach was used to evaluate the total oral bacterial adhesion on PDMS surfaces placed in the oral cavity of five volunteers (the study was approved by the University Ethical Committee). After 24 h, the disks were analyzed using MTT assay and light microscopy. **Results.** In the present pilot study, microwell structures were microfabricated on the PDMS surface via soft lithography with a spacing of 5 μm . Overall, bacterial adhesion did not significantly differ between the flat and micropatterned surfaces. However, individual analysis of two subjects showed greater bacterial adhesion on the micropatterned surfaces than on the flat surfaces. **Significance.** Microfabrication and hMIRS might be implemented to study the cell/biomaterial interactions for dental materials.

1. Introduction

The formation of oral biofilms on natural materials (e.g., enamel and dentin) and restorative biomaterials promotes the development of diseases, such as dental caries, periodontitis, and peri-implantitis [1, 2]. Microbial adhesion is the first step in colonization and the formation of a biofilm, in which microorganisms and extracellular material accumulate on a solid surface [3]. Biofilms have been defined as communities of microorganisms that grow embedded in a matrix of exopolysaccharides that affect inert surfaces or living tissues [4], where such formation can be produced by any microorganism if suitable environmental conditions are provided.

The microenvironment plays a decisive role in the formation of the oral biofilm on dental materials due to direct or indirect interactions [5]. Factors such as pH, temperature, and saliva, among others, affect biofilm composition [6]. These interactions are a challenge in using in vitro approaches (i.e., bacterial static or dynamic culture reactors and microfluidic devices) due to intra- and interindividual variations in the oral environment through health and disease conditions. In addition, surface properties are one of the major microenvironmental factors that substantially influence biofilm formation. Variations in free surface energy and surface roughness promote plaque formation and maturation [7, 8].

Soft lithography allows the production of random or ordered surfaces in a controlled manner. Such surfaces modulate the cellular response [9], specifically cell adhesion, metabolism, orientation, adhesion, growth, and differentiation in vitro [10–12]. The relationship between microfabricated surfaces and bacterial behaviour show limited information [4, 13–15] and human studies are narrow due to bioethical regulations. The challenge to carry out translational research to surface modified biomaterials is a intensive, time-consuming and cost labor. Human rapid screening might provide new successful therapies to patients in a short time. Rimondini et al. [6] introduced a minimally invasive technique to evaluate the adhesion of bacteria and biofilms in dental materials with random topographies generated by chemical or physical processing based on subtractive techniques. However, ordered topographies are hard to produce by traditional processing, but it was solved using microengineered techniques. To the best of our knowledge, a synergy of hMIRS and additive additives such as soft lithography has not been reported to evaluate biofilm formation on dental and implant material surfaces.

The aim of the present study was to evaluate a synergy of microfabrication and hMIRS to study the bacterial adhesion on micropatterned surfaces for dental materials.

2. Materials and Methods

This pilot study had approval from the ethical committee of the Universidad Cooperativa de Colombia, Medellín, Colombia. Five subjects between 18 and 35 years of age were invited, who met the following inclusion criteria: no antibiotic treatment during the 3 months prior to the test, no use of orthodontic appliances, nonsmoker, non-dental student, and have signed informed consent.

Microfabricated surfaces were obtained using biomedical PDMS (FDA approved) processed by soft lithography technology, which included the manufacturing of a master model by UV photolithography for two different purposes: (a) to test pattern transferability using raised and recessed features of different sizes, and (b) to fabricate the test geometries (pillar arrays with a $5\ \mu\text{m}$ diameter, $5\ \mu\text{m}$ height, and $5\ \mu\text{m}$ spacing) needed for the biofilm study [16]. A PDMS substrate was fabricated via replica casting, where PDMS (Silastic MDX4-4210, Dow Corning, USA) was mixed with a curing agent at a 10 : 1 ratio and cast on the master to generate a negative replica of the surface. PDMS flat surfaces were fabricated using the same procedure as microfabricated surface, but without the master. Characterization of the micropatterned and flat surfaces was performed using light microscopy (Primo Star, Zeiss, Switzerland) and scanning electron microscopy (Hitachi, S-3000H, Japan).

Modified Essix retainers were fabricated with two metal baskets per hemiarch where transparent PDMS disks of 6 mm diameter were placed with flat and micropatterned surfaces (Figure 1). All subjects were instructed to wear the modified Essix retainer for 24 hours, removing it only for eating, brushing, and contact sports.

After the plates were removed from the mouth, the disks were washed three times with saline solution



(a)



(b)

FIGURE 1: Intraoral modified Essix retainer with metal baskets.

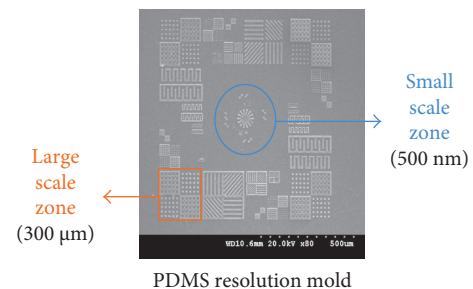


FIGURE 2: Resolution test. Several geometries with scales (from $500\ \text{nm}$ to $300\ \mu\text{m}$) were transferred from silicon wafer to PDMS.

(Baxter, USA). The disks were incubated in a solution of 3-(4,5-dimethylthiazol-2-yl)-2,5-diphenyltetrazolium bromide (MTT, Molecular Probe, USA) at $0.5\ \text{mg/ml}$ in saline solution for 2 hours at 37°C . Quantification of the area covered by the biofilm was performed on 6 random micrographs obtained by optical microscopy through an ad hoc digital image-processing strategy that included binarization, edge detection, segmentation, and pixel counting using ImageJ 1.51 g [17, 18].

2.1. Statistical Analysis. A comparison of the area covered by biofilm was performed for the two evaluated surfaces with a nonparametric Wilcoxon rank-sum test blocked by the subject using R software.

3. Results

Figure 2 shows the results of PDMS micropatterned arrays from $500\ \text{nm}$ to $300\ \mu\text{m}$.

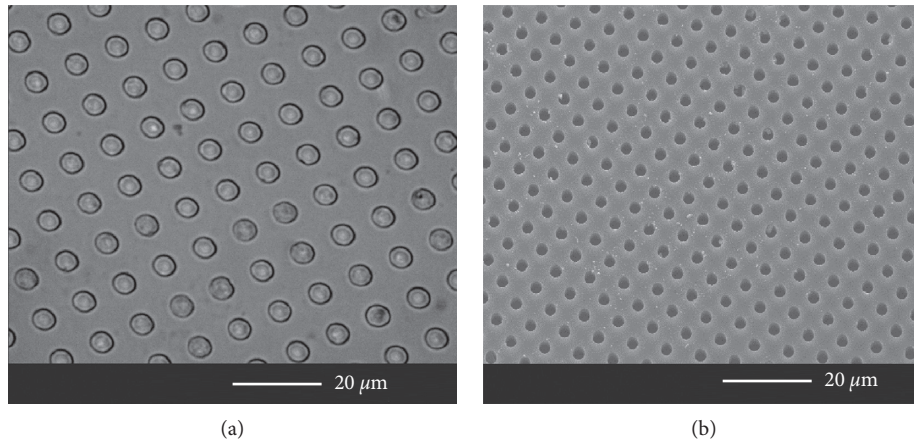


FIGURE 3: Micropatterned surfaces on PDMS: (a) 100x optical micrograph and (b) scanning electron micrograph.

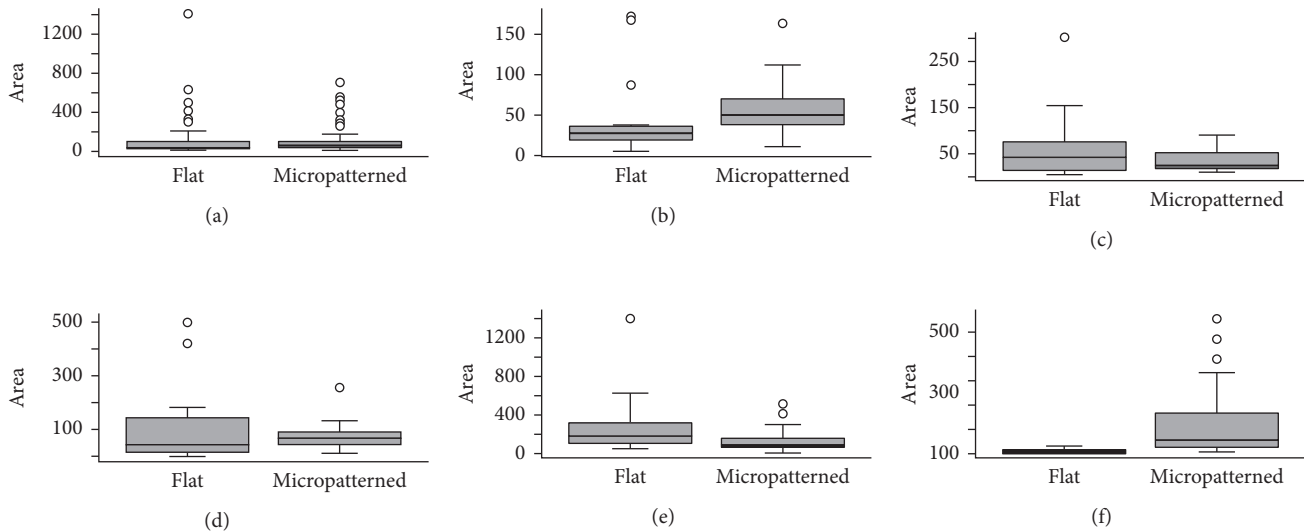


FIGURE 4: Comparison between micropatterned surfaces and flat surfaces. (a) Overall. (b–f) Subjects 1–5.

Figure 3 shows optical and scanning electron micrographs of the micropatterned surfaces on PDMS. A $5\ \mu\text{m}$ well structure (depth, diameter, and spacing) is observed with no defects.

Overall (Figure 4(a)), the area covered by the bacteria did not significantly differ between the micropatterned surfaces and the flat surfaces ($p = 0.06$). Patient-to-patient comparison between the micropatterned surfaces and the flat surfaces did not show statistically significant differences for subjects 2, 3, and 4 (Figures 4(c)–4(e)). For subjects 1 and 5, significantly less biofilm formation was found on the flat surfaces (Figures 4(b) and 4(f)).

4. Discussion

Bacterial adhesion and biofilm formation on biomaterials is a complex process involving environmental factors, physical and chemical surface properties, and bacterial characteristics [19]. The surface has been extensively studied in terms of free

energy and topography and has been associated with bacterial adhesion, growth, and maturation of biofilm [7, 8]. Topography modulates the behavior of eukaryotic cells in terms of adhesion, orientation, growth, differentiation, and apoptosis [20, 21]. Cell adhesion dynamics on ordered microtopographies has been largely studied using in vitro approaches [22, 23], which showed that the response is not universal for all surfaces, materials, and cells. Adherent cells such as rat fibroblasts [22] show a preference for smooth surfaces rather than surfaces with micro/nanopillars. In contrast, glial cells show a positive response for textured surfaces [23].

Andersson et al. [24] studied cell adhesion on smooth and textured surfaces with grooves ($15\ \mu\text{m}$ wide and $185\ \text{nm}$ deep) and pillars ($168\ \text{nm}$ diameter and $100\ \text{nm}$ high) and found that increasing the height of the topography reduced epithelial cell adhesion. In addition, cells on pillars had a smaller area of covering compared to flat surfaces.

Dalby et al. [25] evaluated a topography of $<20\ \text{nm}$ that promoted adhesion in a wide range of cell types (endothelial,

fibroblast, and mesenchymal). These authors [26] show that small pillar (10 nm) topographies improve the adhesion of fibroblasts compared to 50 nm. Rice et al. [27] also showed that osteoblasts had low adhesion to nanopillars with heights of 160 nm.

In contrast, bacterial studies on micropatterned surfaces are limited. Chung et al. [28] developed micropatterned surfaces by recreating shark skin on PDMS to evaluate the in vitro adhesion of *Staphylococcus aureus* when compared to smooth surfaces. Their results showed that the topography inhibited the development of biofilm. Such response was attributed to the fact that the protruding features of the surfaces provide a physical barrier that prevents the expansion of small colonies of bacteria. Hochbaum and Aizenberg demonstrated bacterial ordering and orientated attachment on the single-cell level induced by nanometer scale periodic surface features [15]. The possible clinical implications of these in vitro findings justify studies based on human models. A systematic review [8] concluded that an increase in the surface roughness greater than Ra 0.2 μm or an increase in the free energy of the surface will facilitate the formation of biofilms in restorative materials.

The present pilot study used a surface model of microwells with a diameter, depth, and interspacing of 5 μm and hMIRS in terms of limited contact duration (24 h) and in contact with uncompromised oral mucosa. General comparisons showed no statistically significant difference in bacterial adhesion between flat and microfabricated surfaces on PDMS. These results might be explained by antiadhesive barrier as a consequence of high hydrophobicity in the biomedical PDMS used, which could be reduced with increased exposure time, but this would be opposite to the rapid screening model described. Modified Essix retainer was used for a period of 24 hours, which matched the in vivo human studies reported in the literature [6, 29, 30]. Auschill et al. [31] evaluated the formation of biofilms over a 120-hour period on different dental materials, including glass and ceramics. They found biofilm formation with thicknesses of 1–17 μm , values that are similar to those reported in 24-hour studies [6, 29, 30].

In the present pilot study, the sample size used was similar to that in in vivo human studies, which had sample sizes ranging from 5 to 10 subjects [6, 29, 30]. These results of the present pilot study found that the synergy of microfabrication by soft lithography and hMIRS might be a powerful tool to evaluate the bacterial/implant-biomaterials interface in human with a minimum risk for subjects. The tested biomedical PDMS model surfaces require further research that includes other factors such as different microstructure features, microscale and nanoscale topographies, and contact duration.

Conflicts of Interest

The authors declare that there are no conflicts of interest regarding the publication of this paper.

Acknowledgments

This study was supported by the CONADI funds, Universidad Cooperativa de Colombia, and the “Bonamidi” project (contract FCT/PTDC/CTM/100120/2008).

References

- [1] M. Quirynen and W. Teughels, “Microbiologically compromised patients and impact on oral implants,” *Periodontology* 2000, vol. 33, no. 1, pp. 119–128, 2003.
- [2] C. J. Seneviratne, C. F. Zhang, and L. P. Samaranayake, “Dental plaque biofilm in oral health and disease,” *Chinese Journal of Dental Research*, vol. 14, no. 2, pp. 87–94, 2011.
- [3] K. Hori and S. Matsumoto, “Bacterial adhesion: from mechanism to control,” *Biochemical Engineering Journal*, vol. 48, no. 3, pp. 424–434, 2010.
- [4] L. D. Renner and D. B. Weibel, “Physicochemical regulation of biofilm formation,” *MRS Bulletin*, vol. 36, no. 5, pp. 347–355, 2011.
- [5] C. Hannig and M. Hannig, “The oral cavity—a key system to understand substratum-dependent bioadhesion on solid surfaces in man,” *Clinical Oral Investigations*, vol. 13, no. 2, pp. 123–139, 2009.
- [6] L. Rimondini, L. Cerroni, A. Carrassi, and P. Torricelli, “Bacterial colonization of zirconia ceramic surfaces: an in vitro and in vivo study,” *International Journal of Oral & Maxillofacial Implants*, vol. 17, no. 6, pp. 793–798, 2002.
- [7] M. Quirynen and C. M. L. Bollen, “The influence of surface roughness and surface-free energy on supra- and subgingival plaque formation in man. A review of the literature,” *Journal of Clinical Periodontology*, vol. 22, no. 1, pp. 1–14, 1995.
- [8] W. Teughels, N. Van Assche, I. Sliepen, and M. Quirynen, “Effect of material characteristics and/or surface topography on biofilm development,” *Clinical Oral Implants Research*, vol. 17, no. 2, pp. 68–81, 2006.
- [9] A.-S. Andersson, J. Brink, U. Lidberg, and D. S. Sutherland, “Influence of systematically varied nanoscale topography on the morphology of epithelial cells,” *IEEE Transactions on Nanobioscience*, vol. 2, no. 2, pp. 49–57, 2003.
- [10] A. Carvalho, A. Pelaez-Vargas, D. J. Hansford, M. H. Fernandes, and F. J. Monteiro, “Effects of line and pillar array micro-engineered SiO₂ thin films on the osteogenic differentiation of human bone marrow-derived mesenchymal stem cells,” *Langmuir*, vol. 32, no. 4, pp. 1091–1100, 2016.
- [11] A. Carvalho, A. Pelaez-Vargas, D. Gallego-Perez et al., “Micropatterned silica thin films with nanohydroxyapatite micro-aggregates for guided tissue regeneration,” *Dental Materials*, vol. 28, no. 12, pp. 1250–1260, 2012.
- [12] S. Arango-Santander, S. C. Freitas, A. Pelaez-Vargas, and C. Garcia, “Silica sol-gel patterned surfaces based on dip-pen nanolithography and microstamping: a comparison in resolution and throughput,” *Key Engineering Materials*, vol. 720, pp. 264–268, 2016.
- [13] D. B. Weibel, W. R. DiLuzio, and G. M. Whitesides, “Microfabrication meets microbiology,” *Nature Reviews Microbiology*, vol. 5, no. 3, pp. 209–218, 2007.
- [14] T. R. Garrett, M. Bhakoo, and Z. Zhang, “Bacterial adhesion and biofilms on surfaces,” *Progress in Natural Science*, vol. 18, no. 9, pp. 1049–1056, 2008.
- [15] A. I. Hochbaum and J. Aizenberg, “Bacteria pattern spontaneously on periodic nanostructure arrays,” *Nano Letters*, vol. 10, no. 9, pp. 3717–3721, 2010.
- [16] A. Pelaez-Vargas, D. Gallego-Perez, M. Magallanes-Perdomo et al., “Isotropic micropatterned silica coatings on zirconia

- induce guided cell growth for dental implants,” *Dental Materials*, vol. 27, no. 6, pp. 581–589, 2011.
- [17] J. Schindelin, I. Arganda-Carreras, E. Frise et al., “Fiji: an open-source platform for biological-image analysis,” *Nature Methods*, vol. 9, no. 7, pp. 676–682, 2012.
- [18] C. Restrepo, A. Peláez, E. Alvarez, C. Paucar, and P. Abad, “Digital imaging of patterns of dental wear to diagnose bruxism in children,” *International Journal of Paediatric Dentistry*, vol. 16, no. 4, pp. 278–285, 2006.
- [19] M. Katsikogianni and Y. F. Missirlis, “Concise review of mechanisms of bacterial adhesion to biomaterials and of techniques used in estimating bacteria-material interactions,” *European Cells and Materials*, vol. 8, pp. 37–57, 2004.
- [20] A. Pelaez-Vargas, D. Gallego-perez, D. F. Gomez, M. H. Fernandes, D. J. Hansford, and F. J. Monteiro, “Propagation of human bone marrow stem cells for craniofacial applications,” in *Stem Cells and Cancer Stem Cells*, M. A. Hayat, Ed., vol. 7, pp. 107–122, Springer, Dordrecht, Netherlands, 2012.
- [21] A. Pelaez-Vargas, D. Gallego-Perez, N. Higueta-Castro et al., “Micropatterned coating for guided tissue regeneration in dental implantology,” in *Cell Interaction*, S. Gowder, Ed., pp. 273–302, InTech, Rijeka, Croatia, 2012.
- [22] A. S. G. Curtis, B. Casey, J. O. Gallagher, D. Pasqui, M. A. Wood, and C. D. W. Wilkinson, “Substratum nanotopography and the adhesion of biological cells. Are symmetry or regularity of nanotopography important?,” *Biophysical Chemistry*, vol. 94, no. 3, pp. 275–283, 2001.
- [23] A. M. Turner, N. Dowell, S. W. Turner et al., “Attachment of astroglial cells to microfabricated pillar arrays of different geometries,” *Journal of Biomedical Materials Research*, vol. 51, no. 3, pp. 430–441, 2000.
- [24] A.-S. Andersson, F. Bäckhed, A. von Euler, A. Richter-Dahlfors, D. Sutherland, and B. Kasemo, “Nanoscale features influence epithelial cell morphology and cytokine production,” *Biomaterials*, vol. 24, no. 20, pp. 3427–3436, 2003.
- [25] M. J. Dalby, S. Childs, M. O. Riehle, H. J. H. Johnstone, S. Affrossman, and A. S. G. Curtis, “Fibroblast reaction to island topography: changes in cytoskeleton and morphology with time,” *Biomaterials*, vol. 24, no. 6, pp. 927–935, 2003.
- [26] M. J. Dalby, M. O. Riehle, H. J. H. Johnstone, S. Affrossman, and A. S. G. Curtis, “Nonadhesive nanotopography: fibroblast response to poly(n-butyl methacrylate)-poly(styrene) demixed surface features,” *Journal of Biomedical Materials Research Part A*, vol. 67, no. 3, pp. 1025–1032, 2003.
- [27] J. M. Rice, J. A. Hunt, J. A. Gallagher, P. Hanarp, D. S. Sutherland, and J. Gold, “Quantitative assessment of the response of primary derived human osteoblasts and macrophages to a range of nanotopography surfaces in a single culture model in vitro,” *Biomaterials*, vol. 24, no. 26, pp. 4799–4818, 2003.
- [28] K. K. Chung, J. F. Schumacher, E. M. Sampson, R. A. Burne, P. J. Antonelli, and A. B. Brennan, “Impact of engineered surface microtopography on biofilm formation of *Staphylococcus aureus*,” *Biointerphases*, vol. 2, no. 2, pp. 89–94, 2007.
- [29] F. Bremer, S. Grade, P. Kohorst, and M. Stiesch, “In vivo biofilm formation on different dental ceramics,” *Quintessence International*, vol. 42, no. 7, pp. 565–574, 2011.
- [30] M. M. de Freitas, C. H. da Silva, M. Groisman, and G. M. Vidigal, “Comparative analysis of microorganism species succession on three implant surfaces with different roughness: an in vivo study,” *Implant Dentistry*, vol. 20, no. 2, pp. e14–e23, 2011.
- [31] T. M. Auschill, N. B. Arweiler, M. Brex, E. Reich, A. Sculean, and L. Netuschil, “The effect of dental restorative materials on dental biofilm,” *European Journal of Oral Sciences*, vol. 110, no. 1, pp. 48–53, 2002.

Research Article

Osseointegration of a 3D Printed Stemmed Titanium Dental Implant: A Pilot Study

James Tedesco,¹ Bryan E. J. Lee,² Alex Y. W. Lin,^{1,3} Dakota M. Binkley,⁴ Kathleen H. Delaney,⁵ Jacek M. Kwiecien,^{5,6} and Kathryn Grandfield^{1,2}

¹*Department of Materials Science and Engineering, McMaster University, Hamilton, ON, Canada*

²*School of Biomedical Engineering, McMaster University, Hamilton, ON, Canada*

³*Department of Materials Science and Engineering, Northwestern University, Evanston, IL, USA*

⁴*School of Integrated Science, McMaster University, Hamilton, ON, Canada*

⁵*Department of Pathology and Molecular Medicine, McMaster University, Hamilton, ON, Canada*

⁶*Department of Clinical Pathomorphology, Medical University of Lublin, Lublin, Poland*

Correspondence should be addressed to Kathryn Grandfield; kgrandfield@mcmaster.ca

Received 19 May 2017; Revised 30 August 2017; Accepted 3 October 2017; Published 19 November 2017

Academic Editor: Silvio M. Meloni

Copyright © 2017 James Tedesco et al. This is an open access article distributed under the Creative Commons Attribution License, which permits unrestricted use, distribution, and reproduction in any medium, provided the original work is properly cited.

In this pilot study, a 3D printed Grade V titanium dental implant with a novel dual-stemmed design was investigated for its biocompatibility *in vivo*. Both dual-stemmed ($n = 12$) and conventional stainless steel conical ($n = 4$) implants were inserted into the tibial metaphysis of New Zealand white rabbits for 3 and 12 weeks and then retrieved with the surrounding bone, fixed, dehydrated, and embedded into epoxy resin. The implants were analyzed using correlative histology, microcomputed tomography, scanning electron microscopy (SEM), and transmission electron microscopy (TEM). The histological presence of multinucleated osteoclasts and cuboidal osteoblasts revealed active bone remodeling in the stemmed implant starting at 3 weeks and by 12 weeks in the conventional implant. Bone-implant contact values indicated that the stemmed implants supported bone growth along the implant from the coronal crest at both 3- and 12-week time periods and showed bone growth into microporosities of the 3D printed surface after 12 weeks. In some cases, new bone formation was noted in between the stems of the device. Conventional implants showed mechanical interlocking but did have indications of stress cracking and bone debris. This study demonstrates the comparable biocompatibility of these 3D printed stemmed implants in rabbits up to 12 weeks.

1. Introduction

Bone-anchored implants have been a standard treatment for edentulism since the mid-1980s, after Per-Ingvar Brånemark demonstrated the successful osseointegration of a titanium dental implant placed in human patients [1]. However, failure rates for clinical use dental implants range between 3 and 8% depending on the implant design and/or patients' health factors [2–5]. Although this appears to be a rather successful procedure, an epidemiological study reported 1200 emergency department visits due to dental implant failures from 2008 to 2010 in the US alone [6], signifying the continued burden of edentulism on the healthcare system. As such, methods to improve the clinical outcomes of dental implants are still actively pursued.

Due to its bone-bonding or osseointegrative ability, mechanical and chemical properties, and overall biocompatibility, titanium and titanium alloys have long been the dental implant material of choice [7–9]. Recently, considerable emphasis has been placed on surface treatment of implants, where surface roughness and texture modifications have been shown to facilitate bone integration and cellular activity via microscale and nanoscale features [10–13]. In addition, a range of surface coatings, such as calcium phosphate, magnesium, and titania, have been explored with the intent of encouraging faster osseointegration [14–16]. While it is known that implant geometry can change the response of the bone-implant interface under loading [17], conventional machining processes have traditionally limited implant morphologies to conical- and screw-like designs.

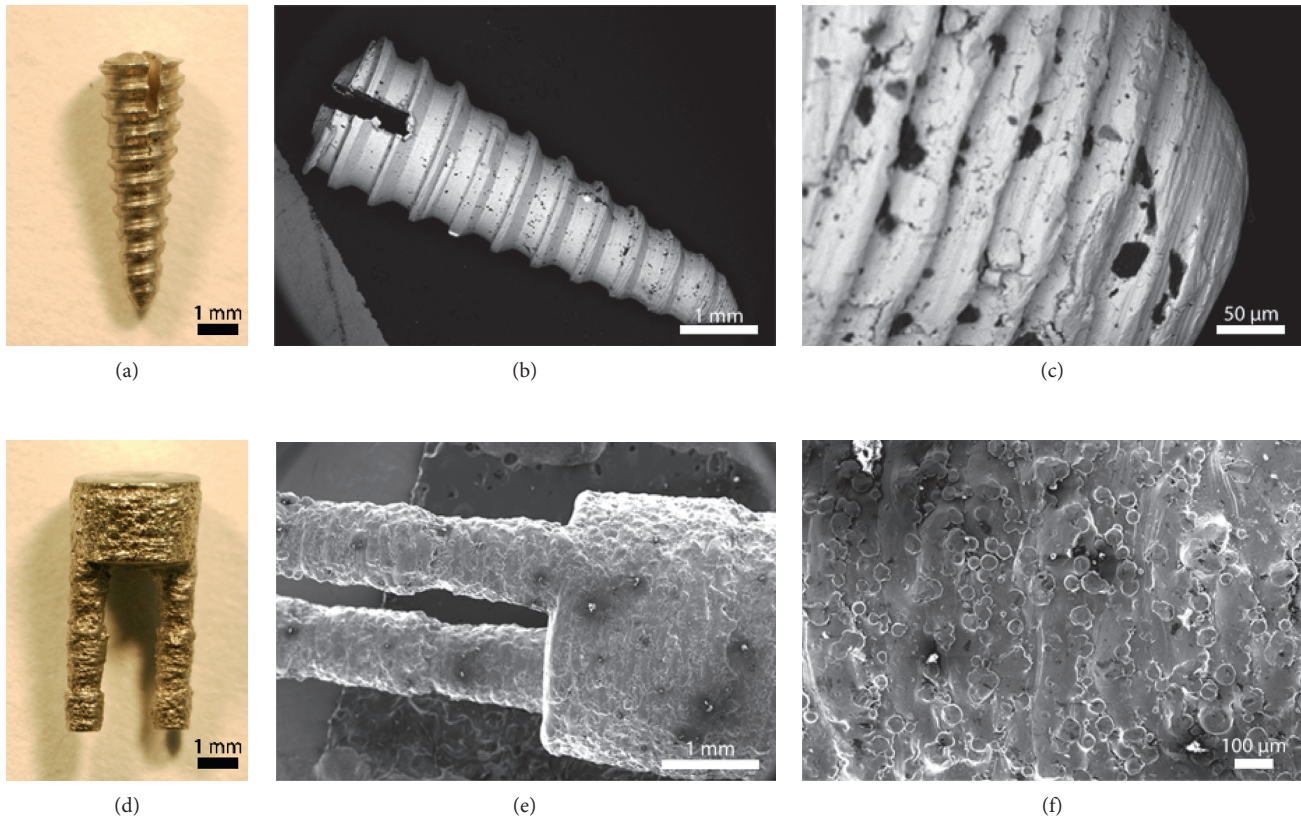


FIGURE 1: (a) Photo of control conical implant ($\text{Ø} = 2 \text{ mm}$, $l = 6 \text{ mm}$). (b, c) SEM images of control surface. (d) Photo of dual-stemmed (SIT) implant ($\text{Ø} = 3 \text{ mm}$, $l = 6 \text{ mm}$). (e, f) SEM images of SIT implant surface. At higher magnification, it is clear that the 3D printed surface (f) retains characteristic surface features representative of the powders used in its production and has a much higher roughness than conventionally machined implants (c).

However, with the technological advances in additive manufacturing, 3D printing of titanium and titanium alloys for new and innovative implant geometries are now possible. Additive manufacturing techniques, such as direct metal laser sintering (DMLS) and electron beam melting (EBM), are processes that can create three-dimensional metallic constructs by selectively melting metal powder in a layer-by-layer fashion. These techniques are capable of creating complex porous features [18–20] and an inherent surface roughness, as the melted powder droplets solidify on the object surface. Current use of this technology for implant manufacturing has focused on creating open pore networks to mimic the trabecular bone, showing improved cellular activity and greater bone ingrowth in both rabbit and sheep models [21–23].

In this pilot study, the osseointegration of a dental implant with a novel dual-stemmed shape, enabled by DMLS, was assessed for the first time. We present complementary histology, high-resolution X-ray, and electron microscopy analyses to investigate the bone-implant interface.

2. Materials and Methods

2.1. Implants. Twelve dual-stemmed implants (herein referred to as the SIT implant) were produced via DMLS using an EOSINT M 280 (EOS GmbH, Krailling, Germany) with

Ti6Al4V powder and were received from Stemmed Implant Technologies Inc. (Niagara Falls, Canada). Implants were 3 mm in diameter, with 1 mm diameter stems. In preparation for implantation, implants were cut into 6 mm in length, briefly sandblasted with 70 psi and a 90% glass bead/10% Al_2O_3 media, and autoclaved. Final implants consisted of a body and stems, both 3 mm in length (Figure 1(b)). Four conical stainless steel mini-implant screws, with a tapered body and maximum of 2 mm diameter, were used as controls. The control implants were received from Stemmed Implant Technologies Inc., cut into a 6 mm length to match the length of the stemmed implants (Figure 1(a)), and autoclaved for sterilization prior to the implantation procedure. At higher magnification, it is clear that the 3D printed surface (f) retains characteristic surface features representative of the powders used in its production and has a much higher roughness than conventionally machined implants (Figures 1(b), 1(c), 1(e), and 1(f)).

2.2. Implant Placement and Retrieval. Eight skeletally mature female-specific pathogen-free New Zealand white (NZW) rabbits (Charles River, Toronto, Canada) weighing between 3 and 4 kg were housed at the Central Animal Facility (CAF) at McMaster University. Animal experiments were carried out under ethical approval (AUP 14-12-54)

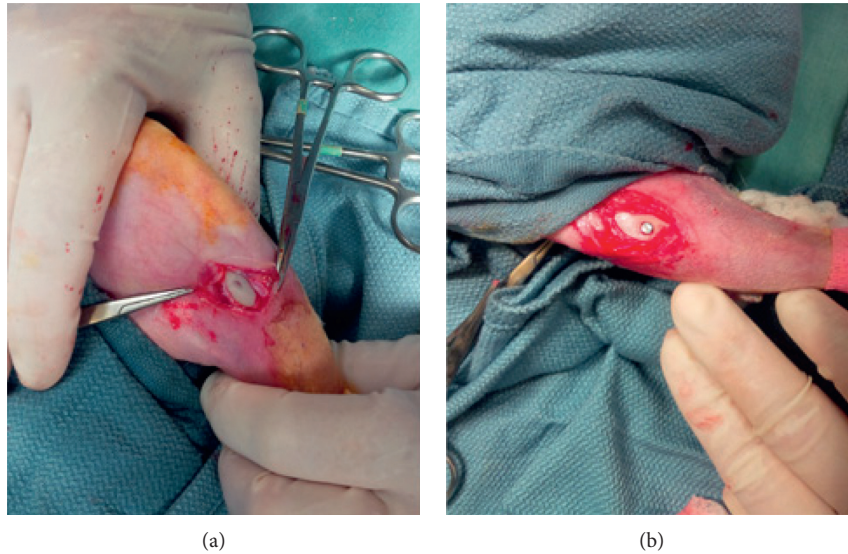


FIGURE 2: Cranial medial surgical approach parallel to the tibial crest. (a) Slow-rotating drill used to create pilot holes perpendicular to the bone crest. (b) SIT implants were pressed to fit into place until flush with bone crest. Control implants were screwed into place (not shown).

from the McMaster Animal Research Ethics Board. The day prior to surgery and over the following four days, all rabbits received 10 mg/kg enrofloxacin (Baytril®, Bayer, Leverkusen, Germany) to prevent infection. During surgery, the rabbits were induced with xylazine, ketamine, and acepromazine, intubated, and placed on isoflurane gas 2-3% inhalation with oxygen. Buprenorphine was administered at 0.5 mg/kg subcutaneously to prevent pain and readministered every 12 hours for 48 hours postoperatively. The surgical method was a cranial medial approach parallel to the tibial crest with a slow-rotating drill and irrigation with saline (Figure 2). The implant bed therefore consisted of cylindrical holes through the cortical bone slightly smaller than the diameter of the implants. One implant of each type was inserted into the tibial metaphysis of each rabbit, where stemmed implants were pressed to fit and conical implants were screwed in until flush with the bone crest. Incisions were closed with a layer of 4-0 Vicryl® (Ethicon, Inc., Somerville, USA), and the skin was closed with stainless steel wound clips. Animals were then randomly split into two groups: one provided a 3-week healing period, and the other, 12 weeks. After the healing period, rabbits were euthanized by overdose of barbiturate. However, one animal at each time point was perfused with 2% glutaraldehyde in 0.1 M sodium cacodylate buffer solution, and bone-implant sections were removed for decalcification with EDTA for histology.

Implants with surrounding bone tissue were collected and prepared into implant-bone blocks following the methodology for preparing undecalcified bone outlined by Donath and Breuner [24]. Approximately 2 cm × 2 cm bone blocks containing the implants were fixed in a solution of 1% glutaraldehyde and 1% paraformaldehyde in 0.1 M sodium cacodylate buffer for 7-10 days and subsequently dehydrated in a graded series of ethanol, followed by

embedding in LR white acrylic resin for the 3-week specimens and Embed-812 epoxy resin for the 12-week specimens. Blocks were longitudinally sectioned using an Isomet® low-speed saw (Buehler, Lake Bluff, USA) and a diamond wafer blade to reveal the bone-implant interface.

2.3. Histology. Rabbits were overdosed with 65 mg/kg body weight sodium pentobarbital I.V. and perfused via the left cardiac ventricle with 1 L lactated Ringer's solution followed by 1 L formalin (10% paraformaldehyde in phosphate buffer, pH 7.2). The fragment of the tibial bone with the metal implant was carefully removed, postfixed in formalin for two days, and then placed in formalin supplemented with 4% EDTA (pH 7.2) for demineralization. Demineralizing solution was exchanged once per week over nine months. The metal implants were carefully removed from the soft bone, and the bone was sectioned for analysis at the site of the implants. The sections were dehydrated with a series of graded concentrations of ethyl alcohol (50-100%) and xylene, embedded in paraffin wax, cut into 5 µm thick, mounted onto glass slides, and stained with both hematoxylin and eosin. The histological analysis was performed under an Eclipse 50i light microscope (Nikon, Tokyo, Japan).

2.4. Microcomputed Tomography. Visualization of whole implant-bone ingrowth was achieved using a SkyScan 1172 (Bruker, Billerica, USA) with a 100 kV X-ray beam, aluminium-copper filter, 2.3 µm-2.6 µm pixel size, and 0.3-1° rotation step. NRecon and CTAn software (Bruker, Billerica, USA) were used to reconstruct and visualize the 3D volumes. The length of bone growth was measured using the image processing and analysis software ImageJ (National Institutes of Health, Bethesda, USA).

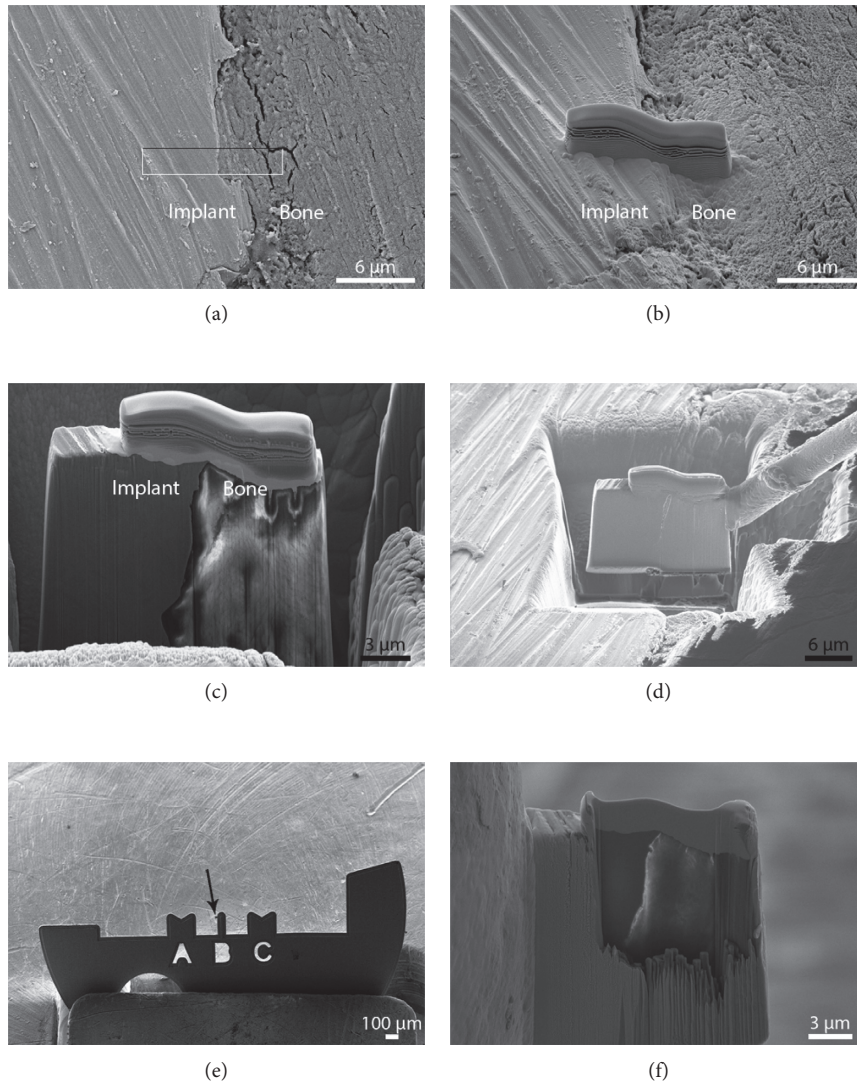


FIGURE 3: TEM sample preparation of a SIT 12-week bone-implant interface using FIB. (a) Selection of ROI. (b) Deposition of protective carbon layer over ROI. (c) Rough milling of the material surrounding the ROI. (d) Lift-out of the lamella containing the ROI via an in situ micromanipulator. (e) Attachment of the lamella on the copper TEM grid (arrow indicates sample location). (f) Cross-sectional view of the electron transparent sample following final thinning.

2.5. Scanning and Transmission Electron Microscopy. Longitudinal implant-bone blocks were sputter coated with gold and imaged with a JSM-6610LV (JEOL Ltd., Tokyo, Japan) scanning electron microscope (SEM) at an accelerating voltage of 10 kV. Backscattered electron (BSE) images with compositional contrast enabled identification of regions of new bone growth along the implant length.

Transmission electron microscopy (TEM) specimens were prepared using an in situ lift-out method (Figure 3) on a NVision 40 (Carl Zeiss GmbH, Germany), a dual-beam instrument comprising a focused ion beam (FIB) milling instrument and a Schottky field emission gun (FEG) filament SEM. Due to implant-bone separation caused during retrieval and sample preparation, an intact bone-implant specimen was not possible. However, the interface between old and new bone was successfully prepared for high-resolution analysis. TEM images were captured using

a Titan 80-300 (FEI, Oregon, USA) operated at 300 kV with a high-angle annular dark-field detector.

3. Results

3.1. Histology. Histological analysis of both SIT implants and control screw implants was completed after 3 and 12 weeks of implantation to determine the cellular activity and remodeling behaviour of the bone tissue with the implanted devices (Figure 4). For both the SIT and control groups, implants resided primarily in the cortical bone. Following extraction of the control implant after 3 weeks, bone debris was present between the implant and the cortical bone (Figure 4(a)). This is in contrast to the cortical bone surrounding the SIT implant after 3 weeks, where there was no debris and the presence of multinucleated osteoclasts and hypertrophied osteoblasts suggested that the bone was being

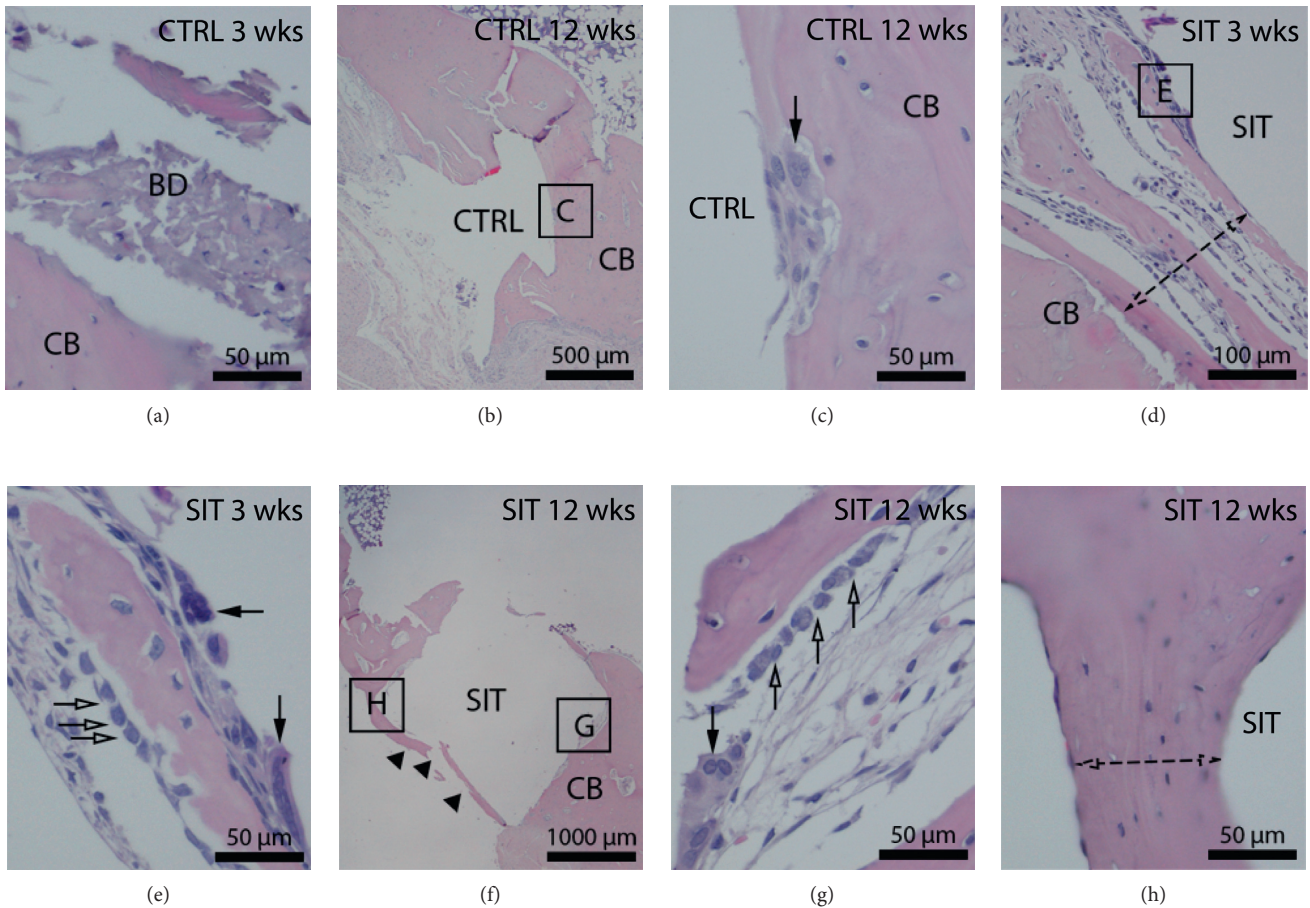


FIGURE 4: H&E staining highlights histological changes in the tibial bone after implantation of the SIT implant (d, e, f, g, h) or control implant (a, b, c) for a duration of 3 weeks (a, d, e) or 12 weeks (b, c, f, g, h). The metal implants have been removed. (a) At 3 weeks post implantation, bone debris is present between the control implant and cortical bone. (b) At 12 weeks post implantation, the cortical bone surrounding the control implant has active bone remodeling at the bone-metal interface (c) which involves osteoclasts (arrow). However, the cortical bone is being actively remodeled (double-headed arrow) around the site of the SIT implant (d) after 3 weeks. At higher magnification (e), multinucleated osteoclasts (black arrows) and hypertrophied osteoblasts (white arrows) participate in bone remodeling. (f) At 12 weeks post implantation, the SIT implant is encased in the cortical bone (arrowheads) which at higher magnification (h) has the morphology of a mature bone (double-headed arrow). The remodeling of the bone surrounding the SIT implant is still active (g) and involves osteoclasts (black arrow) and hypertrophied osteoblasts (white arrows). CTRL = control, SIT = stemmed implant, CB = cortical bone, and BD = bone debris.

actively remodeled around the implant (Figures 4(d) and 4(e)). After 12 weeks of implantation, both the control-implanted (Figure 4(b)) and SIT-implanted (Figure 4(f)) rabbits were observed to have active bone remodeling at the bone-implant interface. The control implants showed active bone remodeling involving osteoclasts (Figure 4(c)), meanwhile, the SIT implant was completely encased in the cortical bone, with a layer of bone forming over its surface. The remodeling of the bone was still active but showed the morphology of more mature bone (Figure 4(h)).

3.2. Microcomputed Tomography. Prior to sectioning for SEM, the entire implant-bone blocks of the SIT and control implants were imaged by microcomputed tomography (μ -CT). Radiographs of both implant types revealed the top portion of the implants to be surrounded by the cortical bone with the remainder of the implant located in the

medullary cavity (Figures 5(a), 5(e), 6(a), and 6(e)). The SIT and control implants were shown to have new bone growing from the preexisting cortical bone, down and around each implant surface and into the medullary cavity, after 3 and 12 weeks (Figures 5 and 6). Three-dimensional renderings (Figures 5(b), 5(f), 6(b), and 6(f)) of both implants provided a holistic perspective of the entire implant and surrounding bone volume. The new bone growth around the implants is simultaneously visualized with the growth down the implant length. The location of the reconstructions shown in Figures 5 and 6 is represented in the 3D renderings by the corresponding cross-sectional and longitudinal planes. At 3 weeks, the new bone is in an immature state, identified by lighter contrast and porous structure when compared to the preexisting cortical bone for both the control (Figures 5(c) and 5(d)) and SIT (Figures 5(h) and 5(g)) implants. Qualitatively, through 12 weeks, the new bone appeared to have developed into mature or remodeled cortical bone

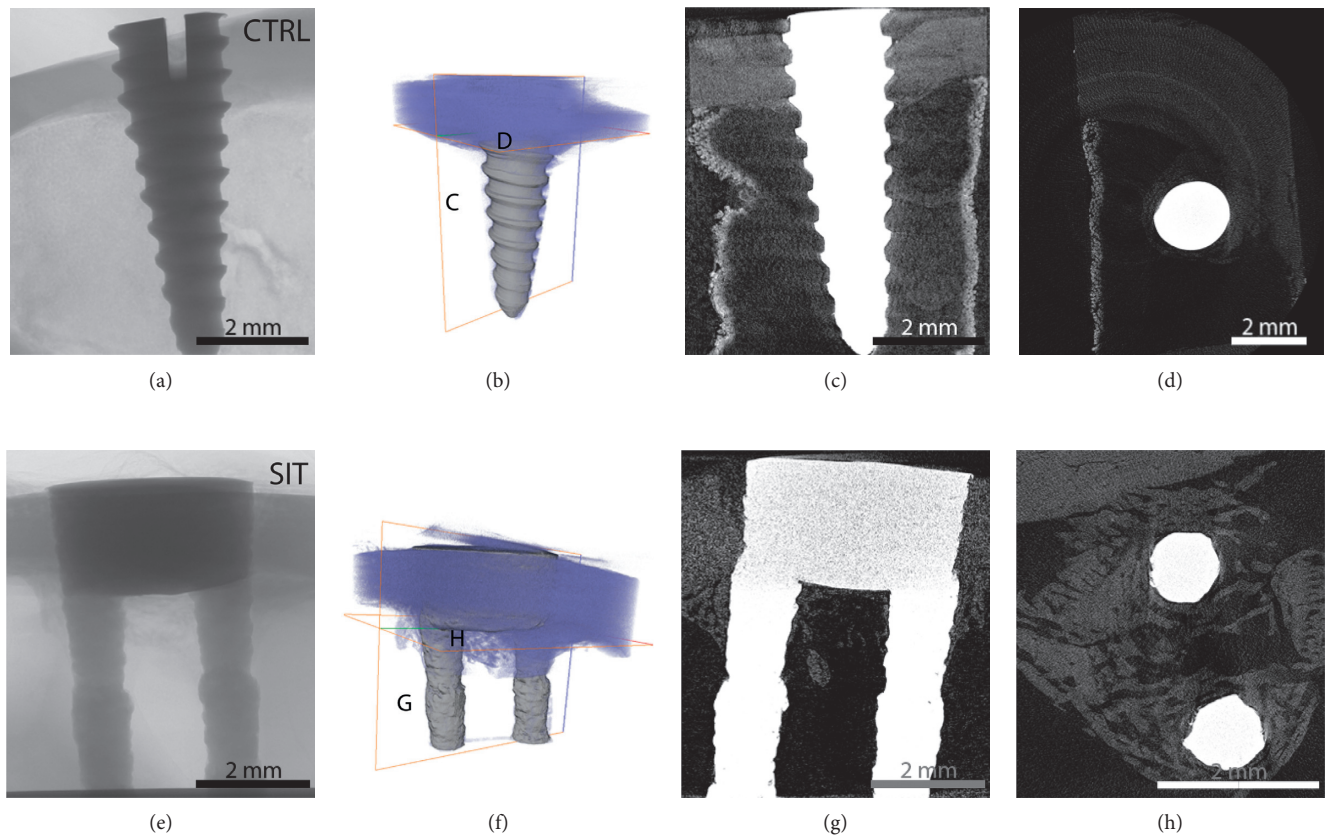


FIGURE 5: Micro-CT analysis following 3-week implantation of CTRL (left column) and SIT (right column) implants. (a, e) Radiographs of each implant type. (b, f) 3D visualization of the implant and bone (purple) with orthogonal planes labelled, (c, d, g, h) corresponding orthoslices from (b, f) where new bone formation (appears lighter in contrast) is noted. Both implants showed bone conduction down the implants from the cortical bone crest, while the SIT implant also showed new bone formation between the implant stems.

with higher levels of mineralization, as a result of the similar contrast and density of the new and old cortical bone for both implant types (Figures 6(c), 6(d), 6(h), and 6(g)). The longitudinal sections of the control (Figures 5(c) and 6(c)) and SIT (Figures 5(g) and 6(g)) implants showed a difference in the extent of bone growth extending from the bone crest down the length of the implant at both time points. The new bone accounted for 25% and 50% of the total bone length residing along the control and SIT implant surfaces, respectively, at 3 weeks (Figure 7). After 12 weeks, the new bone accounted for 35% and 55% of the total bone length residing along the control and SIT implant surfaces, respectively (Figure 7). While the bone growth down the SIT implant surface was greater than that down the control implant surface at both time points, a difference in the extent of radial bone growth between the control and SIT implants was less evident. Qualitative results suggest that over the same time period, bone grows similarly around the SIT implant compared to controls.

3.3. Scanning Electron Microscopy. Similar to the micro-CT results, SEM images did not show a trabecular bone transition underlying the cortical bone, which indicated some misplacement of the implant off the target anatomical

position. As such, bone contact was only possible originating from the cortical bone crest. Imaging of the embedded sections with SEM enabled qualitative assessment of the bone-implant contact in this cortical region. Three weeks after implantation, the cortical bone was present within the threads of the control implant (Figure 8(a)). This mechanically interlocked bone was in contact with the control implant, while the new bone further down the length of the implant was primarily not in direct contact. However, stress cracks were observed at the mechanically interlocked thread tips. In contrast, little to no bone was in contact with the SIT implant after 3 weeks (Figure 8(c)). The absence of threads also indicates a lack in mechanical interlocking. The bone structure around the SIT implant specimens appeared less developed with more porosity and randomly oriented osteocyte lacunae; however, in some cases, new bone formation was observed in between the stems of the SIT implant. Twelve weeks post implantation, the bone surrounding both implant types was more developed and in greater contact with the implant surfaces (Figures 8(b) and 8(d)). The arrow in Figure 8(d) points to bone growth within the microporosities of the SIT implant suggesting improved osteoconduction. As with the 3-week samples, stress cracks were also present within the bone from the 12-week control implant.

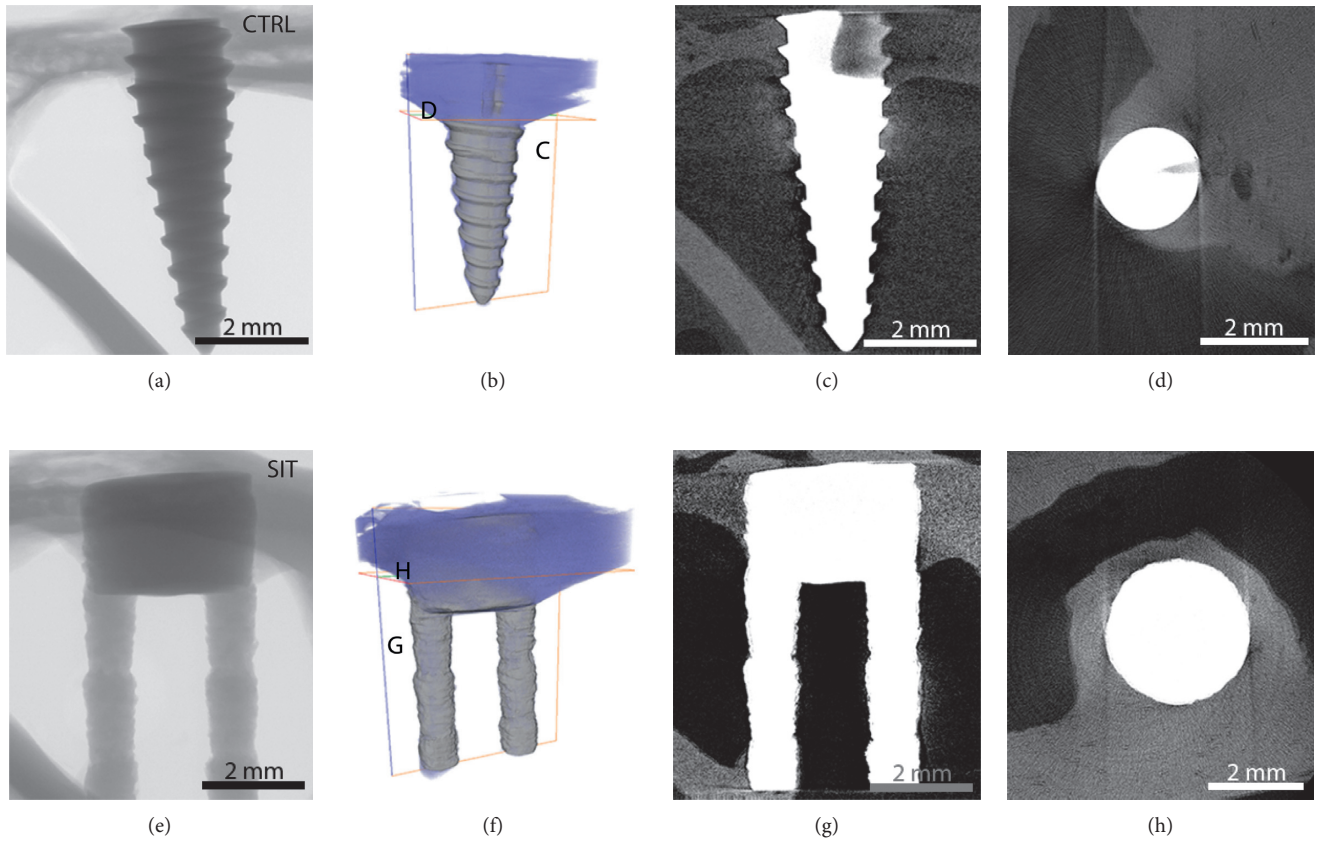


FIGURE 6: Micro-CT analysis following 12-week implantation of CTRL (left column) and SIT (right column) implants. (a, e) Radiographs of each implant. (b, f) 3D visualization of the implant and bone (purple) with orthogonal planes labelled, (c, d, g, h) corresponding orthoslices from (b, f) where the new bone has matured and is of equal intensity to the preexisting bone. Both implants showed bone conduction down the implants from the cortical bone crest; however, bone growth between the stems was not noted in this particular specimen.

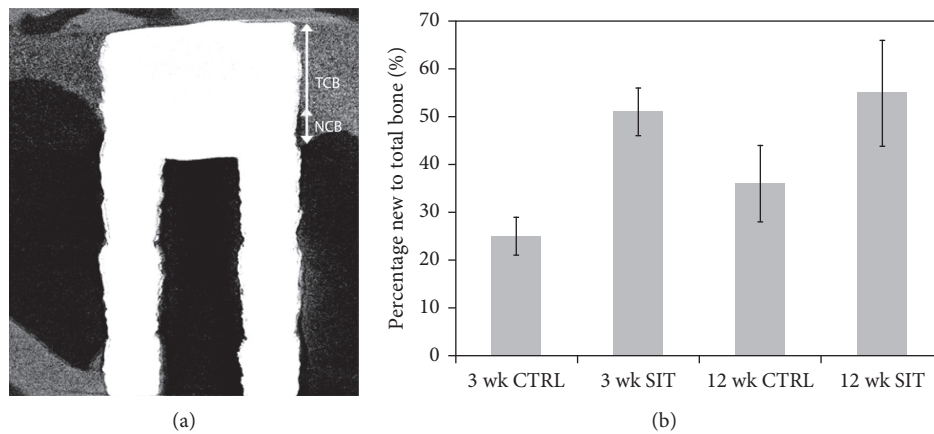


FIGURE 7: (a) Representative micro-CT orthoslice of the SIT device, indicating new cortical bone growth (NCB) and total cortical bone (TCB) from the coronal surface after implantation. (b) Graphical comparison of new bone formation under the cortical bone crest to total bone crest height observed after 3- and 12-week implantation for control and SIT implants.

3.4. *Transmission Electron Microscopy.* To fully assess the osseointegration between the bone and implant and the quality of bone tissue at the interface, higher spatial resolution than that achieved by SEM is required. Figure 9(a)

shows a high-angle annular dark-field (HAADF) image of the SIT implant-bone interface after 12 weeks of healing. A separation at the bone-implant interface, likely due to mechanical stresses during removal and resin infiltration,

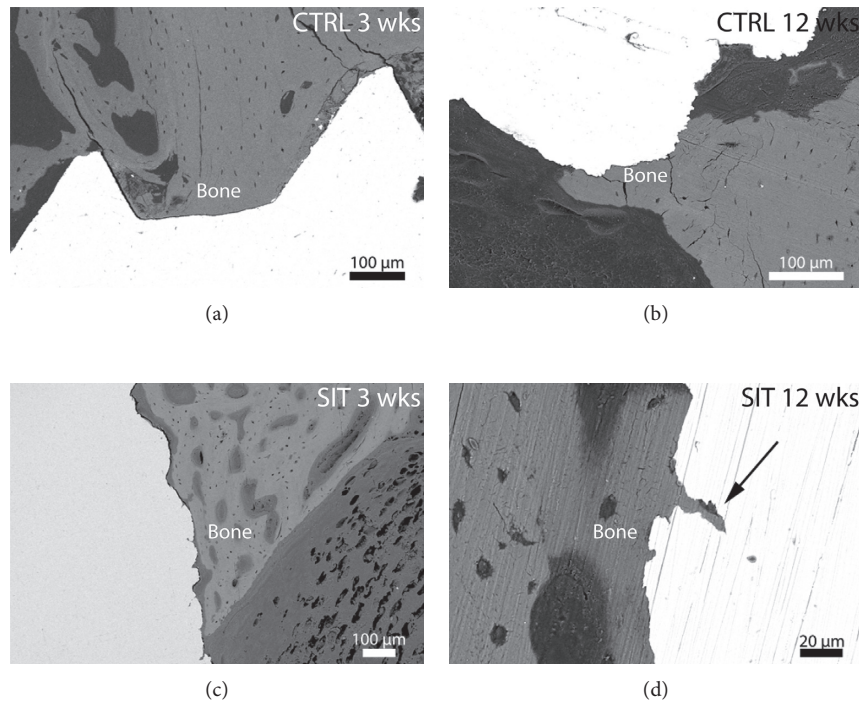


FIGURE 8: BSE-SEM images of the bone-implant interface after 3-week (a, c) and 12-week (b, d) implantation for (a, b) control and (c, d) SIT devices. Bone conduction along and into the microporosities of the SIT implant was observed after 12 weeks (arrowhead).

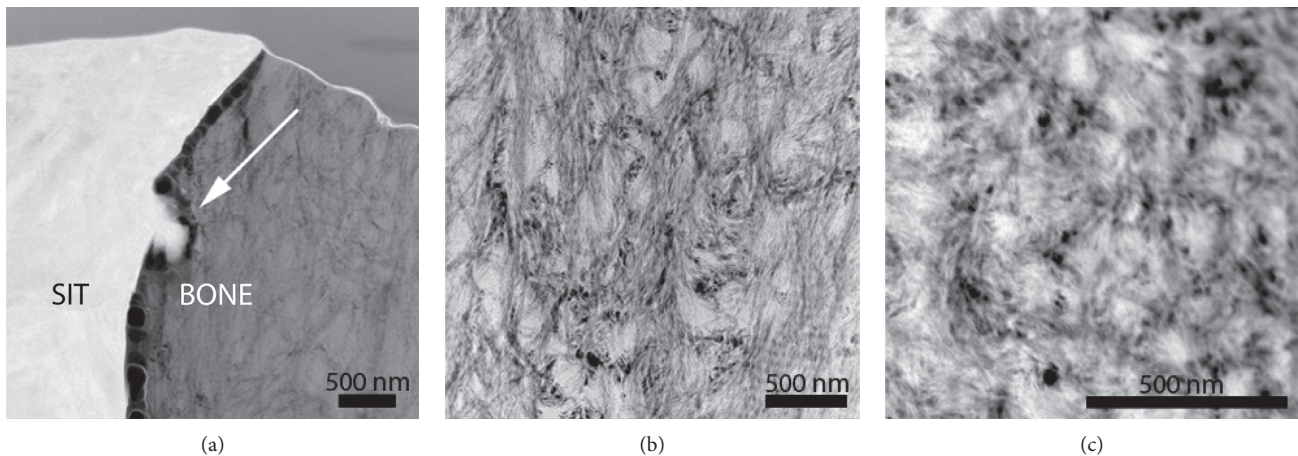


FIGURE 9: HAADF STEM images of (a) the SIT implant-bone interface after 12-week implantation. Bone growth around the nanoscale features was observed (arrow). (b) Ordered collagen fibrils, representative of mature bone, are noted adjacent to the implant at 12 weeks, while at 3-week implantation (c) partially disorganized collagen fibrils, representative of newly developing woven bone, are noted adjacent to the implant, consistent with the new bone structure.

was exaggerated by the FIB during TEM sample preparation. However, the matching contours of the bone and implant surface indicate that the implant and bone were likely in complete contact prior to retrieval. Preparation of a TEM specimen for the SIT implant at 3 weeks was not possible because of a lack of contact at the bone-implant interface. However, a specimen of the bone near the implant interface was removed for TEM. The difference in bone quality near the implant surface at 12 and 3 weeks is shown in Figures 9(b) and 9(c), respectively. The collagen fibers of the 12-week bone are more organized compared to the woven

collagen fibers and visible mineral clusters of the 3-week bone, highlighting the differences in bone maturity.

4. Discussion

A novel implant design by Stemmed Implant Technologies Inc. is marked by a significant geometrical change that employs dual prong-like stems when compared to conventional implants that are generally conical threaded screws. The unique shape of this implant was achieved by the layer-by-layer, bottom-up approach of DMLS. It has been

proposed that the new SIT implant will better resist rotational forces experienced during mastication and bruxism, as well as reducing the amount of bone removed and damaged during surgery and insertion. However, it is important to note that the authors did not evaluate any of these claims in this study. This pilot study aimed to understand the bone-implant interactions of the SIT implant and to predict its potential success in clinical implant scenarios. This was conducted with histology, X-ray, and electron microscopies. While the nature of a pilot study limits this work to a small sample size, the reported findings provide an initial assessment of the biocompatibility of the SIT implant and demonstrate its potential for further animal and clinical studies.

Histological analysis showed active bone growth and remodeling for both the SIT and control implants via osteoclast- and osteoblast-mediated bone matrix resorption and deposition. These observations are similar to previous histomorphometric evaluations of other DMLS implants placed in both sheep and humans [25, 26]. Early bone formation is evident by the presence of osteoblasts connected to the newly formed bone (Figure 4(e)). The observation of bone debris for the control implant at 3 weeks and predominant osteoclast activity at 12 weeks compared to the SIT implant suggests a potential difference in the rate of bone formation and remodeling between the implants. Bone debris in the peri-implant space at early healing time points has been observed previously with threaded implants [26, 27] and may lead to delayed bone formation compared to implants devoid of threads [28]. Histological analysis indicates that the SIT implant shows comparable osseointegration to conventional implants after 12 weeks, marked by complete bone encasement and active remodeling.

The nondestructive basis of micro-CT has been demonstrated as a useful tool for visualizing the entire implant and bone volume in two and three dimensions. Contrast gradients enable differentiation of new bone from old bone and identification of active remodeling sites, as well as sites lacking bone and osseointegration. These micro-CT results indicate that the implants were only anchored in the cortical bone, despite the usually large amount of the trabecular bone present in the metaphysis of rabbits where implants were placed, indicating a potential misplacement. Thus, this study is limited to the evaluation of cortical bone only. A fairly small amount of bone growth was conducted from the cortical bone crest down the implant length for the control implant compared to a slightly larger amount on the SIT implant that was even clearly visible between the implant stems at 3 weeks. Ideally, placement in the trabecular bone would maintain bone trabeculae between the stems for added stability. The reason for the observed difference in bone growth is somewhat unclear due to the potential interplay between differences in both the osteoconductivity of titanium and steel and the radial bone growth required for the control implants due to the threaded design. By three weeks, the majority of the bone volume, which was to encapsulate the implants, had been deposited and was remodeled into more mature dense bone, but not a greater quantity, by 12 weeks.

While micro-CT is ideal for a general overview of bone growth, it lacks the resolution necessary to visualize sub-micron features at the bone-implant contact. The greater extent of bone growth from the cortical region down the implant surfaces for the SIT implant was confirmed by SEM. The SIT implant conducted bone growth along its length and within the stems (Figure 8). The control implant initiated a limited amount of new bone formation, and large cracks were present within the cortical bone, perhaps caused by overtorquing during implant placement. Very tight integration, with no separation, was seen around the SIT implant, as the bone had grown into the micropores of the implant surface, which is an indicator of biocompatibility. Comparison of the bone-implant contact across studies remains challenging because of a lack of standardized methodologies employed to model bone growth and measure the bone-implant contact (BIC). Animal model selection, bone type, surgical procedure, heal time, sample preparation methodology, and selected implant length for BIC measurements varies across studies, all of which can influence the BIC [16, 26, 29, 30]. Nevertheless, previously reported BIC measurements of machined and analogous 3D printed implants after 2 weeks were 20% for both implant types [26]. In this study, we instead looked at the conduction of bone growth down the implant surface, since it was placed primarily in the cortical bone, and found as expected that the titanium SIT implant was a better conductor of bone growth at both early and late time points.

Due to bone-implant interface separation caused by FIB sample preparation, the exact integration between the bone and the SIT implant could not be analyzed; however, the maturity of the bone surrounding the implant could be evaluated to demonstrate the success of bone growth at the implantation site. TEM imaging of the lift-outs revealed differences in the orientation of the collagen fibrils and the presence of mineral clusters after 3 and 12 weeks. This suggests that the mechanism of distant osteogenesis is occurring during healing after the insertion of the implants. In distant osteogenesis, mature bone acts as a substrate for osteogenic cells to form a matrix that gradually encroaches upon the implant surface [31].

This pilot study was limited to an investigation of the structural and biochemical interaction of the implant device in vivo via advanced imaging modalities. To further validate these results, future work should focus on determining the mechanical integrity of the bone-implant interface. Mechanical testing of the implanted devices would also be beneficial to improving the understanding of the overall system and the potential advantages to using additive manufacturing as a production method for dental implants. This could potentially be completed in vivo through methods such as resonance frequency analysis to determine implant stability [32] and via pullout tests to confirm adequate mechanical strength [33]. Complementary information from in vitro testing, such as investigating cell viability [34], may provide additional insight into the biocompatibility of the device. Other works reporting 3D printed implant devices have shown promising cell viability and biocompatibility [35–37].

5. Conclusions

Additive manufacturing provides a means for innovative dental implant designs with inherent surface features which facilitate bone integration. Initial observation of a dual-stemmed 3D printed dental implant has shown successful bone growth and bone-implant contact similar to conventional and other 3D printed implants up to 12 weeks of healing in rabbits. In some cases, new bone formation was noted in between the stems of the device, although the stems were not within a trabecular bone region. Conventional implants showed mechanical interlocking but did have indications of stress cracking and bone debris. This pilot study demonstrates that this 3D printed implant design is biocompatible, as it allows for successful osseointegration in rabbits up to 12 weeks, and supports additional studies to obtain more statistical validation, including mechanical testing.

Conflicts of Interest

The authors declare no conflicts of interest.

Acknowledgments

Financial support for this study was provided by the NSERC Engage Grant Program. Implants and surgical tools for implantation were provided by Stemmed Implant Technologies Incorporated. Electron microscopy was performed at the Canadian Centre for Electron Microscopy, a facility supported by NSERC and other governmental agencies. Staff of the Central Animal Facility and Faculty of Health Science Electron Microscopy Facility are gratefully acknowledged. The authors acknowledge the assistance of Kristoff Malejczuk in optimizing micro-CT operating conditions at the McMaster Automotive Resource Centre.

References

- [1] P. I. Brånemark, B. O. Hansson, R. Adell et al., "Osseointegrated implants in the treatment of the edentulous jaw. Experience from a 10-year period," *Scandinavian Journal of Plastic and Reconstructive Surgery. Supplementum*, vol. 16, pp. 1–132, 1977.
- [2] D. Tran, I. Gay, J. Diaz-Rodriguez, K. Parthasarathy, R. Weltman, and L. Friedman, "Survival of dental implants placed in grafted and nongrafted bone: a retrospective study in a university setting," *International Journal of Oral & Maxillofacial Implants*, vol. 31, no. 2, pp. 310–317, 2016.
- [3] C. A. A. Lemos, M. L. F. Alves, R. Okamoto, M. R. Mendonça, and E. P. Pellizzer, "Short dental implants versus standard dental implants placed in the posterior jaws: a systematic review and meta-analysis," *Journal of Dentistry*, vol. 47, pp. 8–17, 2016.
- [4] H.-J. Han, S. Kim, and D.-H. Han, "Multifactorial evaluation of implant failure: a 19-year retrospective study," *International Journal of Oral & Maxillofacial Implants*, vol. 29, no. 2, pp. 303–310, 2014.
- [5] H. L. Sun, C. Huang, Y. R. Wu, and B. Shi, "Failure rates of short (≤ 10 mm) dental implants and factors influencing their failure: a systematic review," *International Journal of Oral & Maxillofacial Implants*, vol. 26, no. 4, pp. 816–825, 2011.
- [6] S. Elangovan and V. Allareddy, "Estimates of hospital based emergency department visits due to dental implant failures in the United States," *Journal of Evidence Based Dental Practice*, vol. 16, no. 2, pp. 81–85, 2016.
- [7] L. Carlsson, T. Rostlund, T. Albrektsson, B. Albrektsson, and P. Branemark, "Osseointegration of titanium implants," *Acta Orthopaedica Scandinavica*, vol. 57, no. 4, pp. 285–289, 1986.
- [8] C. Oldani and A. Dominguez, Titanium as a Biomaterial for Implants, *Recent Advances in Athroplasty*, S. K. Fokter Ed., InTech, London, UK, 2012.
- [9] M. Geetha, A. K. Singh, R. Asokamani, and A. K. Gogia, "Ti based biomaterials, the ultimate choice for orthopaedic implants—a review," *Progress in Materials Science*, vol. 54, no. 3, pp. 397–425, 2009.
- [10] B. E. J. Lee, S. Ho, G. Mestres, M. Karlsson Ott, P. Koshy, and K. Grandfield, "Dual-topography electrical discharge machining of titanium to improve biocompatibility," *Surface and Coatings Technology*, vol. 296, pp. 149–156, 2016.
- [11] F. A. Shah, X. Wang, P. Thomsen, K. Grandfield, and A. Palmquist, "High-resolution visualization of the osteocyte lacuno-canalicular network juxtaposed to the surface of nanotextured titanium implants in human," *ACS Biomaterials Science & Engineering*, vol. 1, no. 5, pp. 305–313, 2015.
- [12] A. Palmquist, L. Emanuelsson, R. Brånemark, and P. Thomsen, "Biomechanical, histological and ultrastructural analyses of laser micro- and nano-structured titanium implant after 6 months in rabbit," *Journal of Biomedical Materials Research Part B: Applied Biomaterials*, vol. 97B, no. 2, pp. 289–298, 2011.
- [13] R. Brånemark, L. Emanuelsson, A. Palmquist, and P. Thomsen, "Bone response to laser-induced micro- and nano-size titanium surface features," *Nanomedicine: Nanotechnology, Biology and Medicine*, vol. 7, no. 2, pp. 220–227, 2011.
- [14] K. Grandfield, S. Pujari, M. Ott, H. Engqvist, and W. Xia, "Effect of calcium and strontium on mesoporous titania coatings for implant applications," *Journal of Biomaterials and Nanobiotechnology*, vol. 4, no. 2, pp. 107–113, 2013.
- [15] Y. T. Sul, J. Jönsson, G. S. Yoon, and C. Johansson, "Resonance frequency measurements in vivo and related surface properties of magnesium-incorporated, micropatterned and magnesium-incorporated TiUnite®, Osseotite®, SLA® and TiOblast® implants," *Clinical Oral Implants Research*, vol. 20, no. 10, pp. 1146–1155, 2009.
- [16] N. M. Poulos, N. A. Rodriguez, J. Lee et al., "Evaluation of a novel calcium phosphate-coated titanium porous oxide implant surface: a study in rabbits," *International Journal of Oral & Maxillofacial Implants*, vol. 26, no. 4, pp. 731–738, 2011.
- [17] O. E. Ogle, "Implant surface material, design, and osseointegration," *Dental Clinics of North America*, vol. 59, no. 2, pp. 505–520, 2015.
- [18] S. J. Hollister, "Porous scaffold design for tissue engineering," *Nature Materials*, vol. 4, no. 7, pp. 518–524, 2005.
- [19] T. B. Kim, S. Yue, Z. Zhang, E. Jones, J. R. Jones, and P. D. Lee, "Additive manufactured porous titanium structures: through-process quantification of pore and strut networks," *Journal of Materials Processing Technology*, vol. 214, no. 11, pp. 2706–2715, 2014.
- [20] J. Lv, Z. Jia, J. Li et al., "Electron beam melting fabrication of porous Ti6Al4V scaffolds: cytocompatibility and osteogenesis," *Advanced Engineering Materials*, vol. 17, no. 9, pp. 1391–1398, 2015.

- [21] F. A. Shah, A. Snis, A. Matic, P. Thomsen, and A. Palmquist, "3D printed Ti6Al4V implant surface promotes bone maturation and retains a higher density of less aged osteocytes at the bone-implant interface," *Acta Biomaterialia*, vol. 30, pp. 357–367, 2016.
- [22] A. Cheng, A. Humayun, D. J. Cohen, B. D. Boyan, and Z. Schwartz, "Additively manufactured 3D porous Ti-6Al-4V constructs mimic trabecular bone structure and regulate osteoblast proliferation, differentiation and local factor production in a porosity and surface roughness dependent manner," *Biofabrication*, vol. 6, no. 4, p. 45007, 2014.
- [23] E. Baril, L. P. Lefebvre, and S. A. Hacking, "Direct visualization and quantification of bone growth into porous titanium implants using micro computed tomography," *Journal of Materials Science: Materials in Medicine*, vol. 22, no. 5, pp. 1321–1332, 2011.
- [24] K. Donath and G. Breuner, "A method for the study of undecalcified bones and teeth with attached soft tissues. The Säge-Schliff (sawing and grinding) technique," *Journal of Oral Pathology and Medicine*, vol. 11, no. 4, pp. 318–326, 1982.
- [25] C. Mangano, A. Piattelli, S. d'Avila et al., "Early human bone response to laser metal sintering surface topography: a histologic report," *Journal of Oral Implantology*, vol. 36, no. 2, pp. 91–96, 2010.
- [26] S. Stübinger, I. Mosch, P. Robotti et al., "Histological and biomechanical analysis of porous additive manufactured implants made by direct metal laser sintering: a pilot study in sheep," *Journal of Biomedical Materials Research Part B: Applied Biomaterials*, vol. 101, no. 7, pp. 1154–1163, 2013.
- [27] M. Carlo, P. Adriano, M. Francesco et al., "Computed microtomography study of 2 human-retrieved direct laser metal formed titanium implants," *Implant Dentistry*, vol. 22, no. 2, pp. 175–181, 2013.
- [28] A. Piattelli, *Bone Response to Dental Implant Materials*, Woodhead Publishing, Sawston, UK, 2016.
- [29] R. N. Brown, B. E. Sexton, G. Chu et al., "Comparison of stainless steel and titanium alloy orthodontic miniscrew implants: a mechanical and histologic analysis," *American Journal of Orthodontics and Dentofacial Orthopedics*, vol. 145, no. 4, pp. 496–504, 2014.
- [30] A. Palmquist, A. Snis, L. Emanuelsson, M. Browne, and P. Thomsen, "Long-term biocompatibility and osseointegration of electron beam melted, free-form-fabricated solid and porous titanium alloy: experimental studies in sheep," *Journal of Biomaterials Applications*, vol. 27, no. 8, pp. 1003–1016, 2011.
- [31] J. E. Davies, "Understanding peri-implant endosseous healing," *Journal of Dental Education*, vol. 67, no. 8, pp. 932–949, 2003.
- [32] W. Chang, S. Lee, C. Wu et al., "A newly designed resonance frequency analysis device for dental implant stability detection," *Dental Materials Journal*, vol. 26, no. 5, pp. 665–671, 2007.
- [33] C. Aparicio, A. Padrós, and F.-J. Gil, "In vivo evaluation of micro-rough and bioactive titanium dental implants using histometry and pull-out tests," *Journal of the Mechanical Behavior of Biomedical Materials*, vol. 4, no. 8, pp. 1672–1682, 2011.
- [34] S. F. Alves and T. Wassall, "In vitro evaluation of osteoblastic cell adhesion on machined osseointegrated implants," *Brazilian Oral Research*, vol. 23, no. 2, pp. 131–136, 2009.
- [35] G. Li, L. Wang, W. Pan et al., "In vitro and in vivo study of additive manufactured porous Ti6Al4V scaffolds for repairing bone defects," *Scientific Reports*, vol. 6, no. 1, p. 34072, 2016.
- [36] D. J. Cohen, A. Cheng, K. Sahingur et al., "Performance of laser sintered Ti-6Al-4V implants with bone-inspired porosity and micro/nanoscale surface roughness in the rabbit femur," *Biomedical Materials*, vol. 12, no. 2, p. 025021, 2017.
- [37] K. Gulati, M. Prideaux, M. Kogawa et al., "Anodized 3D-printed titanium implants with dual micro- and nanoscale topography promote interaction with human osteoblasts and osteocyte-like cells," *Journal of Tissue Engineering and Regenerative Medicine*, 2016.

Clinical Study

Morse Taper Connection Implants Placed in Grafted Sinuses in 65 Patients: A Retrospective Clinical Study with 10 Years of Follow-Up

Francesco Mangano,¹ Renata Bakaj,¹ Irene Frezzato,² Alberto Frezzato,² Sergio Montini,³ and Carlo Mangano⁴

¹Department of Medicine and Surgery, University of Insubria, 21100 Varese, Italy

²Private Practice, 45100 Rovigo, Italy

³Private Practice, 22019 Tremezzo, Italy

⁴Department of Dental Science, Vita Salute S. Raffaele University, 20132 Milan, Italy

Correspondence should be addressed to Francesco Mangano; francescoguidomangano@gmail.com

Received 19 June 2017; Accepted 10 July 2017; Published 7 August 2017

Academic Editor: Luigi Canullo

Copyright © 2017 Francesco Mangano et al. This is an open access article distributed under the Creative Commons Attribution License, which permits unrestricted use, distribution, and reproduction in any medium, provided the original work is properly cited.

Purpose. To investigate the 10-year survival and complication rates of Morse taper connection implants (MTCIs) placed in grafted sinuses. **Methods.** This study reports on patients treated with maxillary sinus augmentation (with the lateral window technique (LWT) or the transalveolar osteotomy technique (TOT)) and installed with MTCIs supporting fixed restorations (single crowns (SCs) and fixed partial dentures (FPDs)), in two dental clinics. The outcomes of the study were the 10-year implant survival and complication rates. **Results.** Sixty-five patients (30 males and 35 females) with a mean age of 62.7 (± 10.2) years were installed with 142 MTCIs: 79 fixtures were inserted with the LWT and 63 were placed with the TOT. After ten years, five implants failed, for an overall survival rate of 96.5%. Three implants failed in the LWT group, for a survival rate of 96.3%; two implants failed in the TOT group, for a survival rate of 96.9%. The 10-year incidence of biologic complications was 11.9%. Prosthetic complications were all technical in nature and amounted to 7.6%. **Conclusions.** MTCIs seem to represent a successful procedure for the prosthetic restoration of the grafted posterior maxilla, in the long term. This study was registered in the ISRCTN registry with number ISRCTN30772506.

1. Introduction

In the posterior maxilla, sinus pneumatization with ageing [1] and postextraction alveolar crest resorption [2] can severely affect the amount of bone volume, jeopardizing a successful osseointegration, unless a reconstructive osseous surgery is performed to sustain a functional and aesthetic implant-supported restoration [3].

Currently, bone volume increase in the posterior maxilla is mainly obtained by maxillary sinus floor augmentation [4–6]. This surgical procedure was found to be reliable and it can be performed according to two major techniques: the lateral window approach [7], which is still the most common method, and the transalveolar osteotomy technique [8, 9].

Many variables should be taken into consideration by the clinician before choosing the surgical technique, such as the residual bone quantity [9], the type of grafting material [10–12], the use of barrier membranes [13], the implant insertion timing in relation to grafting (one- or two-stage approach) [14, 15], and the type of implants to be placed. The one-stage approach consists of simultaneous implant placement into the augmented sinus graft [14], while the two-stage method involves implant insertion secondary to reconsolidation of the bone graft [15].

Morse taper connection implants (MTCIs) represent a valid treatment option for restoring partially and completely edentulous patients, as demonstrated by several long-term follow-up studies [16–19].

In MTCIs, the implant-abutment connection relies on the “cold welding” achieved through frictional resistance between the surfaces of the abutment and the implant [18, 20]. If the taper angle is less than 2° , the connection is called “self-locking” [17, 20].

Although several studies have confirmed that the use of MTCIs yields excellent survival and success rates [16–19, 21–23], there are currently no clinical studies on the long-term outcomes of MTCIs placed in the grafted sinuses.

In light of the above, the purpose of this retrospective clinical study was to investigate the 10-year survival and complication rates of MTCIs placed in grafted sinuses via the lateral window technique or the transalveolar osteotomy technique.

2. Materials and Methods

2.1. Patient Population. We conducted a retrospective clinical study on patients that have been treated with maxillary sinus augmentation (with the lateral window or the transalveolar osteotomy technique) and with fixed prosthetic restorations (SCs and FPDs) supported by MTCIs, in the period from January 2003 to August 2006, in two private dental clinics (located in Gravedona, Como, Italy, and in Padua, Italy, resp.).

Patients selected for the present study were identified through the records of two dental clinics; these records included all information about each enrolled patient (patient-related information: systemic health, age at surgery, gender, smoking habit, and oral hygiene) and each implant-supported restoration placed (implant-related information: position, premolar or molar; length and diameter; restoration-related information: type of prosthesis, SC or FPD; date of deliveries). The customized records included all information about any implant failure and/or biological/prosthetic complication that occurred during the 10-year follow-up.

Patients were excluded from the present retrospective study in case of (1) systemic diseases or ongoing treatments/conditions that may contraindicate intervention (uncontrolled diabetes, immunocompromised states, chemo/radiotherapy of the head/neck region, treatment with amino-bisphosphonates, psychiatric disorders, and abuse of drugs/alcohol); (2) oral diseases (nontreated periodontal disease and active/chronic/persistent sinus infections); (3) nonacceptance or inability to attend the 10-year follow-up clinical/radiographic examination for different reasons (death, hospitalization, and transferring to another country or city).

All of the enrolled patients were requested to return to the dental clinic and to attend a 10-year control follow-up clinical/radiographic examination. Patients who did not accept to attend the 10-year follow-up control, as well as patients who could not attend it, were excluded from the present study. All included patients read and signed a written consent form for inclusion in this retrospective study. Approval of the Ethics Committee at University of Insubria was obtained for this study; the Helsinki Declaration of 1975, as revised in 2008, was followed. In addition, the study was registered in the publicly available ISRCTN clinical studies

registry, a trial registry recognized by the WHO, with number ISRCTN30772506.

2.2. Implant Design and Surface Characterization. The implants used were screw-shaped and made of grade-5 titanium alloy (Leone Implants®, Florence, Italy). Their surfaces were blasted with $350\ \mu\text{m}$ Al_2O_3 particles and acid-etched with HNO_3 , producing a R_a value (the peak-valley distance of surface irregularities) of $2.5\ \mu\text{m}$ [24] (Figure 1). The implant-abutment connection is based on a Morse taper with an angle of 1.5° combined with an internal hexagon [16–19, 21] (Figure 2).

2.3. Preoperative Work-Up. Each patient underwent a primary investigation within a complete medical examination of the hard and soft oral tissues and panoramic radiographs. Where needed, computed tomography (CT) scans were requested, in selected patients. CT datasets were acquired and then converted into DICOM format. DICOM files were used to obtain a three-dimensional reconstruction of the jaws in implant navigation software, which showed the anatomic tissues including residual bone volume, thickness/density of the cortical and cancellous bone, ridge angulations, and also possible sinus pathology. Each implant site was carefully assessed. An accurate evaluation of the edentulous ridges using casts and diagnostic wax-up were included in the preoperative workups.

2.4. Surgery. Patients were instructed to rinse with 0.2% chlorhexidine mouthwash (Chlorhexidine®, OralB, Boston, MA) for 1 minute twice daily, two days before surgery, and also for 1 minute prior to the surgery. All patients received prophylactic antibiotic therapy of 2 g of amoxicillin + clavulanic acid 1 hour before the surgery. After surgery, they continued taking antibiotics twice daily for 6 days. All patients were treated under local anaesthesia using 4% articaine with adrenaline 1:100000.

When the lateral window technique (LWT) was used, the surgeon proceeded as follows. In order to expose the maxillary sinus lateral side, a horizontal crestal incision and two vertical incisions were performed in the buccal mucosa, in order to raise a mucoperiosteal flap. Using piezosurgery equipment under continuous saline irrigation, it was possible to outline a bone window approximately 1.5×1.5 cm in size. The sinus mucosa was separated from the bony surface of the sinus floor with an elevator and the bony window fragment removed. Great effort was made to prevent disruption of the Schneiderian membrane; when this occurred, a collagen barrier was used to contain the graft. After the elevation of the Schneiderian membrane was completed, the gap created between the maxillary alveolar process and the new sinus floor was filled with coral-derived porous hydroxyapatite (Biocoral®, Biocoral Inc., Saint Gonnerly, France) blocks. These blocks were shaped and modelled by the surgeon, who also used porous hydroxyapatite granules to completely fill in the spaces between the porous material blocks and residual bone crest. The granules were interspersed with tetracycline powder to obtain a local antibiotic effect and moistened with

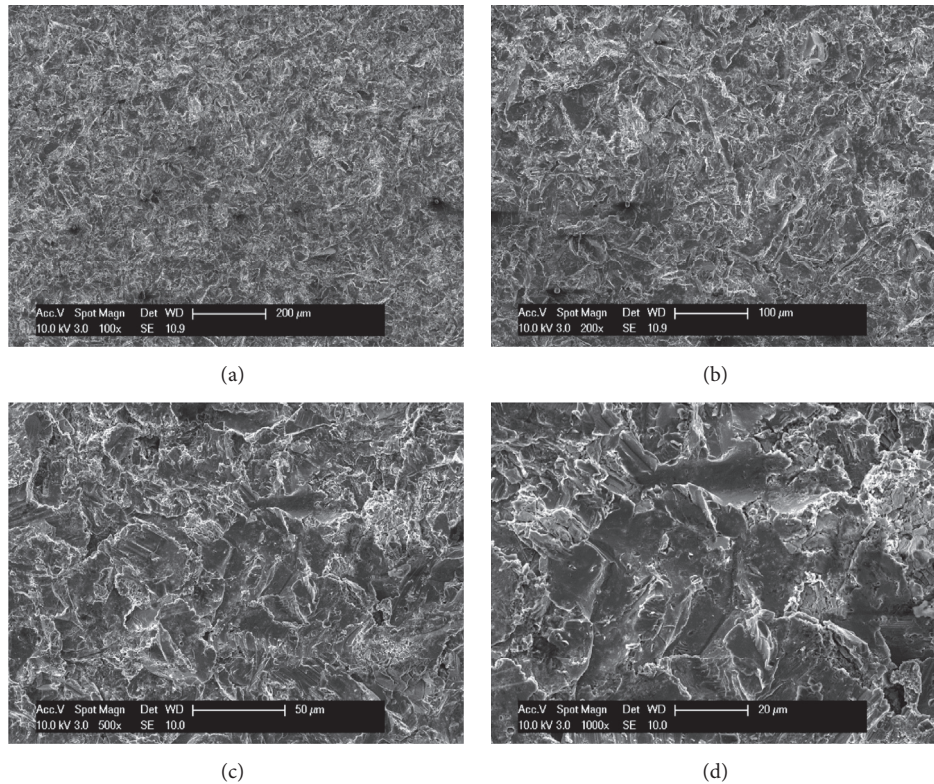


FIGURE 1: The sandblasted-acid-etched surface of the implants used in this study, at different magnification: (a) $\times 100$; (b) $\times 200$; (c) $\times 500$; (d) $\times 1000$. Implant surface was treated with a sandblasting process producing an average roughness R_a of $2.5 \mu\text{m}$; fixtures were blasted with alumina particles. Sandblasting was followed by a decontamination treatment series, including a passivation process with nitric acid.



FIGURE 2: The implants used in this study featured a cone Morse taper interference-fit (TIF) locking-taper, with a taper angle of 1.5° , combined with an internal hexagon.

physiological saline solution so that this mixture could be easily moulded to fit the gaps. The sinus window was then sealed with the bony window fragment, covered by a collagen membrane and the mucosa sutured with non-absorbable sutures. When using a two-stage approach, the healing period for grafted sinuses was 6 months before implant placement. Conversely, in the one-stage approach, simultaneous implant insertion was performed. Implant placement was performed

as follows. Spiral drills of increasing diameter were used under constant irrigation, to prepare the implant site. All implants were placed at the bone crest level.

When the transalveolar osteotomy technique (TOT) was used, the surgeons proceeded as follows. A horizontal crestal incision with minimal lateral releases was performed to expose all implant sites. A mucoperiosteal flap was elevated. The preparation of the site was performed with a speed

reducing gear handpiece under copious saline irrigation. Using the aforementioned drill sequence, the palatal osseous lid was removed and the Schneiderian membrane was meticulously lifted by means of the sequential use of osteotomes and a metal mallet. After the elevation was completed, the sinus cavity was grafted with coral-derived hydroxyapatite granules, mixed with tetracycline powder. The material was packed into the cavity and the implant was placed. The fixture was tightly screwed by means of a hand ratchet until it came into alignment with the crest of alveolar bone. Excessive graft material particles were removed and the flap was repositioned. Primary interrupted tension-free wound closure was accomplished with nonabsorbable sutures. With the transalveolar osteotomy technique, the implants were submerged for a minimum healing period of 3 months before beginning the prosthetic phases.

2.5. Healing Period, Second-Stage Surgery, and Prosthetic Restoration. Postoperative pain was controlled in all patients with 100 mg nimesulide intake every 12 hours for 2 days and detailed oral hygiene instructions were given, including mouth rinses with 0.2% chlorhexidine for 7 days. Sutures were removed around 8–10 days after the surgery.

The submerged healing period lasted around 3–9 months (lateral window technique, two-stage approach = 6 + 3 months; lateral window technique, one-stage approach = 3 months; transalveolar osteotomy technique = 3 months). A second surgery was performed to accede to the healed implants and to place the healing abutments. After two weeks, impressions were taken and, one week later, the provisional restorations were provided. The provisional restorations remained in situ for 3 months, before placing definitive restorations. All definitive restorations (SCs and FPDs) were ceramometallic and cemented with a temporary oxide-cement.

2.6. Implant Survival and Complications. Implants were classified as “surviving” when still functioning at the final follow-up.

Conversely, all implants that were lost and/or had to be removed (for implant mobility due to absence and/or loss of osseointegration in absence of infection, for recurrent/persistent peri-implantitis, and for implant body fracture) were considered as “failed.”

In addition, all biologic and prosthetic complications registered during the entire follow-up period were considered. Among the biologic complications, loss of the graft, sinus infection, peri-implant mucositis, and peri-implantitis were considered [25]. Among the prosthetic complications, all mechanical complications (i.e., complications affecting the prefabricated implant components at the implant-abutment interface such as abutment loosening and abutment fracture) and all technical complications (i.e., complications affecting the superstructures made by the dental technician, such as loss of retention, ceramic chipping/fracture, and fracture of the metallic framework of restoration) were considered [26].

All data were carefully analysed in a statistical software package. Means and standard deviations, ranges,

TABLE 1: Patient distribution.

	Number of patients (%)	* <i>P</i>
Gender		
<i>Males</i>	30 (46.2%)	0.535
<i>Females</i>	35 (53.8%)	
Age at surgery		
<i>20–39 years</i>	2 (3.1%)	<0.0001
<i>40–59 years</i>	21 (32.3%)	
<i>60–79 years</i>	42 (64.6%)	
Smoking habit		
<i>Yes</i>	15 (23.1%)	<0.0001
<i>No</i>	50 (76.9%)	
Oral hygiene		
<i>Satisfactory</i>	35 (53.8%)	0.535
<i>Not satisfactory</i>	30 (46.2%)	
Total	65 (100%)	—

* *P* = Chi-square test.

and confidence intervals were calculated for the available quantitative variables (patients' age). Absolute and relative frequency distributions were calculated for all the available qualitative variables. The distribution of the patients (by gender, age at surgery, smoking, and oral hygiene habits) and the distribution of the implants (by sinus augmentation technique, position, length and diameter, and type of supported restoration) were investigated, and a Chi-square test (with level of significance set at 0.05) was used to calculate the differences in distribution between the groups. Finally, implant survival and complications were calculated using the implant as a statistical unit.

3. Results

3.1. Patients Enrolled and Implants Placed. Sixty-five patients were enrolled in this study: 30 males (30/65: 46.2%) and 35 females (35/65: 53.8%) with an average age of 62.7 ± 10.2 years (median 66, range 38–79, 95% CI: 60.3–65.1). Most of the enrolled patients (42/65 patients, 64.6%) were between the ages of 60 and 79 at surgery, whereas 21 (21/65, 32.3%) were between the ages 40 and 59 and only two patients (2/65: 3.1%) were between the ages of 20 and 39 years. Fifteen patients (15/65: 23.1%) were smokers. Among all patients, 35 (35/65: 53.8%) had satisfactory oral hygiene with low plaque score levels and 30 patients (30/65: 46.2%) had unsatisfactory oral hygiene levels. The distribution of the patients by gender, age at surgery, smoking habit, and oral hygiene is reported in Table 1.

As twelve patients required bilateral maxillary sinus augmentation, the number of sinus augmentation procedures amounted to 77. Forty-five of these procedures were performed with the lateral window technique and 32 were performed with the transalveolar osteotomy technique.

In total, 142 implants were placed: 79 (79/142: 55.6%) were inserted with the lateral window technique and 63 (63/142: 44.4%) were placed with the transalveolar osteotomy technique. With regard to the distribution of the implants,

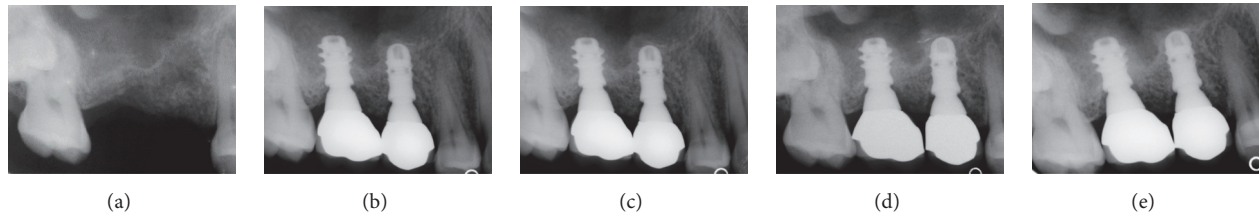


FIGURE 3: Two implants (#15 and #16) inserted with the transalveolar osteotomy technique: (a) preoperative rx; (b) radiographic control at the delivery of final restorations; (c) radiographic control 1 year after implant placement; (d) radiographic control 5 years after implant placement; (e) radiographic control 10 years after implant placement.

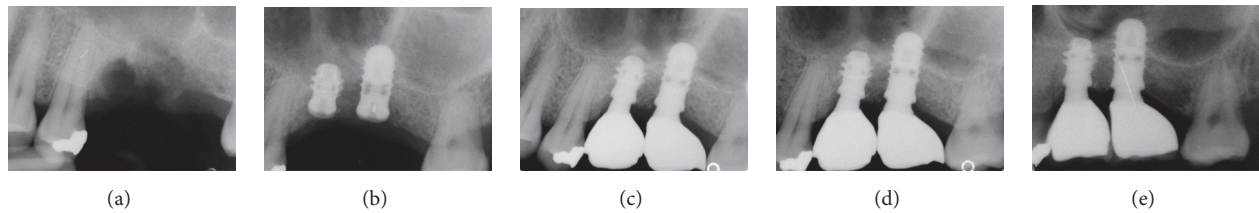


FIGURE 4: Two implants (#25 and #26) inserted with the transalveolar osteotomy technique: (a) preoperative rx; (b) the implants placed after the sinus elevation with the Summers technique; (c) radiographic control 1 year after implant placement; (d) radiographic control 5 years after implant placement; (e) radiographic control 10 years after implant placement.

55 (55/142: 38.7%) were premolars and 87 (87/142: 61.3%) were molars; the most frequent length was 10 mm (49/142 fixtures, 34.5%), followed by 8 mm (35/142 implants, 24.7%), 12 mm (32/142 implants, 22.5%), and 14 mm (26/142 implants, 18.3%). The most frequently used diameter was 4.1 mm (75/142 fixtures, 52.8%), followed by 4.8 mm (43/142 fixtures, 30.3%) and 3.3 mm (24/142 fixtures: 16.9%). Finally, with regard to the prosthetic restoration, as 44 fixtures were used to support SCs, and 98 fixtures were used to support FPDs, the final prosthetic restorations amounted to 44 SCs and 47 FPDs (43 FPDs were supported by two implants and 4 FPDs were supported by three implants, resp.). The distribution of the fixtures by surgical technique, position, length, diameter, and type of supported restoration is reported in Table 2.

3.2. Implant Survival and Complications. At the end of the study, 10 years after implant placement, only five implants failed (5/142), for an overall survival rate of 96.5% (Figures 3–5). Three implants failed in the lateral window group (3/79), for a survival rate of 96.3%. Two implants failed in the transalveolar osteotomy group (2/63), for a survival rate of 96.9%. Three of the failed implants were removed during the second-stage surgery, because they showed clinical mobility due to absence of osseointegration. These failures occurred before the connection of the prosthetic abutment and were therefore defined as “early” failures. Conversely, two implants failed in the same patient due to recurrent peri-implant infection and were removed due to massive bone loss 6 years after placement. All information regarding the failed implants is summarized in Table 3.

With regard to biologic complications, one patient experienced infection and loss of the graft after sinus augmentation with the lateral window technique, probably due to an undetected perforation of the Schneiderian membrane. This

TABLE 2: Implant distribution.

	Number of implants (%)	* <i>p</i>
Sinus augmentation technique		
<i>Lateral window technique</i>	79 (55.6%)	0.179
<i>Transalveolar osteotomy technique</i>	63 (44.4%)	
Position		
<i>Premolars</i>	55 (38.7%)	0.007
<i>Molars</i>	87 (61.3%)	
Length		
<i>8 mm</i>	35 (24.7%)	0.045
<i>10 mm</i>	49 (34.5%)	
<i>12 mm</i>	32 (22.5%)	
<i>14 mm</i>	26 (18.3%)	
Diameter		
<i>3.3 mm</i>	24 (16.9%)	<0.0001
<i>4.1 mm</i>	75 (52.8%)	
<i>4.8 mm</i>	43 (30.3%)	
Restoration		
<i>SC</i>	44 (31.0%)	<0.0001
<i>FPD</i>	98 (69.0%)	
<i>Total</i>	142 (100%)	—

**p* = Chi-square test.

sinus was surgically revisited and cleaned. This intervention was followed by a prolonged systemic antibiotic treatment and a healing period of 6 months and subsequent successful augmentation. Conversely, no biologic complications were found for the implants placed according to the transalveolar osteotomy technique.

In addition, nine implants (9/142: 6.3%) suffered from a reversible inflammation of the peri-implant soft tissues

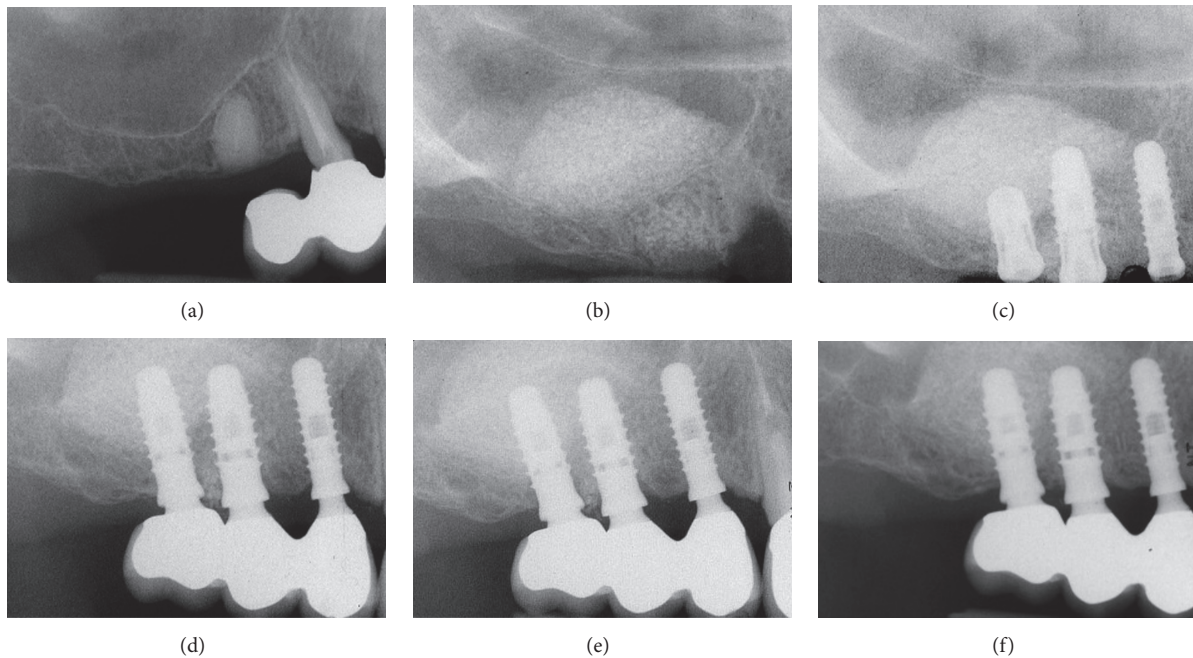


FIGURE 5: Three implants (#14, #15, and #16) inserted with the lateral window technique. (a) preoperative rx; (b) periapical rx after the sinus augmentation procedure according to Tatum; (c) 6 months later the implants are inserted; (d) radiographic control at the delivery of the final restoration; (e) radiographic control 5 years after implant placement; (f) radiographic control 10 years after implant placement.

TABLE 3: Failed implants.

Gender	Age	Smoke	Hygiene	Procedure	Position	Type	Reason/timing
Male	46	No	Poor	LWT	Premolar	4.1 × 10	Failure to osseointegrate after 3 months
Male	66	Yes	Good	LWT	Premolar	4.1 × 10	Failure to osseointegrate after 3 months
Female	59	No	Good	LWT	Molar	4.8 × 8	Failure to osseointegrate after 3 months
Female	66	Yes	Poor	TOT	Premolar	4.1 × 12	Peri-implantitis after 6 years
Female	66	Yes	Poor	TOT	Molar	4.8 × 10	Peri-implantitis after 6 years

(peri-implant mucositis) with exudation and discomfort, but without radiographic evidence of bone loss. Eight implants (8/142: 5.6%) suffered from infection of the hard and soft tissues (peri-implantitis) with associated peri-implant marginal bone loss. Among these implants, however, only two were lost due to untreatable, recurrent peri-implantitis with advanced bone loss; the other five implants were treated with professional oral hygiene and in these cases failure was avoided. Overall, the 10-year incidence of biologic complications affecting implants was 11.9%.

Finally, with regard to prosthetic complications, no mechanical (i.e., at the implant-abutment interface) complications were registered; however, seven restorations (4 SCs and 3 FPDs) experienced ceramic chipping/fractures,

which required intervention from the dental technician. The prosthetic complications amounted to 7.6% (7/91 prosthetic restorations).

4. Discussion

It has been broadly proven that maxillary sinus augmentation is a highly successful and predictable method of obtaining sufficient bone height for posterior maxillary implant placement [3–6, 10].

In an interesting systematic review, which included studies with at least 3 years of follow-up, 18 articles for the LWT (6,500 implants in 2,149 patients) and 7 for the TOT (1,257 implants in 704 patients) were selected [5]. The overall

implant survival was 93.7% and 97.2% for the LWT and the TOT, respectively [5].

These outcomes were confirmed by more recent reviews of the current literature [3, 4]. In fact, Duttenhoefer et al. conducted a meta-analysis to study the influence of various treatment modalities (surgical technique, timing of implant placement, grafting materials, and use of membranes) on the implant survival in the grafted maxillary sinus [3]. This review included 122 publications on 16268 dental implants inserted in grafted sinuses [3]. At the end of this work, no differences were found in the implant survival with respect to each surgical approach, grafting material and implant type. However, the application of membranes showed a positive influence on the long-term implant outcomes, independently of other cofactors [3].

In this retrospective study, we have evaluated the 10-year implant survival and complication rates of MTCIs placed in grafted sinuses using two different surgical techniques (the LWT or the TOT). In accordance with the aforementioned literature, a satisfactorily high implant survival rate was found for both LWT (96.3%) and TOT (96.9%).

Different clinical studies have suggested that autogenous bone is the best reconstructive material, because of its osteogenic, osteoconductive, and osteoinductive properties [27, 28].

However, in recent clinical studies, bone substitutes such as allogeneic [29], xenogenic [11], and synthetic grafts [30, 31] and composite materials [32] have also been successfully employed in maxillary sinus augmentation.

Starch-Jensen et al. found that the 5-year implant survival rate after sinus elevation with autogenous bone graft or bovine bone mineral was 97% and 95%, respectively [4], and the reduction in vertical height of the augmented sinus with the two materials was the same. In this review, similarly high survival rates were found for implants, regardless of the grafting material used [4]. High implant stability, high patient satisfaction, and limited peri-implant marginal bone loss were found [4].

In another review of the literature, Danesh-Sani et al. confirmed that bone substitutes (allografts, xenografts, and synthetic materials) were good alternatives to autogenous bone, avoiding the disadvantages related to autografts (morbidity rate and limited availability) [10].

Here, we used a coral-derived porous hydroxyapatite for maxillary sinus augmentation. In accordance with a previous report [30], the present study has noted excellent results with the use of coralline calcium phosphates for grafting of the maxillary sinus.

It must be pointed out that, recently, the role and the importance of the grafting material has been partially revisited [33]. In a review on clinical studies with a follow-up period of 48 to 60 months, the implant survival rate was 99.6% for surgeries conducted with graft material and 96% for surgeries performed without it [33]. These results suggest that sinus lift can be a safe and predictable treatment procedure with low complication rates, irrespective of the use of biomaterials [33].

Recent studies have reported excellent survival and success rates for sinus grafting and implant placement in both one- and two-stage protocols [14, 15].

A noteworthy systematic review revealed that the placement of implants in combination with sinus elevation is a predictable procedure, showing high implant survival rates with low incidence of complications [6].

Once again, our present study seems to be in accordance with the current literature. In fact, excellent survival rates were found with the LWT, with both staged and simultaneous implant placement.

The choice of simultaneous implant placement and grafting procedure is generally highly influenced by the residual crestal bone height, which must be sufficient to provide adequate primary implant stability [9]. A recent literature review investigated the correlation between the amount of remaining crestal alveolar bone before sinus augmentation and implant survival. The findings indicated that a residual bone height of less than 4 mm may influence the survival/success rates of fixtures placed in combination with sinus elevation using osteotomes [9].

Comparable studies obtained findings that support a positive influence of rough surfaces on osseous integration in the posterior maxilla [34].

In a recent systematic review for implant survival in maxillary sinus augmentation, implants with rough surfaces displayed a higher survival rate (97.6%; 95% CI: 96.7–98.5%) than implants with machined surfaces (89.4%; 95% CI: 83.0–95.8%), within no correlation or influence from the graft type [35].

These results were also confirmed by a previous review of the literature, in which dental implants placed in the posterior augmented maxilla showed an average survival rate of 92.6% [36]. The use of rough-surfaced implants and particulate bone resulted in an increased implant survival rate (94.5%) and the use of a membrane to cover the graft increased the survival rate to 98.6% [36].

In the present study, in accordance with the aforementioned research, the use of sandblasted MTCIs guaranteed excellent implant survival and success rates. Moreover, only a few biologic (11.9%) and prosthetic (7.6%) complications were reported in our present long-term retrospective study.

All implants with screw type connections show a microgap of variable dimensions (40–100 μm) at the interface between the implant and the abutment [37]. Scientific evidence suggests that bacterial leakage and colonization of this microgap may be responsible for inflammatory cell recruitment and activation at the corresponding bone level, causing the development of marginal bone loss [37].

Provided that the absence of the microgaps is associated with reduced inflammation and bone loss, an efficient seal against microbial penetration may be provided by MTCIs [20, 38]. Indeed, this screwless connection reduces the microgap (1–3 μm) dimensions at the implant-abutment interface with a tight closure against the fixture; thus it contributes to a minimal level of peri-implant inflammation [20, 38].

In addition, no prosthetic complications were reported at the implant-abutment interface in our present study. This is similar to results from previous studies on MTCIs [16–20].

The stability of the implant-abutment connection is key for the long-term success of an implant-supported prosthetic restoration [16–19]. In addition, it may contribute to a more favourable load distribution into the bone [20, 39] and therefore to a reduction of the marginal bone loss around implants in the long term. This hypothesis needs further investigation, but, if correct, MTCIs may reduce micromovements at the implant-abutment interface, preventing crestal bone loss [39].

Moreover, MTCIs inherently have “platform switching” [40]. With platform switching, any potential microgap between the implant and the abutment (which harbours bacteria, responsible for toxin production) is displaced horizontally and away from the bone, with the possibility of reducing inflammation and of minimizing bone loss [40]. This aspect may further improve the long-term outcomes of Morse taper connection implants, reducing the incidence of biologic complications. In addition, a larger space exists for the organization of thick soft tissues, that can further protect the bone from resorption [40].

Our present study has limits. First, it is a retrospective clinical study, and the retrospective design is not the best way to investigate the long-term outcomes of dental implants (in fact, a prospective study design would be preferable, but the best solution to draw more specific conclusions about a treatment procedure would certainly be a randomized clinical trial). Second, our conclusions are based on a limited number of patients. Further, long-term prospective clinical studies (or even better, randomized clinical trials) on a larger sample of patients are therefore needed, to confirm the positive outcomes emerging from our present clinical study.

5. Conclusions

Within the limits of the present clinical study (retrospective design and limited number of patients enrolled), it can be stated that MTCIs represent a successful procedure for the prosthetic restoration of the grafted posterior maxilla, with both LWT and TOT, in the long term. In fact, a 10-year overall implant survival rate of 96.5% was found. Three implants failed in the lateral window group (3/79), for a survival rate of 96.3%, and two implants failed in the transalveolar osteotomy group (2/63), for a survival rate of 96.9%. A low incidence of biologic complications was reported in this study, in the long term (11.9%). In addition, the high mechanical stability of MTCIs likely contributed to the limited amount of prosthetic complications observed in this study (7.6%).

Conflicts of Interest

The authors have no conflicts of interest related to the present retrospective clinical study.

References

- [1] F. Wagner, G. Dvorak, S. Nemeč, P. Pietschmann, M. Figl, and R. Seemann, “A principal components analysis: how pneumatization and edentulism contribute to maxillary atrophy,” *Oral Diseases*, vol. 23, no. 1, pp. 55–61, 2017.
- [2] S. Bechara, R. Kubilius, G. Veronesi, J. T. Pires, J. A. Shibli, and F. G. Mangano, “Short (6 mm) dental implants versus sinus floor elevation and placement of longer (≥ 10 mm) dental implants: a randomized controlled trial with a 3-year follow-up,” *Clinical Oral Implants Research*, pp. 1–11, 2016.
- [3] F. Duttonhoefer, C. Souren, D. Menne, D. Emmerich, R. Schön, and S. Sauerbier, “Long-term survival of dental implants placed in the grafted maxillary sinus: systematic review and meta-analysis of treatment modalities,” *PLoS ONE*, vol. 8, no. 9, Article ID e75357, 2013.
- [4] T. Starch-Jensen, H. Aludden, M. Hallman, C. Dahlin, A. Christensen, and A. Mordenfeld, “A systematic review and meta-analysis of long-term studies (five or more years) assessing maxillary sinus floor augmentation,” *International Journal of Oral and Maxillofacial Surgery*, 2017.
- [5] M. Del Fabbro, S. S. Wallace, and T. Testori, “Long-term implant survival in the grafted maxillary sinus: a systematic review,” *The International Journal of Periodontics & Restorative Dentistry*, vol. 33, no. 6, pp. 773–783, 2013.
- [6] B. E. Pjetursson, W. C. Tan, M. Zwahlen, and N. P. Lang, “A systematic review of the success of sinus floor elevation and survival of implants inserted in combination with sinus floor elevation: part I: lateral approach,” *Journal of Clinical Periodontology*, vol. 35, no. 8, pp. 216–240, 2008.
- [7] H. Tatum Jr., “Maxillary and sinus implant reconstructions,” *Dental Clinics of North America*, vol. 30, no. 2, pp. 207–229, 1986.
- [8] R. Summers, “A new concept in maxillary implant surgery: the osteotome technique,” *Compendium*, vol. 15, no. 1, pp. 152–162, 1994.
- [9] C. Călin, A. Petre, and S. Drafta, “Osteotome-mediated sinus floor elevation: a systematic review and meta-analysis,” *The International Journal of Oral & Maxillofacial Implants*, vol. 29, no. 3, pp. 558–576, 2014.
- [10] S. A. Danesh-Sani, S. P. Engebretson, and M. N. Janal, “Histomorphometric results of different grafting materials and effect of healing time on bone maturation after sinus floor augmentation: a systematic review and meta-analysis,” *Journal of Periodontal Research*, vol. 52, no. 3, pp. 301–312, 2016.
- [11] F. Wang, W. Zhou, A. Monje, W. Huang, Y. Wang, and Y. Wu, “Influence of healing period upon bone turn over on maxillary sinus floor augmentation grafted solely with deproteinized bovine bone mineral: a prospective human histological and clinical trial,” *Clinical Implant Dentistry and Related Research*, vol. 19, no. 2, pp. 341–350, 2017.
- [12] M. P. Ramírez-Fernández, J. L. Calvo-Guirado, J. E. Maté-Sánchez del Val, R. A. Delgado-Ruiz, B. Negri, and C. Barona-Dorado, “Ultrastructural study by backscattered electron imaging and elemental microanalysis of bone-to-biomaterial interface and mineral degradation of porcine xenografts used in maxillary sinus floor elevation,” *Clinical Oral Implants Research*, vol. 24, no. 5, pp. 523–530, 2013.
- [13] A. Barone, M. Ricci, R. F. Grassi, U. Nannmark, A. Quaranta, and U. Covani, “A 6-month histological analysis on maxillary sinus augmentation with and without use of collagen membranes over the osteotomy window: Randomized clinical trial,” *Clinical Oral Implants Research*, vol. 24, no. 1, pp. 1–6, 2013.
- [14] M. Silvestri, P. Martegani, F. D’Avenia et al., “Simultaneous sinus augmentation with implant placement: Histomorphometric comparison of two different grafting materials. a multicenter double-blind prospective randomized controlled clinical trial,” *International Journal of Oral and Maxillofacial Implants*, vol. 28, no. 2, pp. 543–549, 2013.

- [15] N. F. Erdem, A. Ciftci, and A. H. Acar, "Three-year clinical and radiographic implant follow-up in sinus-lifted maxilla with lateral window technique," *Implant Dentistry*, vol. 25, no. 2, pp. 214–221, 2016.
- [16] F. Mangano, J. A. Shibli, R. L. Sammons, G. Veronesi, A. Piattelli, and C. Mangano, "Clinical outcome of narrow-diameter (3.3 mm) locking-taper implants: a prospective study with 1 to 10 years of follow-up," *The International journal of oral & maxillofacial implants*, vol. 29, no. 2, pp. 448–455, 2014.
- [17] F. Mangano, A. Macchi, A. Caprioglio, R. L. Sammons, A. Piattelli, and C. Mangano, "Survival and complication rates of fixed restorations supported by locking-taper implants: a prospective study with 1 to 10 years of follow-up," *Journal of Prosthodontics*, vol. 23, no. 6, pp. 434–444, 2014.
- [18] F. G. Mangano, J. A. Shibli, R. L. Sammons, F. Iaculli, A. Piattelli, and C. Mangano, "Short (8 mm) locking-taper implants supporting single crowns in posterior region: a prospective clinical study with 1-to 10-years of follow-up," *Clinical Oral Implants Research*, vol. 25, no. 8, pp. 933–940, 2014.
- [19] C. Mangano, F. Iaculli, A. Piattelli, and F. Mangano, "Fixed restorations supported by Morse-taper connection implants: a retrospective clinical study with 10–20 years of follow-up," *Clinical Oral Implants Research*, vol. 26, no. 10, pp. 1229–1236, 2015.
- [20] G. Sannino and A. Barlattani, "Mechanical evaluation of an implant-abutment self-locking taper connection: finite element analysis and experimental tests," *The International Journal of Oral & Maxillofacial Implants*, vol. 28, no. 1, pp. e17–e26, 2013.
- [21] F. Mangano, I. Frezzato, A. Frezzato, G. Veronesi, C. Mortellaro, and C. Mangano, "The effect of crown-to-implant ratio on the clinical performance of extra-short locking-taper implants," *Journal of Craniofacial Surgery*, vol. 27, no. 7, pp. 675–681, 2016.
- [22] K. Ö. Demiralp, N. Akbulut, S. Kursun, D. Argun, N. Bagis, and K. Orhan, "Survival rate of short, locking taper implants with a plateau design: a 5-year retrospective study," *BioMed Research International*, vol. 2015, Article ID 197451, 8 pages, 2015.
- [23] R. A. Urdaneta, S. Rodriguez, D. C. McNeil, M. Weed, and S.-K. Chuang, "The effect of increased crown-to-implant ratio on single-tooth locking-taper implants," *The International Journal of Oral & Maxillofacial Implants*, vol. 25, no. 4, pp. 729–743, 2010.
- [24] L. Marinucci, S. Balloni, E. Becchetti et al., "Effect of titanium surface roughness on human osteoblast proliferation and gene expression in vitro," *International Journal of Oral and Maxillofacial Implants*, vol. 21, no. 5, pp. 719–725, 2006.
- [25] T. Albrektsson, L. Canullo, D. Cochran, and H. De Bruyn, "'Peri-implantitis': a complication of a foreign body or a man-made 'disease'. facts and fiction," *Clinical Implant Dentistry and Related Research*, vol. 18, no. 4, pp. 840–849, 2016.
- [26] G. E. Salvi and U. Brägger, "Mechanical and technical risks in implant therapy," *International Journal of Oral & Maxillofacial Implants*, vol. 24, pp. 69–85, 2009.
- [27] B. Al-Nawas and E. Schiegnitz, "Augmentation procedures using bone substitute materials or autogenous bone—a systematic review and meta-analysis," *European Journal of Oral Implantology*, vol. 7, supplement 2, pp. S219–S234, 2014.
- [28] W. S. Khan, F. Rayan, B. S. Dhinsa, and D. Marsh, "An osteoconductive, osteoinductive, and osteogenic tissue-engineered product for trauma and orthopaedic surgery: how far are we?" *Stem Cells International*, Article ID 236231, 2012.
- [29] S. P. Xavier, E. R. Silva, A. Kahn, L. Chaushu, and G. Chaushu, "Maxillary sinus grafting with autograft versus fresh-frozen allograft: a split-mouth evaluation of bone volume dynamics," *The International Journal of Oral & Maxillofacial Implants*, vol. 30, no. 5, pp. 1137–1142, 2015.
- [30] C. Mangano, F. Iaculli, A. Piattelli et al., "Clinical and histologic evaluation of calcium carbonate in sinus augmentation: a case series," *The International journal of periodontics & restorative dentistry*, vol. 34, no. 2, pp. e43–e49, 2014.
- [31] C. Mangano, B. Sinjari, J. A. Shibli, and et al., "A Human clinical, histological, histomorphometrical, and radiographical study on biphasic ha-beta-tcp 30/70 in maxillary sinus augmentation," *Clinical Implant Dentistry and Related Research*, vol. 17, no. 3, pp. 610–618, 2015.
- [32] F. G. Mangano, L. Tettamanti, R. L. Sammons et al., "Maxillary sinus augmentation with adult mesenchymal stem cells: a review of the current literature," *Oral Surgery, Oral Medicine, Oral Pathology and Oral Radiology*, vol. 115, no. 6, pp. 717–723, 2013.
- [33] L. D. Silva, V. N. de Lima, L. P. Faverani, M. R. de Mendonça, R. Okamoto, and E. P. Pellizzer, "Maxillary sinus lift surgery—with or without graft material? a systematic review," *International Journal of Oral and Maxillofacial Surgery*, vol. 45, no. 12, pp. 1570–1576, 2016.
- [34] J. A. Shibli, J. T. Pires, A. Piattelli et al., "Impact of different implant surfaces topographies on peri-implant tissues: an update of current available data on dental implants retrieved from human jaws," *Current Pharmaceutical Biotechnology*, vol. 18, no. 1, pp. 76–84, 2017.
- [35] M. Del Fabbro, M. Bortolin, S. Taschieri, G. Rosano, and T. Testori, "Implant survival in maxillary sinus augmentation. an updated systematic review," *Journal of Osteology and Biomaterials*, vol. 1, no. 2, pp. 69–79, 2010.
- [36] S. S. Wallace and S. J. Froum, "Effect of maxillary sinus augmentation on the survival of endosseous dental implants: a systematic review," *Annals of Periodontology*, vol. 8, no. 1, pp. 328–343, 2003.
- [37] A. P. Ricomini Filho, F. S. D. F. Fernandes, F. G. Straioto, W. J. da Silva, and A. A. del Bel Cury, "Preload loss and bacterial penetration on different implant-abutment connection systems," *Brazilian Dental Journal*, vol. 21, no. 2, pp. 123–129, 2010.
- [38] S. Dibart, M. Warbington, M. F. Su, and Z. Skobe, "In vitro evaluation of the implant-abutment bacterial seal: the locking taper system," *International Journal of Oral and Maxillofacial Implants*, vol. 20, no. 5, pp. 732–737, 2005.
- [39] C. M. Schmitt, G. Nogueira-Filho, H. C. Tenenbaum et al., "Performance of conical abutment (Morse Taper) connection implants: a systematic review," *Journal of Biomedical Materials Research A*, vol. 102, no. 2, pp. 552–574, 2014.
- [40] L. Canullo, M. Caneva, and M. Tallarico, "Ten-year hard and soft tissue results of a pilot double-blinded randomized controlled trial on immediately loaded post-extractive implants using platform-switching concept," *Clinical Oral Implants Research*, pp. 1–11, 2016.

Clinical Study

The Ball Welding Bar: A New Solution for the Immediate Loading of Screw-Retained, Mandibular Fixed Full Arch Prostheses

Danilo Bacchiocchi¹ and Andrea Guida²

¹Private Practice, Castelfidardo, 60022 Ancona, Italy

²Fundacao Universitaria Vida Crista (FUNVIC), 12400-010 Pindamonhangaba, SP, Brazil

Correspondence should be addressed to Andrea Guida; prof.andreaguida@funvic.edu.br

Received 15 March 2017; Accepted 24 May 2017; Published 1 August 2017

Academic Editor: Eitan Mijiritsky

Copyright © 2017 Danilo Bacchiocchi and Andrea Guida. This is an open access article distributed under the Creative Commons Attribution License, which permits unrestricted use, distribution, and reproduction in any medium, provided the original work is properly cited.

Purpose. To present a new intraoral welding technique, which can be used to manufacture screw-retained, mandibular fixed full-arch prostheses. **Methods.** Over a 4-year period, all patients with complete mandibular edentulism or irreparably compromised mandibular dentition, who will restore the masticatory function with a fixed mandibular prosthesis, were considered for inclusion in this study. The “Ball Welding Bar” (BWB) technique is characterised by smooth prosthetic cylinders, interconnected by means of titanium bars which are adjustable in terms of distance from ball terminals and are inserted in the rotating rings of the cylinders. All the components are welded and self-posing. **Results.** Forty-two patients (18 males; 24 females; mean age 64.2 ± 6.7 years) were enrolled and 210 fixtures were inserted to support 42 mandibular screw-retained, fixed full-arch prostheses. After two years of loading, 2 fixtures were lost, for an implant survival rate of 97.7%. Five implants suffered from peri-implant mucositis and 3 implants for peri-implantitis. Three of the prostheses (3/42) required repair for fracture (7.1%); the prosthetic success was 92.9%. **Conclusions.** The BWB technique seems to represent a reliable technique for the fabrication of screw-retained mandibular fixed full-arch prostheses. This study was registered in the ISRCTN register with number ISRCTN71229338.

1. Introduction

In 1982, P. L. Mondani and P. M. Mondani published an article in which they fully described the equipment and techniques necessary for intraoral welding, a welding procedure for intraoral implant abutments, developed to obtain an immediate fixed prosthesis without the need for complex and lengthy laboratory procedures [1]. The method was essentially based on the creation of an electric arc between two electrodes under an argon gas flux [1]. Current scientific literature has validated the use of intraoral welding techniques [2–6]. In 2002, Hruska et al. published a study reporting the results of 1301 immediately loaded implants, 436 of which were used to support fixed partial dentures and full arches built over intraorally welded frameworks [2]. In this paper, the authors reported a rather low incidence of implant failures, with three failed implants (0.7%), one due to fracturing and two due to peri-implantitis [2]. The authors showed how, in cases of

extensive reconstruction, intraoral welding had the advantage of simplifying prosthetic procedures and in particular those involving highly disparallel abutments [2]. Intraorally welded frameworks acted as mesiostructures and reduced the incidence of fractures of the provisional prosthesis [2]. More than 20 years after the publication of Mondani’s article [1], Degidi et al. published a study on the immediate loading of multiple implants using a preformed bar that was welded intraorally to the implant abutments and that supported a temporary, metal-reinforced bridge [3]. All 192 immediately loaded implants survived, and no prosthetic complications occurred at the level of the provisional prosthesis [3]. This structure proved to be capable of withstanding load better than a temporary restoration without reinforcement, as demonstrated by finite element analysis [3]. In a later work by the same authors [4], intraoral welding proved to be a reliable technique for the rehabilitation of completely edentulous mandibles. The process they described involved the delivery

and immediate loading of a full arch prosthesis on the day of surgery, using fixtures with butt-joints and conical implant-abutment connections. Once again, in a further prospective clinical work, Degidi et al. showed the rehabilitation of the fully edentulous mandible by inserting 4 implants, splinted to each other through the intraoral welding of a bar to their titanium abutments [5]. The framework thus obtained was used to support an immediately loaded definitive prosthesis [5]. In brief, 22 patients treated with 88 implants were followed for a total period of one year. At the end of the period, only one implant was lost within a month of insertion, for an implant survival rate of 98.9% [5]. No fractures or alterations occurred to the intraorally welded framework, and no fractures of the prosthetic acrylic resin superstructure were recorded [5]. Finally, in 2013, Degidi et al. reported the 6-year follow-up results of the welding technique for the fabrication of immediately loaded maxillary and mandibular fixed full arches [6]. All the patients in this study were rehabilitated on the same day of surgery with a temporary, immediately loaded prosthesis built on a titanium framework obtained by the intraoral welding of a titanium bar to the implant abutments [6]. In total, there were 124 implants placed in the maxilla and 87 implants placed in the mandible; the fixtures were controlled for up to 6 years after loading [6]. Mean peri-implant bone resorption was measured as 1.39 mm (± 0.67) and 1.29 mm (± 0.71) for the maxilla and mandible, respectively [6]. The most frequent complication was the fracture of the resin superstructure. Overall, the intraoral welding technique proved to be effective and reliable in allowing the fabrication of immediately loaded prostheses in edentulous patients [6]. Some possible variations to the classic technique of intraoral welding have been presented in recent scientific literature [7–10]. In the most commonly used methods, the diameter of the bar (generally made of titanium grade 2) is chosen based on the distance between the implants, the extent of the arch, and the available prosthetic volumes. The bar is then shaped to be adherent to the titanium cylinders placed on the abutments and is then welded to them [2–6, 8, 10]. The purpose of our present work is therefore to present a new variant of the intraoral welding technique, which can be used to manufacture full arch screw-retained rehabilitations of the edentulous mandible, under an immediate loading protocol. This innovative type of prosthetic rehabilitation, which the authors refer to as the “Ball Welding Bar” (BWB) technique, is characterised by smooth prosthetic cylinders, interconnected by means of titanium bars (grade 4) which are adjustable in terms of distance from ball terminals and are inserted in the rotating rings of the cylinders. All the components are welded and self-posing and do not cause arcing or tension. This paper reports on a study tracking the results obtained two years after immediate loading of a full arch, screw-retained mandibular prosthesis (Toronto bridges) that was screwed onto the new intraorally welded Ball Welding Bars.

2. Materials and Methods

2.1. Patient Sample. In the period between January 2010 and December 2013, all patients who were referred to two different private dental centres (the private dental clinics of Professor

Andrea Guida and Dr. Danilo Bacchiocchi) for rehabilitation using oral implants were considered for inclusion in this prospective clinical study. Patients considered for inclusion were those with

- (1) complete mandibular edentulism, with functional and aesthetic problems related to the presence of a complete, removable conventional denture (i.e., lack of stability of the complete denture, discomfort during function, and aesthetic embarrassment),
- (2) irreparably compromised mandibular dentition, due to advanced periodontal disease or destructive/massive tooth decay that made the residual dental elements unrestorable,
- (3) sufficient bone volume (bone height \times width) to allow for the placement of implants of at least 8 mm in length and 3.0 mm in diameter,
- (4) will to restore the masticatory function with a fixed mandibular prosthesis supported by dental implants,
- (5) the ability to understand and sign an informed consent form for implant treatment.

Patients excluded from the study were those

- (1) with general medical conditions/systemic diseases that represented an absolute contraindication to surgical and implant treatment, such as severely immunocompromised patients or severely uncompensated diabetics, patients receiving radiotherapy to the head and neck area or chemotherapy, and patients receiving amino-bisphosphonates intravenously and/or orally,
- (2) with psychiatric disorders,
- (3) addicted to alcohol or drugs,
- (4) who needed bone augmentation procedures with autogenous bone or other bone substitutes, to allow for proper implant insertion,
- (5) who had previously undergone major regenerative bone surgery, preliminary to the placement of dental implants. Inclusion and exclusion criteria for the present study were also summarized in Table 1.

Cigarette smoking was not an exclusion criterion for enrollment in this study; nevertheless, patients that smoke were informed of the fact that cigarette smoking is a risk factor for the success of implant treatments [11]. All patients received detailed information about the planned therapy, the related risks, and possible alternatives. Patients were enrolled only after signing an informed consent form for implant treatment. Finally, the present clinical work was carried out in compliance with the principles set out in the Helsinki Declaration on Human Experimentation of 2000 (revised 2008). The present clinical study was registered in the ISRCTN, a publicly available register for clinical trials recognized by WHO and ICMJE, with number ISRCTN71229338.

TABLE 1: Inclusion and exclusion criteria for enrollment of patients in the study.

Inclusion criteria	Exclusion criteria
(1) Complete mandibular edentulism, with functional and aesthetic problems related to the presence of a complete, removable conventional denture.	(1) Severely immunocompromised status, severely uncompensated diabetes, radiotherapy of head and neck area, chemotherapy, and treatment with intravenous and/or intraoral amino-bisphosphonates.
(2) Irreparably compromised mandibular dentition, due to advanced periodontal disease or destructive/massive tooth decay that made the residual dental elements unrestorable.	(2) Psychiatric disorders.
(3) Sufficient bone volume to allow for the placement of implants of at least 8 mm in length and 3.0 mm in diameter.	(3) Alcohol and/or drugs addition.
(4) Will to restore the masticatory function with a fixed mandibular prosthesis supported by dental implants.	(4) Need for bone augmentation procedures with autogenous bone or other bone substitutes, to allow for proper implant insertion.
(5) Ability to understand and sign an informed consent form for implant treatment.	(5) Previous interventions of regenerative bone surgery.

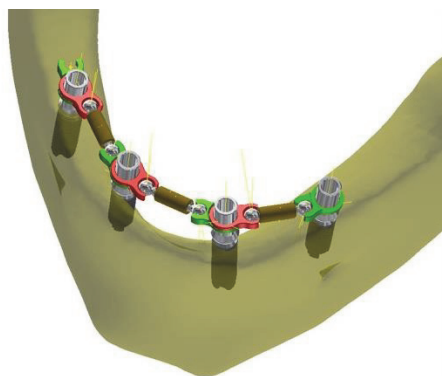


FIGURE 1: The BWB (Ball Welding Bar) consists of smooth prosthetic cylinders, interconnected by means of titanium bars (grade 4) adjustable in distance with ball terminals, which are inserted in the rotating rings of the cylinders. All the components are welded and self-posing, without arcing nor tensions. This BWB has been patented by the authors (patent number AN2014A000111 and variants).

2.2. The Ball Welding Bar (BWB) Concept. The BWB (Ball Welding Bar) consists of smooth prosthetic cylinders, interconnected by means of titanium bars (grade 4) which are adjustable in terms of distance from ball terminals and are inserted in the rotating rings of the cylinders. All the components are welded and self-posing and do not cause arcing or tension (Figure 1). This prosthetic device has been patented by the authors (patent number AN2014A000111 and variants).

2.3. The Implants Used in This Study. The fixtures used in the present work (BT Safe Bone Level®; Biotec BTK, Povolaro di Dueville, Vicenza, Italy) were made of titanium grade 4 (ASTM F67dISO 5832-2). These were tapered implants with double lead threads (Figure 2) and a hexagonal conical connection (11°) and integrated platform switching [12]. The

dual acid etched (DAE) surface of these implants was the result of treatment with a mixture of strong inorganic acids (H₂SO₄, H₃PO₄, HCl, and HF) [13]. The implants were then rinsed and washed with distilled water, to neutralize acid residuals. Finally, implants were taken to a cleaning room (ISO 7 class) to be decontaminated through a plasma spray decontamination process, in an argon atmosphere.

The DAE implant surface (Figure 3) had the following roughness parameters:

- (i) Ra (arithmetic mean of the absolute height of all points) = 1.12 (60.41) μm ,
- (ii) Rq (square root of the sum of the squared mean difference of all points) = 1.34 (60.69) μm ,
- (iii) Rt (difference between the highest and the lowest points) = 3.86 (61.40) μm [13].

2.4. Surgical and Prosthetic Phases. A preliminary clinical and radiographic evaluation with panoramic radiographs (Figure 4) preceded the surgery. Where needed, a cone beam computed tomography (CBCT) scan (I-Max Touch 3D®, Owandy Radiology, Oxford, CT, USA) was performed, in order to collect all anatomical information for optimal surgical and prosthetic planning. The digital imaging and communication in medicine (DICOM) files from CBCT were imported into three-dimensional (3D) reconstruction software, where the surgical and prosthetic planning was performed, and the feasibility of the protocol was investigated. The present protocol involved the fabrication of screw-retained, complete mandibular dentures (Toronto bridge) supported by 5 dental implants. Two implants had to be inserted in the molar areas (3.6 and 4.6, resp.), two in the first premolar areas (3.4 and 4.4, resp.), and the last one in midline or otherwise in the incisal areas (3.1 or 4.1). The prosthesis had to be immediately loaded, supported by multiunit abutments (MUA) splinted together with a Ball Welding Bar (BWB). Prior to surgery, a complete lower

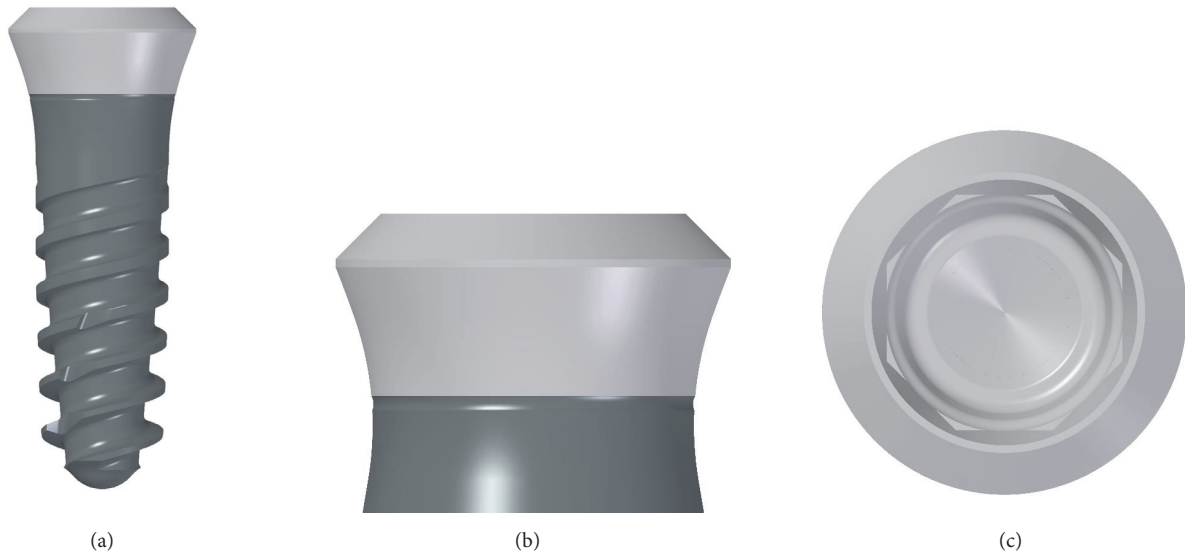


FIGURE 2: Drawing of the tapered, double lead threads implant used in this study. (a) Apical threads, deeper and cutting, favour insertion, and initial stability, whereas squared coronal thread enhances bone condensation. (b) Back-tapered collar provides excellent cortical bone management, improving soft tissue support. (c) Octagonal conical connection (2 mm in depth with 8° cone) that guarantees an excellent seal, reducing the risk of micromovements between the implant and the abutment.

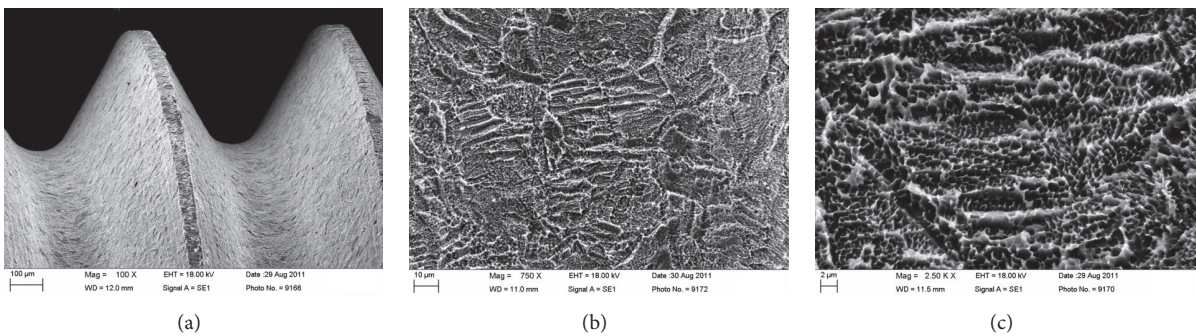


FIGURE 3: Scanning electron microscopy (SEM) evaluation of the dual acid etched (DAE) implant surface. The surface (a) presented micron-sized shallow cavities uniformly covered by submicroscopic pitting (b) limited by razor-sharp cusps and edges (c).



FIGURE 4: Preoperative situation. A 52-year female patient in good general health had a complete removable denture in the maxilla and a severe acute periodontitis in the mandible, with several teeth with reduced bone support and therefore high mobility. The patient asked for a full arch implant supported rehabilitation of the mandible, possibly involving an immediate loading protocol.



FIGURE 5: Prior to surgery, a complete lower denture was fabricated in the dental laboratory, made in composite resin with a transparent vacuum-formed template.

denture was fabricated in the dental laboratory, from composite resin with a transparent vacuum-formed template (Figure 5). In order to achieve this, impressions were taken

and casts were developed and mounted in an articulator, with bite-in wax for definition of the proper occlusion and the selection of the colour and the shape of the teeth. This lower denture was then hollowed in order to be able to accommodate the intraorally welded titanium framework. Flanges



FIGURE 6: The lower denture was emptied internally, in order to subsequently accommodate inside the future intraorally welded titanium framework. The flanges and the supports in the retromolar areas were preserved, in order to facilitate the positioning in the postwelding phase.

and supports were kept on the retromolar areas to facilitate positioning in the postwelding phase (Figure 6). Surgery commenced after infiltration of local anaesthesia. A full-thickness flap was raised after a crestal incision was performed, and two releasing vertical incisions were made. In the case of partially edentulous patients, the nonrestorable teeth affected by severe periodontal disease or decay were then removed, taking care not to damage the socket walls. This was followed by the preparation of the implant sites and the deepening of the apex of the socket (3-4 mm). In the case of fully edentulous patients with completely healed ridges, the preparation of the implant sites was performed in accordance with manufacturer recommendations, taking into account the clinical situation. The implants were then inserted in both extraction sockets and healed sites (the final insertion torque of the fixtures had to be ideally > 55 N/cm). The prosthetic phase started immediately with the placement of multiunit abutments (MUA) with a transmucosal height of 3 mm over the implants. The aforementioned MUA were screwed gently with a torque of 30 N/cm. In all immediate postextraction implants, the remaining gaps between the implant and the walls of the socket were filled and packed with a resorbable β -tricalcium phosphate [14] regenerative material (OXOFIX®, Biotec BTK, Povolaro di Dueville, Vicenza, Italy BTK, Italy). Finally, sutures were made. The prosthetic procedure went as follows. The prosthetic titanium cylinders provided by systematic BWB were first screwed in. Over these cylinders, the adjustable rings and rotating balls were adjusted both horizontally and vertically, taking care to remain well above the crest, and not to occupy extracrestal spaces (Figure 7). The self-locating bar was welded into the mouth, then removed, and finished; after blasting, it was covered with a white opaque light curing composite resin and repositioned onto the MUA abutments (Figure 8). The vacuum-formed template was placed over the bar to control the occlusal fairness and to verify the previously measured vertical dimensions (Figure 9(a)). Holes were made on the prosthesis using the vacuum-formed template which was already perforated in the direction of the cylinders (Figure 9(b)) in order to give access to the cylinders themselves after relining with composite



FIGURE 7: The prosthetic cylinders in titanium were screwed: over these cylinders, the adjustable rings and the rotating spheres were adapted both horizontally and vertically, paying attention to remain well above the bone crest.

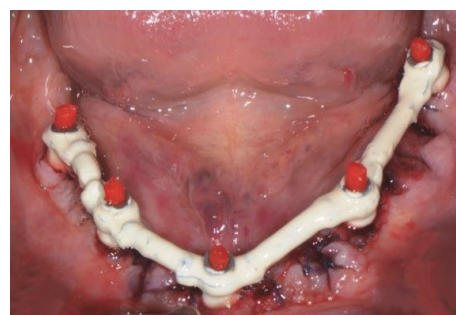


FIGURE 8: After the intraoral welding, the self-locating bar was removed from the mouth and finished, blasted, and then covered with a white opaque composite resin. The bar was subsequently repositioned onto the MUA abutments.

resin flow (Figure 9(c)). Adhesive (Universal Futura B®, Voco, Cuxhaven, Germany) was positioned within the prosthesis and light cured, and the prosthesis was filled with a composite dual fluid (Rebilda, Voco, Cuxhave, Germany) and positioned above the bar. The prosthesis was self-centring, because it had all the support on the retromolar areas and the vestibules like a conventional full denture; therefore it found its natural position and occlusal vertical dimension without any error or unwanted movement (Figure 10(a)). When the dual composite resin was completely polymerized, the prosthesis was removed and sent to the laboratory, which after a few hours finished and returned it. The prosthesis was then delivered to the patient in less than 6 hours (Figures 10(b), 10(c), and 10(d)). The occlusion was carefully checked because it had to be perfectly balanced, and the holes were closed again with Teflon cylinders soaked in chlorhexidine 5% and a flowable light-cured composite. The patients received detailed instructions about oral hygiene and home care procedures and were enrolled in a series of scheduled follow-up controls, every 4 months, for professional oral hygiene sessions and clinical monitoring of their rehabilitation.

2.5. Outcome Variables and Statistical Evaluation. The main outcome variables for the present study were implant survival and the prosthetic success. With regard to implant survival, an implant was classified as “surviving” if it functioned

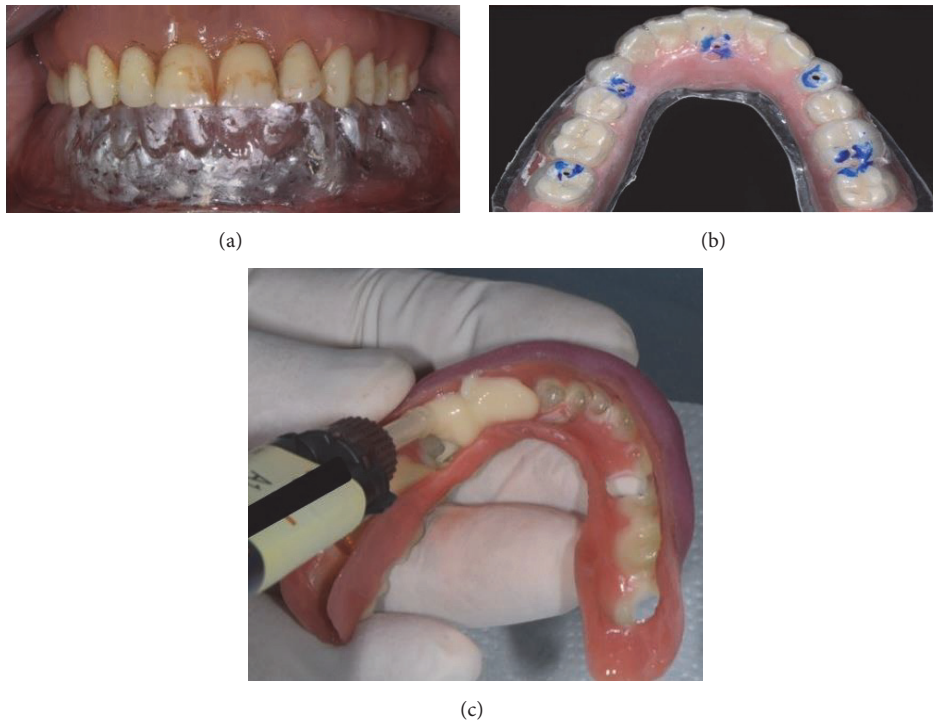


FIGURE 9: The vacuum-formed template was placed over the bar to control the occlusal fairness and to verify the previously measured vertical dimension (a). Holes were made on the prosthesis, using the vacuum-formed template already perforated in the direction of the cylinders, in order to access to the cylinders themselves (b). The prosthesis was relined with composite resin flow (c).

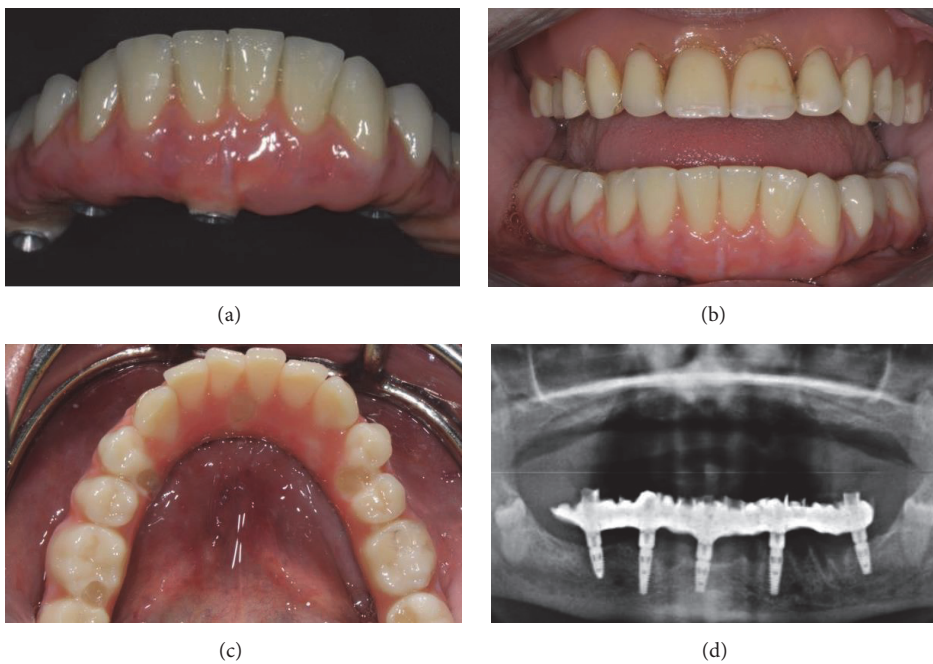


FIGURE 10: The fabrication of the prosthesis is completed in the laboratory (a), which after a few hours return the Toronto Bridge to the dentist for clinical application. The clinician delivers the prosthesis to the patient (b), after a careful check of the occlusion that must be perfectly balanced; then, the clinician closes the holes of the cylinders with Teflon soaked in chlorhexidine 5% and light curing flowable composite resin (c). The panoramic radiograph shows the titanium framework and the perfect adaptation of this structure on implant abutments (d).

regularly at the end of the study, two years after its placement and functional loading. In all cases in which the implant had to be removed, the fixture was defined as “failed.” The causes for implant failure were as follows:

- (1) mobility for lack of osseointegration, which occurred in the early healing period (not later than 4 months after insertion) but in the absence of symptoms/signs of infection,
- (2) infection of the peri-implant tissue (peri-implantitis) that caused massive bone loss and subsequent loosening of the implant [15]. The threshold for diagnosis of peri-implantitis was a probing depth ≥ 4 mm, bleeding on probing, and/or pus secretion associated with evidence of radiographic bone loss (>2.5 mm) [15],
- (3) progressive severe bone loss (>2.5 mm per year) in the absence of specific symptoms/signs of infection,
- (4) fracture of the implant body.

With regard to prosthetic success, a prosthesis was considered successful when no adverse events (such as fractures/alterations of the resin superstructure and of the intraorally welded titanium framework) occurred [3–6, 16]. At the end of the study, after 2 years of functional loading, all relevant patient data (gender, age at surgery, and smoking habits), implant information (position, length, and diameter), and prosthesis information were collected in an Excel spreadsheet. Means (\pm SD) ranges, medians, and confidence intervals (95%) were calculated for quantitative variables and absolute and relative (%) frequency distributions were obtained for all qualitative variables. Implant survival and prosthesis success were finally calculated at the patient level, which meant that if even a single implant out of five failed, the procedure on that patient was classified as a failure, and in the presence of even a single prosthetic complication, the prosthesis could not be considered successful [17].

3. Results

In total, 42 patients (18 males and 24 females) were included in the present study. The mean age of patients was 64.2 (± 6.7), range 54–79 years, median 63.5 years, and confidence interval (95%) 62.1–66.2. Among these patients, 12 (28.5%) were smokers. Overall, 210 fixtures were inserted to support 42 screw-retained, full arches restorations (Toronto bridges) in the edentulous mandible. The distribution of the implants was as follows: 18 fixtures (8.6%) were 3.7 mm in diameter \times 12 mm in length, 40 fixtures (19%) were 3.7 \times 14 mm, 46 fixtures (21.9%) were 3.7 \times 16 mm, 18 fixtures (8.6%) were 4.1 \times 12 mm, 48 fixtures (22.9%) were 4.1 \times 14 mm, and 40 fixtures (19%) were 4.1 \times 16 mm. The positions of the implants were the following: 84 molars (40%), 84 premolars (40%), and 42 incisors (20%). At the end of the study, only 2 fixtures were lost (2/210: 0.9%) during the first months after placement, in a single patient: the implant survival rate was 97.7% (patient-based). With regard to complications, during the follow-up, 5 implants suffered from peri-implant mucositis and 3 implants suffered for peri-implantitis: these fixtures were, however, successfully treated with dedicated

professional oral hygiene sessions and no further biological problems were registered at the end of this work. With regard to prosthetic complication and therefore prosthetic success, 3/42 of the prostheses required repair for fracture (7.1%): this was considered a major complication. In addition, 4 multiunit abutments (1.9%) became loose during the entire follow-up: these were reinserted and screwed and no other abutment loosening was encountered in this study. The loosening of the multiunit abutments was considered as a minor complication.

4. Discussion

In recent years, several clinical studies have reported excellent results obtained using intraoral welding techniques for the rehabilitation of completely edentulous mandibles with screw-retained full arch immediately loaded prostheses and Toronto bridges [2–6]. Similar results have also been reported for procedures on the fully edentulous maxilla [6, 18, 19], giving the impression that intraoral welding can be successfully used for the rehabilitation of edentulous patients. In particular, Degidi et al. published a paper [18] in which 30 patients received 3 axial and 4 tilted implants in the edentulous maxilla and were rehabilitated with an immediately loaded definitive prosthesis achieved using intraoral welding. Patients were followed for a period of 3 years during which the 210 implants inserted were checked, and implant failures, marginal bone resorption around the fixtures, and prosthetic problems were carefully registered [18]. At the end of the study, three implants had biological problems, giving a success rate of 97.8% for axial implants and 99.2% for tilted implants, respectively. The mean marginal bone resorption was 0.92 mm (± 0.75) for the axial and 1.03 mm (± 0.69) for the tilted implants [18]. No fractures or alterations of the intraorally welded titanium framework occurred, for a prosthetic success of 100% [18]. One of the obvious advantages of the intraoral welding technique is the ability to rehabilitate in a very short timeframe and with limited costs fully edentulous patients, without going through lengthy and complex laboratory phases [2–6, 18]. Recently, some potential alternatives to the traditional technique originally proposed by P. L. Mondani and P. M. Mondani [1] and subsequently recovered by Degidi et al. [3, 5, 6, 18] have been proposed [7, 8]. Albiero and Benato [8] published a case report in which the technique of intraoral welding has been combined with modern guided surgical techniques. Using this “guided-welded approach,” the authors were able to obtain a very precise passive fit of a maxillary complete denture supported by 4 implants, loaded immediately [8]. The passive fit contributed to the optimal healing of the implants and the use of guided surgery allowed for the reduction of surgery time and the adaptation of the bar to the implant abutments [8]. Fornaini et al. [7, 9, 10] have presented another possible variant of the intraoral welding technique, using a laser for the welding of a bar (previously prepared from a technician) to 4 implants placed in an edentulous maxilla. In particular, in their clinical report [7] preceded by an *in vitro* evaluation, the authors proved that the use of lasers can produce good results in terms of intraoral welding. The theoretical advantages of the use of lasers for the welding

are different: lasers is effective on all metals and can be used without filler metal and shielding gas and thanks to the fact that the beam has extremely small dimensions and is well focused (0.6 mm), there is no adverse effect (overheating) on the surrounding tissue [7, 9, 10]. In addition, lasers can be used on all patients (even on patients with pacemakers) [7, 9, 10]. In our present clinical research, we have introduced a further possible variant of the classical intraoral welding technique procedure: the so-called “Ball Welding Bar” (BWB) technique. The BWB technique represents a new, simple treatment option for the fabrication of a screw-retained Toronto Bridge that has predictable results. The mechanical properties of this new bar (made of titanium grade 4) and the original assemblage designed and patented by the authors allow for the rapid fabrication of prostheses with no tension. This means that there will be good adaptation when using a variety of loading protocols (including immediate functional loading). Overall, 210 fixtures were inserted to support 42 screw-retained, full arches restorations (Toronto bridges) in the edentulous mandible. At the end of the study, only 2 fixtures were lost (2/210: 0.9%) during the first months after placement, in a single patient: the implant survival rate was 97.7% (patient-based). With regard to prosthetic complication and therefore prosthetic success, 3/42 of the prostheses required repair for fracture (7.1%): this was considered a major complication. The prosthetic success was therefore 92.9%. The main advantages of our method are that it makes it easy to centre the bars over the bone crest (for ease of orientation of the components in the vertical and horizontal dimensions), allows for fine regulation, and makes it easy to solder the framework without distortions. Finally, the procedure is very rapid and can be managed by a single operator, both of which allow for reduced rehabilitation costs. In the present study, we have used tapered implants with a hexagonal conical implant-abutment connection, because these fixtures had all the features necessary to meet the biological and mechanical requirements for immediate loading, both in fully healed edentulous ridges and in postextraction sockets [12]. The tapered design with double lead threads, in fact, allows the surgeon to obtain an excellent primary implant stability even in difficult clinical conditions [12], such as in the case of postextraction sockets [20]. At the same time, the dual acid etched surface of these implants has the potential to accelerate bone healing, as demonstrated by a recent histologic/histomorphometric human study [13]. In modern oral implantology, the presence of an adequate macrostructure (thread design) and microstructure (surface roughness) is considered critical for functional immediate loading [21–23]. Finally, new materials (such as composite resins) are now available for the fabrication of fixed full arch mandibular dentures [24, 25]. These composite resins can effectively replace more conventionally used materials (i.e., acrylic resins) because they offer greater hardness compared to conventional acrylic resins. In addition, they are better in terms of aesthetics, as they come in different shades of pink to mimic the colours of the gum [24, 25]. These features allow the technician to fabricate a prosthesis composed of a single material, in which the titanium framework/bar is incorporated and welded to the cylinders and

the abutments. The resin composite, besides being stronger and more aesthetically pleasing than acrylic resin, has the potential to preserve the occlusion stability over time, and the maintenance and repair are similar to those of a common dental composite [25]. In our present study we have used these materials, and we have obtained excellent functional and aesthetic outcomes. Our present study has limitations, for example, the limited number of patients treated and prostheses fabricated; therefore further studies on a larger sample of patients are needed to confirm the positive clinical outcomes reported here. In addition, the present study has tracked outcomes for only two years and it is necessary to follow the progress of these patients in the long-term, before more specific conclusions can be drawn about the reliability of the new and innovative BWB technique.

5. Conclusions

Fulfilling patient demands for an immediate functional recovery is the main goal of modern dentistry. The novel “Ball Welding Bar” technique proposed in the present study is simple and makes it possible to immediately load a definitive screw-retained fixed full arch prosthesis, without the use of a provisional prosthesis. In our present study, 210 fixtures were inserted to support 42 mandibular screw-retained, fixed full arches restorations (Toronto bridges). After two years of loading, 2 fixtures were lost (2/210: 0.9%) during the first months after placement, in a single patient: the implant survival rate was 97.7% (patient-based). With regard to prosthetic complication and therefore prosthetic success, 3/42 of the prostheses required repair for fracture (7.1%): this was considered a major complication. The prosthetic success was therefore 92.9%. Further studies are needed to confirm these positive outcomes.

Conflicts of Interest

The authors report no conflicts of interest in relation to the present clinical work.

References

- [1] P. L. Mondani and P. M. Mondani, “The Pierluigi Mondani intraoral electric solder. Principles of development and explanation of the solder using syncrystallization,” *Rivista di odontostomatologia e implantoprotesi*, vol. 4, no. 4, pp. 28–32, 1982.
- [2] A. Hruska, P. Borelli, A. C. Bordanaro, E. Marzaduri, and K.-L. Hruska, “Immediate loading implants: a clinical report of 1301 implants,” *The Journal of oral implantology*, vol. 28, no. 4, pp. 200–209, 2002.
- [3] M. Degidi, P. Gehrke, A. Spanel, and A. Piattelli, “Syncrystallization: A technique for temporization of immediately loaded implants with metal-reinforced acrylic resin restorations,” *Clinical Implant Dentistry and Related Research*, vol. 8, no. 3, pp. 123–134, 2006.
- [4] M. Degidi, D. Nardi, and A. Piattelli, “Prospective study with a 2-year follow-up on immediate implant loading in the edentulous mandible with a definitive restoration using intra-oral

- welding," *Clinical Oral Implants Research*, vol. 21, no. 4, pp. 379–385, 2010.
- [5] M. Degidi, D. Nardi, G. Sighinolfi, and A. Piattelli, "Immediate rehabilitation of the edentulous mandible using AnkylosSynCone telescopic copings and a pilot study," in *Proceedings of the Immediate rehabilitation of the edentulous mandible using AnkylosSynCone telescopic copings and intraoral welding: a pilot study*, vol. 32, pp. 189–194, 2012.
 - [6] M. Degidi, D. Nardi, and A. Piattelli, "A six-year follow-up of full-arch immediate restorations fabricated with an intraoral welding technique," *Implant Dentistry*, vol. 22, no. 3, pp. 224–231, 2013.
 - [7] C. Fornaini, E. Merigo, I. Cernavin, G. López de Castro, and P. Vescovi, "Intraoral Laser Welding (ILW) in implant prosthetic dentistry: case report," *Case Reports in Dentistry*, vol. 2012, Article ID 839141, 4 pages, 2012.
 - [8] A. M. Albiero and R. Benato, "Computer-assisted surgery and intraoral welding technique for immediate implant-supported rehabilitation of the edentulous maxilla: case report and technical description," *International Journal of Medical Robotics and Computer Assisted Surgery*, vol. 12, no. 3, pp. 453–460, 2016.
 - [9] C. Fornaini, E. Merigo, P. Vescovi, M. Meleti, and S. Nammour, "Laser welding and syncrystallization techniques comparison: *in vitro* study," *International Journal of Dentistry*, vol. 2012, Article ID 720538, 5 pages, 2012.
 - [10] C. Fornaini, P. Vescovi, E. Merigo et al., "Intraoral metal laser welding: a case report," *Lasers in Medical Science*, vol. 25, no. 2, pp. 303–307, 2010.
 - [11] B. R. Chrcanovic, T. Albrektsson, and A. Wennerberg, "Smoking and dental implants: a systematic review and meta-analysis," *Journal of Dentistry*, vol. 43, no. 5, pp. 487–498, 2015.
 - [12] G. A. Dolcini, M. Colombo, and C. Mangano, "From guided surgery to final prosthesis with a fully digital procedure: a prospective clinical study on 15 partially edentulous patients," *International Journal of Dentistry*, vol. 2016, Article ID 7358423, 7 pages, 2016.
 - [13] F. G. Mangano, J. T. Pires, J. A. Shibli et al., "Early bone response to dual acid-etched and machined dental implants placed in the posterior maxilla: a histologic and histomorphometric human study," *Implant Dentistry*, vol. 26, no. 1, pp. 24–29, 2017.
 - [14] A. Giuliani, A. Manescu, E. Larsson et al., "In vivo regenerative properties of coralline-derived (Biocoral) scaffold grafts in human maxillary defects: demonstrative and comparative study with beta-tricalcium phosphate and biphasic calcium phosphate by synchrotron radiation x-ray microtopograph," *Clinical Implant Dentistry and Related Research*, vol. 16, no. 5, pp. 736–750, 2014.
 - [15] T. Albrektsson, L. Canullo, D. Cochran, and H. De Bruyn, "'Peri-implantitis': a complication of a foreign body or a man-made 'disease'. facts and fiction," *Clinical Implant Dentistry and Related Research*, vol. 18, no. 4, pp. 840–849, 2016.
 - [16] C. Mangano, F. Mangano, J. A. Shibli, M. Ricci, R. L. Sammons, and M. Figliuzzi, "Morse taper connection implants supporting "planned" maxillary and mandibular bar-retained overdentures: a 5-year prospective multicenter study," *Clinical Oral Implants Research*, vol. 22, no. 10, pp. 1117–1124, 2011.
 - [17] C. Mangano, F. Iaculli, A. Piattelli, and F. Mangano, "Fixed restorations supported by Morse-taper connection implants: a retrospective clinical study with 10–20 years of follow-up," *Clinical Oral Implants Research*, vol. 26, no. 10, pp. 1229–1236, 2015.
 - [18] M. Degidi, D. Nardi, and A. Piattelli, "Immediate loading of the edentulous maxilla with a definitive restoration supported by an intraorally welded titanium bar and tilted implants," *International Journal of Oral and Maxillofacial Implants*, vol. 25, no. 6, pp. 1175–1182, 2010.
 - [19] M. Marchesi, C. Ferrari, S. Superbi, R. Jimbo, and S. Galli, "Modified protocol of the intraoral welding technique for immediate implant-supported rehabilitation of the edentulous maxilla," *Implant Dentistry*, vol. 24, no. 1, pp. 110–116, 2015.
 - [20] F. G. Mangano, P. Mastrangelo, F. Luongo, A. Blay, S. Tunchel, and C. Mangano, "Aesthetic of immediately restored single implants placed in extraction sockets and healed sites of the anterior maxilla: a retrospective study on 103 patients with 3 of follow-up," *Clinical Oral Implants Research*, vol. 28, no. 3, pp. 272–282, 2017.
 - [21] H. De Bruyn, S. Raes, P.-O. Östman, and J. Cosyn, "Immediate loading in partially and completely edentulous jaws: a review of the literature with clinical guidelines," *Periodontology 2000*, vol. 66, no. 1, pp. 153–187, 2014.
 - [22] S. M. Meloni, M. Tallarico, M. Pisano, E. Xhanari, and L. Canullo, "Immediate loading of fixed complete denture prosthesis supported by 4–8 implants placed using guided surgery: a 5-year prospective study on 66 patients with 356 implants," *Clinical Implant Dentistry and Related Research*, vol. 19, no. 1, pp. 195–206, 2017.
 - [23] F. G. Mangano, A. Caprioglio, L. Levrini, D. Farronato, P. A. Zecca, and C. Mangano, "Immediate loading of mandibular overdentures supported by one-piece, direct metal laser sintering mini-implants: a short-term prospective clinical study," *Journal of Periodontology*, vol. 86, no. 2, pp. 192–200, 2015.
 - [24] F. Fieri, N. N. Aldini, M. Fini, and G. Corinaldesi, "Immediate occlusal loading of immediately placed implants supporting fixed restorations in completely edentulous arches: A 1-year prospective pilot study," *Journal of Periodontology*, vol. 80, no. 3, pp. 411–421, 2009.
 - [25] B.-W. Park, N.-J. Kim, J. Lee, and H.-H. Lee, "Technique for fabricating individualized dentures with a gingiva-shade composite resin," *Journal of Prosthetic Dentistry*, vol. 115, no. 5, pp. 547–550, 2016.

Clinical Study

Cumulative Success Rate of Short and Ultrashort Implants Supporting Single Crowns in the Posterior Maxilla: A 3-Year Retrospective Study

Giorgio Lombardo,¹ Jacopo Pighi,¹ Mauro Marincola,² Giovanni Corrocher,¹ Miguel Simancas-Pallares,^{2,3} and Pier Francesco Nocini¹

¹School of Dentistry, Department of Surgery, Dentistry, Paediatrics and Gynaecology (DIPSCOMI), University of Verona, Verona, Italy

²Dental Implant Unit, University of Cartagena, Cartagena, Colombia

³Research Department, Faculty of Dentistry, University of Cartagena, Cartagena, Colombia

Correspondence should be addressed to Miguel Simancas-Pallares; msimancasp@unicartagena.edu.co

Received 17 April 2017; Accepted 23 May 2017; Published 2 July 2017

Academic Editor: Luigi Canullo

Copyright © 2017 Giorgio Lombardo et al. This is an open access article distributed under the Creative Commons Attribution License, which permits unrestricted use, distribution, and reproduction in any medium, provided the original work is properly cited.

Aim. To determine cumulative success rate (CSR) of short and ultrashort implants in the posterior maxilla restored with single crowns. **Patients and Methods.** We performed a retrospective study in 65 patients with 139 implants. 46 were ultrashort and 93 short. Implants were placed with a staged approach and restored with single crowns. Success rate, clinical and radiographic outcomes, and crown-to-implant ratio (CIR) were assessed after three years. Statistical analysis was performed by descriptive and inferential statistics. A log-binomial regression model where the main outcome was implant success was achieved. Coefficients and 95% confidence intervals were reported. Analyses were performed with Stata 13.2 for Windows. **Results.** 61.54% of patients were female and mean overall age was 51.9 ± 11.08 years old. Overall CSR was 97.1% (95% CI: 92.4–98.9): 97.9 and 95.1% for short and ultrashort, respectively (P value: 0.33). Four implants failed. Covariates were not associated with CSR (P value > 0.05). Regression model showed coefficients correlated with implant success for ultrashort implants (0.87) and most of covariates but none were statistically significant (P values > 0.05). **Conclusions.** Our results suggest that short and ultrashort implants may be successfully placed and restored with single crowns in the resorbed maxillary molar region.

1. Introduction

The partially edentulous posterior maxilla bone quality is often poorly characterized by large marrow spaces and reduced both vertical and horizontal bone volumes due to the severe atrophy, increased sinus pneumatization, and also iatrogenic prosthesis. Patients with extremely atrophic upper posterior maxilla require major surgical sinus lift procedures [1] or even zygomatic implants to be successfully restored and then recover their oral function [2–5]. These options are clinically challenging, because of the increased patient morbidity and also the greater chance of intra- and postoperative complications [6, 7]. Likewise, the development of innovative implant designs and surface textures

in cases of intermediate atrophy suggests the use of short implants as minimally invasive treatment options in these cases [8].

The definition of a short implant in scientific literature has been a historical debate. At first, “short” implants were defined as those with <11 mm in length [9, 10], 10 mm [11, 12], 8 mm [13], and 6 mm [14], and ultimately “extra-short” implants were defined as those with a ≤ 5 mm intrabony length [15]. However, the most recent European Consensus Conference on short, angulated, and diameter-reduced implants defined short implants as those with ≤ 8 mm in length and ≥ 3.75 mm in diameter, standard implants as those >8 mm in length and ≥ 3.75 mm in diameter, and ultrashort implants as those <6 mm in length [16]. Also they stated that short implants are used primarily to avoid bone augmentation

procedures and they are applicable if vertical bone volume is limited by other anatomical structures such as maxillary sinus or the mandibular canal, but there is sufficient alveolar ridge width to use ≥ 3.75 mm diameter implants [16].

Short implants were historically associated with lower survival rates and with unpredictable long-term outcomes [17–20], but, currently due to their design improvement, scientific evidence suggests that short implants (>6 but ≤ 8 mm) have similar survival rates compared to standard implants (>8 mm) [15]. Splinted restorations were highly recommendable in the posterior area of the jaw in order to avoid unfavorable strains over the prosthesis [21], but further studies showed the success of nonsplinted short implants supporting single restorations, offering a comfortable prosthetic approach including better emergence profiles and oral hygiene access compared to other fixed partial prostheses options [22].

Several types of connections between the implant and its prosthetic abutment are commercially available. Screw-retained hexagonal (internal and external) or locking-taper have been subjected to research in the past [23]. Screw-retained systems exhibits greater rate of complications due to instability at the implant-abutment interface (IAI), poor accuracy of thread coupling, and the presence of microgap allowing microbial colonization at the IAI leading to higher rates of biological complications. To deal with this, the locking-taper connection was introduced. It is defined as a tapered connection with an angle connection <1.5 degrees on both components [24]. Major advantages of the locking-taper connection include increased mechanical stability with no micromovements or microgaps at the IAI, thus leading to fewer rates of biological and prosthetic complications. Numerous studies have shown the high survival rates of dental implants with this type of connection [23, 25, 26].

To the best of our knowledge most of these studies focused mainly on 8 mm length implant clinical outcomes, but the scientific evidence for 5 or 6 mm length implants supporting single crowns in the posterior jaw is scarce, thus leaving no clinical recommendations at this time for its clinical usage. So our aim was to determine cumulative success rates of 5 and 6 mm length implants in the posterior jaw restored with single crowns.

2. Materials and Methods

2.1. Study Design and Sample. We performed a retrospective study in 65 patients who had at least one 5, 6, or 8 mm length Bicon™ dental implant (Bicon Dental Implants, Boston, MA, USA) placed between January 2012 and December 2013 at the University of Verona Dental Clinic. One hundred thirty-nine dental implants were placed overall. Sample was selected by a convenience sampling according to the inclusion criteria described below.

2.2. Inclusion Criteria. Patients with ASA I or II status who voluntarily agreed to participate, aged > 18 years old, being partially edentulous in the posterior area of the maxilla, with a residual ridge that allowed insertion of ≤ 8 mm length implants, with 3 months of healing after tooth extraction and

having at least one 8, 6, or 5 mm Bicon implant in length, and restored with single crowns with at least 3 years of function were included. Amongst all of the 139 implants, 52 were 8 mm, 46 were 6 mm, and 41 were 5 mm in length.

The study was conducted in accordance with the Helsinki statement, and all patients signed a written informed consent form. Also the University of Verona Institutional Review Board approved the protocol.

2.3. Preoperative Steps. Before implant placement, all patients received clinical examinations regarding periodontal diseases, caries, and soft tissue status and, if needed, dentate subjects were periodontally treated in order to obtain good oral health before implant placement. Also complete radiographic evaluation including panoramic and periapical radiographs with parallelism technique was obtained. When more than one implant was needed, surgical templates were delivered. All of the patients were prescribed Amoxicillin plus Clavulanate (Augmentin, GlaxoSmithKline SpA, Verona, Italy) one hour before the implant placement to prevent systemic or local infections.

2.4. Surgical Procedure. Local infiltrative anesthesia was used. 2% Xylocaine (Dentsply Pharmaceutical, York, PA, USA) was used to complete the surgical procedure.

Intrasulcular incisions were performed by using a N°15 blade in a Bard-Parker scalpel. Full thickness flap was obtained in the area and then this surgical protocol was followed for implant placement; we began with pilot (2 mm diameter) drilling to achieve cortical perforation. Initial pilot drilling length (3–4 mm) was determined upon residual bone height (RBH) measurement. This high-speed drill (1100 Revolutions Per Minute (RPMs)) was used with external saline irrigation and had a cutting edge at the apical portion. RBH aimed to determine also implant selection, but final pilot drilling length was calculated by adding 3 mm to the selected implant length. Once pilot drilling was performed, a periapical X-ray was obtained in order to control vertical and horizontal positions with regard to the adjacent anatomical structures.

The following steps were achieved with latch reamers (LRs) at 50 RPMs without external irrigation. LRs were used to widen the osteotomy, but length was always set at the computed final drilling length (by adding 3 mm to the desired implant length). LRs are designed with a 0.5 mm diameter progressive increase and were used until the final implant diameter was reached. Due to the fact that the LRs did not need external irrigation and have low RPMs, we collected autogenous bone from the latch reaming process. This bone was stored in a Silicone Dappen Dish during the procedure. Then the selected implant (Bicon Dental Implants, Boston, MA, USA) was manually inserted into the osteotomy through the healing plug. Healing plug was carefully removed and then, with a seating tip mounted into a straight handle, we seated the implant into the osteotomy. Healing plug was cut ensuring that no sharp edges were present and could irritate soft tissue. Then we placed harvested bone over the implant shoulder.

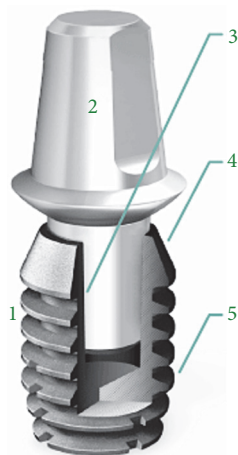


FIGURE 1: Schematic drawing of the Bicon dental implant system and its macrogeometric features. 1 represents the short root-plateau form implant body; 2 represents the abutment; 3 represents the 1.5° internal connection (locking-taper); 4 indicates the convergent crest module (sloping shoulder); and 5 represents the implant plateaus.

Single suture with polyglycolid acid (Vicryl, ACE Surgical Supply Co., Brockton, MA, USA) was used to close the incisions. After implant insertion, immediate postoperative X-ray was performed. The patient received postoperative and homecare instructions as well as antibiotic and analgesic prescriptions to avoid infections and pain/swelling, respectively.

After a 4-to-6-month healing period, the implants were uncovered, temporary abutments were placed, flaps were readapted, and sutures were placed around the temporary abutments. After 3 weeks of soft tissue healing, definitive impressions were taken and within 2 weeks definitive ceramic or composite single crown restorations were delivered. At each recall appointment and when needed, occlusal adjustments were made and the prosthetic restorations were checked for loosening, chipping, or other prosthetic complications.

2.5. Implant System. We used a locking-taper (Morse taper or Morse cone) dental implant system (Bicon Dental Implants, Boston, MA, United States) designed in 1985. Besides the aforementioned clinical advantages of a locking-taper connection with proven bacterial seal [27], this implant has a convergent crest module, platform switching, and a root-form plateau design (Figure 1). Regarding its surface, Integra-Ti™ (grit-blasted and acid-etched) and Integra-CP™ (Hydroxylapatite treated or covered by Hydroxyapatite) are commercially available.

2.6. Follow-Up Examination. After 3 years, patients were recalled for radiographic and clinical examinations. Peri-implant tissues and prostheses were also assessed. Figure 2 depicts a case of two upper posterior-placed implants at the tooth numbers 14 and 15 with porcelain-fused-to-metal restorations. Number 14 was a 5.0 × 8.0 mm and number 15 a 5.0 × 5.0 mm implant, respectively.

2.7. Study Variables. All of the implants had the same diameter (5 mm), but three different lengths were included (5, 6, or 8 mm). The major predictor variable was implant length classified as short (S) (≤ 8 mm in length) or ultrashort (US) (< 6 mm in length) according the proposed criteria of the European Consensus Conference on short, angulated, and diameter-reduced implants [16].

The main outcome was the cumulative success rate (CSR). Secondary variables (covariates) included the following: sex, age, smoking history, NSAIDs consumption, and clinical-related parameters such as implanted tooth type, history of periodontal disease on the treated site, and implant surface. Prosthetic-related covariates were type of restorative material and crown-to-implant ratio.

2.8. Crown-to-Implant Ratio (CIR) Determination. At first, crown height (in mm) was measured on the radiograph immediately after prosthetic loading as the most occlusal point to the implant-abutment interface (IAI) [28]. Then crown-to-implant ratios were calculated by dividing the digital length of the crown over the implant length and were dichotomized as > 2 or < 2 units.

Vertical distortion occurs equally in the crown and in the implant on the radiograph; and because the crown-to-implant ratio is not dependent on absolute values, the effect of vertical distortion on a ratio is then minimal [29].

2.9. Study Outcomes

2.9.1. Primary Outcome: Cumulative Success Rate. Expressed as CSR was the primary outcome variable in our study. Failure was defined as the need of implant removal. Also implant failures were classified in two types: early (or initial) and late that occurred before and after implant loading (crown insertion), respectively.

2.9.2. Secondary Outcomes: Biological and Prosthetic Complications. Biological complications included mucositis (swollen soft tissue and bleeding on probing without bone loss) and peri-implantitis (swollen tissues, bleeding on probing, bone loss, and peri-implant pocket depth > 5 mm) [30].

Prosthetic complications were considered as crown detachment, chipping, or material fracture. However, prosthesis failure was defined as the need to remake the crown due to fracture or loosening.

2.10. Statistical Analysis. We first performed univariate analysis through descriptive statistics. For qualitative variables, we computed proportions and 95% confidence intervals. However, to analyze quantitative data, we first tested normality assumptions by using the Shapiro-Wilks test. If normality criteria were met, we reported mean and standard deviation; otherwise median and interquartile range (IQR) were reported.

In bivariate analysis, we compared proportions using χ^2 or Fisher's exact test, but, to compare means across groups, we used Student's *t*-test or the Mann-Whitney test, considering if normality assumption and homoscedasticity criteria were met (Levene's test).

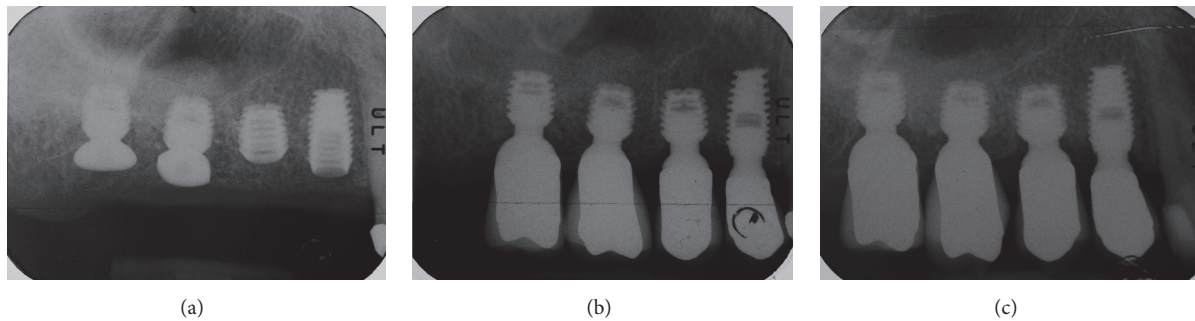


FIGURE 2: (a) Immediate postoperative radiography of premolar implants placed at the upper posterior maxilla (premolars); internal sinus lift cases were not included in this study. (b) Immediate X-ray obtained at crown insertion. (c) X-ray obtained at three-year follow-up showing the implant-restoration success.

Finally, for multivariate analysis, we created a generalized linear model (log-binomial regression) model where the outcome (β) was the implant success rate due to the high rate of the outcome [31]. Major predictors were defined a priori being those with biological plausibility. From this model we reported standardized coefficients and 95% confidence intervals. Marginal probability predictions were also estimated for each group of implant length (short or ultrashort). Statistical analysis was performed using Stata v.13.2 for Windows (StataCorp, College Station, TX, USA).

3. Results

Amongst the 65 patients, 61.5% were females. Overall mean age was 51.9 ± 11.08 years old. Most of the patients were nonsmokers (75.38%), ASA status II (52.31%), and non-NSAIDs consumers. Most of the implanted sites were located in the molar area, coated by the Integra-CP surface and restored using porcelain (porcelain-fused-to-metal (PFM) Technique).

When we analyzed sample distribution according to length definition (short or ultrashort), we only found statistical significance for patients having history of periodontal disease on the implanted site (58.46%), implanted tooth type (molars: 51.8%), and also type of restorative material (porcelain: 76.26%). Overall mean follow-up time was 32.69 ± 15.62 months. Table 1 presents uni- and bivariate demographic and clinical-related outcomes.

Our overall cumulative success rate was 97.12% (95% CI: 92.49–98.92). Among the 139 implants, 4 implants failed: 3 due to peri-implantitis and the other one due to no osseointegration (early failure). When we analyzed failures according to implant length, implanted tooth type, restorative material, and also periodontal status before implantation, we found they were equally distributed amongst groups (P values > 0.05). Nonetheless, most of the failed implants were Integra-CP coated (4 implants) with crown-to-implant ratio > 2 (2 implants). Bivariate analysis for the cumulative success rate is presented in Table 2 showing no statistical significance of the

mentioned parameters with the cumulative success rates (P values > 0.05).

Table 3 shows the descriptive statistics for length definition distribution of the successes and failures according implanted tooth type, implant surface, restorative material, CIR, and also periodontal status before implantation.

Finally, we entered covariates into the log-binomial regression model and coefficients with 95% CI are presented in Table 4. Implant success increases with ultrashort implants in male patients with ASA status I, mostly consuming NSAIDs, and implants covered by Integra-CP. Regarding prosthetic covariates, success increases with crowns made by ceromer and with CIR > 2 . On the other hand, failures increases in periodontally compromised patients. However, none of these parameters were statistically significant (P value > 0.05).

Probability prediction after regression indicated that overall probability of success for short and ultrashort implants are 96.24 and 94.39%, respectively. Finally, according to CIR (> 2), probability of success for short and ultrashort implants was 95.64 and 93.51%, respectively.

4. Discussion

Placed implants in augmented bone in both mandible and maxilla simultaneously or after a staged 6-month period from lateral sinus floor elevation procedure were shown to provide high survival rates [32]. However, these associated procedures are highly invasive and often associated with a high rate of complications such as membrane perforation, sinusitis, and total or partial loss of the grafted material [33–37].

This led to an increase usage of short implants especially in the posterior area of the lower jaw. Also a large number of studies including systematic and narrative reviews suggest that short implants could be considered an alternative treatment to advanced bone augmentation techniques with significantly less complications rates and higher patient's satisfaction [38]. However, several of these reviews clustered short implants outcomes supporting different types of restoration, so the evidence about clinical outcomes of short

TABLE 1: Overall placed implants according to studied covariates. Also distribution of placed implants according to implant length is presented in this table.

Variable	Overall		Short		Ultrashort		P value
	n	%	n	%	n	%	
<i>Sex</i>							
Female	40	61.54	26	65.00	14	56.00	0.46
Male	25	38.46	14	35.00	11	44.00	
<i>Age</i>	51.90 ± 11.08		51.07 ± 10.38		53.24 ± 12.22		0.44
<i>Smoking history</i>							
Yes	16	24.62	7	17.50	9	36.00	0.09
No	49	75.38	33	82.50	16	64.00	
<i>ASA status</i>							
I	31	47.69	21	52.50	10	40.00	0.32
II	34	52.31	19	47.50	15	60.00	
<i>NSAIDs consumption</i>							
Yes	5	7.69	2	5.00	3	12.00	0.36
No	60	92.31	38	95.00	22	88.00	
<i>History of periodontal disease</i>							
Yes	38	58.46	19	47.50	19	76.00	0.02*
No	27	41.54	21	52.50	6	24.00	
<i>Implanted tooth type</i>							
Premolar	67	(48.20)	56	(57.14)	11	(26.83)	0.00*
Molar	72	(51.80)	42	(42.86)	30	(73.17)	
<i>Implant surface</i>							
Integra-CP	117	87.31	80	84.21	37	94.87	0.29
HA-coated	12	8.96	10	10.53	2	8.96	
Integra-Ti	5	3.73	5	5.26	0	3.73	
<i>Restorative material</i>							
Ceromer	33	(23.74)	18	(18.37)	15	(36.59)	0.02*
Porcelain	106	(76.26)	80	(81.63)	26	(63.41)	

* Statistically significant differences between groups. Age is presented as mean ± standard deviation.

implants supporting single crowns in the posterior maxilla is scarce [39, 40].

To the best of our knowledge, there is only one comprehensive systematic review aimed to evaluate the prognosis of the posterior area restoration with single crowns supported by short implants [41]. In this review, even when authors did not find differences between ≤6 and >7 but in ≤8 mm implants in length, they hypothesized that this might be due to the small sample of the 6 mm and 5 mm length implants included, and if, with a larger sample size of the 6 mm and 5 mm implants, the meta-regression analysis results should be different, finding statistically significant differences between implants ≤8 mm and >8 mm in length.

Recently, Lai et al. [42] in a 5–10-year study followed 231 short Straumann implants supporting single crowns. 110 implants were placed in the maxilla and found that the 6 and 8 mm length implants showed, respectively, a cumulative survival rate of 97 and 98.5%, with no differences in regard to the implanted jaw. Gulje et al. examined 41 patients randomly allocated to receive an 11 mm implant in combination with

maxillary sinus floor elevation surgery or to receive a 6 mm implant without any grafting in the posterior maxilla. At the 12-month evaluation implant, survival was 100% in both groups [43]. Schincaglia et al. [44] and Bechara et al. [45], in two studies with similar designs, reported a cumulative survival rate of 100% for the 6 mm implants after 1 and 3 years, respectively. Even when we performed a mid-term (three years) follow-up, our results are also comparable to those at long-term (ten years) follow-up. Mangano et al., on a prospective clinical study including 215 short (8 mm) implants also supporting single crowns in the posterior region of the jaws, showed an implant-based cumulative survival rate of 98.5% [46], also highlighting the clinical applicability of short implants.

Our results show that overall cumulative success rates for short and ultrashort implants was 97.9% and 95.1%, respectively (P value = 0.58), thus being equivalent. These results are also consistent with previous evidence about short implants supporting single crowns in the posterior maxilla and, as a matter of fact, not only short but also

TABLE 2: Bivariate analysis of the success rate according to study included covariates.

Variable	Overall		P value
	Success n (%)	Failure n (%)	
<i>Implant length</i>			
Short	96 (97.96)	2 (2.04)	0.33
Ultrashort	39 (95.12)	2 (4.88)	
<i>Implanted tooth type</i>			
Premolar	65 (97.01)	2 (2.99)	1.00
Molar	70 (97.22)	2 (2.78)	
<i>Implant surface</i>			
Integra-CP	113 (96.58)	4 (3.42)	1.00
Hydroxyapatite (HA) coating	12 (100)	0 (0.00)	
Integra-Ti	5 (100)	0 (0.00)	
<i>Restorative material</i>			
Ceromer	31 (93.94)	2 (6.06)	0.23
Ceramic	104 (98.11)	2 (1.89)	
<i>Crown-to-implant ratio</i>			
<2 Units	71 (98.61)	1 (1.39)	0.60
>2 Units	63 (96.92)	2 (3.08)	
<i>Periodontal status before implantation</i>			
Periodontally compromised	36 (94.74)	2 (5.26)	1.00
Nonperiodontally compromised	25 (92.59)	2 (7.41)	

TABLE 3: Descriptive analysis of the success rate according to study groups.

Variable	Short		Ultrashort	
	Success n (%)	Failure n (%)	Success n (%)	Failure n (%)
<i>Implanted tooth type</i>				
Premolar	55 (57.29)	1 (50.00)	10 (25.64)	1 (50.00)
Molar	41 (42.70)	1 (50.00)	29 (74.35)	1 (50.00)
<i>Implant surface</i>				
Integra-CP	78 (83.87)	2 (100)	35 (94.59)	2 (100)
HA-coated	10 (10.75)	0 (0.00)	2 (5.40)	0 (0.00)
Integra-Ti	5 (5.37)	0 (0.00)	0 (0.00)	0 (0.00)
<i>Restorative material</i>				
Ceromer	18 (18.75)	0 (0.00)	13 (33.33)	2 (100)
Ceramic	78 (81.25)	2 (100)	26 (66.66)	0 (0.00)
<i>Crown-to-implant ratio</i>				
<2 Units	66 (69.47)	1 (50.00)	5 (12.82)	0 (0.00)
>2 Units	29 (30.52)	1 (50.00)	34 (87.17)	1 (100)
<i>Periodontal status before implantation</i>				
Periodontally compromised	20 (52.63)	1 (50.00)	5 (21.73)	1 (50.00)
Nonperiodontally compromised	18 (47.36)	1 (50.00)	18 (78.26)	1 (50.00)

ultrashort implants can support single crowns and remain as a successful treatment in the atrophic posterior maxilla, even with high C/I ratios (>2). It is important to note that the prevalence of crowns with CIR > 2 (47.4%) was higher than the previously published in the literature. Moreover when we analyzed success rates of short and ultrashort implants according to CIR, we did not find any statistical significance,

thus suggesting that either short or ultrashort implants could be restored with single crowns having CIR > 2. Besides this, the multivariate analyses show the positive effect of CIR > 2 on the implant success rate (coefficient = 0.79). Even when our study only included dental implants restored by means of single crowns, our results are also comparable with those of Mangano et al., who showed a high CSR (97,2%), for

TABLE 4: Standardized coefficients derived from log-binomial regression and 95% confidence intervals for factors associated with success rate.

Variable	Estimates		P value
	Coefficients	95% CI	
<i>Implant length</i>			
Ultrashort	0.87	1.05–2.79	0.37
<i>Sex</i>			
Male	0.47	–1.42–2.36	0.62
<i>ASA status</i>			
I	0.09	–1.80–1.99	0.92
<i>NSAIDs consumption</i>			
Yes	1.38	–0.68–3.45	0.19
<i>Implant surface</i>			
Integra-CP	14.85	–4318.28–4348.00	0.99
HA-coated	–14.19	–3787.47–3759.08	
Integra-Ti	–13.88	–5171.07–5143.29	
<i>Restorative material</i>			
IACs (ceromer)	1.16	–0.75–3.08	0.23
<i>Crown-to-implant ratio</i>			
>2 units	0.79	–1.58–3.17	0.51
<i>Periodontal status before implantation</i>			
Periodontally compromised	–0.34	–2.23–1.55	0.72

standard (>10 mm) implants restored using fixed prosthesis with follow-up periods as high as 20 years [47].

Urdaneta et al. evaluated 326 short and ultrashort implants with the same implant design supporting single-tooth crowns with a mean C/IR of 1.6 (ranging from 0.79 to 4.95) and found that after 6 years (70.7 months) of follow-up a CIR up to 4.95 did not lead to an increased risk of implant failures, crown failures, or crown fractures [26]. Malchiodi et al., in a prospective study on 259 tapered truncated cone shaped implants with 5, 7, 9, or 12 mm in length, reported that 36% of the implants presented a C/I ratio >2, showing a CSR of 95.6% [48] being comparable to our results (96.9%). Anitua et al. [49], in a retrospective study with a mean follow-up of 28.9 months, reviewed the clinical outcomes of 128 short implants being mostly restored with bridges or splinted crowns and found a CSR of 100%. Only 42 out of the 128 implants (32.8%) had a >2 CIR. Recently, Mangano et al. [50], in a 5-year prospective study, followed 68 6.5 mm long implants in 51 patients. Twenty-nine out of the 65 implants (72%) were restored by means of single crowns. Twenty-five percent (17 out of 68) of the implants had at baseline CIR \geq 2 and 3 failures were reported, all in the >2 CIR group.

Current scientific evidence demonstrates that implant design can play a determining role to allow higher clinical performance [51], and it is assumed to be particularly true for short implants. Moreover our results support these facts for ultrashort implants. Results from finite element analysis studies show that different implant bodies and abutment connection types may influence peri-implant bone stresses and abutment micromovement, determining the threshold values of tensile and shear stresses that cause resorption of cortical bone, thus affecting implant success rate [52].

Features like a reverse conical neck design, the locking-taper implant-abutment connection, and a plateau root form body are associated with low occlusal stress concentration on the buccal bone and limited harmful abutment micromovement inside the connection [52]. Furthermore, the locking-taper feature inhibits the bacterial leakage at the implant-abutment connection level [27], thus providing numerous benefits in terms of healing and osseointegration, leading to a better biomechanical fixation [53]. From a biomechanical standpoint, a locking-taper connection is mechanically more stable than external-hexagon or butt-joint implant-abutment connections. While the rate of biological and prosthetic complications related to screw-retained systems is high, locking-taper implants demonstrates minimizing all these problems. Also this type of implant-abutment connection can also withstand large lateral forces [54]. Thanks to the Morse taper principle, the high friction between the surfaces of two equal conical parts links them altogether. This phenomenon is known as “cold welding,” since both surfaces undergo a kind of interpenetration and fusion between their asperities as result of contact pressure. This means that both implant and abutment virtually create a single body; so compared to screw-retained systems, stress distribution is homogeneous through the unit [24].

All these facts that aim to elucidate the high CSR from our study are also well supported in scientific evidence from systematic reviews [55]. Implant placement in a subcrestal (submerged) fashion and the usage of an implant with convergent crest module, represented by the sloping shoulder geometry, enhance the platform switching (PS) to occur. This PS allows an increase in residual crestal alveolar bone volume around the neck of the an implant, repositions the papilla to

a more esthetic and apposite level, reduces mechanical stress in the crestal alveolar bone area, and assists in enhancing the vascular supply to hard and soft tissue in case of reduced interdental space.

Even when our study was able to demonstrate the high cumulative success rate and low rate of biological complications, some limitations are evident such as the relatively small sample size, the mid-term follow-up, and imbalanced distribution across groups (short versus ultrashort). These factors might partially explain our nonstatistically significant associations presented here.

5. Conclusions

Results from our study suggest the adequate clinical performance of short and ultrashort implants. After 3 years of loading, the clinical applicability of these implants with locking-taper connection, sloping shoulder, and plateau-form which are supporting single crowns in the posterior maxilla is evident. Since we did not find any statistical difference between groups, even according to CIR, this is the first evidence to hypothesize that short and ultrashort implants are clinically equivalent and could be used either on premolar or on molar areas. However, in most cases where residual bone height in the molar area is limited, ultrashort implants are recommended for implant-supported restorations.

Conflicts of Interest

The authors declare no conflicts of interests.

Acknowledgments

This paper is supported by Department of Surgery, Dentistry, Paediatrics and Gynaecology (DIPSCOMI). University of Verona.

References

- [1] B. E. Pjetursson, W. C. Tan, M. Zwahlen, and N. P. Lang, "A systematic review of the success of sinus floor elevation and survival of implants inserted in combination with sinus floor elevation: part I: lateral approach," *Journal of Clinical Periodontology*, vol. 35, Supplement 8, pp. 216–240, 2008.
- [2] G. Lombardo, A. D'Agostino, L. Trevisiol et al., "Clinical, microbiologic and radiologic assessment of soft and hard tissues surrounding zygomatic implants: a retrospective study," *Oral Surgery, Oral Medicine, Oral Pathology and Oral Radiology*, vol. 122, no. 5, pp. 537–546, 2016.
- [3] P. F. Nocini, L. Trevisiol, A. D'Agostino, G. Zanette, V. Favero, and P. Procacci, "Quadruple zygomatic implants supported rehabilitation in failed maxillary bone reconstruction," *Oral and Maxillofacial Surgery*, vol. 20, no. 3, pp. 303–308, 2016.
- [4] A. D'Agostino, P. Pasquale, F. Ferrari, L. Trevisiol, and N. P. Francesco, "Zygoma implant-supported prosthetic rehabilitation of a patient after subtotal bilateral maxillectomy," *Journal of Craniofacial Surgery*, vol. 24, no. 2, pp. e159–e162, 2013.
- [5] P. F. Nocini, A. D'Agostino, L. Chiarini, L. Trevisiol, and P. Procacci, "Simultaneous le fort I osteotomy and zygomatic implants placement with delayed prosthetic rehabilitation," *Journal of Craniofacial Surgery*, vol. 25, no. 3, pp. 1021–1024, 2014.
- [6] P. Boffano and T. Forouzanfar, "Current concepts on complications associated with sinus augmentation procedures," *Journal of Craniofacial Surgery*, vol. 25, no. 2, pp. e210–e212, 2014.
- [7] A. D'Agostino, L. Trevisiol, V. Favero, M. Pessina, P. Procacci, and P. F. Nocini, "Are zygomatic implants associated with maxillary sinusitis?" *Journal of Oral and Maxillofacial Surgery*, vol. 74, no. 8, pp. 1562–1573, 2016.
- [8] A. Y. Alqutaibi and F. Altaib, "Short dental implant is considered as a reliable treatment option for patients with atrophic posterior maxilla," *Journal of Evidence-Based Dental Practice*, vol. 16, no. 3, pp. 173–175, 2016.
- [9] F. das Neves, D. Fones, S. Bernardes, C. do Prado, and A. Neto, "Short implants-an analysis of longitudinal studies," *The International Journal of Oral & Maxillofacial Implants*, vol. 21, no. 1, pp. 86–93, 2006.
- [10] F. P. Strietzel and P. A. Reichart, "Oral rehabilitation using Camlog screw-cylinder implants with a particle-blasted and acid-etched microstructured surface. Results from a prospective study with special consideration of short implants," *Clinical Oral Implants Research*, vol. 18, no. 5, pp. 591–600, 2007.
- [11] M. Morand and T. Irinakis, "The challenge of implant therapy in the posterior maxilla: providing a rationale for the use of short implants," *The Journal of oral implantology*, vol. 33, no. 5, pp. 257–266, 2007.
- [12] G. Tawil and R. Younan, "Clinical evaluation of short, machined-surface implants followed for 12 to 92 months," *The International Journal of Oral & Maxillofacial Implants*, vol. 18, no. 6, pp. 894–901, 2003.
- [13] F. Renouard and D. Nisand, "Impact of implant length and diameter on survival rates," *Clinical Oral Implants Research*, vol. 17, supplement 2, pp. 35–51, 2006.
- [14] M. Srinivasan, L. Vazquez, P. Rieder, O. Moraguez, J.-P. Bernard, and U. C. Belser, "Efficacy and predictability of short dental implants (<8 mm): a critical appraisal of the recent literature," *International Journal of Oral and Maxillofacial Implants*, vol. 27, no. 6, pp. 1429–1437, 2012.
- [15] D. Nisand and F. Renouard, "Short implant in limited bone volume," *Periodontology 2000*, vol. 66, no. 1, pp. 72–96, 2014.
- [16] J. Neugebauer, H. Nickenig, and J. Zöller, "Update on short, angulated a diameter-reduced implants," in *Proceedings of the 11th European Consensus Conference (EuCC '16)*, pp. 1–9, European Association of Dental Implantologists, Bonn, Germany, February, 2016.
- [17] O. Bahat, "Branemark system implants in the posterior maxilla: clinical study of 660 implants followed for 5 to 12 years," *International Journal of Oral and Maxillofacial Implants*, vol. 15, no. 5, pp. 646–653, 2000.
- [18] S. Winkler, H. F. Morris, and S. Ochi, "Implant survival to 36 months as related to length and diameter," *Annals of periodontology*, vol. 5, no. 1, pp. 22–31, 2000.
- [19] L. Pierrisnard, F. Renouard, P. Renault, and M. Barquins, "Influence of implant length and bicortical anchorage on implant stress distribution," *Clinical Implant Dentistry and Related Research*, vol. 5, no. 4, pp. 254–262, 2003.
- [20] D. Weng, Z. Jacobson, D. Tarnow, M. B. Hürzeler, O. Faehn, and F. Sanavi, "A prospective multicenter clinical trial of 3i machined-surface implants: results after 6 years of follow-up," *The International Journal of Oral & Maxillofacial Implants*, vol. 18, no. 3, pp. 417–423, 2003.

- [21] B. R. Rangert, R. M. Sullivan, and T. M. Jemt, "Load factor control for implants in the posterior partially edentulous segment," *International Journal of Oral and Maxillofacial Implants*, vol. 12, no. 3, pp. 360–370, 1997.
- [22] G. S. Solnit and R. L. Schneider, "An alternative to splinting multiple implants: use of the ITI system," *Journal of Prosthodontics*, vol. 7, no. 2, pp. 114–119, 1998.
- [23] K. O. Demiralp, N. Akbulut, S. Kursun, D. Argun, N. Bagis, and K. Orhan, "Survival rate of short, locking taper implants with a plateau design: a 5-year retrospective study," *BioMed Research International*, vol. 2015, Article ID 197451, 8 pages, 2015.
- [24] G. Sannino and A. Barlattani, "Mechanical evaluation of an implant-abutment self-locking taper connection: finite element analysis and experimental tests," *The International Journal of Oral & Maxillofacial Implants*, vol. 28, no. 1, pp. e17–e26, 2013.
- [25] F. Mangano, A. Macchi, A. Caprioglio, R. L. Sammons, A. Piattelli, and C. Mangano, "Survival and complication rates of fixed restorations supported by locking-taper implants: a prospective study with 1 to 10 years of follow-up," *Journal of Prosthodontics*, vol. 23, no. 6, pp. 434–444, 2014.
- [26] R. A. Urdaneta, S. Daher, J. Leary, K. M. Emanuel, and S. K. Chuang, "The survival of ultrashort locking-taper implants," *The International Journal of Oral & Maxillofacial Implants*, vol. 27, no. 3, pp. 644–654, 2012.
- [27] S. Dibart, M. Warbington, M. F. Su, and Z. Skobe, "In vitro evaluation of the implant-abutment bacterial seal: the locking taper system," *International Journal of Oral and Maxillofacial Implants*, vol. 20, no. 5, pp. 732–737, 2005.
- [28] R. J. Blanes, J. P. Bernard, Z. M. Blanes, and U. C. Belsler, "A 10-year prospective study of ITI dental implants placed in the posterior region. II: influence of the crown-to-implant ratio and different prosthetic treatment modalities on crestal bone loss," *Clinical Oral Implants Research*, vol. 18, no. 6, pp. 707–714, 2007.
- [29] H. Birdi, J. Schulte, A. Kovacs, M. Weed, and S.-K. Chuang, "Crown-to-implant ratios of short-length implants," *The Journal of Oral Implantology*, vol. 36, no. 6, pp. 425–433, 2010.
- [30] M. Sanz, I. L. Chapple, and Working Group 4 of the VEWoP, "Clinical research on peri-implant diseases: consensus report of working group 4," *Journal of Clinical Periodontology*, vol. 39, Supplement 12, pp. 202–206, 2012.
- [31] T. Skov, J. Deddens, M. R. Petersen, and L. Endahl, "Prevalence proportion ratios: estimation and hypothesis testing," *International Journal of Epidemiology*, vol. 27, no. 1, pp. 91–95, 1998.
- [32] A. Aloy-Prosper, D. Peñarrocha-Oltra, M. Penarrocha-Diago, and M. Penarrocha-Diago, "The outcome of intraoral onlay block bone grafts on alveolar ridge augmentations: a systematic review," *Medicina Oral, Patología Oral y Cirugía Bucal*, vol. 20, no. 2, pp. e251–e258, 2015.
- [33] W. C. Tan, N. P. Lang, M. Zwahlen, and B. E. Pjetursson, "A systematic review of the success of sinus floor elevation and survival of implants inserted in combination with sinus floor elevation Part II: Transalveolar technique," *Journal of Clinical Periodontology*, vol. 35, Supplement 8, pp. 241–254, 2008.
- [34] H.-L. Chan and H.-L. Wang, "Sinus pathology and anatomy in relation to complications in lateral window sinus augmentation," *Implant Dentistry*, vol. 20, no. 6, pp. 406–412, 2011.
- [35] H.-W. Lee, W.-S. Lin, and D. Morton, "A retrospective study of complications associated with 100 consecutive maxillary sinus augmentations via the lateral window approach," *International Journal of Oral and Maxillofacial Implants*, vol. 28, no. 3, pp. 860–868, 2013.
- [36] O. Camps-Font, G. Burgueno-Barris, R. Figueiredo, R. E. Jung, C. Gay-Escoda, and E. Valmaseda-Castellon, "Interventions for dental implant placement in atrophic edentulous mandibles: vertical bone augmentation and alternative treatments. a meta-analysis of randomized clinical trials," *Journal of Periodontology*, vol. 87, no. 12, pp. 1444–1457, 2016.
- [37] F. G. Draenert, P. W. Kammerer, M. Berthold, and A. Neff, "Complications with allogeneic, cancellous bone blocks in vertical alveolar ridge augmentation: prospective clinical case study and review of the literature," *Oral Surgery, Oral Medicine, Oral Pathology and Oral Radiology*, vol. 122, no. 2, pp. e31–e43, 2016.
- [38] B. Pommer, G. Mailath-Pokorny, R. Haas, D. Busenlechner, R. Furhauser, and G. Watzek, "Patients' preferences towards minimally invasive treatment alternatives for implant rehabilitation of edentulous jaws," *European journal of oral implantology*, vol. 7, Supplement 2, pp. S91–109, 2014.
- [39] D. S. Thoma, J. Cha, and U. Jung, "Treatment concepts for the posterior maxilla and mandible: short implants versus long implants in augmented bone," *Journal of Periodontal & Implant Science*, vol. 47, no. 1, p. 2, 2017.
- [40] C. A. A. Lemos, M. L. Ferro-Alves, R. Okamoto, M. R. Mendonça, and E. P. Pellizzer, "Short dental implants versus standard dental implants placed in the posterior jaws: a systematic review and meta-analysis," *Journal of Dentistry*, vol. 47, pp. 8–17, 2016.
- [41] L. A. Mezzomo, R. Miller, D. Triches, F. Alonso, and R. S. A. Shinkai, "Meta-analysis of single crowns supported by short (<10 mm) implants in the posterior region," *Journal of Clinical Periodontology*, vol. 41, no. 2, pp. 191–213, 2014.
- [42] H.-C. Lai, M.-S. Si, L.-F. Zhuang, H. Shen, Y.-L. Liu, and D. Wismeijer, "Long-term outcomes of short dental implants supporting single crowns in posterior region: a clinical retrospective study of 5–10 years," *Clinical Oral Implants Research*, vol. 24, no. 2, pp. 230–237, 2013.
- [43] F. L. Gulje, G. M. Raghoebar, A. Vissink, and H. J. Meijer, "Single crowns in the resorbed posterior maxilla supported by either 6-mm implants or by 11-mm implants combined with sinus floor elevation surgery: a 1-year randomised controlled trial," *European Journal of Oral Implantology*, vol. 7, no. 3, pp. 247–255, 2014.
- [44] G. P. Schincaglia, D. S. Thoma, R. Haas et al., "Randomized controlled multicenter study comparing short dental implants (6 mm) versus longer dental implants (11–15 mm) in combination with sinus floor elevation procedures. Part 2: Clinical and radiographic outcomes at 1 year of loading," *Journal of Clinical Periodontology*, vol. 42, no. 11, pp. 1042–1051, 2015.
- [45] S. Bechara, R. Kubilius, G. Veronesi, J. T. Pires, J. A. Shibli, and F. G. Mangano, "Short (6-mm) dental implants versus sinus floor elevation and placement of longer (≥ 10 -mm) dental implants: a randomized controlled trial with a 3-year follow-up," *Clinical Oral Implants Research*, 2016.
- [46] F. G. Mangano, J. A. Shibli, R. L. Sammons, F. Iaculli, A. Piattelli, and C. Mangano, "Short (8-mm) locking-taper implants supporting single crowns in posterior region: a prospective clinical study with 1-to 10-years of follow-up," *Clinical Oral Implants Research*, vol. 25, no. 8, pp. 933–940, 2014.
- [47] C. Mangano, F. Iaculli, A. Piattelli, and F. Mangano, "Fixed restorations supported by Morse-taper connection implants: a retrospective clinical study with 10–20 years of follow-up," *Clinical Oral Implants Research*, vol. 26, no. 10, pp. 1229–1236, 2015.

- [48] L. Malchiodi, A. Cucchi, P. Ghensi, D. Consonni, and P. F. Nocini, "Influence of crown-implant ratio on implant success rates and crestal bone levels: a 36-month follow-up prospective study," *Clinical Oral Implants Research*, vol. 25, no. 2, pp. 240–251, 2014.
- [49] E. Anitua, L. Pinas, and G. Orive, "Retrospective study of short and extra-short implants placed in posterior regions: influence of crown-to-implant ratio on marginal bone loss," *Clinical Implant Dentistry and Related Research*, vol. 17, no. 1, pp. 102–110, 2015.
- [50] F. Mangano, I. Frezzato, A. Frezzato, G. Veronesi, C. Mortellaro, and C. Mangano, "The effect of crown-to-implant ratio on the clinical performance of extra-short locking-taper implants," *Journal of Craniofacial Surgery*, vol. 27, no. 7, pp. 675–681, 2016.
- [51] K.-J. Lee, Y.-G. Kim, J.-W. Park, J.-M. Lee, and J.-Y. Suh, "Influence of crown-to-implant ratio on periimplant marginal bone loss in the posterior region: a five-year retrospective study," *Journal of Periodontal and Implant Science*, vol. 42, no. 6, pp. 231–236, 2012.
- [52] Y. Yamanishi, S. Yamaguchi, S. Imazato, T. Nakano, and H. Yatani, "Influences of implant neck design and implant-abutment joint type on peri-implant bone stress and abutment micromovement: three-dimensional finite element analysis," *Dental Materials*, vol. 28, no. 11, pp. 1126–1133, 2012.
- [53] P. G. Coelho, M. Suzuki, M. V. M. Guimaraes et al., "Early bone healing around different implant bulk designs and surgical techniques: a study in dogs," *Clinical Implant Dentistry and Related Research*, vol. 12, no. 3, pp. 202–208, 2010.
- [54] K. Gotfredsen, T. Berglundh, and J. Lindhe, "Bone reactions adjacent to titanium implants subjected to static load: a study in the dog," *Clinical Oral Implants Research*, vol. 12, no. 1, pp. 1–8, 2001.
- [55] C. M. Schmitt, G. Nogueira-Filho, H. C. Tenenbaum et al., "Performance of conical abutment (Morse Taper) connection implants: a systematic review," *Journal of Biomedical Materials Research A*, vol. 102, no. 2, pp. 552–574, 2014.

Clinical Study

Immediate Loading of Single Implants in the Anterior Maxilla: A 1-Year Prospective Clinical Study on 34 Patients

Miguel Stanley, Filipa Calheiros Braga, and Beatriz Mota Jordao

White Clinic, Rua Dr. António Loureiro Borges, Edifício 5, 1º Andar 131, 1495 Algés, Portugal

Correspondence should be addressed to Filipa Calheiros Braga; filipabraga@whiteclinic.pt

Received 2 March 2017; Accepted 13 March 2017; Published 22 May 2017

Academic Editor: Eitan Mijiritsky

Copyright © 2017 Miguel Stanley et al. This is an open access article distributed under the Creative Commons Attribution License, which permits unrestricted use, distribution, and reproduction in any medium, provided the original work is properly cited.

Purpose. To present the outcomes of immediately loaded single implants placed in the anterior maxilla. *Methods.* Over a 2-year period, all patients referred to a private clinic were considered for enrolment in this study. Inclusion criteria were single-tooth placement in postextraction sockets or healed sites of the anterior maxilla. All implants were immediately loaded and followed for a period of 1 year after the placement of definitive crowns. The outcome measures were implant stability, survival, and success. *Results.* 34 patients were selected and 43 tapered implants with a knife-edge thread design and a nanostructured, calcium-incorporated surface (Anyridge®, Megagen, Gyeongsang, Korea) were installed. Two implants were not sufficiently stable at placement (ISQ < 60) and were considered failed for immediate loading; 41 implants had an ISQ ≥ 60 at placement and were immediately loaded. One year after the placement of definitive crowns, no implant failures were reported, for a survival rate of 100%. No biological complications were found, but 2 implants had their prosthetic abutments loosened: the implant success rate was 95.2%. *Conclusions.* In the present study on the immediate loading of single implants in the anterior maxilla, positive outcomes were reported, with high survival (100%) and success (95.2%) rates (*the present study has been registered in the ISRCTN registry, a publicly available trial register recognized by WHO and ICMJE, with number ISRCTN12935478*).

1. Introduction

Dental implants are a viable solution for the restoration of single-tooth gaps, with high survival and success rates in the short [1] and long term [2]. Nowadays, the placement of an implant-supported single crown allows the rapid and predictable restoration of function (mastication) and aesthetics [3, 4].

A good biological integration is an essential prerequisite for the success of a fixed implant-supported restoration [5]. In fact, a dental implant has to effectively integrate into the bone, in order to functionally support the prosthetic restoration [5]; at the same time, of fundamental importance is the integration with the soft tissues, which is a guarantee of the maintenance of osseointegration over time, and it is an essential condition for the aesthetic success of the rehabilitation [4–6].

In recent years, the aesthetic requirements of the patients have become increasingly important and difficult to

satisfy [4–6]; furthermore, patients require a treatment that should be fast, minimally invasive, and of low cost [5].

In order to meet the modern needs of patients, new surgical and prosthetic protocols have been proposed and are gaining acceptance, which reduce the number of operating sessions (and with them the stress and costs for the patient): among them, there are the placement of implants in fresh extraction sockets [4, 7, 8] and the immediate prosthetic loading [9].

The placement of implants in fresh extraction sockets, that is, immediately after the extraction of the nonrestorable, compromised teeth, can reduce the number of surgical sessions (from two to one) with a reduction in the patients' stress and costs [4, 7, 8]. This strategy is compatible with the insertion of implants with a flapless technique (i.e., without having to raise a full-thickness, mucoperiosteal flap) and is therefore minimally invasive: this represents a further advantage of the method [8, 10]. Finally, some researchers believe that the insertion of an implant into a fresh extraction

socket may facilitate the correct three-dimensional (3D) positioning of the fixture, with benefits for the emergence profile [4, 7, 8].

Although all these benefits of immediate implant placement have been recognized, this surgical technique does not allow (in contrast to what had been assumed in the past) a reduction or counteracting of the physiological resorption that occurs in the alveolar bone after tooth extraction [11, 12], and that particularly affects the delicate buccal bone plate in the anterior maxilla [12]. In addition, the placement and primary stabilization of an implant in a fresh postextraction socket (which is generally larger) can be technically difficult and can be a challenge for the surgeon [7, 8, 13]. If the implant is placed too buccally, the final aesthetic outcome can be compromised [8, 13]; if the implant is placed too palatally (lingually), this situation may not be compatible with adequate prosthetic emergence profile [8, 13].

The immediate prosthetic loading is a viable strategy to reduce the time of treatment: the placement of a temporary restoration immediately after the insertion of the fixture (within 48–72 hours after surgery) is certainly an aesthetic and functional benefit to the patient, who can avoid wearing uncomfortable removable dentures during the healing period [9]. Finally, the placement of an immediate provisional restoration involves benefits with respect to gingival tissues, which can be modeled around it immediately [4, 6, 14].

However, there is a risk to be calculated in immediate loading of dental implants, especially when they support single crowns [15, 16]: in order to obtain a valid osseointegration, it is indeed necessary that the forces applied on the system in the early healing period are controlled, and they do not generate micromotions [17]. The presence of micromovements at the interface between bone and implant can, in fact, affect bone healing and osseointegration, leading to a mobilization and failure of the implant [17, 18].

In order to meet the new challenges of modern implantology, the manufacturers now offer implant systems with specific designs (macrotopographies) and surfaces (micro/nanotopographies) that can help to maximize the primary stabilization in difficult contexts (such as the placement in postextraction sockets) and at the same time speed up and enhance osseointegration, in order to anticipate the prosthetic loading without risk [19–22].

The aim of this prospective clinical study is therefore to present the clinical outcomes of single implants with a knife-edge thread design and a nanostructured calcium-incorporated surface, when placed in postextraction sockets and healed sites of the anterior maxilla and subjected to immediate loading.

2. Materials and Methods

2.1. Study Sample. The patients were enrolled in this prospective study and treated with the insertion of dental implants in the course of two years (2013–2014) in one private dental center (White Clinic®, Lisbon, Portugal). Inclusion criteria were as follows: (1) patients with one to four single-tooth gaps or patients in need of replacement of one to four severely compromised, nonrestorable teeth in the anterior areas of the

maxilla (incisors, canines, and first and second premolars); (2) good state of systemic health; (3) good oral hygiene; (4) age > 18 years; (5) dentition in the opposite arch; (6) willingness to participate in the follow-up study, attending all annual periodic examinations/controls. The general exclusion criteria included the presence of medical conditions that contraindicated surgery, such as (1) uncontrolled or not properly treated diabetes with high blood sugar levels, (2) the presence of immunosuppression, (3) history of head and neck cancer with radio- and chemotherapy, (4) the presence of blood diseases, (5) the presence of psychological or psychiatric diseases, (6) patients in treatment with anticoagulants, and (7) patients in treatment with oral/intravenous aminobisphosphonates. The local exclusion criteria were as follows: (1) the absence of enough bone to place an implant of at least 10.0 mm in length and 3.5 mm in diameter; (2) the need of major regenerative bone techniques (such as onlay/inlay bone grafting) before implant insertion (minor procedures including guided bone regeneration with granulate and membranes or buccal grafting and interproximal procedures were not exclusion criteria); (3) the presence of oral diseases (vesiculobullous diseases, ulcerative diseases, white or red lesions, diseases of the salivary glands, the connective tissue or lymphoid lesions, cystic lesions, and benign or malignant tumors of the oral cavity); (4) the lack of occlusal contacts in the antagonist arch. History of periodontal disease, the habit of cigarette smoking, and the presence of parafunctions were not exclusion criteria for this study; however, patients were advised that these conditions could represent a risk factor for implant therapy [23]. All patients were informed in detail about the nature of this study and signed informed consent for implant therapy. The present study was carried out in full compliance with the criteria established by the Declaration of Helsinki on clinical trials involving human subjects (2008).

2.2. Preoperative Evaluation. The preoperative evaluation included a careful clinical and radiographic analysis (Figures 1 and 2). In particular, all patients underwent two-dimensional radiographic evaluation (intraoral periapical radiographs or panoramic radiograph) for a first assessment of the surgical site; when requested, this assessment was supplemented by a three-dimensional (3D) evaluation of bone anatomy by means of a low-dose cone beam computed tomography (CBCT) (CS9300®, Carestream Health, Rochester, USA). The DICOM files resulting from the CBCT were then loaded into visualization software, in order to evaluate in detail the height and thickness of the bone crest. The surgical planning then proceeded through a simulation of implant placement: this was helpful for deciding the length and diameter of the different fixtures and to better study location, depth, and inclination of the same fixtures. Radiographic evaluation was completed by taking two alginate impressions and pouring of plaster models, on which the dental technician made a diagnostic wax-up, in order to better understand the patient's prosthetic needs.

2.3. The Implants. The tapered implants used here (Anyridge, Megagen, Gyeongsang, Korea) had a knife-edge thread design and a nanostructured, calcium-incorporated surface.

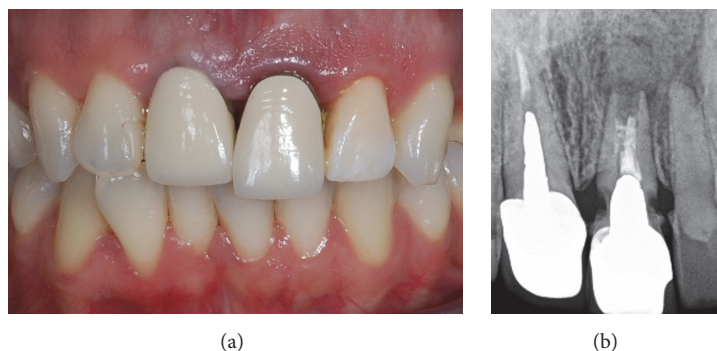


FIGURE 1: Preoperative situation. The patient complains because the left central incisor, which was restored with a single crown several years before, appears extruded and presents a high mobility (a). The periapical radiograph shows a severe resorption (b): the tooth is nonrestorable and needs to be extracted.

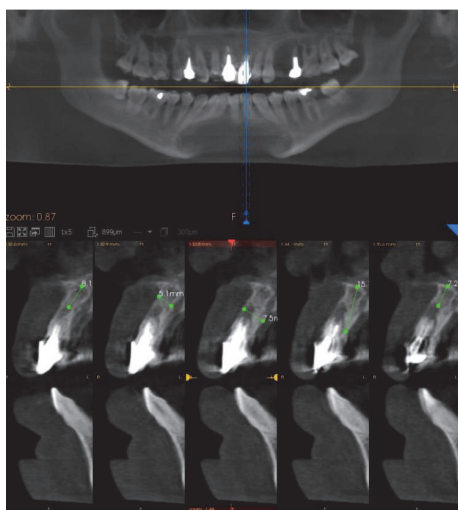


FIGURE 2: Cone beam computed tomography (CBCT). The cone beam computed tomography (CBCT) examination confirms the presence of the tooth resorption. A careful 3D analysis of the height and width of the alveolar ridge is performed, in order to better plan the implant placement.

The nanostructured surface of these implants (Xpeed®) was the result of a conventional sandblasting procedure (resorbable blast media treatment) and the subsequent incorporation of calcium ions by means of a hydrothermal method [24]. The implants had a 5 mm deep conical connection (10°) combined with an internal hexagon [6, 15, 20] and were available in different lengths (7.0, 8.5, 10.0, 11.5, 13.0, and 15.0 mm) and diameters (3.5, 4.0, 4.5, 5.0, 5.5, and 6.0 mm).

2.4. Surgical and Prosthetic Procedures. All surgeries were performed under local anesthesia, using articaine with adrenaline (1:100,000) by the same experienced clinician (M.S.). In the case of single-tooth gaps in healed ridges, a midcrestal incision was performed connected with two lateral releasing incisions; a full-thickness flap was raised; then the surgeon prepared the implant sites using drills

of increasing diameter, strictly following the manufacturer's recommendations. In the case of nonrestorable teeth that had to be extracted, the extraction was performed gently with the purpose of avoiding any damage to the buccal bone wall; the socket was carefully cleaned and the integrity of the socket walls was verified. Then, the surgeon prepared the implant site, without rising any flap apically and pushing 3 to 4 mm to the peak of the postextraction socket. In cases with high aesthetic demands (such as the central and lateral incisors) care was taken to prepare the implant site palatally, in order to avoid any contact with the delicate and thin buccal wall. In postextraction cases, after the insertion of the implants, the gaps between the fixture and the alveolus walls were filled with autogenous bone chips, recovered during the preparation of the surgical site (Figures 3 and 4); the autogenous bone could be mixed with highly porous hydroxyapatite granules, where needed. In all cases, the implants were placed slightly subcrestal and their primary implant stability was measured by means of RFA; the ISQ values were measured at four sites (buccal/palatal/mesial/distal) in order to calculate the mean ISQ value for each implant. When the mean ISQ < 60, the implants could not be loaded immediately and were therefore considered failed for immediate loading; they were left unloaded placing a transmucosal healing abutment for a period of 3-4 months, during which the patient had to wear a small removable prosthesis, for aesthetic reasons. If the mean ISQ value at placement was ≥ 60 , conversely, the implants were immediately loaded (within 48 hours after implant placement) by means of a single provisional resin crown. A titanium prefabricated abutment was prepared and screwed on the implant; a provisional resin crown was then adapted. The provisional crowns could be obtained from a direct impression (from the laboratory) or from preformed shells which were relined intraorally. Care was taken to polish well all crowns and to obtain a satisfactory, natural emergence profile (Figure 5). In the healed ridge group of patients, interrupted sutures were performed to adapt the flap to the restoration; in the postextraction group, the provisional crown protected the alveolus, maintaining the clot formation subgingivally; in some cases, these crowns could be splinted with composite resin to the adjacent teeth, in the period

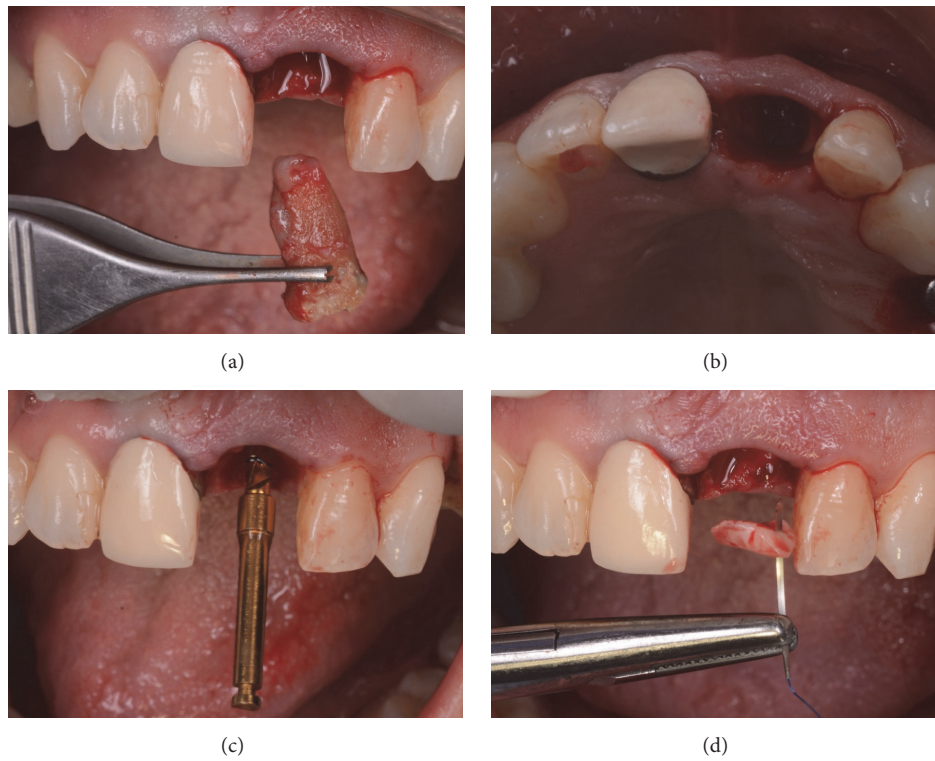


FIGURE 3: Surgery. The nonrestorable tooth is extracted (a) and the socket is carefully debrided (b), in order to remove all infected tissue; then, the implant site is prepared with sequential drills, exceeding the alveolar apex 3-4 mm (c) and before to place the implant, a connective tissue graft is harvested from the palate, in order to thicken the soft tissues in the delicate buccal area (d).

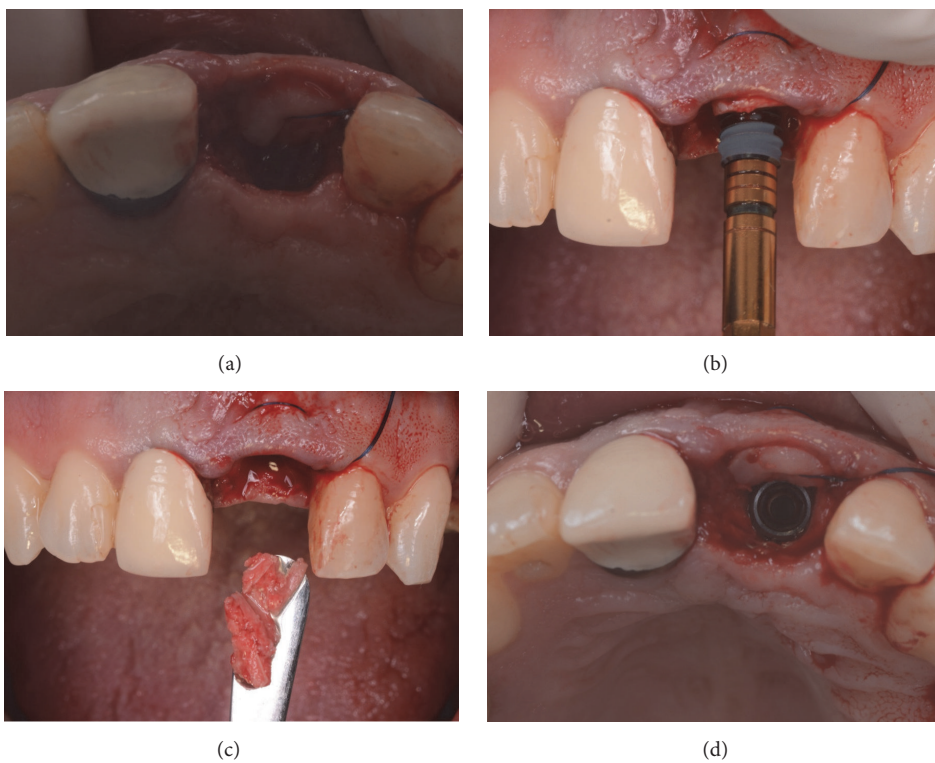


FIGURE 4: Surgery. The connective tissue graft is secured in position, within the envelope flap (a); then the implant (Anyridge, Megagen) is inserted slightly subcrestal and in palatal position (b); the autogenous bone chips collected during the preparation of the implant site are then placed in the alveolus (c), in order to fill the gaps between the socket and the implant (d).

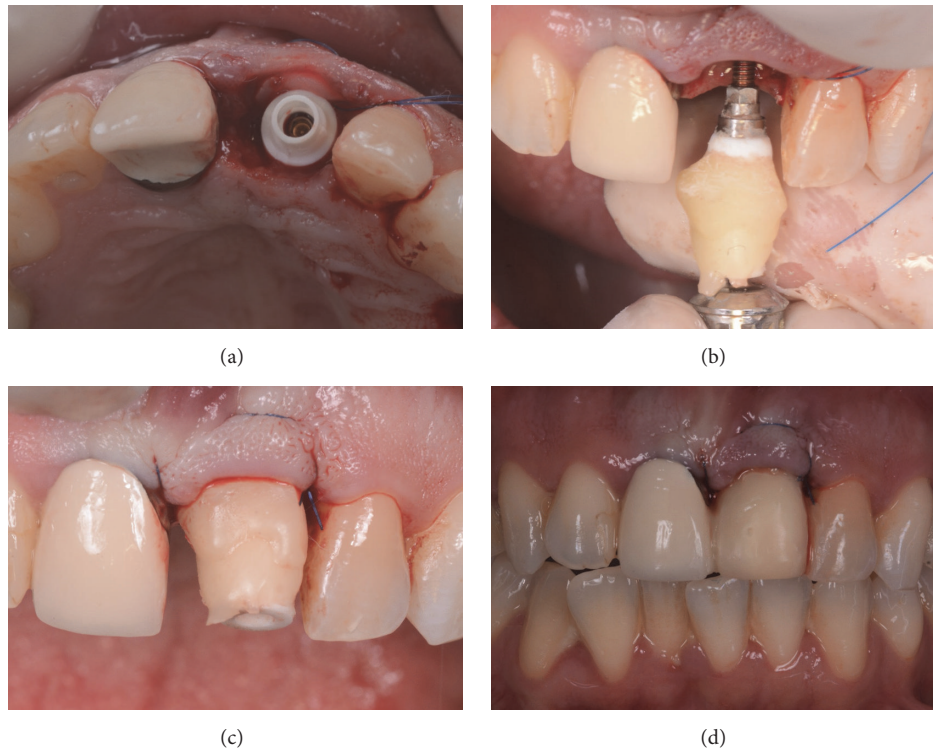


FIGURE 5: Immediate provisionalization. A provisional abutment is screwed on the implant (a) and the individual emergence profile is obtained with composite resin (b) in order the correct pressure that is exerted on the soft tissues (c); in this case, the immediate temporary restoration is then splinted to the adjacent teeth, for a short period after the surgery, in order to reduce the effects of prosthetic loading on the immediately inserted implant (d).

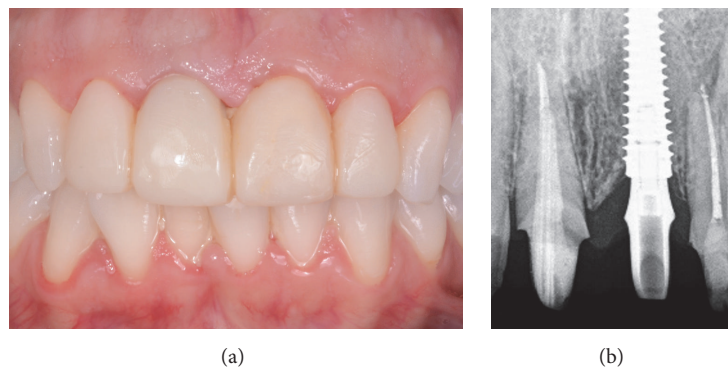


FIGURE 6: The provisional restoration after 2 months. The soft tissues outline has been modeled by the temporary and the level and curvature of the facial mucosa look better, even if oral hygiene should be improved. (a) Clinical view; (b) radiographic control.

immediately following the surgery. The provisionals were screw-retained or cemented, depending on the case. A careful check of the occlusion with articulating papers completed the provisional prosthetic phase: light and well distributed static contacts were left, and care was taken to remove any possible overloading. An intraoral periapical radiograph was taken, and the patient was left with prescriptions of oral antibiotics (amoxicillin + clavulanic acid, 2 gr/day for a period of 6 days) and analgesics (600 mg ibuprofen, 2/3 times a day for a maximum period of 2 days). All patients were recalled at

1 week, for a control and the removal of the sutures (where present). The provisional crowns remained in situ (Figure 6) for a period of 3-4 months, after that they were replaced by the definitive ceramic (zirconia ceramic) restorations; the final restorations were cemented (Figure 7). At the delivery of the final crowns, occlusion was carefully checked again, and a new periapical radiograph was taken. All patients were then enrolled in a follow-up program, with visits every 4 months; the patients were followed for a period of 1 year of loading (Figure 8), after the delivery of the final restorations.



FIGURE 7: The definitive ceramic restoration in position. (a) The definitive ceramic crown is delivered to the patient, along with the other planned definitive, tooth-supported restorations. (b) The aesthetic result 4 months after implant placement.

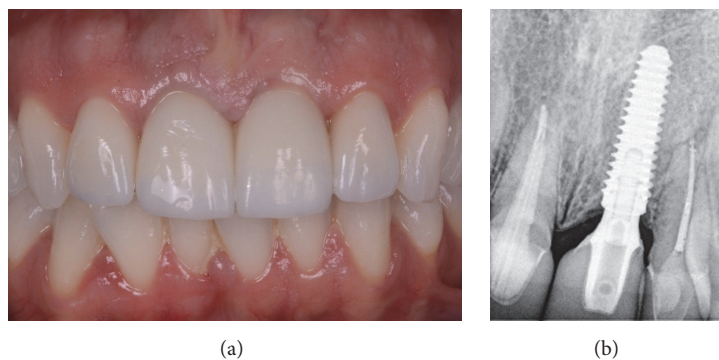


FIGURE 8: The definitive ceramic crown 1 year after the delivery. (a) An aesthetically pleasing result has been maintained clinically, and the patient is fully satisfied; (b) the radiographic control confirms the stability of the hard tissues around the implant.

2.5. Outcomes of the Study. During each follow-up visit (every 4 months) and until the end of the study (1 year after the placement of the definitive crowns) a clinical and radiographic assessment of the implants, peri-implant tissues, and prostheses was carried out by a periodontologist and a prosthodontist, who were not directly involved in the placement of the implants. The main outcomes of the study were implant stability, implant survival, and implant success.

2.5.1. Implant Stability. Resonance frequency analysis (RFA) was the method used to measure implant stability, immediately after placement (primary implant stability) and at each follow-up session. A dedicated instrument (Osstell Mentor®; Osstell, Integration Diagnostic, Sweden) was used to register implant stability. This portable device emitted magnetic pulses to a small magnet (Smartpeg®) screwed directly on the implant with 5 Ncm; the magnet started to vibrate, and the probe listened to the tone and translated it to a value named implant stability quotient (ISQ) [25]. For each fixture, ISQ values (scaled 1–100) were measured from the four sites (mesial, distal, buccal, and palatal sites). The mean of all measurements was rounded to a whole number and regarded as the final ISQ of the implant [25, 26]. At each follow-up session, after each measurement, the abutments were repositioned and screwed again on the implants so that the prostheses could be reinserted. In general, the acceptable

stability range is 55–85 ISQ; however, in the present study, in the case of ISQ < 60, implants could not be immediately functionalized/loaded and were therefore considered failed for immediate loading, as previously reported [20].

2.5.2. Implant Survival. A fixture was defined as “surviving” if still present and regular in function, at the end of the study, one year after the placement of the definitive crown. In all cases in which the fixture had to be removed, the implant was defined as “failed.” The causes for which an implant could be removed were (1) lack of osseointegration and mobility, which occurred in the early healing period/provisionalization or even after the placement of the final restoration, but in the absence of symptoms/signs of infection; (2) recurrent and intractable infection of the peri-implant tissues (peri-implantitis) that caused massive bone loss and subsequent implant loosening; (3) fracture of the implant body.

2.5.3. Implant Success. The implant success was defined as the condition in which no biological or prosthetic complications occurred, at the implant and at the restoration level, in the course of the whole study. Among the biological complications, there were (1) postoperative pain/discomfort and edema/swelling; (2) peri-implant mucositis; (3) peri-implantitis; (4) peri-implant bone loss >1.5 mm, without any symptoms or signs of infection, at the 1-year follow-up

session. Peri-implant mucositis was defined as a reversible clinical situation in which bleeding on probing and/or suppuration were present, associated with a pocket depth ≥ 4 mm but with no radiographic bone loss; conversely, peri-implantitis was defined as a nonreversible clinical situation characterized by pocket depth ≥ 4 mm and bleeding on probing and/or pus secretion associated with evidence of radiographic bone loss (>2.5 mm) [27]. Among the prosthetic complications, there were mechanical complications such as abutment screw loosening and abutment fracture, but also technical complications such as chipping/fracture of the ceramic restorations [2, 28].

2.6. Statistical Evaluation. Two independent, experienced observers (a periodontist and a prosthodontist) collected and evaluated all data. Data were entered into a statistical sheet (Excel®, Microsoft, Redmond, USA) where the statistical analysis was performed. The evaluation of patients' demographics (gender, age at surgery, smoking habit, history of periodontal disease, and presence of parafunctions) as well as the implant characteristics (site, position, length and diameter, minor bone augmentation, and connective tissue graft procedures) was carried out. All qualitative variables were evaluated by calculating absolute and relative frequency distributions; the Chi-square test was used to calculate the differences in distribution between the groups, with the significance level set at 0.005. Conversely, quantitative variables (such as patients' age) were analyzed by calculating means, standard deviations (SD), and medians and 95% confidence intervals (CI). Implant survival and success were calculated at the implant level.

3. Results

3.1. Patient Demographics and Implant Distribution. In total, 34 patients (13 males; 21 females) were enrolled in the present study. The mean age of these patient was 45.58 years (± 10.15 ; median 44; range 20–69; CI 95% 42.14–49.02). The distribution of the patients is reported in Table 1. Although more females were enrolled (21/34: 61.8%), the distribution of patients did not differ significantly in relation to gender ($p = 0.170$). Conversely, most of the selected patients were young adults (with an age comprising between 35 and 49 years, 21/34: 61.8%), with only 7 patients with an age comprising between 50 and 64 years (7/34: 20.6%) and 3 patients with an age < 35 years and ≥ 65 years (3/34: 8.8%), respectively. Accordingly, the distribution of the patients was nonhomogeneous with respect to the age at surgery ($p < 0.0001$). Most of the patients were nonsmokers (28/34: 82.4%) so that the distribution of patients was not homogeneous with regard to the smoking habit ($p = 0.0002$); however, the percentage of smokers was quite high (6/34: 17.6%). Finally, no statistically significant differences were found in the patients demographics with regard to history of periodontal disease ($p = 0.303$) or presence of parafunctions (bruxism and/or clenching) ($p = 0.086$). In fact, 20 patients had a previous history of chronic periodontal disease (20/34: 58.8%) while 14 patients had not experienced this condition before (14/34: 41.2%). Similarly, 22 patients had no history

TABLE 1: Patient demographics.

	Number of patients (%)	p^*
<i>Gender</i>		
Males	13 (38.2%)	0.170
Females	21 (61.8%)	
<i>Age at surgery</i>		
20–34 years	3 (8.8%)	<0.0001
35–49 years	21 (61.8%)	
50–64 years	7 (20.6%)	
≥ 65 years	3 (8.8%)	
<i>Smoke</i>		
Yes	6 (17.6%)	0.0002
No	28 (82.4%)	
<i>History of periodontal disease</i>		
Yes	20 (58.8%)	0.303
No	14 (41.2%)	
<i>Parafunctions</i>		
Yes	12 (35.3%)	0.086
No	22 (64.7%)	
Total	34	—

p^* = Chi-square test.

of parafunctions (22/34: 64.7%), while 12 patients (35.3%) suffered from bruxism and/or clenching.

A total of 43 implants were inserted in this study. Six patients had multiple indications for implant therapy (one patient had four implants installed, another patient received three implants, and four patients had two implants installed). With regard to the distribution of the implants, almost one-third of them were placed in postextraction sockets (14/43: 32.6%), while 29 (29/43: 67.4%) were placed in fully healed sites: these groups did not differ significantly ($p = 0.022$). With regard to the position of the implants, however, a high number of premolars (28/43: 65.1%) were installed, when compared to the incisors (11/43: 25.6%) and with the cuspids (4/43: 9.3%): the distribution of the fixtures in these groups was significantly nonhomogeneous ($p < 0.0001$). No statistically significant differences were found in the distribution of implants by length ($p = 0.010$) and diameter ($p = 0.026$). In almost all cases (37/43: 86.0%) a bone regeneration with autogenous bone particles (collected during the preparation of the implant site) was performed; consequently, there was a significant difference in the distribution of the implants, with regard to the use of bone regeneration procedures ($p < 0.0001$). Finally, in a high number of cases (10/43: 23.3%) a connective tissue graft was harvested from the palate and used to thicken the soft tissues in the buccal area. The connective tissue grafts were placed in almost all cases of central incisors (10/11: 90.9%). In 33 cases, however (33/43: 76.7%) no connective tissue grafts were harvested, and the p value observed (0.0005) did not reveal a statistically significant difference in the distribution of the fixtures, with regard to the use of connective tissue grafts. All information about the distribution of the implants is summarized in Table 2.

TABLE 2: Distribution of the implants.

	Number of implants (%)	<i>p</i> *
<i>Surgical protocol</i>		
Postex. sockets	14 (32.6%)	0.022
Healed sites	29 (67.4%)	
<i>Position</i>		
Incisors	11 (25.6%)	<0.0001
Cuspids	4 (9.3%)	
Premolars	28 (65.1%)	
<i>Length</i>		
10.0 mm	3 (7.0%)	0.010
11.5 mm	9 (20.9%)	
13.0 mm	13 (30.2%)	
15.0 mm	18 (41.9%)	
<i>Diameter</i>		
3.5 mm	15 (34.9%)	0.026
4.0 mm	16 (37.2%)	
4.5 mm	8 (18.6%)	
5.0 mm	4 (9.3%)	
<i>Bone regeneration</i>		
Yes	37 (86.0%)	<0.0001
No	6 (14.0%)	
<i>Connective tissue graft</i>		
Yes	10 (23.3%)	0.0005
No	33 (76.7%)	
Total	43	—

*p** = Chi-square test.

3.2. Implant Stability, Survival, and Success. In the present study, only two implants (2/43: 4.6%) did not show sufficient primary implant (ISQ < 60) and were therefore considered failed for the immediate loading. These implants were not loaded and remained with the healing abutments in position, for a period of 3 months; after this period, they were successfully loaded with a provisional restoration. Both these implants were premolars, placed in the extraction sockets of two different adult patients (49- and 67-year-old females). Conversely, 41 implants (41/43: 95.4%) were satisfactory stable (ISQ ≥ 60) at placement and were therefore loaded immediately.

At the end of the study, one year after the placement of the definitive crowns, no implants failed, for an overall survival rate of 100% (43/43 implants, 41/41 immediately loaded implants in functions).

Finally, with regard to the implant success, no biological complications were reported. In fact, no postoperative pain/discomfort and/or edema/swelling occurred after surgery; in addition, no peri-implant mucositis or peri-implantitis was registered during the entire follow-up period, and the marginal bone loss was <1.5 mm in all implants. However, two prosthetic abutments (2/41: 4.8%) became loose, in two premolars; the abutment screw loosening was registered as prosthetic (mechanical) complication, since it was complication affecting implant components. The abutment screws were tightened again and no other complications

occurred at this level. Overall, the rate of complications was therefore 4.8%, for an implant success of 95.2% after 1 year of functional loading.

4. Discussion

Nowadays, patients are increasingly demanding and asking for early and immediate prosthetic loading protocols [9, 14]; in the same way, the immediate placement of implants in fresh postextraction sockets represents a valid therapeutic option for the clinician, to reduce the times and costs of implant-prosthetic treatment, the invasiveness of the therapy, and the patient stress [4, 7, 8, 10].

Although the placement of immediate, postextraction implants and the immediate loading protocols can represent today predictable solutions, characterized by high rates of survival and success [7–10], there is no doubt that these methods are more challenging for the clinician, at least when compared to more conventional protocols (such as the insertion of fixtures in fully healed edentulous bone ridges and the conventional, delayed loading after a period of 4–6 months of undisturbed bone healing) [7, 13]. In fact, the placement of implants in extraction sockets can be difficult [7, 13]. First, the postextraction alveolus is generally of larger size than the diameter of the implant: it can therefore be difficult to obtain adequate primary stability of the implant in the surgical site [1, 7, 13]. It is known that primary stability is a fundamental requirement for the survival of the implant, in the short term: an insufficiently stable implant may have a mobilization and failure in the early months of healing, immediately after insertion [17, 18]. In fact, during the first two months following insertion, a bone remodeling with partial loss of initial mechanical stabilization of the implant (resulting from the initial contact between the implant surface and the preexisting alveolar bone) occurs [17, 18]. If this remodeling is not effectively counteracted and balanced by an adequate and rapid deposition of new bone on the implant surface, an adequate secondary stabilization (or osseointegration) of the implant is not possible, with a high risk of failure [17, 18]. Some colleagues have suggested the use of fixtures of larger diameter, in order to get a better primary stability in postextraction sockets: this solution is certainly feasible and viable in the posterior regions [16] but may even be counterproductive in the anterior regions (characterized by high aesthetic impact), where the contact between the implant and the delicate buccal bone plate must be avoided, to prevent the risk of an aesthetic failure [8, 29–31]. For these reasons, generally, the stabilization of the postextraction implants is obtained via an apical preparation that is brought 3–4 mm deeper than the alveolus, for a better apical engagement of the fixture [7, 8, 30, 32, 33]. These surgical strategies are certainly of great validity, but even better results can be obtained if these methods are accompanied by the use of an implant with a design (macrotopography) conceived to maximize the primary stabilization [19, 20, 33].

In the present study on the immediate loading of single implants placed in the anterior areas of the maxilla, almost one-third of all fixtures (32.6%) were placed in postextraction

sockets. Despite this, only two implants (4.6%) did not show sufficient primary implant (ISQ < 60) and were therefore considered failed for the immediate loading. This valuable result was certainly possible because long implants were used (72% of the fixtures used in this study were ≥ 13 mm in length) for a better apical engagement and stabilization in the socket; however, the use of tapered implants with knife-edge threads helped to obtain these positive outcomes, because this implant design is potentially able to guarantee a valid primary stabilization even in difficult contexts, as indicated previously in the literature [6, 15, 20].

Immediate loading represents the second possible strategy to reduce the duration of the implant-prosthetic treatment and the cost of therapy: for these reasons, this procedure is more and more appreciated and requested by the patients [9, 16]. Although the immediate loading of implants represents today a reliable procedure in clinically controlled contexts [9], there is no doubt that it could represent a potential risk for treatment failure [17, 18]. In fact, uncontrolled forces and exceeding the physiological limits, transmitted from the crown to the implant, can interfere in the early healing processes at the bone/implant interface and determine the mobilization and failure of the fixture [17, 18].

In our present study, the immediate loading of single implants installed in postextraction sockets and healed sites gave positive clinical outcomes, with high survival rates (100%: no implants were lost during the follow-up). The careful treatment planning and the care and attention devoted to compliance with the strict surgical protocols and prosthetic may explain the excellent results obtained here [34], with a low (4.8%) incidence of complications (no biological complications were reported; only a few prosthetic complications were registered, with two prosthetic abutment loosening encountered during the entire follow-up). However, once again, the use of implants with a specific thread design and macrotopography, able to optimize the primary stabilization, may have contributed to the excellent clinical result obtained in our present work. The threads of the fixtures used in this study, in fact, result in maximized bone-to-implant contact and compressive force resistance and minimized shear force production: this can help in maintaining implant stability in the immediate postplacement healing period, as previously reported in the literature [6, 15, 20]. It should be added, however, that in our present work, all immediately loaded implants were subjected to a controlled load. In fact, all temporary crowns were adjusted with light occlusal marks, so that the occlusal surfaces were in slight static contact with the opposite dentition but with no contact in lateral movements, as previously described in the literature [15]. This procedure allows control and reduces in some way the forces acting on the system, through the prosthetic restoration [15]. In addition, in the present study, some of the single, implant-supported crowns (12/41: 29.2%) were splinted with the neighbouring teeth, for a period of two weeks after surgery. These procedures were particularly important in fresh extraction sockets: in these areas, where the primary stabilization may be more difficult, it is generally considered prudent to avoid overloading the fixture, to prevent the risk of mobilization and failure [17, 18]. In fact, there must be

sufficient time to guarantee the transition from the primary (mechanical) stabilization of the implant, to the secondary (biological) stabilization, due to the deposition of new bone directly on the fixture surface [17, 18]. This transition should be as undisturbed as possible, that is, without the occurrence of micromovements at the interface between the bone and the implant, which beyond a certain threshold may interfere with the phenomena of osseointegration [17, 18]. Finally, in the present study, we have used an implant system characterized by a specific micro/nanotopography, with a sandblasted, microstructured surface, which was subsequently treated with incorporation of calcium ions, to become nanostructured. The scientific literature has evidenced that the treatment of implant surfaces stimulates a better and faster bone-implant integration and rapid deposition of new bone on the implant surface [21, 22, 24, 35]. Numerous systematic reviews [21, 22] have shown that the treatment of implant surfaces can be a very important strategy to reduce the conventional healing times, thanks to an increased surface area and surface energy, which are able to promote a better interaction with biological fluids and blood.

The present study has limits, such as the limited number of patients treated (and fixtures inserted) and the short follow-up time. In addition, in this study, only implants placed and immediately loaded in the anterior maxilla have been included. The implants placed in the molar regions of the maxilla were excluded from this evaluation. This is not a trivial matter since in the posterior areas the prosthetic load is higher, and the quality of bone is generally lower: therefore, there may be a higher risk of implant failure, when the immediate functional loading protocol is performed [9, 15, 16]. Finally, it must be pointed out that in the present study in almost all cases of immediate postextraction implants, the provisional resin crowns were splinted with the neighbouring teeth, for a period of two weeks, in order to reduce the possible negative effects of loading (micromotion) at the bone-implant interface, in the first period of healing. In conclusion, the implants inserted in this study should be followed for a longer period of time, and further studies on a larger sample of patients (and possibly including fixtures placed and immediately loaded in the posterior maxilla) will be needed before drawing more specific conclusions.

5. Conclusions

In this prospective clinical study with a follow-up of 1 year, the immediate loading of single implants with knife-edge thread design and nanostructured calcium-incorporated surface placed in the anterior maxilla gave positive clinical outcomes, with high survival (100%) and success (95.2%) rates. Only a few, minor prosthetic complications (two abutment screws became loose) were reported, for an overall complication rate of 4.8%. Further long-term studies on a larger sample of patients are needed to confirm these results; in addition, it will be necessary to evaluate the effects of immediate loading on single implants placed in the posterior areas of the maxilla (molar regions), where the prosthetic load is higher.

Disclosure

No materials, grants, or other sources of financial supports were provided for the publication of this study.

Conflicts of Interest

The authors report no conflicts of interest for the present prospective clinical study.

References

- [1] M. Tallarico, E. Xhanari, M. Pisano, G. De Riu, A. Tullio, and S. M. Meloni, "Single post-extractive ultra-wide 7 mm-diameter implants versus implants placed in molar healed sites after socket preservation for molar replacement: 6-month post-loading results from a randomised controlled trial," *European Journal of Oral Implantology*, vol. 9, no. 3, pp. 263–275, 2016.
- [2] L. Canullo, M. Caneva, and M. Tallarico, "Ten-year hard and soft tissue results of a pilot double-blinded randomized controlled trial on immediately loaded post-extractive implants using platform-switching concept," *Clinical Oral Implants Research*, 2016.
- [3] R. E. Jung, A. Zembic, B. E. Pjetursson, M. Zwahlen, and D. S. Thoma, "Systematic review of the survival rate and the incidence of biological, technical, and aesthetic complications of single crowns on implants reported in longitudinal studies with a mean follow-up of 5 years," *Clinical Oral Implants Research*, vol. 23, no. 6, pp. 2–21, 2012.
- [4] F. G. Mangano, P. Mastrangelo, F. Luongo, A. Blay, S. Tunchel, and C. Mangano, "Aesthetic outcome of immediately restored single implants placed in extraction sockets and healed sites of the anterior maxilla: a retrospective study on 103 patients with 3 years of follow-up," *Clinical Oral Implants Research*, vol. 28, no. 3, pp. 272–282, 2017.
- [5] D. Buser, L. Sennerby, and H. De Bruyn, "Modern implant dentistry based on osseointegration: 50 years of progress, current trends and open questions," *Periodontology 2000*, vol. 73, no. 1, pp. 7–21, 2017.
- [6] F. G. Mangano, F. Luongo, G. Picciocchi, C. Mortellaro, K. B. Park, and C. Mangano, "Soft tissue stability around single implants inserted to replace maxillary lateral incisors: a 3D evaluation," *International Journal of Dentistry*, vol. 2016, Article ID 9393219, 9 pages, 2016.
- [7] B. R. Chrcanovic, T. Albrektsson, and A. Wennerberg, "Dental implants inserted in fresh extraction sockets versus healed sites: a systematic review and meta-analysis," *Journal of Dentistry*, vol. 43, no. 1, pp. 16–41, 2015.
- [8] F. Mangano, C. Mangano, M. Ricci, R. L. Sammons, J. A. Shibli, and A. Piattelli, "Single-tooth Morse taper connection implants placed in fresh extraction sockets of the anterior maxilla: an aesthetic evaluation," *Clinical Oral Implants Research*, vol. 23, no. 11, pp. 1302–1307, 2012.
- [9] B. R. Chrcanovic, T. Albrektsson, and A. Wennerberg, "Immediate nonfunctional versus immediate functional loading and dental implant failure rates: a systematic review and meta-analysis," *Journal of Dentistry*, vol. 42, no. 9, pp. 1052–1059, 2014.
- [10] R. Kolerman, E. Mijiritsky, E. Barnea, A. Dabaja, J. Nissan, and H. Tal, "Esthetic assessment of implants placed into fresh extraction sockets for single-tooth replacements using a flapless approach," *Clinical Implant Dentistry and Related Research*, vol. 19, no. 2, pp. 351–364, 2017.
- [11] M. G. Araújo, C. O. Silva, M. Misawa, and F. Sukekava, "Alveolar socket healing: what can we learn?" *Periodontology 2000*, vol. 68, no. 1, pp. 122–134, 2015.
- [12] V. Chappuis, M. G. Araújo, and D. Buser, "Clinical relevance of dimensional bone and soft tissue alterations post-extraction in esthetic sites," *Periodontology 2000*, vol. 73, no. 1, pp. 73–83, 2017.
- [13] M. Al-Sabbagh and A. Kutkut, "Immediate implant placement: surgical techniques for prevention and management of complications," *Dental Clinics of North America*, vol. 59, no. 1, pp. 73–95, 2015.
- [14] D. Farronato, F. Mangano, F. Briguglio, V. Iorio-Siciliano, F. Riccitiello, and R. Guarnieri, "Influence of Laser-Lok surface on immediate functional loading of implants in single-tooth replacement: a 2-year prospective clinical study," *The International Journal of Periodontics & Restorative Dentistry*, vol. 34, no. 1, pp. 79–89, 2014.
- [15] C. Mangano, F. Raes, C. Lenzi et al., "Immediate loading of single implants: a 2-year prospective multicenter study," *The International Journal of Periodontics & Restorative Dentistry*, vol. 37, no. 1, pp. 69–78, 2017.
- [16] G. I. Benic, J. Mir-Mari, and C. H. F. Hämmerle, "Loading protocols for single-implant crowns: a systematic review and meta-analysis," *The International Journal of Oral & Maxillofacial Implants*, vol. 29, supplement 1, pp. 222–238, 2014.
- [17] S.-S. Gao, Y.-R. Zhang, Z.-L. Zhu, and H.-Y. Yu, "Micromotions and combined damages at the dental implant/bone interface," *International Journal of Oral Science*, vol. 4, no. 4, pp. 182–188, 2012.
- [18] N. Lioubavina-Hack, N. P. Lang, and T. Karring, "Significance of primary stability for osseointegration of dental implants," *Clinical Oral Implants Research*, vol. 17, no. 3, pp. 244–250, 2006.
- [19] M. Alshehri and F. Alshehri, "Influence of implant shape (tapered vs cylindrical) on the survival of dental implants placed in the posterior maxilla: a systematic review," *Implant Dentistry*, vol. 25, no. 6, pp. 855–860, 2016.
- [20] C. H. Han, F. Mangano, C. Mortellaro, and K. B. Park, "Immediate loading of tapered implants placed in postextraction sockets and healed sites," *Journal of Craniofacial Surgery*, vol. 27, no. 5, pp. 1220–1227, 2016.
- [21] A. Jemat, M. J. Ghazali, M. Razali, and Y. Otsuka, "Surface modifications and their effects on titanium dental implants," *BioMed Research International*, vol. 2015, Article ID 791725, 11 pages, 2015.
- [22] R. Smeets, B. Stadlinger, F. Schwarz et al., "Impact of dental implant surface modifications on osseointegration," *BioMed Research International*, vol. 2016, Article ID 6285620, 16 pages, 2016.
- [23] C. A. Bain, D. Weng, A. Meltzer, S. S. Kohler, and R. M. Stach, "A meta-analysis evaluating the risk for implant failure in patients who smoke," *Compendium of Continuing Education in Dentistry*, vol. 23, no. 8, pp. 695–708, 2002.
- [24] F. G. Mangano, G. Iezzi, J. A. Shibli et al., "Early bone formation around immediately loaded implants with nanostructured calcium-incorporated and machined surface: a randomized, controlled histologic and histomorphometric study in the human posterior maxilla," *Clinical Oral Investigations*, 2017.
- [25] M. A. Atieh, N. H. Alsabeeha, and A. G. Payne, "Can resonance frequency analysis predict failure risk of immediately loaded implants?" *International Journal of Prosthodontics*, vol. 25, no. 4, pp. 326–339, 2012.
- [26] S. Bechara, R. Kubilius, G. Veronesi, J. T. Pires, J. A. Shibli, and F. G. Mangano, "Short (6-mm) dental implants versus sinus floor

- elevation and placement of longer (≥ 10 -mm) dental implants: a randomized controlled trial with a 3-year follow-up," *Clinical Oral Implants Research*, 2016.
- [27] American Academy of Periodontology, "Peri-implant mucositis and peri-implantitis: a current understanding of their diagnoses and clinical implications," *Journal of Periodontology*, vol. 84, no. 4, pp. 436–443, 2013.
- [28] G. E. Salvi and U. Bragger, "Mechanical and technical risks in implant therapy," *The International Journal of Oral and Maxillofacial Implants*, vol. 24, supplement 1, pp. 69–85, 2009.
- [29] S.-C. Cho, S. J. Froum, A. R. Kamer, P. M. Loomer, G. Romanos, and B. Demiralp, "Implants in the anterior maxilla: aesthetic challenges," *International Journal of Dentistry*, vol. 2015, Article ID 152420, 2 pages, 2015.
- [30] F. G. Mangano, C. Mangano, M. Ricci, R. L. Sammons, J. A. Shibli, and A. Piattelli, "Esthetic evaluation of single-tooth Morse taper connection implants placed in fresh extraction sockets or healed sites," *Journal of Oral Implantology*, vol. 39, no. 2, pp. 172–181, 2013.
- [31] U. Covani, L. Canullo, P. Toti, F. Alfonsi, and A. Barone, "Tissue stability of implants placed in fresh extraction sockets: a 5-year prospective single-cohort study," *Journal of Periodontology*, vol. 85, no. 9, pp. e323–e332, 2014.
- [32] M. Gómez-Polo, R. Ortega, C. Gómez-Polo, C. Martín, A. Celemín, and J. del Río, "Does length, diameter, or bone quality affect primary and secondary stability in self-tapping dental implants?" *Journal of Oral and Maxillofacial Surgery*, vol. 74, no. 7, pp. 1344–1353, 2016.
- [33] R. M. Shadid, N. R. Sadaqah, and S. A. Othman, "Does the implant surgical technique affect the primary and/or secondary stability of dental implants? A systematic review," *International Journal of Dentistry*, vol. 2014, Article ID 204838, 17 pages, 2014.
- [34] B. Butler, "Masking buccal plate remodeling in the esthetic zone with connective tissue grafts: immediate implant concepts, techniques," *Compendium of Continuing Education in Dentistry*, vol. 35, no. 7, pp. 486–493, 2014.
- [35] M. Shokri and A. Daraeighadikolaie, "Measurement of primary and secondary stability of dental implants by resonance frequency analysis method in mandible," *International Journal of Dentistry*, vol. 2013, Article ID 506968, 5 pages, 2013.